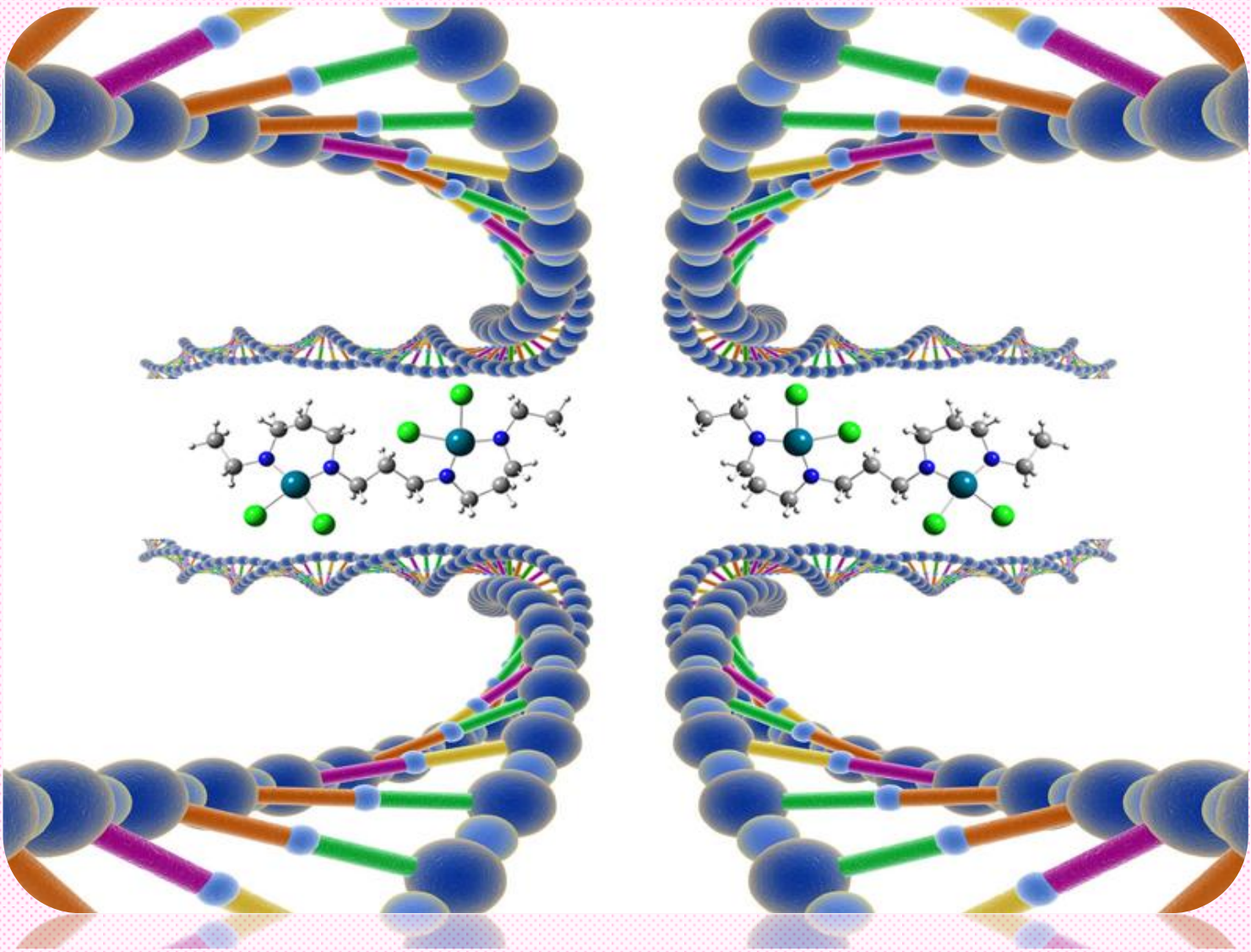

Tânia Raquel de Magalhães e Silva

Polyamine-Based Anticancer Strategies

The Role of Modified Polyamines

2013

· U C ·

Universidade de Coimbra

Tânia Raquel de Magalhães e Silva

Polyamine-Based Anticancer Strategies

The Role of Modified Polyamines

Dissertação apresentada à Universidade de Coimbra para cumprimento dos requisitos necessários à obtenção do grau de Doutor em Bioquímica, especialidade em Biologia Celular e Molecular.

Orientação: **Doutora Maria Paula Marques**

Doutora Stina Oredsson

Departamento de Ciências da Vida – Faculdade de Ciências e Tecnologia

Universidade de Coimbra

Coimbra, 2013

Tânia Raquel de Magalhães e Silva

Polyamine-Based Anticancer Strategies

The Role of Modified Polyamines

Dissertation presented to the University of Coimbra as requirement for the achievement of the PhD degree in Biochemistry, specialisation in Cellular and Molecular Biology.

Supervisors: **Doctor Maria Paula Marques**

Doctor Stina Oredsson

Life Sciences Department – Faculty of Sciences and Technology

University of Coimbra

Coimbra, 2013

Tânia M. Silva gratefully acknowledges the Institutions that supported this PhD work:

- Portuguese Foundation for the Science and Technology (FCT) – PhD fellowship (SFRH/BD/46364/2008), funded by POPH-QREN and financed by ESF
- Project PEst-OE/Qui/UIOO700/2011 – co-financed by FCT
- Project research grant PTDC/QUI/66701/2006 – co-financed by the European Community fund FEDER
- Swedish Gunnar Nilsson Cancer Foundation

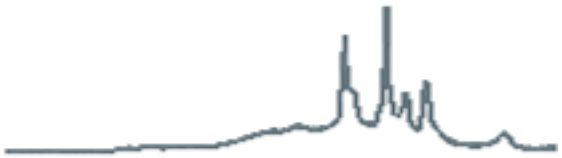

R&D Unit – Coimbra University PORTUGAL

LUNDS UNIVERSITET

This research work was conducted at:

- Molecular Physical-Chemistry R&D Unit, Faculty of Sciences and Technology, University of Coimbra, Coimbra, Portugal
- Biology Department, University of Lund, Lund, Sweden
- Department of Experimental Medical Science, University of Lund, Lund, Sweden

This PhD work had the collaborations of:

- Dr. Lo Persson – Department of Experimental Medical Science, University of Lund, Sweden
- Dr. Patrick Woster – Department of Drug Discovey and Biomedical Sciences, Medical University of South Carolina, Charleston, SC, USA
- Dr. Sunil Kumar Sukumaran – Anthem Biosciences Pvt. Ltd, Bangalore, India
- Chemistry Department – University of Aveiro, Aveiro, Portugal

To my wonderful and unique Parents

To my beautiful Family and Friends

To the two real Loves of my life

“The greatest thing you’ll ever learn is just to love and be loved in return!”

Moulin Rouge

Acknowledgements

I would like to extend my sincere gratitude and appreciation to everybody who helped me during my PhD and that truly made my stay, both in Coimbra and Lund, forever memorable over these 4 years as a PhD student. Therefore, I especially want to thank to:

Professor Maria Paula Marques, my Portuguese supervisor, for introducing me to the spectacular Polyamines field and for inviting me to join your group, thereby giving me the opportunity to follow my dreams and do research! I admire you so much, not only as a professor but, most important, as a person and friend! Thank you for all your invaluable help, your advices and for making this project possible. You were the initiator of my scientific life! Without you I wouldn't be here today!

Professor Stina Oredsson, my Swedish supervisor, for being the way you are! I never met anyone with such enthusiasm, passion, and love for their work as you! I wish I could be more like you, always seeing the good and also the bad things in science! You are simply a unique, incredible and unforgettable scientist! I'm so happy and grateful to have met you! I will never forget the way you lived my experiments with me! All the screams, the laughs, the smiles, the happiness we both felt…Thank you for your invaluable scientific guidance, encouragement, precious motivation and support and endless inspiration. Thank you for the meals shared, for giving me the opportunity to visit your house and family and for letting me hear you singing (and what a singer you are!!)!! My doors in Portugal will always be wide open for you and your family!

Professor Lo Persson, my Swedish co-supervisor and splendid guide through science (and, without any doubt, the best golf player of Sweden!) for all your invaluable help, advices, fruitful scientific ideas, support, for always having time for a talk, as well as fun comments on daily life. I don't have words to express how much I am grateful for your unique encouragement and motivation, moral support when I was feeling frustrated, never ending enthusiasm and patience and for your invaluable scientific guidance. It has been an honour and a pleasure working with you! Thank you for your true friendship and for making possible some of my trips to conferences, especially to Japan (it was so fantastic and unforgettable), as well as for always taking care of everything regarding my accommodation in Lund! You and Mari-Ann will always be very welcome to visit us in Portugal whenever you want! We will be delightful to have you here!

Fundação para a Ciência e Tecnologia (FCT), for the PhD fellowship that supported and made this work possible.

Molecular Physical-Chemistry Research Unit, especially to *Prof. Dr. António Marinho Amorim da Costa* for receiving me in this research unit where I developed my work and for always being so kind and nice to me. I also would like to thank to *Dr. Luís Alberto de Carvalho* for his help and kindness, for teaching me how to work properly with the spectroscopic apparatus, and for all the nice moments shared in this research unit.

My colleagues at the *Molecular Physical-Chemistry Research Unit* for the good moments shared, as well as for the bad ones, and for making me see life in a different perspective. A very special thank to *Sónia Fiuza* and *Ana Margarida Amado* for all your incredible help and scientific guidance as work colleagues. Thank you so much for listening to me, for teaching me so many things about the synthesis and vibrational spectroscopy and for answering to all my questions no matter what! You are the best!

Ewa Dahlberg for all the expert technical assistance (without you, it would have been crazy in the lab!), fabulous company and advices and invaluable help inside and outside the lab. I will terribly miss our morning hugs and kisses, our funny moments in the cell culture room (in particular everytime we were singing "Ai se eu te pego"!), our dances and to always see you with a big and beautiful smile on your face! You were my shining sun in Lund and my favourite Swedish cook of all! I will always bring you in my heart! Jag kommer att sakna dig så mycket!

Helena Cirenajwis, my sweet little sister, for your never ending help, support, assistance, friendship and marvellous company in the lab. All our shared meals, namely cakes and pizzas, talks, confidences, trips to conferences, everything will last in my mind forever! You are a very special and unique friend and my home in Portugal will always have all the doors open to receive you whenever you want! I don't have any doubt that you will be a famous and brilliant scientist and that we will be friends for life! I'm so proud of you honey! I also would like to thank to Anna-Carin (my Swedish Mum) for taking care of me as a daughter, for always giving me so much food and for living with me all my problems and good things!!! My love for you and Helena will last forever because I see you as family!

My colleagues and friends at the *Biology Department*, namely *Erika Söderstjerna*, my dearest and enthusiastic partner, *Catja Freiburghaus*, my precious western blot master, *John*

Stegmayr, my dear office partner, *Xiaoli Huang*, my sweet Chinese friend, *Sara Andersson* for the amazing collaboration in one of the published papers, *Kristina Attoff* and all the others (*Kersti*, *Birgit*, *Martin* (may your soul rest in peace!), *Leif*, *Inger*, *Fredrik*, *Lisa*, *Olena*, *Marianne*, *Henrik*) for everything you taught me and for all the funny and unforgettable moments we shared. Your friendship, collaboration and encouragement were simply amazing and helped me a lot during these years!!! I do appreciate all the knowledge I have learned with you during our scientific and non-scientific discussions. Without you, the lab would have been much smaller in every sense. Thank you so much!!!! I will never forget you!

Ana Carolina Moreira, for just being you, for appearing in my life and making me incredibly happy! Our true friendship is the best and most beautiful thing that I am taking with me from the University of Coimbra. I want you in my life for all the eternity my sweetie! Thank you for your invaluable help, for always showing me that I am stronger than I think, for your outstanding support and for always being there for me no matter what! I will never forget all the incredible and beautiful moments we shared over the years, specially the basketball games and our funny study days at the Botanical Department!!!:) You are an amazing friend and a model to follow! I love you so much my beautiful Carol!!!

Sónia Fiuza, the sweetest person (and fantastic tea lover!) that I met during these years! Although we are not sharing an "old" friendship, it seems that I was waiting for such a friend like you for all my entire life! Thank you for all your kindness, for your love, support, never ending friendship, happiness, enthusiasm, for sharing the salsa classes with me, for always understand me, for all the advices, for the picnics, for the surprise parties and gifts, for simply being the best friend I could ever asked for! I want you to know that now we are strongly binding (emotionally) for the rest of our lives and there is nothing or anyone that could ever break this unique bond! I admire you so much darling!

My two wonderful and sweet best friends "*Mariana Martins*", for all your support, motivation, love and friendship during all these years! You are truly unique and strong friends and occupy a very special place in my heart! Thank you for being the way you are, don't ever change!!! I will always be here for you and I know for sure that our friendship will last forever!

Sandra Smiljanic, min kära vän for always being there for me, for helping me both at work and home, for going shopping with me (especially to Ullared!), for bringing to my life

your marvellous and unique family and for taking me as part of your family! I will never forget our trips to Jönköping, our vacation in Croatia and our nights at the cinema watching Twilight!!! Thank you for making this eternal friendship so beautiful and shinning! I love you and I will miss you all (especially *Bella*!) like crazy!!!

Ana Margarida Amado, for all your help, support, kindness and friendship during these years! For making our lunches so funny and nice with all the stories about Beatriz! It was a pleasure to meet and work with such a wonderful friend (and amazing scientist) for life!!!

All my friends that share with me the love for the Biochemistry, in special Carolina Moreira, Mariana Martins, Inês Santarino and Joana Serôdio (caloirinhas), Marisa Baptista, Sara Lemos, Ana Marisa Henriques and little David, Cláudia Pereira, Vera Francisco, João Costa and João Silva, *for the basketball*, particularly Silvia Andrade, Ana Gomes Costa and sweet Carolina, Inês Santarino, Joana Serôdio, Ana Coelho, Mariana Inácio, Catarina Soares, Manakes, Joana Arieiro, Rafaela Tomé and mister coach Fernando Guimarães and also *for the afrolatin dances*, in special my lovely Fiuzinha, sweet Irma and the greatest Paul Many! Thank you for being there for me, for your support, encouragement and true friendship! All of you are a big part of my life and the best friends ever!

My friends in Lund, especially my sweet and the best flatmate ever *Beatrice Zangrilli* (ti voglio tanto bene mia bella amica! Mi manchi tantissimo!), min flickvän *Therese Reber* (our trip to the Baltic countries, Valborg and our shared meals will stay in my life forever! I miss you min vackra vän!), Magnus, Sara, Cristiana, Maria, Miguel, Tiago, Sara, Natalia, Irem, Tripta, Shilpi, Clara and Massimo for making my time in Lund so much fun and unforgettable. My memories of Lund wouldn't be the same without you and I hope that our friendship will last forever! I will never forget you!

My beautiful, extraordinary and beloved family, the one that I love the most! I am so proud of all of you and it is such a pleasure to share my life with you all! Thank you for your never ending love, protection, support, help, laughs, for making me feel stronger and full of energy and for giving me lots of kisses and hugs every time I need you! You are the best family I could ever ask for and your huge love, motivation and support were my main strength that helped me to carry on with my PhD work, particularly during the time I was in

Sweden! I also want to thank to my sweet and dear nephew *Rafael* for making my days brighter and happier with his beautiful smile and funny expressions! I love you so much!!!:)

My fantastic, beautiful, exceptional and sweet mum and *dad* for your continuous love, protection, support, encouragement and for always believing and having faith in me. You are my pillar, the source of my being and I will be forever grateful for all the sacrifices that you've done for me over the years! I am here today because of you and so this thesis will be mainly dedicated to you! Thank you for raising me in such a loving and devoted way, making me the person I am today! I am so proud of both of you!!! You are the best parents in the whole world and I will love you forever and ever!

My fabulous brother Miguel, my Best friend and my idol, my hero, the person that knows me the best, for your never ending love, support, protection, incentive and encouragement, for just being the way you are! You have been in my life from the very first start and there is no other person that I admire and love more than you! Thank you for giving me the strength to carry on when I was feeling down, for making me laugh and extremely happy with your company and for understanding my feelings just by a simple look. You're an incredible and outstanding person and the greatest brother in the entire Universe! I'm very proud, lucky and grateful to have you in my life and my adoration and love for you has no end! I want you to know that I will always be by your side no matter what because my life has no sense without you! There is no love like ours! I also want to thank to *Andreia* for always being there for me and for your true friendship! You're a person with a big heart and I am very happy and lucky to have you in my life forever, my favourite and sweet sister-in-law! You are so adorable and loving! Adoro-te demais gigantinha!!!:)

Last but far from least, *Bruno Rodrigues, my soul mate!* Words cannot express what you mean to me and how my life has completely improved since we met! You are my life, my sweet, big, unique and greatest love, my heaven, my everything and your never endless love, support, protection, strength, inspiration and encouragement were absolutely crucial for my performance during all these years! Thank you so much for all your unbelievable help and contribute to this thesis, for your honesty, for trusting in me no matter what and for always having a simple smile, an adoring hug and a sweet kiss when I needed you the most! I would be completely lost without you in my life and I could never have finished this without you by my side! I promise you that from now on, there won't be no more "goodbyes" min kärlek! You are my paradise! Jag älskar dig för evigt!:)

Abstract

Worldwide, cancer is still one of the major leading causes of death. In particular, breast cancer is the one presenting the highest incidence rates in women. Therefore, new approaches for breast cancer treatment based on the development of promising anticancer agents that can efficiently improve patient survival are of utmost relevance.

In the present work, several modified biogenic polyamines and their newly synthesised Pt(II) and Pd(II) complexes were studied regarding their conformational behaviour by vibrational spectroscopy (infrared and Raman). Since Pt(II) and Pd(II) complexes have shown good anticancer activity, an accurate knowledge of the structural profile of these compounds is essential for understanding the molecular basis of their cytotoxic activity. The *all-trans* geometry was found to be favoured for all the alkylated polyamines, in their totally protonated state. In the other hand, their polynuclear complexes presented a stable geometry very similar to that previously obtained for the analogous chelates with spermidine and spermine, comprising two or three cisplatin-like ($MCl_2(NH_3)_2$) moieties.

The *in vitro* cytotoxic activity of these compounds was then evaluated in established human breast cancer cell lines (JIMT-1, L56Br-C1, MCF-7 and MDA-MB-231) and in one normal-like immortalised breast cell line (MCF-10A) as model systems. The MCF-10A cells were found to be least affected by the tested compounds, while significant growth inhibition and apoptotic cell death was observed for some of the cancer cell lines, L56Br-C1 being the most sensitive to this type of treatment.

Norspermidine (NSpd) and its Pd(II) complex were generally shown to have a stronger antiproliferative effect, as compared to its Pt(II) analogue. Also they were found to reduce the cellular activity of the growth-related enzyme ornithine decarboxylase to a lower level than the Pt(II) complex, in most of the cell lines examined. Moreover, treatment with NSpd or Pd-NSpd decreased colony formation, *i.e.* the malignancy of the breast cancer cells, to a much larger extent than the Pt(II) counterpart. None of these agents appeared to act as a genotoxin at a 25 μM concentration.

Regarding the spermine analogues, palladination of N^1,N^{11}-bis(ethyl)norspermine (BENSpm) led to enhanced cytotoxicity, in contrast to platination of N^1-cyclo-propylmethyl-N^{11}-ethylnorspermine (CPENSpm), that reduced cytotoxicity, which may be explained by differences in the cellular uptake of the chelates. BENSpm and Pd-BENSpm treatment reduced the putative cancer stem cell population $CD44^+CD24^-$ (evaluated by flow cytometry).

Furthermore, Pd-BENSpm was the most efficient compound of those investigated regarding induction of DNA damage and decrease in colony formation. Pt-CPENSpm and Pd-Spm, in the other hand, were shown to be the least toxic compounds of all tested. Pd-Spm efficiently reduced the cellular glutathione levels, which probably was a consequence of its metabolic inactivation by conjugation to this endogenous thiol.

Overall, the results show that the polynuclear Pd(II)-polyamine complexes display a stronger anticancer effect than their Pt(II) homologues, which renders them promising new metal-based therapeutic agents against breast cancer, coupling increased efficiency to a slightly lower toxicity.

Keywords: breast cancer; modified biogenic polyamines; Pt(II)/Pd(II) polynuclear complexes; anticancer agents; vibrational spectroscopy; cytotoxicity; cell cycle; apoptosis; DNA damage; stem cells; glutathione.

Resumo

O cancro continua a ser uma das principais causas de morte em todo o mundo. O cancro de mama, em particular, é um dos que apresenta a maior taxa de incidência em mulheres. Desta forma, novas abordagens para o tratamento do cancro de mama baseadas no desenvolvimento de compostos anticancerígenos promissores que permitam uma eficiente melhoria na sobrevivência do paciente, são de extrema importância.

No presente trabalho, várias poliaminas biogénicas modificadas e correspondentes complexos de platina (Pt(II)) e paládio (Pd(II)) foram estudados relativamente ao seu comportamento conformacional, através de espectroscopia vibracional (infravermelho e Raman). Uma vez que os complexos de Pt(II) e Pd(II) têm demonstrado uma boa actividade anticancerígena, um conhecimento rigoroso do perfil estrutural destes compostos é essencial para compreendermos a base molecular da sua atividade citotóxica. A geometria *all-trans* foi reconhecida como sendo a mais favorável para todas as poliaminas alquiladas, em condições totalmente protonadas. Po outro lado, os respetivos complexos polinucleares apresentaram uma geometria estável muito semelhante àquela previamente obtida para os quelatos análogos com espermidina e espermina, contendo duas ou três unidades análogas da cisplatina ($MCl_2(NH_3)_2$).

A atividade antineoplásica destes compostos *in vitro* foi avaliada em linhas celulares humanas de cancro de mama (JIMT-1, L56Br-C1, MCF-7 e MDA-MB-231), assim como numa linha imortalizada não-neoplásica (MCF-10A), como sistema modelo. As células MCF-10A mostraram ser menos afetadas pelos compostos testados, no entanto uma inibição significativa do crescimento e uma indução de morte celular (por apoptose) foram detetadas em algumas das linhas cancerígenas estudadas. As células L56Br-C1 foram as mais sensíveis a este tipo de tratamento.

A norespermidina (NSpd) e o seu complexo de Pd(II) apresentaram um efeito antiproliferativo mais forte relativamente ao análogo de Pt(II). Verificou-se ainda que estes compostos reduziam a atividade celular da enzima ornitina descarboxilase na maioria das linhas celulares analisadas, para doses inferiores relativamente às do complexo de Pt(II). Além disso, o tratamento com NSpd ou com Pd-NSpd diminuíram a formação de colónias, *i.e.* a malignidade das células de cancro de mama, com maior eficiência do que o homólogo de Pt(II). Nenhum destes compostos aparentou atuar como uma genotoxina (na concentração de 25 μM).

Relativamente aos análogos da espermina, a paladinação do N^1,N^{11}-bis(etil)norespermina (BENSpm) levou a um aumento da citotoxicidade, em contraste com a platinação do N^1-metilciclopropil-N^{11}-etilnorespermina (CPENSpm) que reduziu a citotoxicidade, o que pode ser explicado por diferenças na entrada celular dos dois quelatos. O BENSpm e o Pd-BENSpm apresentaram um efeito redutor face à população de células estaminais cancerígenas $CD44^+CD24^-$ (avaliada por citometria de fluxo). O Pd-BENSpm foi o composto mais eficiente de todos os investigados relativamente à indução de danos no ADN e redução na formação de colónias. O Pt-CPENSpm e o Pd-Spm, por sua vez, mostraram ser os compostos menos tóxicos de todos os testados. O Pd-Spm diminuiu eficientemente os níveis intracelulares de glutationa, o que provavelmente foi uma consequência da sua inativação metabólica por conjugação a este tiol endógeno.

Os resultados obtidos mostram que os complexos polinucleares de poliaminas com Pd(II) possuem uma atividade anticancerígena mais elevada do que os seus homólogos de Pt(II), podendo assim serem considerados promissores agentes terapêuticos inorgânicos contra o cancro de mama, acoplando uma maior eficiência a uma toxicidade mais reduzida.

Palavras-chave: cancro de mama; poliaminas biogénicas modificadas; complexos polinucleares de Pt(II)/Pd(II); agentes anticancerígenos; espectroscopia vibracional; citotoxicidade; ciclo celular; apoptose; danos no ADN; células estaminais; glutationa.

List of Publications

The majority of the work performed during this PhD research, which constitutes the present thesis, is already published (or submitted) in international scientific peer-reviewed journals of the field.

- T. M. Silva, S. Oredsson, L. Persson, P. M. Woster and M. P. M. Marques
  "Novel Pt(II) and Pd(II) Complexes with Polyamine Analogues: Synthesis and Vibrational Analysis"
  Journal of Inorganic Biochemistry, **108**: 1–7 (**2012**)
  DOI: 10.1016/j.jinorgbio.2011.11.021

- T. M. Silva, S. Andersson, S. K. Sukumaran, M. P. M. Marques, L. Persson and S. Oredsson.
  "Norspermidine and Novel Pd(II) and Pt(II) Polynuclear Complexes of Norspermidine as Potential Antineoplastic Agents Against Breast Cancer"
  PLoS One, **8**(2): e55651 (**2013**)
  DOI: 10.1371/journal.pone.0055651

- T. M. Silva, S. M. Fiuza, M. P. M. Marques, L. Persson and S. Oredsson
  "Increased Breast Cancer Cell Toxicity by Palladination of the Polyamine Analogue N^1,N^{11}–bis(ethyl)norspermine"
  Submitted to **Amino Acids** in July 2013

- T. M. Silva, S. M. Fiuza, P. M. Woster, S. Oredsson, L. Persson, M. P. M. Marques and A. M. Amado
  "Full Vibrational Assignment of Modified Polyamines"
  (Manuscript in preparation)

Index

I - Introduction

“Try not to become a man of success but rather to become a man of value.”

Albert Einstein

1. Introduction

1.1. Cancer

1.1.1. History of Cancer

The name cancer was first applied and described by the Greek physician Hippocrates (460–370 BC), also entitled the "Father of Medicine". This word was derived from "karkinos", the Greek word for crab, as cancer, with its irradiating blood vessels, can resemble a crab with its claws. At that time, Hippocrates assumed that one of the human fluids was black bile and that cancer developed by an excess of this fluid in any location of the human body, causing an inflammation and then cancer [1]. However, it was only in the 19th century that cancer was classified as a disease of cells [2]. Since then, this has been an extensively studied area of medicinal chemistry and pharmacology and the search for new approaches for the early detection and diagnosis of this severe pathology became imperative. In 1911, Carrel and Burrows established the technique of cell culture, widely used nowadays for the development of new anticancer agents [3].

1.1.2. Epidemiology and Definition of Cancer

Worldwide, cancer is one of the major leading causes of death. Actually, cancer is the second leading cause of death, being only exceeded by cardiovascular diseases [4]. An initial short term predictive study performed for the entire European Union estimated that in the year of 2012 approximately 717000 men and 566000 women would die of cancer [5]. Similarly, in the United States about 302000 men and 275500 women were also expected to die of cancer in 2012 [6], which represents an enormous burden on society (both sociologically and economically). In 2008, approximately 7.6 million of people died from cancer worldwide, which represents about 13% of all deaths. Estimations for the number of deaths in the whole world have been projected, with the data showing a big rise: approximately 13.1 million of people are expected to die of cancer in 2030 [7].

Cancer comprises a very complex and diverse class of disorders characterised by an uncontrolled growth of abnormal cells in the body. It can affect all parts of the human body and is usually classified according to the tissue from which the cancerous cells originate, as well as the normal cell type they resemble the most [8].

Tumours are formed in the body by abnormal growth and division of cells, forming a clump of cells that are not affected by surrounding normal cells. Tumours can be benign (non-cancerous and non-invasive) or malignant (cancerous and invasive) [8]. In the latter case, quickly growing cancerous cells have the ability to move throughout the body using the blood and lymph flows, leading to the invasion and destruction of healthy tissues in distant organs, in a process named metastasis.

Therefore, cancer can be defined as a malignant tumour originating from permanently growing cells. Unlike normal cells, cancer cells do not follow an orderly path of growth, division and death. Actually, they often cannot execute programmed cell death (apoptosis) and, instead, continue to grow and divide [9].

Extensive experimental evidence has shown that the biology of cancer is very complex and diverse, comprising over 100 distinct types determined, for instance, by their histology and hormone dependency. Tumour subtypes can be found within specific organs, and cancers from the same subtype can exhibit a great variability and heterogeneity [8,10].

1.1.3. Histological Classification of Cancer

Based on its histological type (type of tissue in which the cancer cell has its origin), cancer can be classified into seven distinct groups (one of the many possible histological cancer classifications) [11,12]:

- **Carcinoma:** tumour originating from epithelial cells. Since epithelial tissues are the most abundant in the body, carcinomas are responsible for approximately 80–90% of cancers, in organs such as breast, lung, pancreas, colon and prostate;

- **Sarcoma:** tumour originating from connective and supportive tissues (muscles, bones, cartilage and fat);

- **Myeloma:** tumour originating from plasma cells. These plasmocytes (generated in the bone marrow) are white blood cells responsible for antibody production;

- **Leukemia:** tumour originating from hematopoietic cells. This type of cancer mainly affects the bone marrow (where blood cells are produced) and often accumulates in the bloodstream. In these conditions, the bone marrow produces excessive immature

white blood cells that fail to perform their normal functions, often leading to an infection;

- **Lymphoma:** tumour originating from lymphatic cells. This type of cancer begins and develops in the nodes or glands of the lymphatic system and immune system tissues;

- **Central Nervous System Cancers:** tumour originating from the tissues of the brain and spinal cord.

1.1.4. Hallmarks of Cancer

Cancer development proceeds *via* a series of premalignant stages in which a succession of genetic alterations drives the progressive conversion of normal human cells into highly malignant cells [13]. Cancer cells have defects in regulatory circuits that control normal cell proliferation and homeostasis [14].

Earlier studies have shown that most, if not all, human cancers share six common main physiological cellular alterations, acquired during tumour development, that allow malignant growth and metastatic dissemination. These distinct and complementary acquired traits or capabilities include (Fig. 1) [2]:

- Sustained proliferative signalling – cancer cells can induce and sustain positively acting growth stimulatory signals;

- Evading growth suppressors – cancer cells evade processes that depend on the action of tumour suppressor genes to negatively regulate cell growth and proliferation;

- Activation of invasion and metastasis – ability of cancer epithelial cells (carcinoma cells) to invade surrounding tissue and blood vessels and disseminate in the human body giving rise to metastasis;

- Enabling replicative immortality – ability of cancer cells to indefinite proliferate without evidence of either senescence (irreversible entrance into a non-proliferative but viable status) or crisis/apoptosis;

- Induction of angiogenesis – during tumour progression, the tumour-associated neovasculature is stimulated — angiogenesis. This process allows the normally

quiescent vasculature to develop new vessels that support the expansion of the cancer growth and, therefore, has to be continuously activated;

- Resistance to cell death – cancer cells have a number of strategies that limit or evade programmed cell death (by apoptosis).

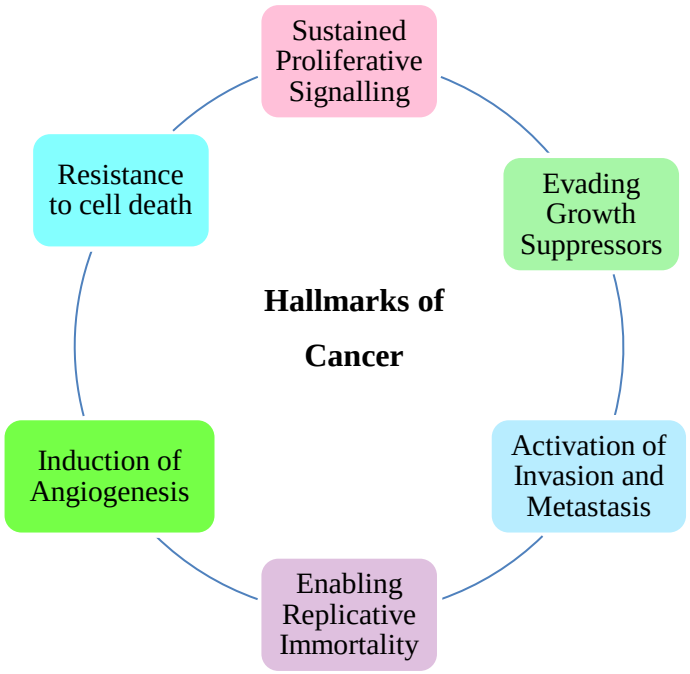

Figure 1: Schematic representation of the six hallmarks of cancer.

Acquisition of these six modifications is feasible by two so-called enabling or consequential characteristics of malignant tumours that contribute to the multistep carcinogenesis: the development of genomic instability and a consequent accumulation of mutations in cancer cells [2,9], and the development of inflammation in innate cells of the immune system. Both characteristics are recognised to promote tumour progression [2].

In the last decade, two additional and important traits of malignant cells that support tumour progression have been reported, although they are not yet fully validated. These two emerging hallmarks of cancer include: reprogramming the cellular energy metabolism (to allow continuous cell proliferation) and evading destruction by the immune system (mainly involving T and B lymphocytes, macrophages and natural killer cells) [2].

1.1.5. Cancer – A Genetic Disease

Cancer is usually considered a genetic disease, due to the involvement of dynamic changes in the genome that are responsible for its progression [9,14,15]. In cancer, the uncontrollable cell growth arises from the occurrence of errors/mutations in the cellular DNA, resulting in damages in the genes involved in cell division [16]. There are four critical types of genes responsible for the cell division process: oncogenes (stimulate cell proliferation), tumour suppressor genes (limit cell growth), suicide genes (control apoptosis and activate cell death if something goes wrong), and DNA repair genes (recognise and repair cellular DNA damage). Tumours can be produced by a change or combination of changes in any of these genes [17], being often linked to a genomic instability and variability along with the generation of multiple mutations [15].

1.2. Breast Cancer

1.2.1 Epidemiology

Although there has been a significant improvement in prognosis and survival, breast cancer is still one of the most widely malignant tumour forms among women [18,19]. Breast cancer can also occur in men, with an incidence approximately 100 times lower, but with a similar statistical survival rate [20,21].

A recent breast cancer research study performed by the Institute for Health Metrics and Evaluation and the University of Queensland (Australia) showed that globally, breast cancer incidence increased from approximately 641000 cases in 1980 to 1643000 cases in 2010. In 2010, roughly 425000 women died from breast cancer in developing countries, 68000 of these being within the age range 15 to 49 [22]. In the European Union, breast cancer is the major cause of female cancer death (representing 16% of all cancers), with about 88000 women having died from this disease in 2012 [5].

The incidence of breast cancer is normally higher in developed countries as compared to less developed ones, with more than half of the incident cases worldwide being diagnosed in Europe and North America [23]. This might be due to an enhanced life expectancy, an increase in obesity, a rise in alcohol consumption, the lack of physical exercise, delayed childbirth and less breast feeding, or later menopause in women [18,24]. However, most of breast cancer-related deaths occur in low and middle income countries, where the majority of

the patients are diagnosed in very late stages of the disease, essentially due to economical reasons, as well as to a lack of awareness of early signs and symptoms, and to the difficulty to get access to health care services [23].

1.2.2. Types of Breast Cancer

Breast cancer is any type of malignant growth in the breast tissue, mainly in the ducts (connecting the lobules to the nipples) and lobules (group of glands responsible for milk production). The ductal carcinomas comprise 85–90% of all cases and the lobular carcinomas comprise 8% of all cases. In addition, breast cancer can be either classified as *in situ* (cells are confined to the region where they originated) or invasive (cells have invaded the surrounding breast tissue including the lymph and blood systems) [21,25]. In invasive forms, cells from the primary tumour can travel through the lymph or blood vessels to any place in the human body, giving rise to a secondary cancer of the same type as the primary one. The majority of breast cancers are invasive (or infiltrating) and their therapy success is deeply influenced by the stage of the disease when diagnosed.

In order to choose the most suitable treatment, it is of utmost importance to identify the histology and stage of the tumour. Staging is the process of finding out how widespread a cancer is at the time of diagnosis. One of the most widely accepted classifications for staging breast cancer is the TNM stage classification [26,27], that is based on three essential characteristics: the size of the tumour (T), the lymph node involvement (N) and the distant tumour metastasis (M). However, currently, this classification has been revised and improved to allow a better determination of breast cancer prognosis [28,29].

Breast cancer development can be identified as hereditary. While 90–95% of breast cancer cases are considered spontaneous, the remaining 5–10% are hereditary because of inherited mutations, mainly in the well-known breast cancer genes BRCA1 and BRCA2. Mutations in these genes account for approximately 80% of all hereditary breast cancer [21,25,30].

1.2.3. Tumour Classification Based on Receptor Expression

Breast cancer treatment is initially governed by the expression status of the most widely studied markers in breast tissue: estrogen receptor (ER), progesterone receptor (PR)

and human epidermal growth factor receptor 2 (HER2) [31-33]. Breast cancers that are ER- and/or PR-positive are correlated with the most favourable prognosis, since expression of these markers usually results in response to hormonal therapy [32]. On the other hand, breast cancers that overexpress HER2, lack ER and PR expression or triple-negative breast cancers (ER-, PR- and HER2-negative) are associated with a less favourable prognosis and higher risk of death [31,32].

1.2.4. Tumour Classification Determined by Gene Expression Data

The genome broad expression patterns of tumours are suggested to represent their biology, with the multiplicity in patterns reflecting biological diversity. Thus, relating the gene expression profile to clinical outcomes is a crucial issue in understanding this diversity. The analysis of the gene expression patterns suggests a division of breast carcinomas into five distinct subgroups with different prognosis: luminal-like subtypes A (in general ER- and PR-positive) and B, HER2-overexpressing (ErbB2+), basal-like (usually triple negative) and normal-like [32-36]. These subtypes also differ markedly in prognosis and in the therapeutic targets they express. The difference in gene expression patterns among these groups is likely to represent distinct tumour phenotypes, thereby influencing response to treatment and overall survival. The basal-like tumour subclass, for instance, has been correlated with a more aggressive cancer outcome [37].

1.2.5. Treatment Options

Depending on the profile and development stage of breast cancer, several therapeutic strategies can be applied. The main options used nowadays in the clinic are:

- Local treatment:
  - **Surgery:** the most common treatment for breast cancer and, most of the times, it is the first one to be used. It consists in the removal of the tissue containing the cancer cells as well as of the surrounding tissue, in order to stop further spreading and to reduce the risk of cancer relapse.
  - **Radiotherapy:** uses carefully measured and controlled high-energy radiation (usually X-rays) to destroy the cancer cells or shrink the tumours, with the advantage of

affecting only the cells in the part of the body containing the cancer. It may be used after surgery to destroy breast cancer cells that remain in the chest area by damaging their DNA.

- Systemic treatment:

  - **Chemotherapy:** consists in the intravenous or oral administration of anticancer agents (either of natural origin or synthetic), with a view to kill or stop proliferation of cancer cells. It can be used before or after surgery. Combination of drugs with synergetic effects may also be applied (cocktails). This is a systemic treatment, as the whole organism is exposed to the drugs.

  - **Hormone therapy:** applied to hormone-dependent breast cancers that contain hormone receptors within the cells (ER- and/or PR-positive). The purpose is to block these receptors or to reduce hormone production in the body, thereby stopping or slowing the growth of cancer cells that require these natural hormones.

  - **Targeted therapy:** consists in the intravenous or oral administration of drugs or other substances (often named missile drugs), that target specific characteristics of the cancer cells, which are responsible for tumour growth by using specifically designed carrier and targeting agents (*e.g.* magic bullet [38]). This kind of strategy is designed to have a higher specificity and lower toxicity (*e.g.* less damage to normal cells) [39]. It can be applied, for instance, to women with a higher level of HER2 expression in the tumour [39,40].

In conclusion, breast cancer is a heterogeneous disease with distinct morphologies, metastatic behaviour and therapeutic response. Despite the availability of several different approaches for its treatment, the mortality rate is still too high in patients displaying metastases (metastatic breast cancer, which is triple negative). Therefore, the search for new options and the cytotoxicity evaluation of novel potential anticancer agents that can efficiently prevent, detect and treat breast cancer (particularly its metastatic forms) are major goals in breast cancer research.

1.2.6. Breast Cancer Stem Cells

Breast cancer cells in a tumour are not the same, *i.e.* different phenotypes can be found within the breast cancer cells that form the tumour.

Al-Hajj and co-workers [41] were the first to identify and prospectively discriminate a minority subpopulation of cells in a human solid breast cancer that had the total capacity of forming tumours *in vivo*, while the remaining bulk of cancer cells from the tumour could not [41-43]. This tumourigenic population had the ability to extensively proliferate, divide and maintain the same phenotype, but also to differentiate into all other phenotypes found in the tumour [44]. This population was recognised as cancer stem cells (CSCs) and was identified based on its cell surface phenotype: $CD44^{+}/CD24^{-/low/}$epithelial-specific antigen $(ESA)^{+}$ phenotype, which is most common in the breast cancer basal-like type (triple negative) [44-47]. Thus, the cellular heterogeneity of human breast cancer has been characterised based on the combined expression of two cell surface markers: CD44 and CD24. While CD44 expression was positively associated with stem cell-like properties, the CD24 expression was linked to differentiated epithelial characteristics [37].

The characteristic of the CSC is that it can divide and produce new CSCs and that it also can differentiate into all the other phenotypes found in the cancer [44,45]. The CSC model has been recognised as the promoter of tumour development and maintenance [44,47-49]. CSCs appear to survive conventional treatment and support tumour regrowth, while the bulk cells (that display other phenotypes) die, therefore leading to treatment failure [47]. For this reason, one of the major concerns in breast cancer research is to identify the minority population of CSCs and eradicate them from cancer patients, as they are the basis for treatment failure and tumour regrowth.

Human breast cancer cell lines contain these subpopulations with stem-like features [50]. Experimental evidence has shown that cells with a $CD44^{+}/CD24^{-}$ phenotype in breast cancer cell lines had an enhanced tumour formation ability *in vivo [46]*. Additionally, some studies showed that the $CD44^{+}/CD24^{-}$ phenotype population is linked to an increased expression of pro-invasive genes, as well as to the ability to form distant metastasis [51], therefore becoming a suitable candidate for breast cancer therapy.

In conclusion, targeting CSC is currently one of the most promising means to efficiently treat breast cancer. Therefore, the search for new anticancer agents that can efficiently affect or reduce the breast CSCs, thereby enhancing the effect of cancer treatment, is crucial.

1.3 Polyamines

1.3.1 Polyamines as Essential Molecules

The polyamine family has a very long history and its crucial role in a vast array of biochemical functions has been recognised over the years. In 1678, the Dutch tradesman and scientist Antonie Van Leeuwenhoek, also known as the "Father of Microbiology" and inventor of the microscope, became the pioneer in the research and discovery of the polyamines, when he isolated some "three-sided" crystals from human semen [52-55]. Much later, these crystals were correctly identified as spermine phosphate by Ladenburg and Abel. Spermidine was discovered, in tissue, almost forty years later. Putrescine was isolated from tissues after bacterial decomposition and it is largely responsible for the foul odour of putrefying flesh [52,53,55,56]. The polyamines putrescine, spermidine and spermine (Fig. 2) are ubiquitous substances virtually present in significant amounts in most prokaryotic and all eukaryotic cells [54,57,58]. They are low molecular weight and flexible multivalent polycations, with spatially distributed charges. At physiological pH, these molecules are positively charged, fully protonated at their primary and secondary amino groups [53,55,57]. Therefore, at physiological pH, putrescine has two, spermidine three and spermine four positive charges. Due to their cationic nature, polyamines interact electrostatically with negatively charged molecules, such as nucleic acids, proteins and phospholipids [53]. Cells depend on polyamines for growth and they can produce them internally or obtain them from exogenous sources (*e.g.* food or intestinal bacteria) [56,57,59]. Exogenously acquired polyamines enter cells by active energy requiring uptake across the plasma membrane. Once inside the cells, they will probably be distributed to all cellular compartments, due to their high solubility [60].

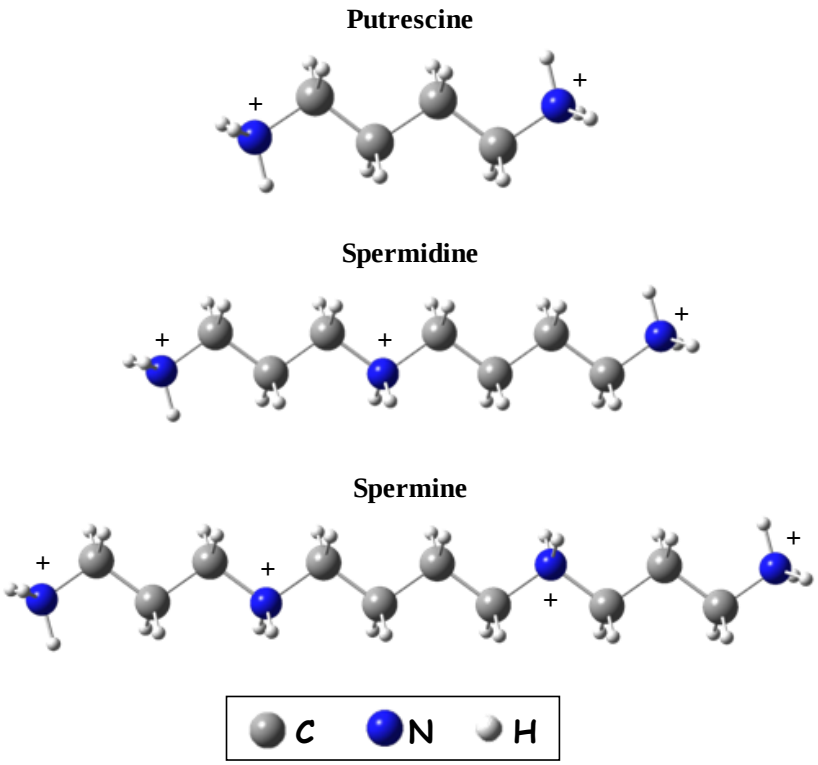

Figure 2: Structural representation of the biogenic polyamines putrescine, spermidine and spermine under physiological conditions.

1.3.2 Polyamine Function and Homeostasis

The polyamines are critical for a variety of fundamental cellular processes like proliferation, differentiation and apoptosis [53,61-64]. The effects on these processes are presumably caused by various specific molecular interactions such as involvement in:

- DNA replication and repair [65]
- DNA conformation by allowing the transition of the conformation B-DNA to Z-DNA [53,60,66]
- DNA condensation by neutralising the negative charges on the phosphate backbone [65,66]
- RNA synthesis and processing [63,65]
- Gene transcription and translation [53,55,62]

- Protein synthesis [55,63,65]
- Stabilisation of membranes and cytoskeletal structures [63,67];
- Cellular protection by binding cations like Cu and Fe and thus acting as strong metal chelators [60]
- Modulation of the membrane polarity and rigidity by forming complexes with phospholipids and proteins [53,60]
- Lipid peroxidation prevention, by acting as antioxidants [53,60]
- Regulation of ion channels [63,68]

It has been reported that polyamine function depends on their electrical charge, with their binding energy increasing from putrescine to spermine. Spermine appears to be the most active biogenic polyamine in several biological processes, whereas putrescine was found to be the least active one [69,70]. This can be explained because spermine is displaying the greatest charge, is the longest polyamine and has the highest flexibility [53].

The polyamine levels are elevated in proliferating cells and low in non-proliferating cells. In eukaryotes, due to the crucial roles of the polyamines in essential cellular functions, there is a strict regulatory control of the intracellular polyamine levels by multiple mechanisms involving biosynthesis, catabolism, uptake and excretion [63,64,71,72]. These mechanisms are then required for normal cellular polyamine homeostasis. Both polyamine uptake and biosynthesis are increased during cellular responses to proliferative stimuli. Conversely, polyamine degradation and excretion are induced upon a rise in the polyamine content, along with the inhibition of polyamine biosynthesis and uptake [73]. The polyamine pool is limited, at the lower limit, by its importance for cellular proliferation and at the upper limit by its cytotoxicity, which may induce cell death [53,71].

1.3.3 Polyamine Metabolism

The complete polyamine metabolism involves seven enzyme-catalysed reactions (Fig. 3) that keep the intracellular polyamine content in agreement with the cellular requirements [55].

In mammalian cells, the first step of the polyamine biosynthetic pathway consists of the conversion of arginine to ornithine through the action of arginase. Ornithine is available for polyamine production not only by the action of arginase within the cells, but can also be obtained from the circulating plasma [55,64]. Thereafter, ornithine is decarboxylated by the rate-limiting enzyme ornithine decarboxylase (ODC) to produce putrescine. Then, two aminopropyl groups, provided by decarboxylated *S*-adenosylmethionine (dcAdoMet), are successively added to putrescine to form spermidine and to spermidine to form spermine. Putrescine is converted to spermidine by the aminopropyltransferase spermidine synthase, while spermidine is converted to spermine by a second closely related but distinct aminopropyltransferase, spermine synthase. Both the aminopropyltransferases are stable and constitutively expressed [53]. The aminopropyl moiety is derived originally from the amino acid methionine, which together with ATP forms *S*-adenosylmethionine (AdoMet) in a reaction catalysed by methionine adenosyltransferase. AdoMet is then decarboxylated by *S*-adenosylmethionine decarboxylase (AdoMetDC), resulting in dcAdoMet, the aminopropyl donor [53,64,68,72,74,75]. The by-product formed after the spermidine and spermine synthase reactions is 5′-methylthioadenosine, which is recycled back to adenosine for further use by a phosphorylase [64,76].

Although the reactions involving the aminopropyltransferases are essentially irreversible, spermidine and spermine can be recycled into putrescine and spermidine, respectively, through a reverse metabolic pathway [64,70]. The first step of the interconversion pathway consists of the acetylation of the primary nitrogen of the aminopropyl group of spermine and spermidine into N^1-acetylspermine or N^1-acetylspermidine, respectively, catalysed by the rate-limiting enzyme spermidine/spermine N^1-acetyltransferase (SSAT). The acetyl group is provided by acetyl-CoA. Then, the resultant acetyl derivatives N^1-acetylspermine and N^1-acetylspermidine can be either excreted from the cells or oxidised by the flavin adenine dinucleotide-dependent acetylpolyamine oxidase (APAO) to form 3-acetamidopropanal (3-AAP) and hydrogen peroxide (H_2O_2), together with either spermidine and putrescine, respectively [53,70,72,74,75]. Nevertheless, spermine can be directly converted into spermidine, without the need for the acetylation step, through the action of the spermine oxidase (SMO). The oxidative products of SMO activity are spermidine, the reactive oxygen species H_2O_2 and 3-AAP [76,77].

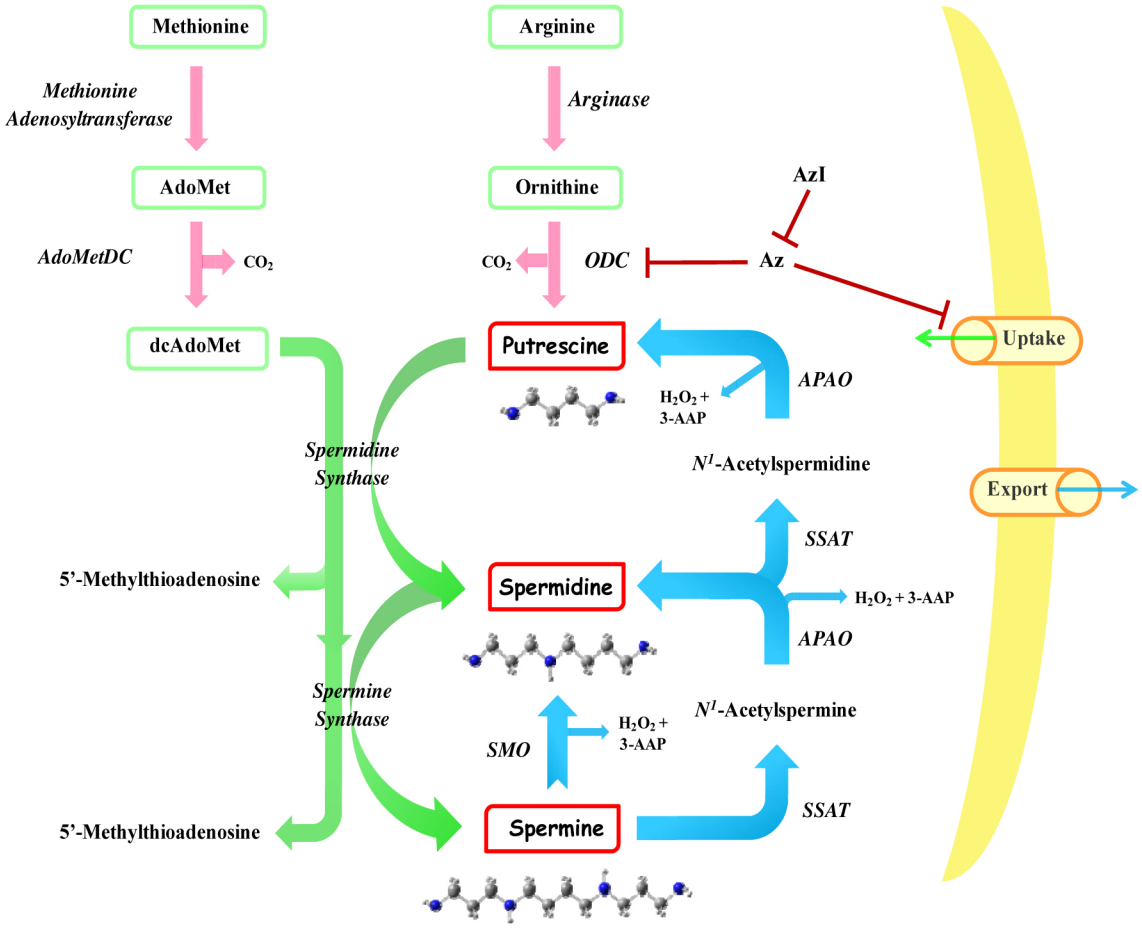

Figure 3: Schematic representation of the polyamine metabolic pathways.

It is important to highlight that polyamine levels are carefully controlled by the combination of three key enzymes: while biosynthesis is regulated by ODC and AdoMetDC, the catabolism is regulated by SSAT [74]. The activities of the biosynthetic enzymes are low in non-proliferating cells, but increase as the cells enter the cell cycle in response to various growth stimuli [78].

The major features of these rate-limiting enzymes are shown in Table 1.

Table 1: Main characteristics of the metabolic enzymes ODC, AdoMetDC and SSAT.

Enzymes	Important characteristics
ODC	▶ Mammalian ODC was first discovered in 1968 [55] ▶ Pyridoxal 5'-phosphate dependent enzyme [53,55,70] ▶ Cytosolic protein [75] ▶ Short half-life protein [53,55,70-72,75] ▶ Highly regulated in eukaryotic cells at transcriptional, translational and pos-translational levels [70,75,79,80] ▶ ODC activity induced by growth-promoting stimuli including hormones, growth factors, tissue regeneration and several drugs [79] ▶ ODC overexpression can cause cellular transformation [79] ▶ ODC degradation by the 26S proteosome is ubiquitin-independent [53,79] ▶ ODC feedback regulation by polyamines: down-regulation in the presence of polyamine excess [71,72] and up-regulation in the presence of low polyamine levels [53,72]
AdoMetDC	▶ Pyruvoyl-containing and dependent enzyme [72,74,75] ▶ Short half-life protein (but longer than that of ODC) [72,75] ▶ Activated by an autocatalytic serinolysis reaction that creates the pyruvoyl group [81] ▶ Well-regulated at transcriptional, translational and protein turnover levels [68,70,72,75] ▶ AdoMetDC activity stimulated by putrescine [75,81] ▶ Acts as a regulatory control point in AdoMet metabolism [55] ▶ AdoMetDC degradation requires polyubiquitination [68] ▶ AdoMetDC feedback regulation by polyamines: down-regulation in the presence of polyamine excess and up-regulation in the presence of low polyamine levels [72,75]

Table 1: Main characteristics of the metabolic enzymes ODC, AdoMetDC and SSAT. (Continuation)

SSAT	▶ Readily inducible enzyme that requires acetyl-CoA as a substrate [53,68,70,82] ▶ SSAT is a predominantly cytosolic protein, although recently it has been also found in the mitochondria [82] ▶ Short half-life [53,72,75,80,82,83] ▶ Present in very small amounts in the cell [83] ▶ Highly-regulated at several levels, including transcription, translation, mRNA processing and protein stabilisation [72,80,82] ▶ Induced by spermidine and spermine, but not by putrescine [53] ▶ Induced by polyamine analogues [53,72,80] and by a large variety of stimuli, such as hormones, toxins (H_2O_2), cytokines and growth factors [68,72,75,80,82,83] ▶ SSAT activity is induced in the presence of increased polyamine levels [75] ▶ Changes in SSAT levels have recently been linked to a variety of pathological stages, including carcinogenesis [82]

1.3.4. Polyamine Transport

De novo synthesis is the main source of polyamines in the majority of mammalian cells. However, in addition to the metabolic pathway, cellular polyamine transport mechanisms also largely contribute to the homeostatic regulation of the polyamine levels [70,72,84]. Therefore, the significant acquisition of exogenous polyamines from diet and the small contribution from the intestinal microbial flora to balance the intracellular polyamine content have to be taken into account [53,75,76,84,85].

The polyamine transport system (PTS) comprises the uptake and efflux of polyamines into and out of the cell and it is extremely important for the salvage of polyamines [68,72,75]. Although the molecular structure of the mammalian PTS still remains to be identified, evidence from yeast and bacteria suggest that most cell types exhibit two separate classes of PTS: one that is sodium dependent with a preference for putrescine (and probably other diamines) but also able to transport spermidine and spermine, and one that is sodium independent with a preference for spermidine and spermine, but not putrescine. The PTS is

energy-, time-, temperature-, and concentration-dependent and saturable, suggesting it is a carrier-mediated transport [53,55,76,85]. However, this system is not highly specific and can be responsible for the transport of several different molecules, such as paraquat, antiproliferative agents such as methylglyoxal bis(guanylhydrazone) (MGBG), mepacrine and polyamine-based compounds, into the cell [68,86]. In general, and since the transporter is not specific for putrescine, spermidine or spermine, the affinity of the carrier increases for amines which have chain lengths resembling those of spermidine or spermine. It has also been shown that the primary nitrogen groups of the polyamines seem to be critical for uptake [87].

Recently, two different models for the mammalian PTS have been described: one through an endocytic-mediated pathway using cell surface heparin sulfate proteoglycans (polyamines bind to heparin sulfate and enter into the cell by endocytosis) and one through a membrane transporter that requires an electronegative membrane potential [72,85,86].

Polyamines can also be transported out of the cells by a polyamine efflux system, *e.g.* excretion of the products formed by the SSAT reaction steps in the catabolic pathway. N^1-acetylspermidine and putrescine are the major products readily excreted from cells. Besides being excreted, putrescine can also be degraded by diamine oxidase [53,68,72,86]. Excretion is a selective process and is regulated by the growth status of the cell, being activated when cell growth decreases and inhibited by initiation of cell growth (in response to a growth stimulus) [53].

The cellular polyamine content plays a key role in the regulation of the polyamine transporters by a feedback mechanism. Thus, when cells are depleted of polyamines, polyamine transport is up-regulated, whereas in the presence of a polyamine excess, the polyamine transporter is down-regulated [72,75].

In 1976, Canellakis and his co-workers [88] discovered a unique small protein inhibitor of ODC, which was induced upon addition of putrescine. They called this protein antizyme (Az), which later was shown to be widely distributed among eukaryotes [89]. Az is synthesised by a unique mechanism from two open reading frames via a polyamine-stimulated ribosomal translational frameshifting [72,79,84,90-92]. Az binds with high affinity to transient ODC monomer subunits forming Az-ODC heterodimers, and thereby preventing the formation of the enzymatically active ODC homodimer. In mammalian cells, this binding of Az to ODC forms the enzymatically inactive Az-ODC complex, which is degraded by the 26S proteosome [53,70,72,74,79,80,91-93]. The ODC degradation by the 26S proteosome occurs in an ATP-dependent but ubiquitin-independent manner [53,91].

Several lines of evidence have shown that Az, which is induced by increased intracellular polyamine levels, besides regulating the degradation of ODC, inhibits the cellular polyamine transport, although the exact mechanism is not known [68,74]. Expression of high levels of Az have been linked to growth inhibition by the decrease in ODC, as well as the occurrence of a marked down-regulation of polyamine uptake [68,75,93]. Therefore, Az is a key regulatory protein in polyamine homeostasis [62].

Mammalian cells also contain another protein very important for cellular polyamine homeostasis named antizyme inhibitor (AzI). This is a 49 kDa protein, originally purified from rat liver extracts by Hayashi and colleagues [94]. AzI is a protein with a short half-life and highly homologous to ODC [72,79,92,93]. Although a number of residues required for ODC activity are conserved in AzI, this is a distinct protein that lacks enzymatic activity [79,80,93]. AzI binds to Az with a higher affinity than ODC does. [79]. AzI acts as a positive regulator of the polyamine pathway by strongly binding to Az and thus rescuing the ODC subunits from interaction with Az, thereby preventing Az-mediated ODC degradation by the 26S proteosome [72,79,80,93]. AzI is also a rapidly degraded protein. Like ODC, the AzI degradation is mediated by the 26S proteosome but, in contrast to ODC, AzI is degraded in an ubiquitin-dependent manner [72,79,89,92]. Moreover, binding of Az actually stabilises AzI by preventing its ubiquitination [79].

Several lines of evidence indicate that AzI is also involved in cell proliferation and tumour progression. High levels of AzI have been correlated with increases in ODC protein, polyamine synthesis and cell proliferation [79,80,93]. It has been reported that AzI overexpression gives rise to increased polyamine content, therefore leading to increased cellular proliferation and transformation, while down-regulation results in reduced polyamine content and inhibition of cell proliferation [79,80,89]. Since AzI is known to stimulate cell proliferation, increased antizyme inhibitor levels may directly promote tumourigenesis [93].

1.3.5. Polyamines and Cancer

One of the most important goals in cancer research is to study and characterise the molecular basis of the uncontrolled proliferation of cancer cells. The association of increased polyamine levels with rapid cell proliferation is well established [95]. Deregulation of cellular polyamine levels is linked with diverse pathological conditions. It has been demonstrated that polyamines are able to affect numerous processes in carcinogenesis, with their synthesis

becoming a potential target for antitumour drugs [74,76,96]. Therefore, from a pharmacological point of view, the polyamine metabolism has been identified as a target for cancer chemotherapy and chemoprevention, mainly due to five major reasons [67,76,80]:

- Polyamines are necessary for cell proliferation;
- Polyamine levels are significantly increased in cancer cells and tissues;
- The ODC gene has been recognised as an oncogene and its activity is also increased in cancer cells;
- Inhibition of polyamine biosynthesis with consequent depletion of the intracellular polyamine pools may reduce or prevent cellular growth;
- Polyamine metabolism is essential for all cancers.

In addition, a strong correlation between the growth rate of cancer cells and their polyamine levels has been reported, in a way that human cancer cells require more polyamines than the equivalent normal cells. Increased polyamine content has also been found in the urine from a majority of patients with various types of cancer [76,96], which may be useful in the diagnosis of cancer and evaluation of the efficiency of chemotherapy. However, since not all cancer patients present an increased content of polyamines in their urine, new prognostic markers for cancer screening are required [57,96].

The potential cancer chemopreventive strategies include the inhibition of polyamine synthesis or induction of polyamine catabolism. Increased polyamine levels are correlated with increased rate of cell proliferation, decreased apoptosis and increased expression of genes affecting tumour invasion and metastasis. On the other hand, inhibition of polyamine levels is correlated with decreased cell proliferation, increased apoptosis and decreased expression of genes affecting tumour invasion and metastasis [57].

In breast cancer, a positive association between the polyamine content in the tumour and its recurrence has been recognised. In the same way, it has been shown that there is frequently a positive relationship between increased polyamine levels and poorer cancer prognosis [70].

Cancer, including breast cancer, is usually associated with an increase in biosynthesis, decrease in catabolism and rise in the uptake of exogenous polyamines. In order to obtain 100% inhibition of cancer cell proliferation *in vivo*, it is essential to affect all these steps in

polyamine homeostasis [97]. In this thesis, cell cultures were used to demonstrate the involvement of polyamines in the proliferation and development of breast cancer [96].

1.3.6. Polyamine Depletion

Polyamine homeostasis is often altered in cancer, with cancer cells exhibiting higher polyamine levels. Since the polyamine biosynthetic pathway has become a target for chemotherapeutic intervention, two approaches can be used to deplete the intracellular polyamine pools: the use of inhibitors of the biosynthetic enzymes or the use of synthetic polyamine analogues. Agents that cause changes in polyamine metabolism or function can become promising compounds in cancer treatment (including breast cancer), either alone or in combination with other agents [98].

1.3.6.1. Polyamine Biosynthesis Inhibitors

Induction of polyamine synthesis, usually leading to the accumulation of intracellular polyamine levels, plays a very important role in cancer biology, including breast cancer.

In terms of therapeutic intervention, most of the research has focused on the biosynthetic enzymes ODC and AdoMetDC, but especially on ODC [99]. Inhibition of these enzymes would be expected to decrease the polyamine levels. Since ODC activity was increased in cancer cells, this enzyme became a promising target for possible prevention of tumour growth [76]. In addition, higher levels of polyamines and ODC activity have been detected in human breast cancer cells, compared to normal and benign breast cells, therefore increasing the evidences that the polyamine pathway plays an essential role in breast cancer development [74]. ODC inhibitors have been shown to deplete putrescine and spermidine contents, while the spermine content is not affected [99-101]. However, although less is known about the role played in cancer of the other rate-limiting biosynthetic enzyme (AdoMetDC), this enzyme is also an evident target [76]. AdoMetDC inhibitors have been shown to deplete spermidine and spermine pools, but not the putrescine pool [99-101].

Over the last decades, there has been an intense research on the use of polyamine biosynthesis inhibitors to efficiently deplete the intracellular polyamine levels. Therefore, a number of single enzyme inhibitors were specifically designed and synthesised with the hope of finding a new and effective anticancer drug [53,76,99].

One of the first efficient and rationally designed inhibitors was α-difluoromethylornithine (DFMO) (Fig. 4). DFMO was synthesised by scientists at the Merrel Dow Research Institute [102]. It is an irreversible, suicide inhibitor of ODC [99,101,102]. DFMO binds to the active site of ODC and is enzymatically decarboxylated, which activates the inhibitor. Although initially this was thought to be a very promising agent, it was found to be poorly efficient as a single agent for inhibition of tumour growth and progression, thereby failing to cure cancer patients [70,101,103]. This selective ODC inhibition stopped proliferation in several cells lines, but it was not enough to inhibit tumour growth [100]. In phase II studies of several cancers (breast, colon and small-cell lung cancers), DFMO did not show antitumour activity and its addition to conventional therapy in solid tumours had no significant inhibitory effect in cancer progression [103,104]. This lack of efficiency can be explained by the availability of polyamines from the intestinal microbial flora and by the activation of an up-regulation in polyamine transport caused by biosynthesis inhibition, thereby allowing the uptake of exogenous polyamines (from bacteria as well as from the food) [99,101,102]. Therefore, compounds that prevent polyamine transport can increase the antiproliferative activity of DFMO. In addition, inhibition of ODC is maintained only with high doses of DFMO. DFMO uptake occurs slowly by facilitated diffusion, while its excretion from the body occurs rapidly [53].

Currently, DFMO is being evaluated and used as a chemopreventive agent in low non-toxic doses [102] against several types of cancer, including colorectal, prostate, non-melanoma, neuroblastoma and breast cancer [57,99,103,104]. Moreover, DFMO is highly efficient as an antiparasitic agent in the treatment of African sleeping sickness [99,100,103].

In an effort to overcome the disappointing results obtained with DFMO as a single agent in chemotherapeutic intervention, DFMO was combined with a number of other cytotoxic agents [70,101].

In conclusion, the results obtained with DFMO in cell culture clearly demonstrate that prevention of polyamine biosynthesis may be a possible strategy for inhibiting cancer cell proliferation. However, for this strategy to be effective also *in vivo* the following conditions need to be considered [101]:

→ Polyamine depletion may need to encompass all three polyamines;

→ Polyamine depletion may be hampered by compensatory mechanisms in polyamine biosynthesis.

→ Polyamine depletion may be hampered by a compensatory increase of polyamine uptake.

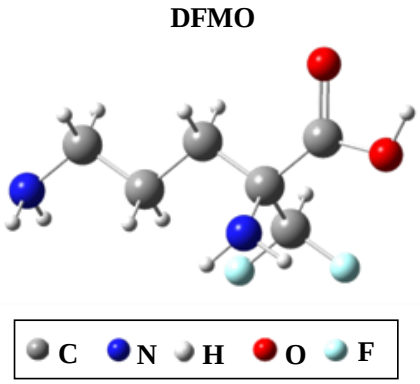

Figure 4: Structural representation of the polyamine biosynthetic inhibitor DFMO.

Other polyamine biosynthetic inhibitors that have been synthesised include the AdoMetDC inhibitors: 4-amidinoindan-1-one-2'-amidinohydrazone (CGP48664, also known as SAM486A) [78,99] and MGBG [66,99].

Taking all of this into account, it may be concluded that the polyamine pathway, with its crucial role in cell proliferation, is still a worthy target for the development of new antiproliferative agents [101].

1.3.6.2. Polyamine Analogues

In the cancer field, apart from the use of inhibitors of polyamine metabolism, new studies on the potential use of synthetic polyamine analogues to achieve more efficient polyamine depletion are of utmost relevance.

The first generation of polyamine analogues (symmetrically substituted analogues) as an alternative approach to interfere with the polyamine biosynthesis were first developed by Porter, Bergeron and colleagues in the 80's [101,105]. Since then, several groups have synthesised polyamine derivatives, the unsymmetrically substituted ones (second generation) having been developed by Dr. Woster's group [53,101]. A third generation of polyamine analogues was developed by the SLIL Biomedical Corporation and covers conformationally restricted analogues, cyclic analogues and oligoamine analogues [53,101].

Worldwide, several research groups and companies have synthesised and are currently synthesising different polyamine analogues. These analogues are compounds structurally

similar to the biogenic polyamines that negatively regulate ODC and AdoMetDC without, however, being able to functionally substitute the natural polyamines [53,101]. These analogues are efficiently taken up by the PTS and, once intracellular, they will accumulate to high concentrations in the cell. Consequently, increased cellular level of the polyamine analogues activates the feedback control, down-regulates biosynthesis and up-regulates catabolism of the natural polyamines [106,107]. Since the modified polyamines cannot functionally substitute for the biogenic ones, several different cellular processes are disrupted, leading to growth inhibition, and sometimes cell death (by apoptosis) is induced (Trojan horse effect) [101,107,108].

A large number of polyamine analogues are able to induce a total and rapid depletion of the three biogenic polyamines in the cells due to the combined homeostatic responses, which include induction of SSAT and PAO (catabolism activation), feedback inhibition of polyamine biosynthesis and activation of the export from the cell [75]. Polyamine analogues also compete for uptake with the natural polyamines [101]. These features, together with the relatively non-toxic response in normal tissues, have contributed to the use of polyamine analogues as single therapeutic agents.

Since rapidly proliferating cells (including cancer cells) have a higher requirement for polyamines than normal cells, agents that are effective in rapidly depleting cells of their polyamine pools can be used in cancer treatment [108]. In addition, polyamine analogues may be particularly attractive to use in cancers that are resistant to other forms of chemotherapeutic treatment.

According to their function, the analogues can be divided into two groups [53,106]:

- **Polyamine mimetic:** a polyamine analogue that enters into the cell and mimics the function of the biogenic polyamines, usually without causing depletion of the intracellular polyamine pools, but causing a reduction in cell growth.

- **Polyamine anti-metabolite:** a polyamine analogue that enters into the cell and depletes the intracellular polyamine pools by activation of polyamine catabolism and export (along with the biosynthetic down-regulation). This results in growth inhibition. These agents can be useful used as anticancer drugs.

The major polyamine analogues synthesised up to this date have been modified spermidine and spermine, by alkylation at specific sites. These analogues may be symmetrically- or unsymmetrically-alkylated derivatives of polyamines, varying in the length

of the intermediate carbon chains [101,103,106]. Some symmetrically substituted polyamine analogues include N^1,N^{11}-bis(ethyl)norspermine (BENSpm), N^1,N^8-bis(ethyl)spermidine (BES), N^1,N^{12}-bis(ethyl)spermine (BESpm) and N^1,N^{14}-bis(ethyl)homospermine (BEHSpm). Some unsymmetrically substituted polyamine analogues include N^1-cyclo-propylmethyl-N^{11}-ethylnorspermine (CPENSpm), N^1-ethyl-N^{11}-((cycloheptyl)methyl)-4,8-diazaundecane (CHENSpm) and N^1-ethyl-N^{11}- ((isopropyl)methyl)-4,8-diazaundecane (IPENSpm).

The polyamine analogues used in this study were BESpm, BENSpm, CPENSpm and norspermidine (NSpd) (Fig. 5) and their most important characteristics are described in Table 2.

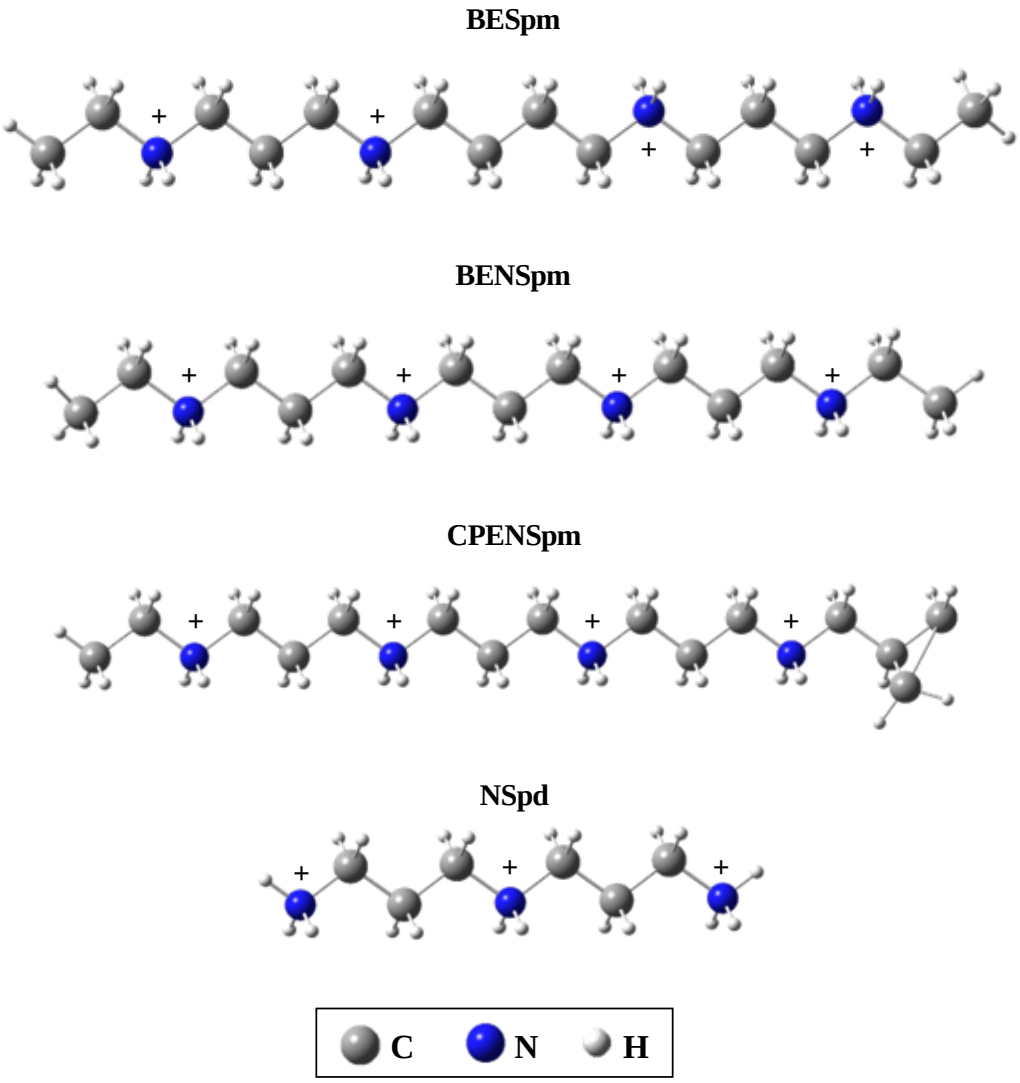

Figure 5: Structural representation of the polyamine analogues BESpm, BENSpm, CPENSpm and NSpd under physiological conditions.

Table 2: Main features of the polyamine analogues BES, BENSpm, CPENSpm and NSpd.

Polyamine analogues	Important features
BESpm	• Spermine analogue • First generation of polyamine analogues • Uses the PTS to be readily transported into mammalian cells [103] • Down-regulates ODC and AdoMetDC and induces SSAT [74,103,109,110] • Induces cell death by apoptosis in leukaemia, lung and melanoma cancer cell lines [103,111] • Significantly inhibits cell growth in breast cancer cell lines [110,111]
BENSpm	• Spermine analogue • First generation of polyamine analogues • Uses the PTS to be readily transported into mammalian cells [103] • Down-regulates ODC and AdoMetDC and super-induces SSAT [74,103,107,109,110] • Efficiently depletes the three intracellular polyamines in several breast cancer cell lines [107] • Growth inhibition and cytocidal effects in some cancer cell lines [74,112] • Induces cell death by apoptosis in breast, lung and melanoma cancer cell lines [107] • Effectively inhibits cell proliferation in breast cancer cell lines [107,112-114] • Antitumour activity in experimental models including breast, prostate, melanoma and lung cancer models and has undergone phase I and II clinical trials [103,110,114-116] • No significant therapeutic effects are shown in breast and lung cancer patients due to low efficacy in clinical activity → did not pass phase II clinical trials [101,103,114,117]

Table 2: Main features of the polyamine analogues BES, BENSpm, CPENSpm and NSpd. (Continuation)

CPENSpm	• Spermine analogue • Second generation of polyamine analogues • Down-regulates ODC and super-induces SSAT [74,109] • Effectively inhibits cell proliferation in breast cancer cell lines [107,112-114] • Induces cell death by apoptosis in breast, prostate and lung cancer cell lines [103,109] • Its cytotoxicity it is not exclusively dependent on SSAT induction [110] • Displays a cell type specific cytotoxicity [109,104]
NSpd	• Spermidine analogue • Naturally occurring triamine polyamine in some species of plants, bacteria and algae [118-120] • Antineoplastic activity against some types of tumours in mice [121]

Several polyamine analogues and polyamine pathway drugs are presently being tested in human cancer patients as potential new chemotherapeutic agents. These compounds are being evaluated individually, collectively and in combination with other anticancer drugs or traditional chemotherapeutics, since good results were achieved *in vitro*, namely in breast cancer cells [97,113,122].

In conclusion, the polyamine analogues are able to target more than one step in the polyamine biosynthetic pathway, therefore providing potentially better polyamine depletion than, for instance, single enzyme biosynthetic inhibitors. The use of particular analogues will then result in greater antiproliferative effects [101].

1.4. Cell cycle

1.4.1. Cell Cycle Phases

In eukaryotes, the cell cycle process is more complex than in prokaryotes, consisting of a highly ordered series of four coordinated and discrete phases (Fig. 6), in which the cell duplicates its components (growth phase) and then divides into two new cells (division phase). The four consecutive phases that constitute the cell cycle are [9,123-127]:

- **Gap 1 (G_1):** is the first phase of the cell cycle and is initiated after the mitosis phase is finished. During G_1 phase, the metabolically active and continuously growing cell prepares for DNA synthesis by synthesising the required RNA and proteins to make its DNA copies. Also in this phase, the cell integrates growth stimulatory and inhibitory signals and decides whether to proceed into the next phase, pause, or exit the cell cycle.

- **Synthesis (S):** corresponds to the interval between the two gap phases (G_1 and G_2, respectively). During S phase, DNA synthesis takes place, the DNA is replicated and two exact copies of the chromosome are formed (duplication of the genetic material).

- **Gap 2 (G_2):** is initiated after the S phase of the cell cycle is completed. During G_2 phase, cells continue to grow and prepare for the next phase (division) by synthesising the required proteins and structural components.

- **Mitosis (M):** corresponds to the interval between the two gap phases (G_2 and G_1, respectively). During M phase, cell division takes place, after chromosome segregation, separation and distribution of the duplicated chromosomes to the daughter cells. The two identical daughter cells contain equal amounts of the same genetic material as the original parental cell. M phase can be divided into four mitotic phases entitled prophase, metaphase, anaphase and telophase.

However, many eukaryotic cells do not undergo continuous division and, instead, they will mature or differentiate in order to execute specific functions in the organism [123]. These cells become quiescent (temporarily or permanently out of cell cycle) and no longer divide. Resting cells in this quiescent state are in another gap phase of the cell cycle entitled G_0. In this state, proteins and signalling molecules responsible for cell growth are down-regulated. In

order to re-enter the cell cycle into the G_1 phase and undergo further division into two daughter cells, cells can exit the quiescent state if stimulated by external growth signals (mitogenic stimulation) [74,124,125,127]. Actually there are some cells that remain in this quiescent state for their entire lifetime, thereby not experiencing cell division [125]. On the other hand, newborn cells can enter this phase to rest for a while before entering into a new the cell cycle [128].

Initially the cell cycle was only divided into two phases because these were the only two that could be distinguished in the microscope:

- **Interphase:** where nothing seemingly happened but increase in cell size → It includes the G_0, G_1, S and G_2 phases. Eukaryotic cells spend the majority of their lifetime in interphase.

- **Mitosis:** where the cell was observed to divide into two daughter cells → It comprises the M phase (cell nuclei division) followed by cytokinesis (cytoplasm division).

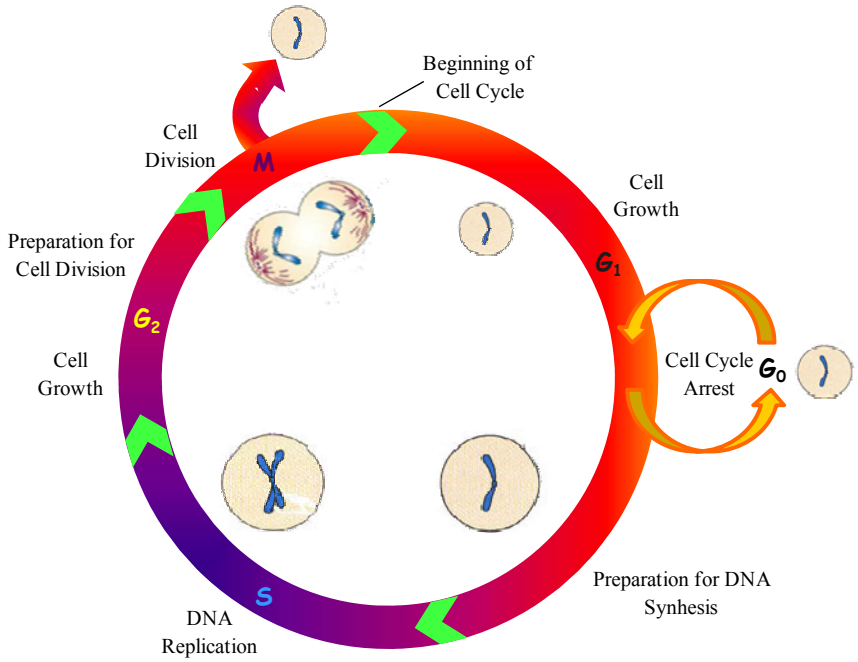

Figure 6: Schematic representation of the cell cycle in eukaryotic cells.

Usually, the time spent by the cells in each phase of the cell cycle differs considerably (especially for the G_0/G_1 phase), depending on the type of cells. However, a typical

eukaryotic cell (rapidly proliferating human cell) approximately divides every 24 h, with G_1, S, G_2 and M phases lasting around 11, 8, 4 and 1 h, respectively [123,125].

1.4.2. Checkpoint Controls in the Cell Cycle

Of the four cell cycle phases described, the two critical steps are DNA replication and cell division [127]. The regulation of the normal cell cycle must certify that the events in each phase are completed before proceeding into the next. The loss of control will lead to abnormal development and can cause causer.

Hence, the cell must pass through a series of checkpoints (known as restriction checkpoints) for checking the DNA integrity. These checkpoints controls are activated in response to DNA damage or other error signals in the cell and are placed in late G_1 and at the G_2/M interface, in order to prevent proliferation and development of mutated or damaged cells [124]. There are also checkpoint control mechanisms within mitosis to guarantee that conditions are favourable for cell division to be completed [125].

When DNA is damaged, the progression of the cell cycle through S phase may be slowed down or a cell cycle arrest may occur at checkpoints in G_1 or G_2. The arrest in G_1 may allow repairing the damaged DNA before the cell enters into the S phase, where the damaged DNA otherwise would be replicated [123]. In mammalian cells, the arrest in G_1 can be mediated by the action of the well-known protein p53. This protein is rapidly induced as a response to DNA damage [123]. However, in human cancer cells the p53 gene is often mutated, resulting in damaged DNA being replicated and transmitted to the daughter cells, instead of being repaired. This will cause instability of the cellular genome and allow cancer development [123]. Actually, it has been reported that defects in many genes coding for proteins that regulate the cell cycle have been implicated in human cancer [126]. Therefore, new researches over the mechanisms that regulate the cell cycle are of utmost importance.

1.4.3. Cyclins and Cyclin Dependent Kinases

The cell cycle is regulated and driven by different groups of proteins named cyclins and cyclin dependent kinases (CDKs), which control the major transitions occurring in the cell cycle of eukaryotic cells [126,129,130]. Cyclins are regulatory proteins sequentially synthesised and degraded in a cyclic way during the cell cycle progression [131]. CDKs are protein kinases constitutively expressed, that positively or negatively regulate the activity of

proteins essential for cell cycle progression by phosphorylation [9,129,130]. Specific cyclins can be found in each cell cycle phase, with cyclins D and E being found in G_1 phase, cyclin A in S and G_2 phases and cyclin B in the M phase [124,127,130,131]. As the cell cycle proceeds, cyclins can interact and bind to CDKs, forming active cyclin/CDK complexes, in which the cyclin is the regulatory unit and CDK is its catalytic partner [124]. Cyclin/CDK complexes phosphorylate specific protein substrates and are the force that drives the cells through the cycle with activation of DNA replication (in S phase), and formation of the structural components correlated with mitosis (in late G_2 and M phases) [124]. Nevertheless, the cell cycle system also comprises a group of other proteins that bind to the cyclin/CDK complexes and negatively regulate their activity (by inhibition). These are called CDK inhibitors (CDKIs) and are the inhibitory force of the cell cycle, since their binding gives rise to the inactivation of the cyclin/CDK complexes [129].

1.4.4. Polyamines and the Cell Cycle

The polyamines have been shown to be required for normal cell cycle progression, with their cellular levels being changed during cell cycle [129]. Polyamine levels are increased through polyamine biosynthesis, after the cell receives growth stimulatory signals [127]. Polyamine biosynthesis exhibits a bicyclical variation during the cell cycle and, when inhibited (for instance by the interference with a drug), cell cycle progression is delayed [98]. Polyamine biosynthesis inhibition may be followed by growth arrest and, sometimes, also apoptosis. However, this effect may be reversed by the addition of exogenous polyamines [129].

The cell cycle phase most sensitive to inhibition of polyamine biosynthesis is the S phase, with DNA replication being negatively affected when polyamine levels are reduced or not allowed to increase normally during cell growth. Nevertheless, some effects also occur later, namely in the G_1 phase (of the next cycle) and in the G_2/M phases transition [130]. Since in G_0 cells are not proliferating, cells in this phase contain lower polyamine levels than those in the other cell cycle phases.

Since polyamine biosynthesis is essential for normal cell cycle progression, the studies of the enzymes acting in the polyamine metabolic pathway (ODC and AdoMetDC) are crucial. Distinct changes in both enzyme activities and intracellular polyamine levels have been shown to take place during the cell cycle. It has been reported that ODC and AdoMetDC

activities have their peak levels at the G_1/S and S/G_2 transitions, while displaying reduced levels in quiescent cells [127,130] Thus, polyamine biosynthesis appears to be strongly activated during these two transitions. While elevated polyamine levels (due to increases in ODC and AdoMetDC activities) have a positive role and are necessary for DNA replication, reduced polyamine levels (*e.g.* due to the induction of SSAT) will affect DNA replication in a negative manner, possibly by decreasing the DNA elongation rate [70,132].

It has been shown that when cells in G_0/G_1 are seeded in the presence of agents preventing the increase in polyamine levels, the S phase of the first cell cycle is prolonged, while the other cell cycle phases are not affected. Thereafter, polyamine depletion can result in cell cycle arrest after one to several cell cycles, depending on the efficacy of polyamine depletion [127].

1.5. Metal-Based Anticancer Agents

One of the main causes for breast cancer treatment failure is related with the development of resistance to the anticancer agents used [14]. For this reason, the search for new treatment strategies is required, with an urgent need to develop improved chemotherapeutic compounds able to efficiently eradicate cancer cells while displaying minimal adverse effects [133].

In the last decades, there has been an intense research aiming at the design and development of new anticancer drugs, namely metal-based compounds, exhibiting highly suitable features for clinical practice [134]. Currently, the most studied ones include platinum (Pt(II)) and (Pt(IV)), palladium (Pd(II)), gold (Au(I)) and Au(III), ruthenium (Ru(II)) and Ru(III), bismuth (Bi(III)), rhenium (Re(I)), gallium (Ga(III)) and cooper (Cu(II))-based and Cu(II) agents [135,136].

1.5.1. Platinum-Based Compounds

1.5.1.1. Cisplatin

Cis-Diamminedichloroplatinum (II), ($Pt(NH_3)_2Cl_2$, cisplatin), is an inorganic neutral complex comprising one metal centre (Pt(II)) (Fig. 7). In 1845, in Turin, Michael Peyrone was the first to synthesise this compound, and its structure (square planar configuration) was deduced in Zurich, by Alfred Werner, forty-eight years later [137]. Werner also distinguished

between cisplatin's *cis* and *trans* isomers [138]. However, it was only in 1965 that Barnett Rosenberg, a biophysics and chemistry professor at the Michigan State University in USA, discovered, quite by chance, the anticancer properties of cisplatin [139]. While studying electrical currents using an *Escherichia coli* culture, Barnet and his colleagues observed that a specific Pt-containing compound inhibited bacterial binary fission (cell division) [139]. A group of compounds was tested and it was found that the *cis* form of the Pt(II)-diamminedichloro complex (cisplatin) was the most effective one. Its *trans* isomer was demonstrated to be ineffective as a chemotherapeutic agent [137].

In order to investigate the anticancer properties of cisplatin, Rosenberg and his group tested it *in vivo* (in 1969) [140]. They observed a total regression in the tumour mass in rats with sarcomas, thus proving that cisplatin was indeed a promising anticancer agent, namely for solid tumours [140]. Since then, several research groups extended cisplatin's testing to other types of tumours, confirming its potential as chemotherapeutic agent. In the end of 1978, cisplatin was approved by the Food and Drug Administration (FDA) for clinical use in the USA and became the first metal-based drug to be successfully used for cancer therapy [141-143].

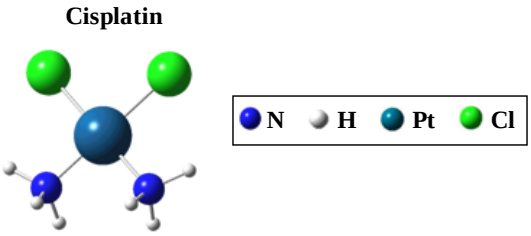

Figure 7: Schematic representation of cisplatin.

Cisplatin has a central role in cancer chemotherapy, its activity relying on particular and specific interactions with DNA, leading to induction of severe DNA damage and finally cell death (by apoptosis) [135]. This drug has been widely used as first line therapy for the treatment of several types of cancer, including lymphomas, testicular, ovarian, head and neck, bladder and a few types of lung cancers, due to its high cytotoxic efficiency [135,143-145]. However, the occurrence of severe side effects, specifically neuro- and nephrotoxicity (due to the interaction of activated cisplatin with critical renal and nervous system tissues), and the development of acquired resistance in most types of cancer, were found to be limiting factors for cisplatin's use in the clinic [137,144,146-149].

Tumour resistance to cisplatin can be either intrinsic or acquired (after exposure to the drug for some time) [137]. The cellular cisplatin resistance mechanisms include a diminished accumulation in the cells by a reduced uptake or increased efflux of the drug, cytoplasmic inactivation of the drug through binding of cisplatin to nucleophiles and cellular thiol-containing molecules (such as glutathione, methionine and metallothionein [150]), an increased ability of the cells to repair or tolerate the DNA damage caused by cisplatin, and a rise in the capacity of cancer cells to avoid cisplatin-induced cell death [137,143,149].

Additionally, since cisplatin therapy also affects normal cells by causing strong secondary effects, its use must be limited.

1.5.1.2. Mechanism of Action of Cisplatin

Cisplatin's mechanism of action has not yet been totally clarified, although it is widely accepted that it includes several specific steps.

For many years, the general conviction was that cisplatin and its analogues entered the cell by passive diffusion across the plasma membrane. However, in the last decades it has been reported that this agent can also enter the cell by active transport, *via* a specialised carrier-mediated mechanism. Recently, two transmembrane proteins involved in copper homeostasis (copper transporter 1 and 2, CTR1 and CTR2, respectively) were found to modulate the uptake of Pt(II)-based anticancer drugs, such as cisplatin [137,143,149,151].

After its entrance into the cells, the neutral cisplatin complex is activated by a series of spontaneous reactions with water, where its chloride ligands are successively substituted by one or two water molecules (*mono*- or *diaqua* species) at physiological pH, thus generating positively charged species that cannot readily leave the cell [143,150]. This cisplatin hydrolysis is due to a large decrease in the chloride concentration inside the cell (3–20 mM) as compared to the extracellular environment (100 mM), thereby favouring the aquation process [137,143,149]. The *monoaqua* platinum species are the most highly reactive ones and they are responsible for at least 98% of the platinum binding to DNA [137].

Thus, once inside the nucleus, and in contrast with classical alkylating agents, the complex interacts with DNA through coordination of the Pt(II) centre to the nitrogen atoms of the nucleotide bases (mostly N_7 of the purines adenine and guanine). This will lead to the formation of characteristic DNA adducts, preferentially through 1,2-intrastrand crosslinks, *via* two consecutive guanine bases (GpG) or with an adenine and a guanine (ApG) within the same DNA strand (corresponding to about 80% of the total DNA lesions) [137,143,150,151].

The formation of these bifunctional adducts causes the purines to become destacked and the DNA helix to bend and unwind [135]. Since it has been shown that transplatin is inefficient in eradicating cancer cells, due to the favoured formation of the hydroxo species (stable) instead the aqua (unstable) ones, the 1,2-intrastrand adducts (only formed between cisplatin and DNA) are critical for the anticancer activity of cisplatin.

Formation of cisplatin-DNA adducts will further affect normal DNA replication (by blocking the action of DNA polymerase) and transcription, as well as the DNA repair mechanisms. It will also be responsible for disruption of the native DNA conformation, which will be further recognised by cellular DNA binding proteins (high mobility group (HMG) proteins) that are known to recognise and repair DNA damage (*e.g.* drug-induced), by tightly binding to the Pt-complex [149]. It has been shown that the HMG domain proteins are important for the activity of cisplatin, since cells that lack the corresponding gene were shown to be less sensitive to treatment with this drug, as compared to those containing this gene [137,152]. In an attempt to repair the induced damage, cisplatin causes cell cycle arrest in the S and G_2 phases [143]. If damage due to cisplatin-DNA adducts cannot be efficiently repaired, the cells will eventually die by apoptosis [152]. Besides this strong interplay with DNA, cisplatin can also interact with RNA and sulphur-containing biomolecules in the cytoplasm (known to present a higher affinity for the soft Pt(II) centre than the purine nitrogens [137,148]), leading to drug deactivation and to an increased toxicity with severe side effects [137].

1.5.1.3. Platinum-Based Drugs Approved for Clinical Use

Cisplatin's approval for clinical use (by FDA and European Medicines Agency) along with the occurrence of severe side effects and development of resistance with cisplatin treatment, urged the pursuit for novel Pt-based agents able to bind to DNA and exhibiting improved anticancer properties (at lower doses), coupled with lower toxicity and lack or minimal acquired resistance [135]. Therefore, in order to overcome the adverse side effects of cisplatin and to enhance its clinical performance, several new cisplatin-based agents have been synthesised and tested. Currently, the Pt-based anticancer agents in clinical use worldwide are:

- **Cisplatin:** approved by FDA as Platinol in 1978. It is the leading and most common Pt(II)-based anticancer agent, used to treat a wide spectrum of human malignancies

[135,153,154]. In testicular germ cell cancer, cisplatin activity is exceptional, displaying a cure rate beyond 90% [144,155]. However, it also exhibits diverse drawbacks, including severe toxicity and development of resistance [151,156].

- **Carboplatin:** second-generation Pt(II) compound (*cis*-diammine (1,1-cyclobutanedicarboxylato)platinum (II)) (Fig. 8), that entered the US market as Paraplatin in 1989, initially for the treatment of advanced ovarian cancer. Carboplatin owes its lower toxicity to the ligand change, from diammine to the bidentate dicarboxylate moiety, which slows down the degradation of carboplatin into potentially toxic derivatives [135,144,151,155]. In addition, the slower hydrolysis rate of carboplatin is responsible for a longer plasma lifetime of the drug – retention time of about 30 h for carboplatin as compared to 1.5 to 3.6 h for cisplatin [157]. This agent yields the same type of DNA adducts as cisplatin and it is effective against the same type of cancers [135,144]. In comparison to cisplatin, the greatest benefit of carboplatin lies in its reduced side effects, particularly the eradication of nephrotoxic effects [135,145].

- **Oxaliplatin:** third generation compound and the third Pt(II) approved for standard chemotherapy use in 2002 ([(1*R*,2*R*)-cyclohexane-1,2-diamine](ethanedioato-*O*,*O'*)platinum(II)) (Fig. 8). It is active against many cisplatin and carboplatin resistant tumours, such as widespread colorectal cancer [144,145,151,157]. Oxaliplatin differs from cisplatin in that the two monodentate ammine groups are substituted by a bidentate 1,2-diaminocyclohexane stable ligand [135,151,157,158]. Oxaliplatin's cytotoxicity is mainly due to the formation of DNA lesions *via* intra- and interstand crosslinks [158]. As a single agent, oxaliplatin presentes a poor outcome with no curative properties in cisplatin resistant cancers. Thus, it is currently combined with other drugs, such as 5-fluorouracil and leucovorin (displaying a different mechanism of action), aiming at a synergetic effect, for the standard treatment of metastatic colorectal cancer [135,144,155,158]. Apart from its success in this type of cancer, oxaliplatin has also been used against gastroesophageal and pancreatic tumours [158]. It has shown enhanced activity and the lack of cross resistance, coupled to a decreased toxicity relative to the other Pt(II) agents, and is a promising treatment option in cancers where cisplatin and carboplatin therapies have failed [135,144].

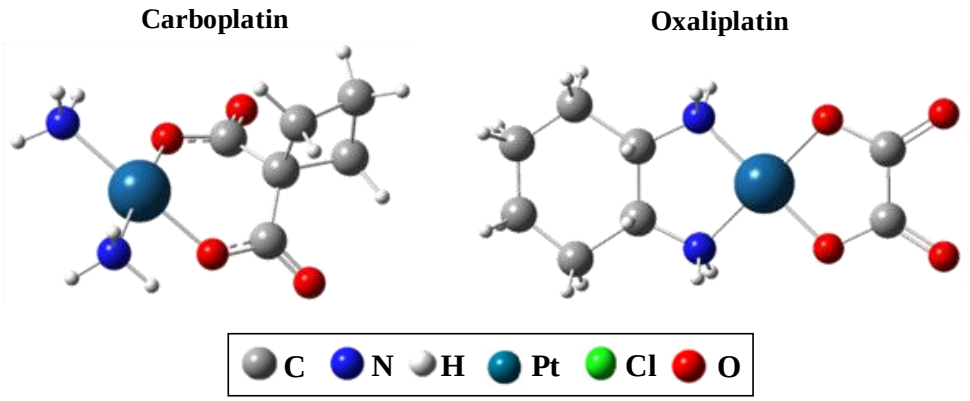

Figure 8: Schematic representation of carboplatin and oxaliplatin.

1.5.1.4. Platinum-Based Drugs in Advanced Clinical Trials

Apart from the Pt-based compounds presently under clinic use, there are other similar and promising agents that are currently being tested in advanced clinical trials. These include:

- Satraplatin: the first Pt(IV)-based chemotherapeutic drug that can be administered orally (in contrast to the Pt(II) compounds that are intravenously administered) [144,145,151,157]. It is an octahedral Pt(IV) complex (Fig. 9) and the most interesting candidate for treatment of advanced clinical stage (phase III) cancers, specially for hormone-refractory prostate cancer [136,151,153,157]. It displays an increased activity in cisplatin resistant cancers and a minimal *in vivo* toxicity (either nephro- or neurotoxicity) [144,153].

- Picoplatin: an orally administered Pt-based drug, particularly designed to overcome glutathione-mediated platinum resistance [135,157,159-161]. Picoplatin is a sterically hindered mononuclear Pt(II) agent (Fig. 9) undergoing phases I and II clinical trials. It has shown a high activity against cancer cell lines resistant to cisplatin, carboplatin and oxaliplatin, as well as in the treatment of patients with solid tumours [135,151,157].

- ProLindac: a novel diaminocyclohexane (DACH) Pt(II) prodrug (nanopolymer-oxaliplatin conjugate) presently being tested in phase II clinical trials in patients with solid tumours (mainly for recurrent ovarian cancer [135,151]). This therapeutic

polymer uses a safe, water soluble nanoparticulate system to specifically deliver Pt-DACH into tumours, concomitantly reducing drug concentrations in normal tissue. As a result, there is an increased drug effectiveness and a significant decrease in its deleterious side effects. ProLindac's activity has been shown to be either equal or higher than oxaliplatin's, coupled with a greater tolerability, mainly in low pH environments (solid tumours) [135,151,162].

- Lipoplatin: a novel liposomal cisplatin formulation, in which the Pt-based drug is encapsulated into liposome nanoparticles specially developed to reduce the drug's systemic toxicity [135,163-166]. This formulation aims at increasing tumour targeting and therapeutic activity, since this small molecule is able to circulate in the body for a longer time, accumulating mainly in primary tumour sites and metastatic tissues, thereby providing a selective delivery to the target [151,163,164]. Lipoplatin has shown significantly reduced neuro-, nephro- and ototoxicity relatively to other clinically used Pt-based drugs, and has been successfully administered in phases I, II and III clinical trials with greater or similar efficiency than cisplatin [135,163,167,168]. This agent has been mainly applied to non-small-cell lung cancer, but also to pancreatic, breast, and head and neck tumours [151,163,164].

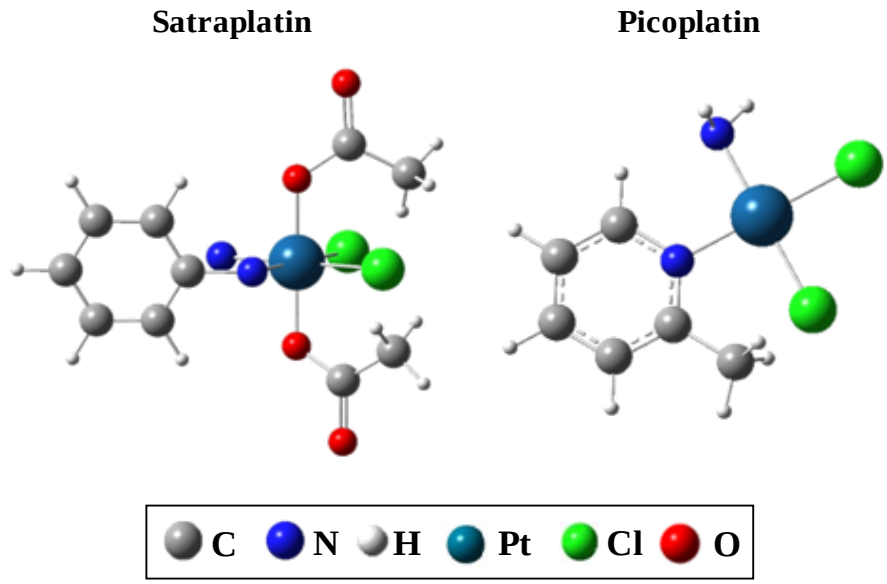

Figure 9: Schematic representation of satraplatin and picoplatin.

1.5.1.5. Polyamine-Bridged Polynuclear Complexes

The design and development of new Pt-based anticancer agents coordinated by biologically active molecules has been the target of an intense research in the last decades. In addition, mononuclear Pt complexes have been replaced by polynuclear complexes, comprising two or three metal centres [135], and Pt has been substituted by Pd with promising results [135,169-171].

There are three key pharmacological features influencing the clinical success of any type of Pt-based anticancer therapy. These include the drug's cellular uptake and efflux, the number and type of DNA adducts and the extent of metabolic drug deactivation [172,173].

The biogenic polyamines putrescine, spermidine and spermine have been used as suitable ligands for the design of new anticancer metal-based agents, since they yield stable and reasonably water soluble coordination compounds, with the advantage of a high conformational flexibility and an increased affinity for DNA [135,174-177]. In fact, linear alkylpolyamines have proved to be very suitable ligands for both Pt(II) and Pd(II) ions, yielding polynuclear chelates that will severely disrupt the DNA native conformation, through the formation of non-conventional interactions (long-range, interstrand) with the N_7 atom of the purine bases, allowing a cross linking of DNA nucleobases over a long distance [133,178-180].

Nicholas Farrell and his co-workers were the first to introduce (in 1988) a Pt(II) chelate comprising two metal centres coordinated to 1,4-diaminebutane [181], as a promising anticancer agent [182]. These complexes, displaying two or three metal centres and a polyamine bridging linker, constitute a unique class of potential anticancer agents active towards cisplatin resistant model systems [135,179,182,183]. Additionally, their cellular uptake is more efficient than that of the mononuclear analogues, and increases as the overall positive charge gets higher. Therefore, the cationic feature of these complexes may be directly associated with their cellular accumulation and DNA affinity [154]. The most promising multinuclear Pt complex synthesised by this group was the trinuclear Pt(II) compound BBR3464 (triplatinum BBR3464 – Triplatin, [{*trans*-$PtCl(NH_3)_2$}$_2$-*trans*-$Pt(NH_3)_2$ $\{NH_2(CH_2)_6NH_{22}](NO_3)_4$, Fig. 10), which has an overall positive charge of 4+ and has shown to induce a higher cytotoxic effect than conventional mononuclear Pt-based drugs, through an identical mechanism of action [135,179,180,183], leading to irreversible changes in the DNA conformation, from B to Z type [184,185]. It exhibited antitumour activity in cisplatin resistant tumour models with much lower therapeutic doses [179,184-186]. However, despite

having reached clinical phases I and II (mainly in ovarian and lung cancer, but also in melanoma and pancreatic cancers), it has gone no further due to poor response rates and severe toxicity (namely irreversible protein bonding in human plasma) [172,179].

In recent years, a cytotoxic trinuclear complex with three tetramineplatinum(II) moieties and an overall charge of 8+, TriplatinNC, has been investigated (Fig. 10). This is a "non-covalent" derivative of BBR3464, not capable of binding to DNA in a coordinative, conventional way [136,172]. Instead, TriplatinNC associates with the nucleic acid's double helix through hydrogen bonds and electrostatic interactions (phosphate clamp) [135,154,172,187]. TriplatinNC is the first Pt(II) anticancer complex that interacts with biomolecules solely in a non-coordinative fashion [154]. It accumulates in significant amounts in cancer cells, leading to a similar or higher toxicity compared to cisplatin [172].

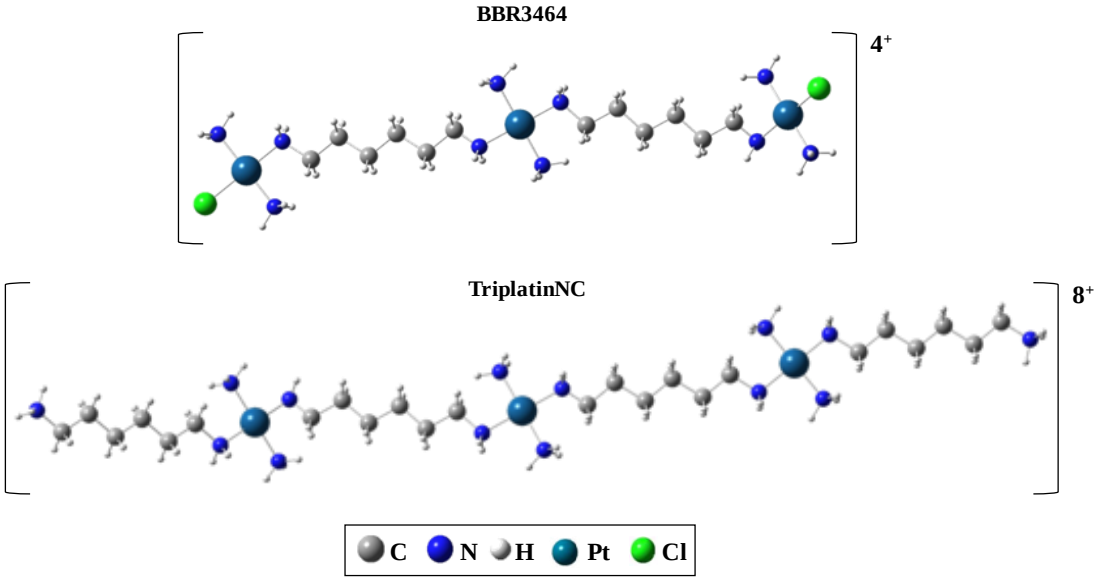

Figure 10: Schematic representation of BBR3464 and TriplatinNC.

In summary, Pt-based agents are widely used as chemotherapeutic compounds in today's oncological practice, based on their ability to enter the cell nucleus and covalently bind to DNA, yielding stable adducts [135,146-148,188]. The formation of several crosslinks in DNA leads to a conformational distortion of the DNA molecule. Thus, essential biological processes, such as DNA transcription and replication are inhibited and protein synthesis, as well as cell division, will also be affected [147,148]. In addition, since the discovery of BBR3464, novel polynuclear metal-based complexes containing biogenic or modified biogenic polyamines of variable chain length as ligands have been synthesised and tested as

promising anticancer agents, particularly Pt(II)- and Pd(II)-chelates [133,134,144,156,169-171,178,189-193].

1.5.2. Palladium-Based Agents

Pd(II) for Pt(II) substitution has been tried over the last few decades, with a view to increase the therapeutic spectrum of the complex and hence its activity profile, despite the initial belief that Pd(II) compounds were biologically inactive as anticancer agents due to the high lability of the Pd(II) centre [135]. The Pd(II) ion is chemically very similar to Pt(II), displaying an identical affinity for polyamine ligands, and hence binding strongly to DNA's purine and pyrimidine bases [135,194,195].

However, the higher lability of Pd(II) complexes (regarding both ligand exchange and ability to form *trans* isomers) relative to their Pt(II) analogues was found to be a major drawback in their use as chemotherapeutic agents. This is due to the lower stability of the drug-DNA adducts [135,196]. Additionally, the leaving groups in the Pd(II) complexes are more rapidly hydrolysed than their Pt(II) counterparts, yielding highly reactive species that will probably fail to reach their pharmaceutical target [135,195,196].

In order to overcome these initial limitations, a tailored design of improved Pd(II) anticancer agents was created. This involves particular conditions such as the binding of the metal to a strongly coordinated ligand to allow the stabilisation of the Pd-based complex (*e.g.* N-containing donor), coupled to a reasonably non-labile leaving group (*e.g.* nitrate) in order to ensure that the complex has time to reach and efficiently interact with its target [135,195]. This can be achieved through the use of specific bidentate ligands (such as polyamines), that are able to confer a higher stability to the complexes, hindering *cis→trans* isomerisation [192,196]. These ligands may not bind to DNA but instead interact with it *via* Van der Walls intermolecular interactions and hydrogen type close contacts. These complexes have been shown to yield non-directional and mainly intrastrand DNA adducts (both short and long range) and, similarly to their Pt(II) counterparts, the presence of more than one metal centre will cause a more severe and less reparable DNA damage, thereby enhancing their anticancer activity [135].

It has been shown that Pd(II) complexes are often more efficient than their analogous Pt(II) complexes. Some Pd(II) complexes have shown improved antitumour activity against different cancer cell lines, coupled to less deleterious side effects (such as nephrotoxicity) and

higher efficacy compared to cisplatin and also to their Pt(II) homologues [133,169,171,192,195]. Several promising results have also been obtained for the Pd(II) counterparts of the polyamines presently studied, specifically for a spermine dinuclear Pd(II) chelate [192]. Despite the good antiproliferative effects displayed by several Pd(II) complexes both *in vitro* and *in vivo*, none of these compounds has yet entered clinical practice [135].

In conclusion, Pd(II) and Pt(II) complexes were developed in order to overcome the limitations associated to the classical mononuclear Pt-drugs (such as cisplatin or carboplatin), aiming at attaining a higher efficiency, a reduced systemic toxicity, lack of cross resistance, enhanced specificity regarding DNA binding and, overall, improved pharmacological properties [144,153,156,169-171,190-193].

In this work, four Pd(II) or Pt(II)-based chelates containing modified polyamines as linkers were synthesised (Fig. 11).

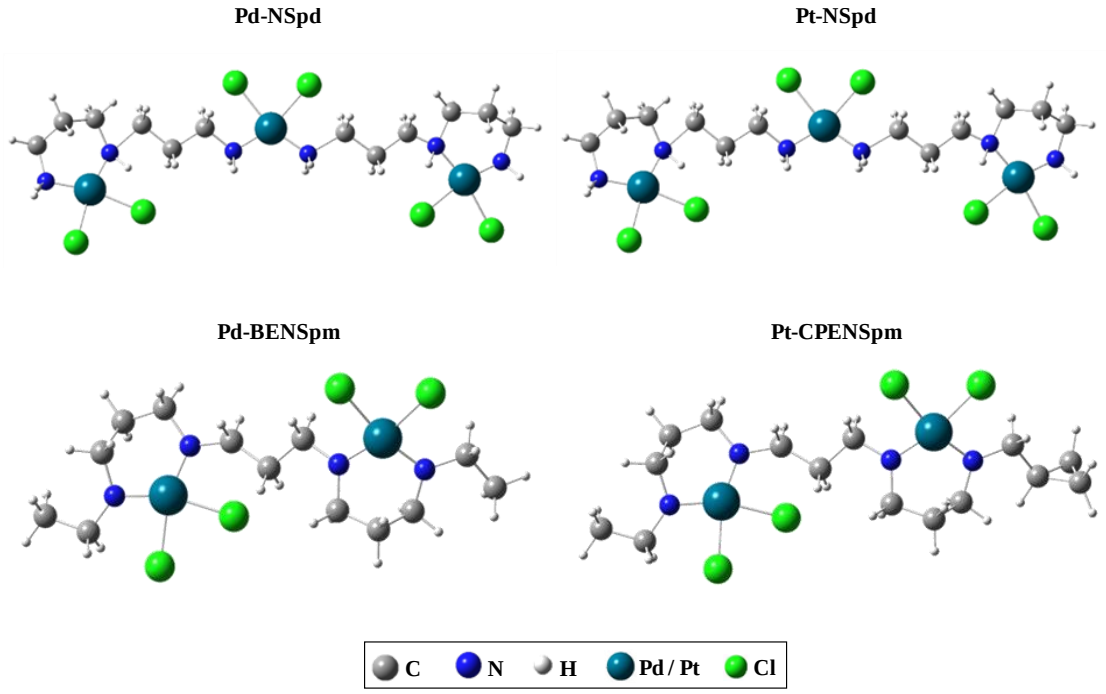

Figure 11: Structural representation of the Pd(II) and Pt(II) complexes Pd-NSpd**,** Pt-NSpd, Pd-BENSpm and Pt-CPENSpm.

1.6. Spectral Identification and Characterisation by Vibrational Spectroscopy

Spectroscopy can be defined as "the study of the interaction of radiation with matter". The name derives from the latin word *spectare* that means to observe, and it is one of the most important experimental techniques for determining the electronic structure of atoms and molecules and for obtaining information about the molecular structure and conformation of a sample, irrespective of its physical state [197].

In order to understand essential processes in life sciences, it is necessary to acquire a detailed knowledge underlying these biochemical mechanisms, namely an accurate structural information. Since the biological activity of an anticancer agent strongly depends on its structure and conformational preferences, along with its chemical characteristics, an accurate knowledge of these properties is essential for a better understanding of the biological behaviour of this type of therapeutic agents at the molecular level (Structure-Activity Relationships – SAR's) [135,170,190,198]. This can be obtained by a number of modern spectroscopic methods, such as vibrational spectroscopy [199].

Vibrational spectroscopy is one of the most powerful and useful physical techniques to study the molecular structure and conformational preferences of biologically relevant compounds [190,200-205]. Vibrational spectroscopy has been used to identify and characterise compounds by the study and analysis of its molecular vibrational modes, therefore providing important structural evidence within the molecule [206]. It is a fast technique that can be applied to solids, liquids, solutions, gases, films or adsorbed species, and offers the potential to explore molecular events under conditions closely related to the physiological environment. Depending on its geometry, conformation and electronic structure, each molecule yields distinctive vibrational spectra that can be measured with the help of different methods, such as infrared (IR), Raman or inelastic neutron scattering (INS) spectroscopies. From the measured vibrational data it is possible to draw conclusions about a compound's structure, since it can be used as a "fingerprint" of the molecule. Vibrational spectroscopy also provides essential information concerning the intramolecular and/or intermolecular interactions occurring within the system (namely in condensed phases), and the nature and strength of the chemical bonds [206].

All spectroscopic techniques work on the principle that, under certain conditions, materials can absorb, emit or diffuse energy, upon interaction with the incident radiation [197]. However, the diverse spectroscopic techniques refer to different and limited frequency

ranges within this broad spectrum, depending on the physical process underlying each specific technique. The total energy of a molecule includes the electronic, vibrational, rotational and translational levels. The energetic levels of a molecule can be obtained if we analyse the respective spectra in different regions of the electromagnetic radiation [207]. The electromagnetic spectrum covers all possible frequencies (Fig. 12), ranging from radio waves at low energy (capable of inducing nuclear spin transitions), up to X-rays at high energy (causing ionisation of the sample).

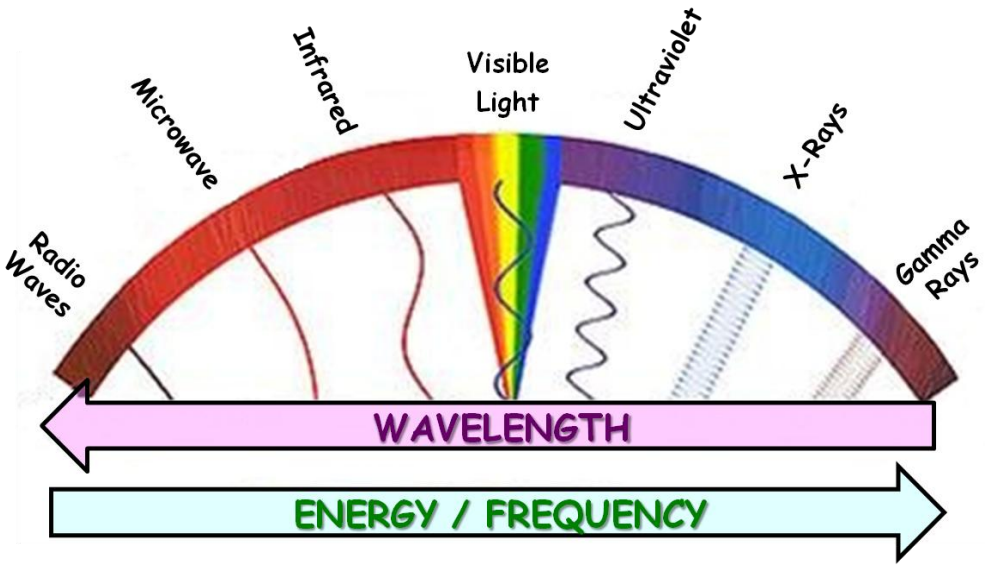

Figure 12: Electromagnetic radiation spectrum.

All electromagnetic waves contain inherent energy expressed and quantised by the Planck equation:

$$E = hv \tag{1.1}$$

where ***h*** is the Planck constant and ***v*** is the frequency of the electromagnetic wave [207,208].

The different possible vibrations within a molecule are called vibrational modes or vibrational degrees of freedom, and are determined by all the different ways the atoms in the molecule can move relative to each other (in the *x*, *y*, and *z* directions, corresponding to three independent degrees of freedom) [209]. Thus, for a molecule with *N* atomic nuclei, a linear molecule will present a total of 3N-5 vibrational degrees of freedom (or normal vibrational modes), while a non-linear one will display 3N-6 such modes. The vibrational degrees of freedom and, consequently, the number of molecular vibrations, are then a characteristic of a

particular compound and are exclusively determined by the number of atoms in the molecule [197,207,208,210].

The simplest model representing the concept of molecular vibrations is a diatomic molecule AB with masses m_A and m_B connected by a massless spring [208,210] (Fig. 13):

Figure 13: Schematic representation of a diatomic molecule AB.

The vibrational motion of this diatomic molecule can be approximated by the Hooke's law for a simple harmonic oscillator:

$$v = \frac{1}{2\pi}\sqrt{\frac{k}{\mu}} \quad , \quad \mu = \frac{mAmB}{(mA + mB)} \tag{1.2}$$

where ***k*** represents the force constant of the oscillator, ***ν*** is the vibrational frequency, ***μ*** is the reduced mass of the oscillator and ***m*** is the atomic mass of each atom [208].

The two major optical vibrational techniques available are the IR and Raman spectroscopies. These are complementary techniques that often give rise to similar spectra and aim at determining the chemical functional groups in the analysed sample, but are based on different physical mechanisms. Briefly, in IR spectroscopy, the molecules are exposed to a continuum radiation in the IR region and those photons that have energies corresponding to the frequencies of the normal modes can be absorbed to excite the respective vibrations. In Raman spectroscopy, in turn, the vibrational transitions are induced after an inelastic scattering of monochromatic light by the molecule, such that the frequency of the scattered light is shifted by the frequency of the molecular vibration, thereby providing information about the vibrational modes in the system [210]. Therefore, IR spectroscopy is a direct absorption process while Raman spectroscopy is a scattering process.

For a given compound, absorption- and scattering-induced vibrational transitions may display different vibrational band patterns in IR and Raman spectra, respectively, which is an additional source of information on the structural and conformational properties of the molecule [210]. Vibrations along a molecular bond (change in bond length) are called stretching modes (Fig. 14 (A)), while vibrations involving a variation in bond angles are

named deformation modes (Fig. 14 (B)). In addition, vibrations corresponding to a free rotation over a simple bound within the molecule, and that involve the variation of a dihedral angle (defined by four atoms) are called torsional modes. Vibrational modes can be further classified as symmetrical or antisymmetrical (depending on its symmetry), in-plane or out-of-plane and in-phase or out-of-phase (Fig. 14) [208].

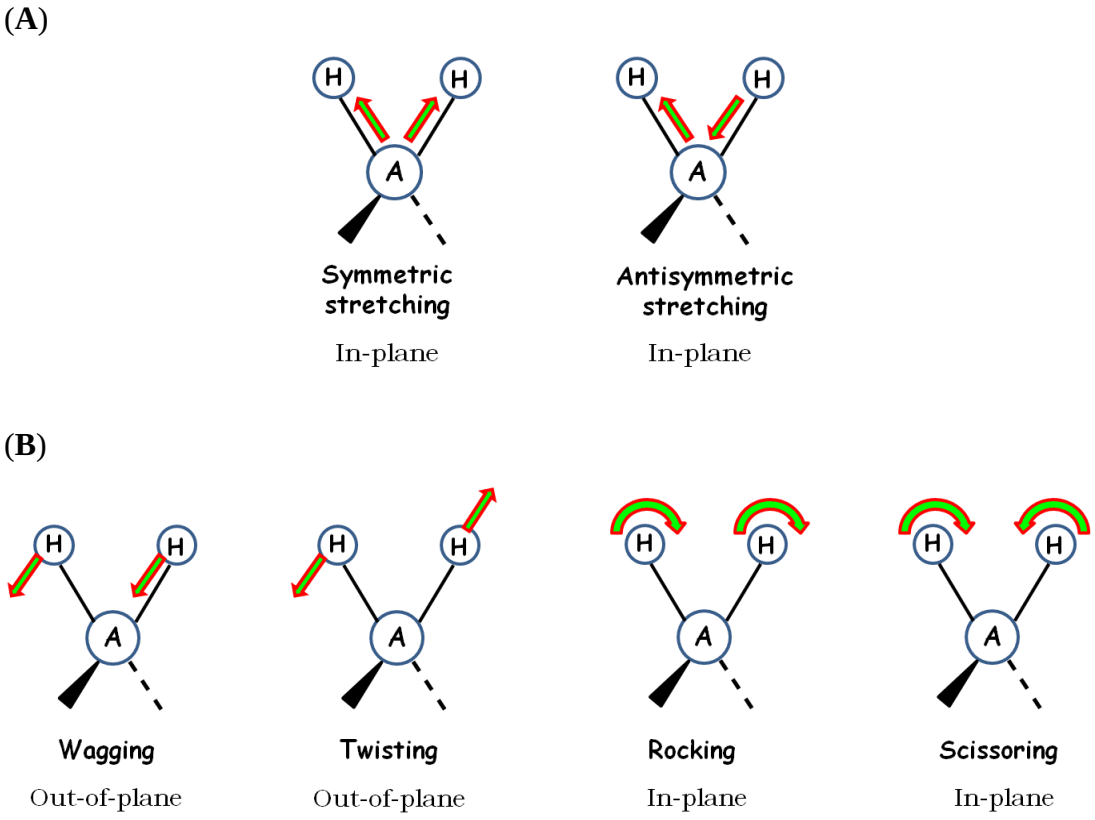

Figure 14: Schematic representation of stretching (**A**) and deformation (**B**) vibrational modes in a molecule (A represent heavy atoms).

Experimental vibrational bands can be ascribed by comparison with vibrational spectra of reference systems (spectroscopic databases). However, a consistent assignment of experimental vibrational spectra presently relies on quantum mechanical calculations, capable of predicting the vibrational pattern of a molecule with very high accuracy [199-201,204,205,211,212].

1.6.1. Infrared Spectroscopy

In 1800, Sir William Herschel, a famous astronomer and also a musician, discovered the IR light [213]. During his studies, Herschel hypothesised that colours themselves could

contain different levels of heat. In order to investigate this theory, he exposed a glass prism to the sunlight creating a "rainbow", and measured the temperature of each colour of the spectrum thus obtained. Three thermometers were used in the experiment and Herschel noticed that the temperature increased from violet to red, being even higher in the region beyond the red. This invisible radiation, currently known as IR radiation, was named by Herschel as "calorific rays". In later studies, Herschel also demonstrated that this radiation could be absorbed, transmitted, reflected or refracted similarly to the visible light. The discovery of IR radiation was of utmost importance in science, since this was the first time that a form of light invisible to the eye was identified. From then on, IR spectroscopy was developed and IR spectrometers were commercially available since the 1940's [213-215]. These can analyse a large range of samples (gases, liquids, and solids) and measure the frequency of IR radiation which is absorbed by the analysed sample [214,215]. An IR spectrometer comprises three basic components: radiation source, monochromator, and detector.

Not all molecular vibrations absorb IR radiation. A sample can only absorb when the frequency of the incoming IR beam matches the frequency of the fundamental modes of vibration of the molecule and also when there is a net change in dipole moment [215]. In general, when this occurs, the bond's stretching frequency causes absorption of the IR radiation and the substance is IR active. If a bond is symmetrically substituted and has a zero dipole moment, there will be no absorption of energy and its stretching mode will be absent from the IR spectrum – the substance is IR inactive. Smaller changes in the dipole moment will give rise to less intense IR bands and *vice-versa*. Therefore, symmetric molecules will have weaker IR active vibrations than antisymmetric compounds [214,215].

The IR spectrum can be divided into three main regions: *far-IR* (low energy, wavenumbers below *ca.* 400 cm^{-1}), *mid-IR* (400–4000 cm^{-1}) and *near-IR* (high energy, 4000–14000 cm^{-1}). In the present study, the *mid-IR* region was used to obtain information on the compounds under investigation, since their fundamental molecular vibrations are within this region [215,216]. The low frequency vibrational modes (*e.g.* skeletal vibrations) are characteristic of the *far-IR* region, while the *near-IR* interval comprises overtones and combination bands [213].

Over the last decades, many useful applications using infrared radiation in several fields of science have been reported [210,217-223] (Table 3). IR microscopy has been applied to analyse the vibrational spectra of the biochemical components of a cell [224]; *mid-IR* lasers

have been widely used in biology, chemistry and medicine since almost most of the molecules of importance to medicinal and clinical chemistry have unique spectra or 'fingerprints' in this specific region [216,225]. *Near-IR* spectroscopy and IR-imaging have been applied in cardiovascular radiology and brain imaging, as well as in cancer diagnosis and therapy [220,223,226]. In fact, Fourier-transform infrared spectroscopy (FTIR) has been shown to distinguish between normal and cancer cells, thus being an important tool for pathologists in clinical applications [227].

Table 3 displays the most important advantages and disadvantages of this technique.

Table 3: Main advantages and disadvantages of IR spectroscopy.

Infrared Spectroscopy	
Advantages	**Disadvantages**
❋ Simple sample preparation ❋ Highly sensitivity technique ❋ Allows the quantitative determination of compounds in mixtures	❋ Analysis of aqueous solutions can be difficult to obtain ❋ With certain IR techniques, the sample cannot be recovered ❋ Background solvent or solid matrix must be relatively transparent in the spectral region of interest

1.6.2. Raman Spectroscopy

In 1923, the Austrian quantum physicist Adolf Smekel theoretically predicted the inelastic scattering of light. However, it was not until 1928 that this phenomenon was successfully observed experimentally by the Indian scientist C. V. Raman, and was therefore named Raman effect [228].

There are two types of scattered light [208] (Fig. 15):

→ **Rayleigh scattering:** the primary scattering process is an elastic scattering event resulting in scattered light comprising the same vibrational or rotational energy and having the same frequency as the incident light, meaning that no energy transfer occurs between the incident and scattered lights at the sample with no frequency change observed. In Rayleigh scattering the incident photon is absorbed and the

molecule is instantaneously raised into a virtual state. The molecule soon relaxes again, emitting a photon with identical frequency and energy to that absorbed, but in a random direction.

→ **Raman scattering:** a small proportion of the light is scattered non-elastically and is thus associated to a change in frequency, meaning that an energy transfer occurs between the incident and scattered lights at the sample.

Rayleigh scattering is 10^3 times more intense than the Raman scattering process, which is typically a low sensitivity technique. Therefore, an intense and monochromatic source of light is usually employed – laser (light amplification by stimulated emission of radiation).

Raman spectroscopy is based on an inelastic scattering of monochromatic radiation and allows the observation of the vibrational modes in a system. It differs from IR spectroscopy mainly in that it is based on the scattering of photons by the sample, rather than on their absorption [210]. The energy difference between the incident and the scattered light corresponds to one or more normal vibrational modes.

A simple Raman spectrometer usually consists of four major components: a monochromatic excitation source, a sample illumination system (presently a laser) and light collection optics, a wavelength selector (spectrophotometer) and a detector. Briefly, after irradiating the sample with an intense light source at a specific wavelength (usually in the visible, near-IR or near-ultraviolet), the scattered light is collected and sent to a monochromator, and finally detected in a photomultiplier tube or a charge coupled device (CCD).

There are two types of Raman scattering [229] (Fig. 15):

- If the final vibrational state of the molecule is more energetic than the initial one, the emitted photon will transfer energy to the sample and will be shifted to a lower frequency relative to the incident light (in order to maintain the total energy of the system). In this case, the photon raises the molecule from the ground to a virtual state and then it drop backs down to a higher energy vibrational state. Therefore, the scattered photon has less energy and a longer wavelength than the incident photon. → **Stokes Raman scattering**.

- If the final vibrational state is less energetic than the initial state, then the emitted photon will catch energy from the sample and will be shifted to a higher frequency. In this case, the molecule is in a vibrational excited state to begin with and, after being scattered into a virtual state, the molecule returns to its ground state (lower energy level). Here, the scattered photon has more energy and a shorter wavelength than the incident photon → **Anti-Stokes Raman scattering**.

The Stokes and anti-Stokes vibrational pattern are thus the mirror image of each other (Fig. 16). Most Raman studies rely on the analysis of the Stokes lines because they are significantly more intense than the anti-Stokes ones [229].

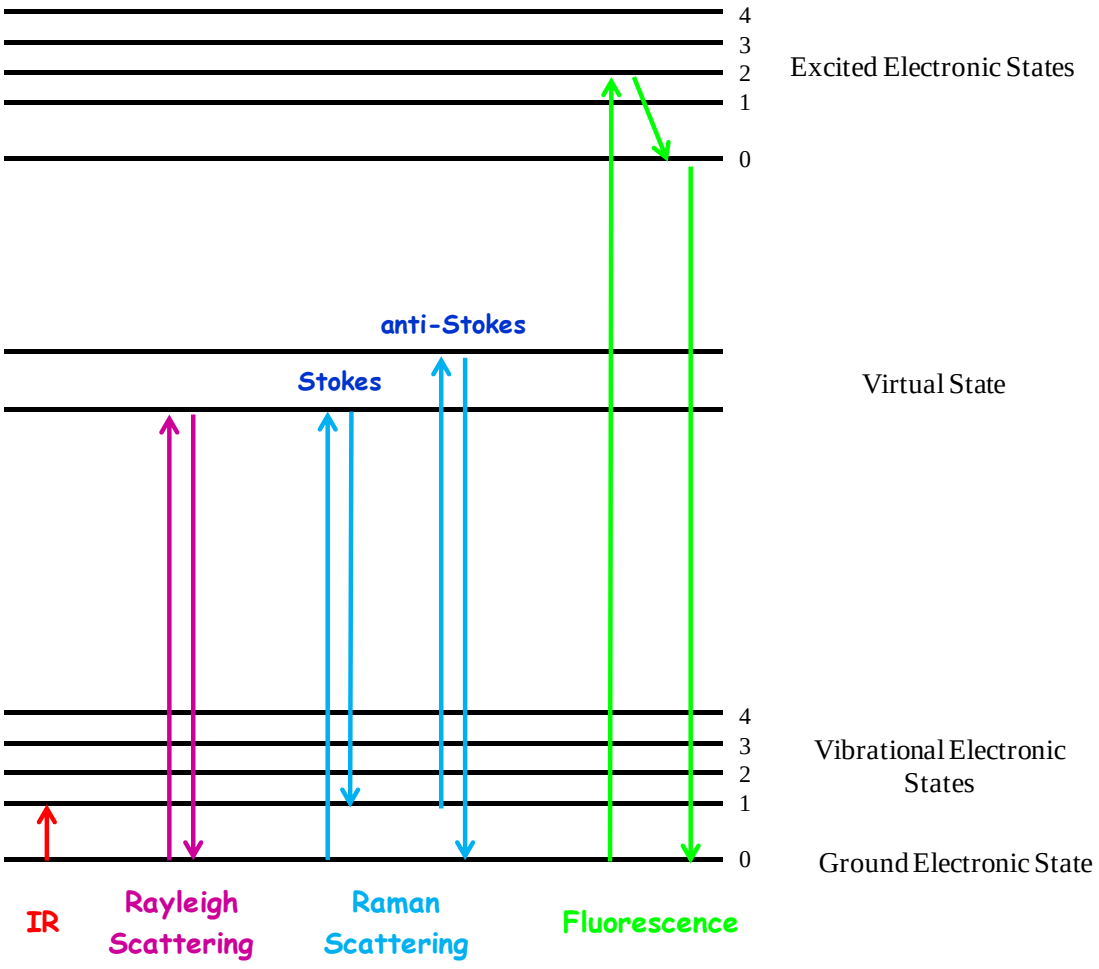

Figure 15: Schematic representation of the vibrational/electronic transitions characteristic of IR absorption, Raman and Rayleigh scattering, and fluorescence.

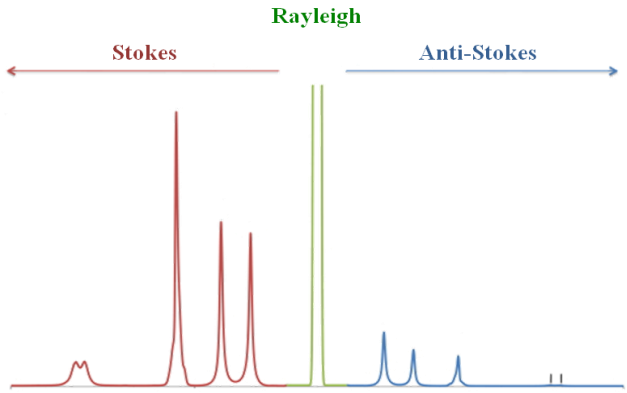

Figure 16: Schematic representation of the Rayleigh, Stokes and anti-Stokes lines (adapted from [230]).

In Raman spectroscopy, when the electric field of the incident radiation interacts with the sample, a change in the molecular polarisability is induced. A molecular vibration will only be Raman active if the vibration that scatters Raman light is accompanied by a change in the polarisability of the molecule [207]. This tendency of the electron cloud of a molecule to distort from its normal shape is a response to an electric field and determines the Raman scattering intensity (Raman activity) [229].

Although many approaches have been explored to reduce the fluorescence impact in Raman spectroscopy, this is still one of the main limitations of the technique [208,231]. Fluorescence is a process that involves excitation of a molecule by absorption of light, from the ground electronic state to an excited electronic state, followed by emission without change in the sample's spin state (fluorescence) [208,224]. Typically, fluorescence is a much more intense process than Raman scattering. Therefore, when fluorescence occurs (either intrinsic to the sample or caused by impurities), it can overrule the Raman features of the analysed compound, rendering the acquisition of Raman data very difficult if not impossible. Therefore, the continuous search for methods to avoid fluorescence emission is of utmost importance. Currently there are several approaches to overcome fluorescence, such as: selecting an appropriate laser excitation wavelength that does not allow absorption to take place between electronic states d [208,231]; purifying the sample when the fluorescence is due to impurities (extrinsic); using low laser intensities and with long integration times in order to improve spectral acquisition and minimise fluorescence interference; by means of a sensitive CCD device as the detection system [231].

Raman spectroscopy can be used to study solid, liquid and gaseous samples and is extremely useful for chemical identification and characterisation of molecular structure and

conformation (*e.g.* environment changes) [231]. Since vibrational information is specific to the chemical bonds, this spectroscopy provides a molecular fingerprint by which the molecule can be identified.

In the last years, Raman spectroscopy has been widely applied in a variety of fields that include biology [224,233,234], biomedicine [233,235] pharmacology [229,235], drug development [229,235], chemistry and biochemistry [208,234,236], forensic sciences [237], and medical diagnosis [235], including early detection of cancer [233]. In addition, the combination of optical microscopy with Raman scattering – Raman microspectroscopy – has proved to be a powerful technique in many areas, namely in clinical oncology applications [223,235,238]. This technique discriminates between normal and malignant tissues in different types of cancer, through *in vivo* and *in situ* observation (chemical imaging), and also provides information about the constitution and distribution of cellular components in individual living cells [239,240], therefore being an invaluable tool in the early diagnosis of cancer. The use of this method overcomes the intrinsic limitation of X-ray diffraction and permits the examination of single crystals displaying high signal-to-noise ratio [235].

Table 4 contains the main advantages and disadvantages of this technique.

Table 4: Main advantages and disadvantages of Raman spectroscopy.

Raman Spectroscopy	
Advantages	**Disadvantages**
❋ No particular sample preparation is required	❋ Sample's intrinsic fluorescence can overrule the Raman spectrum
❋ Samples can be recovered	❋ An intense laser radiation can harm the sample
❋ Very small amounts of sample are required → allowing to detect and analyse trace amounts of sample	❋ Raman effect is very weak → low sensitivity
❋ Non-invasive technique (allows *in situ* analysis)	❋ Raman effect is very weak → highly optimised instrumentation and very sensitive detectors are needed
❋ Allows the analysis of aqueous solutions (water hardly interferes)	❋ Equipment is expensive
❋ Great flexibility of experimental setups	

Table 4: Main advantages and disadvantages of Raman spectroscopy. (Continuation)

❋ Allows the analysis of organic and inorganic compounds → the spectral ranges can reach very low wavenumbers ❋ Short time scale: the spectra can be acquired very quickly, yielding near-instantaneous results	

As described above, IR and Raman are complementary techniques. Usually, vibrations yielding intense bands in IR (involving a large dipole moment variation), are weak in Raman. Similarly, non-polar functional groups giving rise to strong Raman features typically yield weak IR signals.

1.6.3. Fourier Transform Spectroscopy

Fourier transform (FT) spectrometers were developed to overcome the limitations of the dispersive instruments and have been widely used in numerous distinct fields (from chemical analysis to pharmacological or even industrial applications) [227,229,241]. This type of instrument employs a specific interferometer (Michelson interferometer) and exploits the well-established mathematical process of Fourier transformation. In the present study, a FT technique was used both for IR and Raman spectroscopies. The FT-Raman technique was used to overcome the interference from fluorescence in some of the presently investigated samples [213].

A simple FT spectrometer usually consists of three basic components: a radiation source, an interferometer and a detector. Briefly, the radiation rising from the source is passed through an interferometer to the sample, before reaching the detector. The interferometer divides the radiant beams, generates an optical path difference between the beams and then recombines them in order to produce repetitive interference signals, which will be then measured as a function of optical path difference by a detector. Then the data is converted to a digital form and transferred to a computer for Fourier transformation [214].

The interferometer used in FT spectroscopy is based on the principle of the Michelson interferometer that consists of two perpendicular plane mirrors (one movable and one fixed) and a beamsplitter, which is a semi-reflecting device (Fig. 17). When the incoming light

strikes the beamsplitter, two beams of roughly the same intensity are produced. The beamsplitter ideally transmits half of the beams to the fixed mirror and reflects the remaining half to the movable mirror. The movable mirror then produces a change in the optical path length between the two arms of the interferometer. Afterwards, the divided beams reflected by the two mirrors return to the beamsplitter where they recombine and interfere with each other. [210]. Due to changes in the relative position of the two mirrors, an interference pattern is created. If the distance travelled by the two beams is the same, the recombination will result in a constructive interference. If the beam from the movable mirror has travelled a different distance than that from the fixed mirror, they will interfere destructively. The reconstructed beam then goes through the sample and is focused onto the detector, and an interferogram is obtained. This interferogram, that represents the radiation output as a function of time, has the unique property that every data point (a function of the movable mirror position) has information about every frequency of the light collected from the sample. However, the measured interferogram signal cannot be interpreted directly and has to be Fourier transformed in order to convert it into a spectrum (intensity as a function of energy) [214,215].

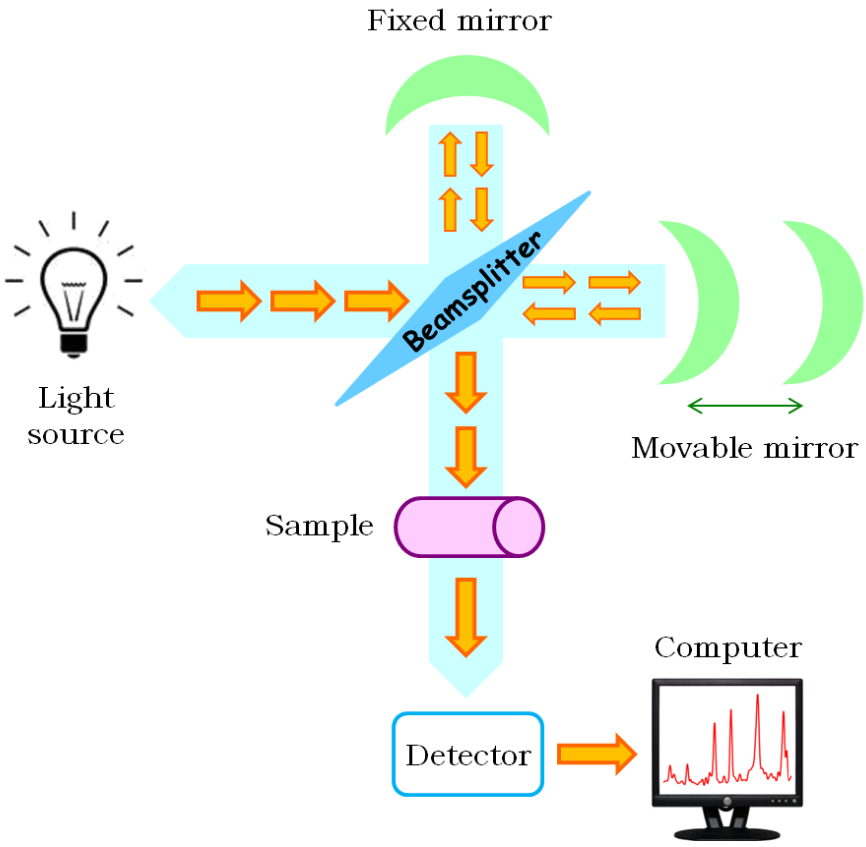

Figure 17: Schematic representation of a Michelson interferometer.

The main advantage of using FT spectroscopy over the dispersive techniques is the fact that information is gathered simultaneously for all frequencies, which allows a quick collection of the spectra and with a higher signal-to-noise ratio ("multiplex" advantage).

1.7. Aims of the Study

Disruptions in cellular polyamine homeostasis have long been closely associated with proliferative disorders. Thus, depletion of the intracellular polyamine pools through the use of polyamine analogues may constitute a promising therapeutic anticancer strategy. In fact, several polyamine analogues deplete cells of their natural polyamines, both *in vitro* and *in vivo*, leading to the retardation of cell growth and, in some cases, initiation of cell death.

Since the clinical use of cisplatin leads to the occurrence of various side effects and to the development of acquired resistance, it is of great relevance to search and test for new metal-based antitumour agents, particularly polyamine Pd(II) and Pt(II) chelates that can exhibit a higher anticancer activity along with lower deleterious side effects.

The main goal of the present work (Fig. 18) was to develop new improved antiproliferative agents by combining the recognised antitumour activity of polyamine analogues (N-alkylated biogenic amines) with the anticancer properties of Pd(II) and Pt(II) complexes. Novel Pd(II) and Pt(II) chelates with polyamine analogues were synthesised and their anticancer properties were tested in several human breast cancer cell lines with different genetic backgrounds (reflecting different breast cancer sub groups), with a view to consider the heterogeneity of breast cancer.

The specific aims were:

<u>Section 3.1:</u>

- To synthesise novel Pd(II) and Pt(II) complexes of the polyamine analogues NSpd, BENSpm and CPENSpm.

- To characterise these compounds with respect to their structure and conformational behaviour, by vibrational spectroscopy – FTIR and Raman – coupled to quantum mechanical calculations.

- To investigate the influence of the structural and conformational preferences of both ligands and complexes (*e.g.* type, number and chemical environment of the metal

centre, nature and coordination mode of the ligands) on their biological activity, and compare it with previously obtained data for biogenic polyamines and their Pd(II) and Pt(II) chelates.

Section 3.2:

- To assess the cytotoxicity profile, including cytostatic and cytocidal effects, of the spermidine analogue NSpd and its newly synthesised trinuclear Pd-NSpd and Pt-NSpd complexes in different human breast cancer cell lines and one immortalised normal-like breast epithelial cell line.

- To determine the effect of the compounds on various aspects of polyamine homeostasis.

- To investigate the ability of the compounds to induce DNA damage.

Section 3.3:

- To determine the cytotoxicity profile, including cytostatic and cytocidal effects, of BENSpm, CPENSpm and the Pd-BENSpm, Pt-CPENSpm and Pd-Spm in different human breast cancer cell lines and one immortalised normal-like breast epithelial cell line.

- To evaluate the effect of the compounds on various aspects of polyamine homeostasis.

- To evaluate the effect of the compounds on CSC and on the ability of treated cells to form colonies in soft agar.

- To assess the capacity of the compounds to induce DNA damage.

- To investigate if glutathione may have a role in the cytotoxic profile.

The results obtained within this study will hopefully allow the development of reliable SAR models, which will enable a rational design of new polynuclear Pd(II)- and Pt(II)-polyamine complexes, with optimised antiproliferative and cytotoxic activities, coupled to low toxicity and minimal acquired resistance.

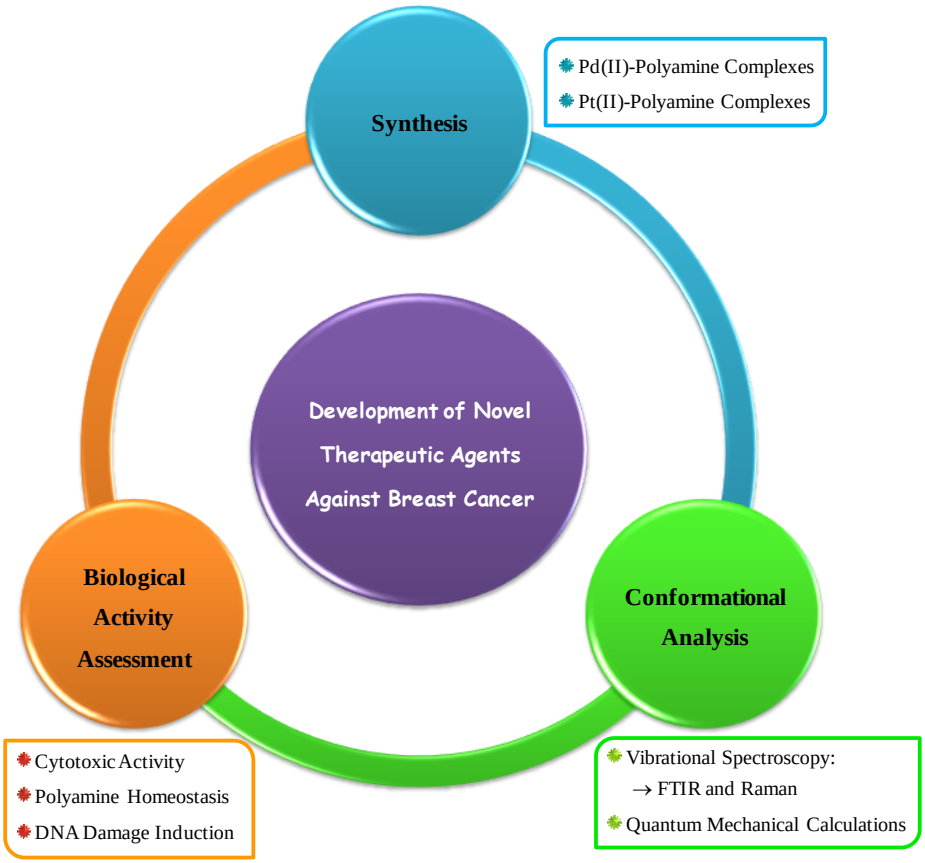

Figure 18: Schematic representation of the aims of the study.

II - Materials and Methods

“Pleasure in the job puts perfection in the work.” “Happiness depends upon ourselves.”

Aristotle

2. Materials and Methods

In this study, a full conformational characterisation of several modified biogenic polyamines and their newly synthesised Pd(II) and Pt(II) complexes was performed through vibrational spectroscopic techniques (infrared and Raman). Furthermore, their cytotoxic effect against human breast cancer cell lines (as well as towards a non-tumourigenic line) was evaluated, using several biological methods. The detailed experimental procedures will be described in this chapter.

2.1. Reagents

Table 5: List of the reagents used along the study.

Reagent	Supplier
Synthesis	
Potassium tetrachloropalladate 98%	Sigma-Aldrich Chemical S.L., Sintra, Portugal
Potassium tetrachloroplatinate > 99.9%	Sigma-Aldrich Chemical S.L., Sintra, Portugal
NSpd trihydrochloride 98%	Sigma-Aldrich Chemical S.L., Sintra, Portugal
BESpm tetrahydrochloride	Biogen Cientifica S.L., Madrid, Spain
BENSpm tetrahydrochloride	Dr. Patrick Woster, Charleston, SC, USA
CPENSpm tetrahydrobromide	Dr. Patrick Woster, Charleston, SC, USA
Pd-Spm complex	Synthesised at the Molecular Physical-Chemistry Research Group, Coimbra University [243], Coimbra, Portugal
Hydrochloric acid 37%	Sigma-Aldrich Chemical S.L., Sintra, Portugal
Sodium hydroxide 99%	Sigma-Aldrich Chemical, S.L., Sintra, Portugal
Acetone $\geq$ 99.5%	Absolve, Odivelas, Portugal
Ethanol	Absolve, Odivelas, Portugal

Table 5: List of the reagents used along the study. (Continuation)

Cell Culture	
[a]DMEM/Ham's F12 medium	Biochrom, Berlin, Germany
[b]RPMI medium 1640	Biochrom, Berlin, Germany
Fetal calf serum	Biochrom, Berlin, Germany
Culture medium components	Biochrom, Berlin, Germany
Aminoguanidine	Sigma, Stockholm, Sweden
Cholera toxin	Sigma, Stockholm, Sweden
Epidermal growth factor	Invitrogen AB, Stockholm, Sweden
Insulin	Sigma, Stockholm, Sweden
Hydrocortisone	Sigma, Stockholm, Sweden
Phosphate-buffered saline	Oxoid Ltd., Basingstoke, Hampshire, UK
Trypsin-EDTA	Sigma, Stockholm, Sweden
MTT Assay	
3-(4,5-dimethyl-thiazolyl-2)-2,5 Diphenyltetrazolium bromide	Sigma, Stockholm, Sweden
Dimethyl sulphoxide	Merck KGaA, Darmstadt, Germany
Radioactivity-Based Uptake Assay	
Hydrochloric acid	VWR, Stockholm, Sweden
Sodium hydroxide	VWR, Stockholm, Sweden
Spermidine trihydrochloride (^{3}H-Spd)	PerkinElmer, Boston, MA, USA
Enzyme Activity Assays	
L-[1-^{14}C]Ornithine	New England Nuclear, DuPont, Scandinavia AB,
Dithiothreitol	Sigma, Stockholm, Sweden
Pyridoxal-5-phosphate	Sigma, Stockholm, Sweden
^{14}[C]Acetyl-coenzyme A	New England Nuclear, DuPont, Scandinavia AB, Stockholm, Sweden
Spermidine	Sigma, Stockholm, Sweden
Sucrose	VWR, Stockholm, Sweden

Table 5: List of the reagents used along the study. (Continuation)

Polyamine Analysis	
Perchloric acid	Merck, Stockholm, Sweden
θ-Phthalaldehyde	Sigma, Stockholm, Sweden
Flow Cytometry	
Nonidet P-40	VWR, Lund, Sweden
Propidium iodide	Sigma , Stockholm, Sweden
Ribonuclease A	Sigma , Stockholm, Sweden
Bromodeoxyuridine	DAKO Cytomation Denmark A/S, Glostrup,
Primary monoclonal antibody against BrdUrd (M744)	Dakopatts, Glostrup, Denmark
Secondary fluorescein isothiocyanate (FITC)-conjugated antibody (F313)	Dakopatts, Glostrup, Denmark
Accutase	Sigma, Stockholm, Sweden
Antibody against CD24-phycoerythrin (PE)	Becton Dickinson**,** Stockholm, Sweden
Antibody against CD44-FITC	Becton Dickinson**,** Stockholm, Sweden
PE-conjugated mouse immunoglobulin 1 (IgG1)	Becton Dickinson**,** Stockholm, Sweden
FITC-conjugated mouse IgG1	Becton Dickinson**,** Stockholm, Sweden
Colony Forming Efficiency Assay	
Agarose	FMC BioProducts, Rockland, ME, USA
Poly(2-hydroxyethyl methacrylate)	Sigma, Stockholm, Sweden
Formaldehyde	VWR, Stockholm, Sweden
Intracellular Metal Accumulation	
Nitric acid	VWR, Stockholm, Sweden

Table 5: List of the reagents used along the study. (Continuation)

Comet Assay	
Agarose gel supporting medium	FMC BioProducts, Rockland, ME, USA
Nusieve® GTG low-melting-point agarose	FMC BioProducts, Rockland, ME, USA
Ethidium bromide	Sigma, Stockholm, Sweden
GSH-Glo™ Glutathione Assay	
GSH-Glo™ Glutathione kit	Promega Biotech AB, Nacka, Sweden
Western Blot	
Bromophenol blue	VWR, Stockholm, Sweden
Glycerol	VWR, Stockholm, Sweden
Sodium dodecyl sulfate	VWR, Stockholm, Sweden
β-Mercaptoethanol	VWR, Stockholm, Sweden
NuPAGE® MOPS running buffer	Invitrogen Corporation, Carlsbad, California, USA
NuPAGE® antioxidant	Invitrogen Corporation, Carlsbad, California, USA
Magic Marker™ XP standard	Invitrogen Corporation, Carlsbad, California, USA
Sea Blue® Pre-stained standard	Invitrogen Corporation, Carlsbad, California, USA
Antizyme inhibitor antibody	Dr. Senya Matsufuji, Tokyo, Japan
Horseradish peroxidase-conjugated goat anti-mouse antibody (P0447)	DAKO Cytomation Denmark A/S, Glostrup, Denmark
Enhanced Chemiluminescence® nitrocellulose membranes	GE Healthcare, Buckinghamshire, United Kingdom
Tween® 20	Sigma, Stockholm, Sweden
Enhanced Chemiluminescence™ Advanced Blotting Detection Kit	GE Healthcare, Buckinghamshire, United Kingdom

[a]Culture medium used for JIMT-1 cells.

[b]Culture medium used for L56Br-C1, MCF-7, MDA-MB-231 and MCF-10A cells.

2.2. Equipment

Table 6: List of the equipment used along the study.

Equipment	Supplier
Synthesis	
AB54-S/FACT Analytical Balance	Mettler Toledo, Switzerland
pH-meter BASIC 20^{+}	Crison Instruments, Barcelona, Spain
E2M2 High Vacuum Pump 2 stage	Edwards, Sussex, England
Cell Culture	
[c]Class II Safety Cabinet Biowizard (BW)-100	Kojair Tech Oy, Vilppula, Finland
[d]Class II Biological Safety Cabinet	ESCO, Wiltshire, England
[c]MCO-19A Incubator	Sanyo Electric Co. Ltd., Japan
[d]Heraeus HERAcell 150 Incubator	Thermo Scientific, Stockholm, Sweden
[c]NE1B-14 Water bath	Clifton, England
[d]GFL-1083 Shaking Water bath	GFL, Manchester, United Kingdom
[c]Olympus CKX41 Microscope with an Olympus DP20-5E Digital	Olympus Optical Co. Ltd., Japan
[d]Olympus CKX41 Microscope with an Olympus SC30 Digital Camera	Olympus Optical Co. Ltd., Japan
[c]MPW-350R Centrifuge	MPW Medical Instruments, Poland
[d]Heraeus Megafuge 16 Centrifuge	Thermo Fisher Scientific, Gothenburg, Sweden
MTT Assay	
[d]Labsystems iEMS Reader MF	Labsystems Oy, Helsinki, Finland
Radioactivity-Based Uptake Assay	
Tri-Carb 2800TR Liquid Scintillation Counter	PerkinElmer, Sweden

Table 6: List of the equipment used along the study. (Continuation)

Enzyme Activity Assays	
Sonicator	Optilab Instruments AB, Stockholm, Sweden
Tri-Carb 2800TR Liquid Scintillation Counter	PerkinElmer, Sweden
Polyamine Analysis	
Hewlett Packard 1100 series HPLC system	Agilent Technologies Sweden AB, Kista, Sweden
Flow Cytometry	
Ortho Cytoron Absolute Flow Cytometer	Ortho Raritan, NJ, USA
Accuri C6 Flow Cytometer	BD Biosciences , San Jose, CA, USA
Intracellular Metal Accumulation	
Thermo X7 Mass Spectrometer	Thermo Elemental, Winsford, UK
Comet Assay	
Electrophoresis device	Invitrogen Corportation, Carslbad. CA, USA
Olympus AX70 Fluorescence Microscope	Olympus Optical Co Ltd., Japan
Olympus DP50 Digital Camera	Olympus Optical Co Ltd., Japan
GSH-Glo™ Glutathione Assay	
Labsystems iEMS Reader MF	Labsystems Oy**,** Helsinki, Finland
Western Blot	
Xcell Sure Lock™ Mini-cell system	Invitrogen Corporation, Carlsbad, CA, USA
iBlot™ Dry Blotting system	Invitrogen Corporation, Carlsbad, CA, USA
ChemiDoc XRS system	Bio-Rad Laboratories Inc., Hercules, CA, USA

[c]"Molecular Physical-Chemistry Research Unit", University of Coimbra, Portugal.

[d]Biology Department, University of Lund, Sweden.

2.3. Synthesis

The synthesis of Pd(II) and Pt(II) complexes with polyamine analogues, one of the goals of this work, was performed according to optimised procedures based on previously reported methods for similar compounds, namely the synthesis of Pt(II) and Pd(II) chelates of natural polyamines [176,244].

The modified polyamines used were the symmetrically (BENSpm) or unsymmetrically (CPENSpm) substituted spermine analogues and the alkylpolyamine NSpd (Fig. 4). The corresponding chelates were $(PdCl_2)_3(NSpd)_2$ (abbreviated Pd-NSpd), $(PtCl_2)_3(NSpd)_2$ (abbreviated Pt-NSpd), $(PdCl_2)_2$(BENSpm) (abbreviated Pd-BENSpm), $(PtCl_2)_2$(CPENSpm) (abbreviated Pt-CPENSpm) (Fig. 10) and $(PdCl_2)_2$(Spm) (abbreviated Pd-Spm).

2.3.1. Palladium Complexes

Two mmol of K_2PdCl_4 were dissolved in a minimal amount of water and an aqueous solution containing 3 or 1 mmol of the ligand (NSpd or BENSpm, respectively) was added dropwise, under continuous stirring, in the dark. The pH was then adjusted to approximately 8 (with 1 M HCl for the NSpd chelate and 1 M NaOH for the BENSpm complex). Upon stirring for about 5 to 6 h, followed by overnight rest, a yellow powder of the complex was obtained. This powder was filtered, washed repeatedly with cold acetone and ethanol and dried under vacuum. Yield: **81.2%** and **88.6%** for Pd-NSpd and Pd-BENSpm, respectively.

The Pd-Spm complex was previously synthesised [170] and kindly provided by S. M. Fiuza from the "Molecular Physical-Chemistry" Research Unit of the University of Coimbra, Portugal.

- $[(PdCl_2)_3$-(norspermidine$)_2]$ – **Pd-NSpd**

$$3\ K_2PdCl_4\ (aq) + 2\ H_2N(CH_2)_3NH(CH_2)_3NH_2\ (aq) \rightarrow \quad (2.1)$$
$$\rightarrow [Pd_3(H_2N(CH_2)_3NH(CH_2)_3NH_2)_2Cl_6]\ (s) + 6\ KCl\ (aq)$$

- $[(PdCl_2)_2$-(N^1,N^{11}-diethylnorspermine)] – **Pd-BENSpm**

$$2\ K_2PdCl_4\ (aq) + C_2H_5NH(CH_2)_3NH(CH_2)_3NH(CH_2)_3NHC_2H_5\ (aq) \rightarrow \quad (2.2)$$
$$\rightarrow [Pd_2Cl_4(C_2H_5NH(CH_2)_3NH(CH_2)_3NH(CH_2)_3NHC_2H_5)]\ (s) + 4\ KCl\ (aq)$$

2.3.2. Platinum Complexes

A solution containing 3 or 1 mmol of the ligand (NSpd or CPENSpm, respectively) was added dropwise to an aqueous solution containing 2 mmol of K_2PtCl_4, under continuous stirring, in the dark. The pH was then adjusted to approximately 8 and 12, respectively for the NSpd and CPENSpm chelates (with 1 M HCl and 1 M NaOH). Upon stirring for about 5 to 6 h, followed by overnight rest, a white-yellow powder of the complex was obtained. This powder was filtered, washed repeatedly with cold acetone and ethanol and dried under vacuum. Yield: **45.7%** and **66.3%** for Pt-NSpd and Pt-CPENSpm, respectively.

- $[(PtCl_2)_3$-(norspermidine$)_2]$ – **Pt-NSpd**

$$3\ K_2PtCl_4\ (aq) + 2\ H_2N(CH_2)_3NH(CH_2)_3NH_2\ (aq) \rightarrow \quad (2.3)$$
$$\rightarrow [Pt_3(H_2N(CH_2)_3NH(CH_2)_3NH_2)_2Cl_6]\ (s) + 6\ KCl\ (aq)$$

- $[(PtCl_2)_2$-(N^1-cyclopropyl-methyl-N^{11}-ethylnorspermine)] – **Pt-CPENSpm**

$$2\ K_2PtCl_4\ (aq) + C_2H_5NH(CH_2)_3NH(CH_2)_3NH(CH_2)_3NHC_4H_7\ (aq) \rightarrow \quad (2.4)$$
$$\rightarrow [Pt_2Cl_4(C_2H_5NH(CH_2)_3NH(CH_2)_3NH(CH_2)_3NHC_2H_5)]\ (s) + 4\ KCl\ (aq)$$

2.4. Characterisation of the Complexes

The complexes were first fully characterised by elemental analysis, carried out at the Central Analysis Laboratory and Chemistry Department (Mass Spectrometry Laboratory) of the University of Aveiro, Portugal (**C**, **N** and **H** analysis), and at the Elemental Analysis Laboratory of the University of Santiago de Compostela, Spain (**Pt** and **Pd** analysis).

Table 7: Elemental analysis results for the complexes Pd-NSpd, Pt-NSpd, Pd-BENSpm and Pt-CPENSpm.

Complex	Experimental (%)				Calculated (%)			
	C	**H**	**N**	**Pd / Pt**	**C**	**H**	**N**	**Pd / Pt**
Pd-NSpd	18.10	4.20	10.32	39.90	18.14	4.32	10.58	40.18
Pt-NSpd	13.33	3.16	7.89	55.01	13.6	3.24	7.92	55.19
Pd-BENSpm	25.88	5.10	9.13	35.25	26.06	5.39	9.36	35.52
Pt-CPENSpm	22.03	4.12	6.77	48.10	22.45	4.28	6.98	48.62

Full identification of the complexes was carried out by vibrational analysis, using both FTIR and FT-Raman spectroscopies, clearly evidencing the presence of the bands characteristic of these particular metal-polyamine chelates.

2.5. FTIR Spectroscopy

The FTIR spectra were recorded at room temperature in a Bruker Optics Vertex 70 FTIR spectrometer, in the range 400–4000 cm^{-1}, using KBr discs (*ca.* 2% (w/w)), a KBr beamsplitter and a liquid nitrogen-cooled Mercury Cadmium Telluride (MCT detector). The spectra were collected for *ca.* 75 scans, with a 2 cm^{-1} resolution. The errors in wavenumbers were estimated to be less than 1 cm^{-1}.

2.6. Raman Spectroscopy

The Raman spectra were obtained for the pure compounds, at room temperature, in a triple monochromator Jobin-Yvon T64000 Raman system (focal distance 0.640 m, aperture *f*/7.5) equipped with holographic gratings of 1800 grooves.mm^{-1}. The premonochromator stage was used in the subtractive mode. The detection system was a liquid nitrogen cooled non-intensified 1024x256 pixel (1") CCD chip.

The 514.5 nm line of an Ar^+ laser (Coherent, model Innova 300-05) was used as the excitation radiation, providing *ca.* 90 mW at the sample position. A 90º geometry between the incident radiation and the collecting system was employed. The entrance slit was set to 200 μm, as well as the slit between the premonochromator and the spectrograph. Samples were

sealed in Kimax glass capillary tubes of 0.8 mm inner diameter. Under the above mentioned conditions, the error in wavenumbers was estimated to be within 1 cm^{-1}.

FT-Raman spectra were obtained at room temperature in a RFS 100/S Bruker spectrophotometer. The 1064 nm line provided by a Nd:YAG laser was used, yielding 200 mW at the sample position. Resolution was set at 2 cm^{-1} and a 180^{o} geometry was employed.

2.7. Quantum Mechanical Calculations

The quantum mechanical calculations were performed using the GAUSSIAN 03W program [245] within the Density Functional Theory (DFT) approach. The widely employed hybrid method denoted by B3LYP, which includes a mixture of HF and DFT exchange terms and the gradient-corrected correlation functional of Lee, Yang and Parr [246,247], as proposed and parameterised by Becke [248,249] was used, along with the double-zeta split valence basis set 6-31G** [250].

Molecular geometries were fully optimised by the Berny algorithm, using redundant internal coordinates [251]: The bond lengths to within *ca.* 0.1 pm and the bond angles to within *ca.* 0.1º. The final root-mean-square (rms) gradients were always less than $3x10^{-4}$ hartree.$bohr^{-1}$ or hartree.$radian^{-1}$. No geometrical constraints were imposed on the molecules under study.

The harmonic vibrational wavenumbers, as well as the Raman activities and infrared intensities, were also obtained, at the same theory level as the geometry optimisation procedure. The widely employed scale factors of Merrick *et al.* [252] were used for wavenumbers above 600 cm^{-1}, leading to a quite good agreement between theoretically predicted and experimental frequencies.

2.8. Stock Solutions

Stock solutions (2 mM) of the polyamine analogues NSpd, BENSpm and CPENSpm were made by dissolving each compound in phosphate-buffered saline (PBS: 8 g/L NaCl, 0.2 g/L KCl, 1.15 g/L Na_2HPO_4, 0.2 g/L KH_2PO_4, pH 7.3), followed by sterile-filtration and storage at 4°C.

Stock solutions of the complexes Pd-NSpd (2 mM), Pt-NSpd (2 mM), Pd-BENSpm (1 mM), Pd-Spm (1 mM) and Pt-CPENSpm (2 mM) were prepared by dissolving the compounds in 4% dimethyl sulphoxide (DMSO) in PBS, followed by sterile-filtration and storage at -20°C.

Further dilutions of these stock solutions were made in complete cell culture medium, in order to obtain the final concentrations required for the biological assays. In all the experiments performed with NSpd, Pd-NSpd and Pt-NSpd, aminoguanidine (1 mM) was added to the culture medium with the view to inhibit the activity of the polyamine oxidase present in the fetal calf serum (FCS). In all the experiments, the highest concentration of DFMO used in the cell for both control and treated samples was 0.2%.

2.9. Cell Lines and Cell Culture Conditions

Four human breast cancer cell lines and one immortalised normal-like breast epithelial cell line were tested in the present work. The cell lines were cultured as monolayers at 37°C in a humidified incubator with 5% CO_2 in air. The MCF-10A, JIMT-1 and MDA-MB-231 cell lines were sub-cultured twice a week, while the L56Br-C1 and MCF-7 cells were sub-cultured once a week with an additional change of growth medium once a week.

2.9.1. JIMT-1

The human ductal carcinoma breast cancer cell line JIMT-1 was isolated from the pleural effusions of a 62-year old breast cancer female patient presenting clinical and intrinsic resistance to trastuzumab, the first immunotherapeutic drug used for breast cancer treatment [253]. It was purchased from the German Collection of Microorganisms and Cell Cultures, DSMZ, Braunschweig, Germany.

JIMT-1 cells (Fig. 19) show an epithelial-like morphology and have mutated p53. This cell line is classified as HER-2 positive since it has an amplification of the HER-2 oncogene, however it is insensitive to HER-2-inhibiting drugs. JIMT-1 is the only cell line used in this study displaying HER-2 overexpression [253-255]. JIMT-1 cells were cultured in DMEM/Ham's F12 medium supplemented with 10% FCS, non-essential amino acids (1 mM), insulin (10 µg/ml), penicillin (100 U/ml) and streptomycin (100 µg/ml). The JIMT-1 cell line has a population doubling time of approximately 24 h.

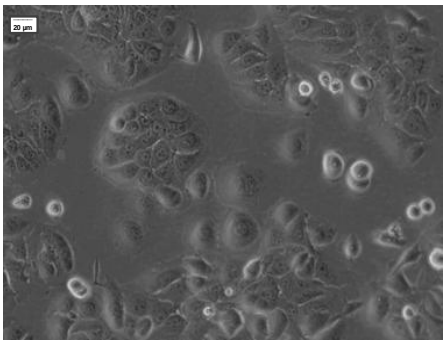

Figure 19: Phase contrast image of JIMT-1 cells, after 48 h of seeding.

2.9.2. L56Br-C1

The human breast adenocarcinoma cell line L56Br-C1 was derived from the human tumour xenograft L56Br-X1 that originated (in the 1990s) from the mammary lymph node metastasis of a 53-year old Swedish Caucasian female carrying a BRCA1 germ-line mutation, one of the most commonly detected alterations in hereditary breast cancer [256]. It was established at the Department of Oncology, Clinical Sciences, Lund University, Sweden.

L56Br-C1 cells (Fig. 20) have a somatic p53 mutation and possess no wild type BRCA1 allele [256,257]. A highly distinctive characteristic of these cells is the spontaneous occurrence of about 10 to 20% cell death by apoptosis. L56Br-C1 cells were maintained in RPMI 1640 medium supplemented with 10% heat-inactivated FCS, non-essential amino acids (1 mM), insulin (10 µg/ml), penicillin (100 U/ml), streptomycin (100 µg/ml) and sodium-pyruvate (1 mM). The L56Br-C1 cell line has a population doubling time of approximately 32 h.

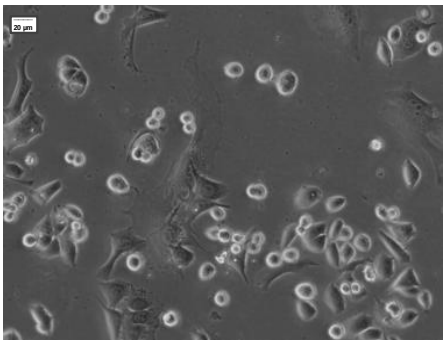

Figure 20: Phase contrast image of L56Br-C1 cells, after 48 h of seeding.

2.9.3. MCF-7

The human epithelial breast adenocarcinoma cell line MCF-7 was isolated from a pleural effusion of a 69-year old Caucasian female in 1970 [258]. It was purchased from the American Type Culture Collection, Manassas, VA, USA.

MCF-7 cells (Fig. 21) have a wild type p53 protein and lack normal expression of caspase-3 mRNA and protein due to a gene deletion. No DNA laddering occurs in these cells when apoptosis is induced. MCF-7 is the only estrogen receptor positive breast cancer cell line used in this study [259-261]. MCF-7 cells were maintained in RPMI 1640 medium supplemented with 10% FCS, non-essential amino acids (1 mM), insulin (10 µg/ml), penicillin (100 U/ml) and streptomycin (100 µg/ml). The MCF-7 cell line has a population doubling time of approximately 34 h.

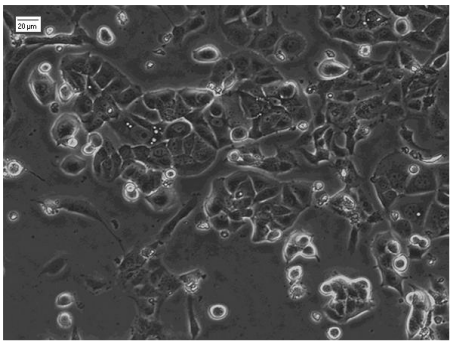

Figure 21: Phase contrast image of MCF-7 cells, after 48 h of seeding.

2.9.4. MDA-MB-231

The human epithelial breast adenocarcinoma cell line MDA-MB-231 was established in 1973 from a pleural effusion of a 51-year old Caucasian female patient with invasive ductal breast cancer [262]. It was purchased from the American Type Culture Collection, Manassas, VA, USA.

MDA-MB-231 cells (Fig. 22) have mutated p53 and express the WNT7B oncogene [263,264]. These cells were grown and maintained in RPMI 1640 medium supplemented with 10% FCS, non-essential amino acids (1 mM), insulin (10 µg/ml), penicillin (100 U/ml), streptomycin (100 µg/ml) and sodium pyruvate (1 mM). The MDA-MB-231 cell line has a population doubling time of approximately 28 h.

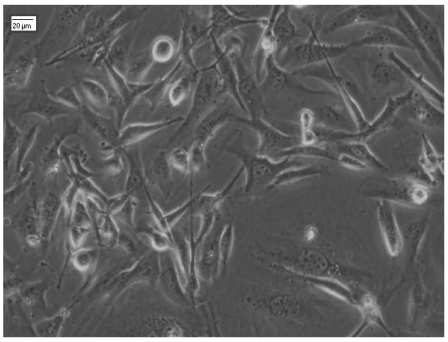

Figure 22: Phase contrast image of MDA-MB-231 cells, after 48 h of seeding.

2.9.5. MCF-10A

MCF-10A is a spontaneously transformed normal-like breast epithelial cell line originating from a fibrocystic mammary gland tissue of a 36-year old female with no family history of breast malignancy [265]. It was obtained from the American Type Culture Collection, Manassas, VA, USA.

MCF-10A cells (Fig. 23) have wild type p53 and do not form tumours in nude mice [265,266] nor do they form colonies in soft agar. MCF-10A cells were maintained in RPMI 1640 medium supplemented with 10% heat-inactivated FCS, non-essential amino acids (1 mM), insulin (10 µg/ml), penicillin (100 U/ml), streptomycin (100 µg/ml), epidermal growth factor (20 ng/ml), cholera toxin (50 ng/ml) and hydrocortisone (500 ng/ml). The MCF-10A cell line has a population doubling time of approximately 15 h.

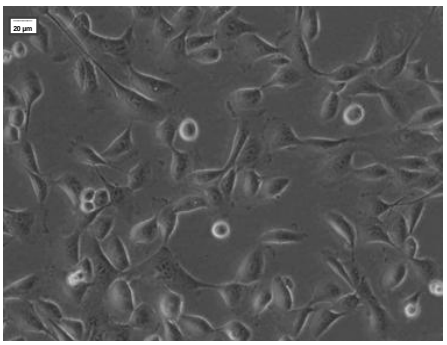

Figure 23: Phase contrast image of MCF-10A cells, after 48 h of seeding.

2.10. Cell Proliferation Studies

Cell proliferation can be defined as the increase in the number of viable cells as a result of growth and division and may be determined by direct cell counting using a hemocytometer. In this thesis, *in vitro* cell proliferation experiments have been carried out. To determine the effect of the compounds under study on cell proliferation, two types of growth curve experiments were set up.

2.10.1. One Treatment Cycle

Cells were seeded in a number of Petri dishes (5 cm diameter) at a density of 0.3 x 10^6 cells/Petri dish (MCF-10A) or 0.6 x 10^6 cells/Petri dish (JIMT-1, L56Br-C1 and MCF-7) and were allowed to attach and grow for 24 h, prior to the addition of the test compounds to a given concentration based on earlier studies, and also on information regarding clinically feasible doses. In each experiment, the number of Petri dishes seeded with cells was at least so many to be able to harvest cells in at least three for each treatment at each time point. After seeding, the cells in each Petri dish were treated independently. For NSpd, Pd-NSpd and Pt-NSpd two different concentrations were tested: 25 μM and 100 μM, while for BENSpm, Pd-BENSpm, CPENSpm, Pt-CPENSpm and Pd-Spm a concentration of 10 μM was used. Twenty-four, 48 or 72 h after seeding, the cells were harvested by trypsinisation and counted in a hemocytometer, and the data were used to draw growth curves.

2.10.2. Repeated Treatment Cycles

One of the goals in cancer treatment is to kill the cancer cells, while the normal cells should be reversibly damaged. In cancer therapy, patients are treated with repeated cycles of chemotherapeutic drugs, to give time for normal cells to recuperate.

The repeated treatment experiments were aimed at investigating the extension of damage caused by this type of therapeutic scheme, and the ability of the cells to recover after each treatment. Cells were seeded in a number of 25 cm^2 cell culture flasks in 5 ml of medium at a density of 0.3 x 10^6 cells/25cm^2 flask (MCF-10A) or 0.7 x 10^6 cells/25cm^2 flask (JIMT-1, L56Br-C1 and MCF-7) and were allowed to attach and grow for 24 h, prior to addition of the test compounds at the desired concentrations (25 μM for NSpd, Pd-NSpd or Pt-NSpd and 10 μM for BENSpm, Pd-BENSpm, Pd-Spm, CPENSpm or Pt-CPENSpm). In each experiment,

the number of flasks seeded with cells was at least so many to be able to harvest at least three for each treatment at each time point. After seeding, the cells in each flask were treated independently. After 72 h of treatment, the medium was removed and new fresh culture medium was added to the vessels. The cells were harvested by trypsinisation, counted in a hemocytometer and reseeded at the same density as before, 72 h after removal of the drugs. Cells were cultivated in cycles using the same treatment procedure, resulting in a long total treatment time of 5 cycles (35 days). The data are presented as the total amount of cells that theoretically would have accumulated if all cells had been reseeded with a known cell density after the end of each treatment cycle. Thus, by using the cell number obtained at each passage of a culture seeded with a known cell density, it was possible to calculate the number of cells that would have been obtained if all cells were reseeded at a lower density at each passage.

2.11. Dose Response Assay – MTT Assay

The MTT (3-[4,5-Dimethylthiazol-2-yl]-2,5 diphenyl tetrazolium bromide) colorimetric assay was established by Mosmann in 1983 [267]. It is based on the reduction of the soluble yellow tetrazolium salt MTT (Fig. 24) into insoluble purple formazan crystals, by mitochondrial NADH-dependent dehydrogenases of metabolically active cells. The amount of formazan formed reflects the cell's metabolic activity, and is assumed to be directly proportional to the number of viable cells. An alteration in cell number results in a concomitant change in the amount of formazan formed, indicating the degree of cytotoxicity caused by the test compound. This is an easy, rapid, convenient, reliable and economic method for obtaining dose response data when treating cells with a wide concentration range of a compound [267-269].

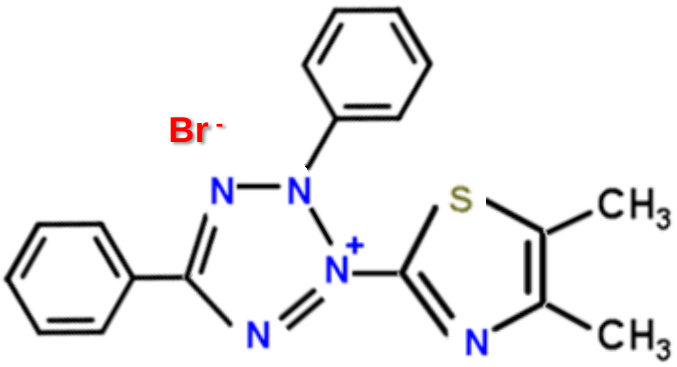

Figure 24: Molecular structure of 3-[4,5-Dimethylthiazol-2-yl]-2,5 diphenyl tetrazolium bromide (MTT).

In the present study, the MTT assay was performed as previously described [112]. Briefly, cells were trypsinised, counted in a hemocytometer, pelleted and resuspended in cell culture medium. Aliquots of 180 µl cell suspension containing 3000 (MCF-10A), 5000 (JIMT-1) or 8000 (L56Br-C1 and MCF-7) cells were seeded in 96-well plates and the compounds to be tested were added 24 h later. At 24, 48 and 72 h of drug treatment, 20 µl of MTT solution (5 mg/ml in PBS) was added to the cell culture medium of each well. After incubation with MTT for 1 h, the MTT containing medium was removed and DMSO was added to each well to dissolve the purple formazan crystals formed by reduction in live attached cells. The plates were swirled gently at room temperature for 10 minutes to dissolve the precipitate. Absorbance was measured at 540 nm using a Labsystems iEMS Reader MF and the software DeltaSoft II v.4.14 (Biometallics Inc., Princeton, NJ, USA) was used for data analysis. The results are presented as percentage of control.

2.12. Methods to Study Polyamine Metabolism

Polyamines are essential for eukaryotic cell proliferation and differentiation. Polyamine levels have to be maintained within very narrow limits because a decrease in their intracellular concentrations inhibits cell proliferation while an excess of polyamines appears to be toxic. Therefore, polyamine metabolism has to be controlled by the use of four different mechanisms: *de novo* synthesis, catabolism and transport (cellular uptake and efflux) [64].

In this thesis, polyamine metabolism was evaluated using radio-labelling and enzymatic assays and also by measuring the intracellular polyamine content.

2.12.1. Radioactivity-Based Uptake Assay

The uptake of extracellular polyamines and export of intracellular polyamines are known to be well-regulated events in cells. Most cells seem to have a single transporter with different affinities instead of specific ones for putrescine, spermidine or spermine since other polyamines, like cadaverine and homospermidine, can also use the same transporter [87].

The present assay was set up to determine the capacity of the compounds under study to competitively inhibit ^{3}H-spermidine uptake in the normal-like and in the breast cancer cell lines (Fig. 25). Cells (0.1 x 10^{6} cells per well) were seeded in replicates into 1.5 ml of medium in 12-well plates. Forty-eight h later, the medium was removed and 1 ml new medium containing 2% FCS, 1 µM ^{3}H-spermidine (0.5 Ci/mmol) and NSpd, Pd-NSpd or Pt-NSpd (0 – 10 mM) was added to the wells. After an incubation period of 30 minutes at 37°C, the cells were washed three times with PBS, followed by addition of 200 µl NaOH (1 M) with gentle shaking of the plates. The cells were again incubated for 1 h, followed by addition of 200 µL HCl (1.5 M) to each well. After gentle swirling of the plates, the radioactivity was measured in an aliquot using scintillation counting. The results are presented as a percentage of the control.

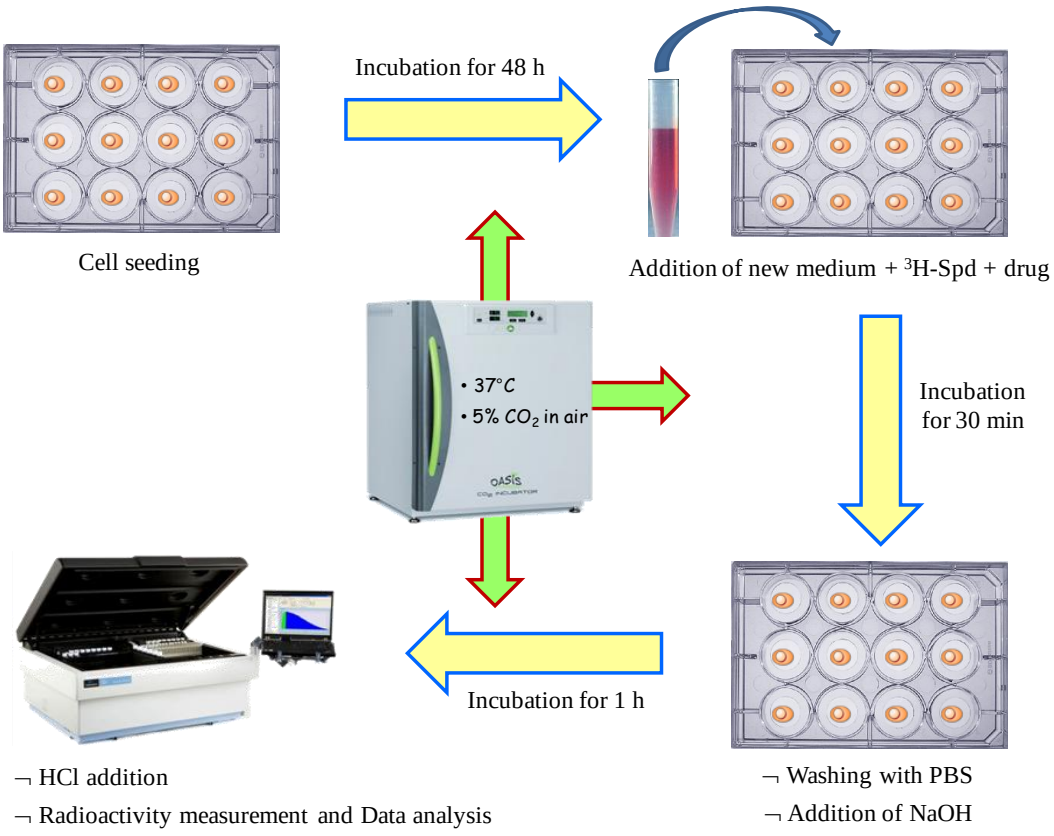

Figure 25: Schematic representation of the radioactivity-based uptake assay.

2.12.2. Enzyme Activity Assays

The activity of the biosynthetic enzyme ODC and of the catabolic enzyme SSAT can be measured by using radioactively-labelled precursors. The labelled end products are captured and quantified by liquid scintillation counting [270].

2.12.2.1. ODC activity

ODC is the first rate-limiting enzyme in polyamine biosynthesis and its activity is closely related to cell proliferation. The measurement of ODC activity can be very useful in clinical oncology since the ODC activity can be affected by treatment with different substances that deplete the intracellular polyamine pools [76].

To determine the ODC activity, cells were seeded as described for the proliferation assay. After 24, 48 and 72 h of treatment with 25 µM NSpd, Pd-NSpd or Pt-NSpd, cells were collected, counted in a hemocytometer, pelleted and stored at -80°C until analysis. Samples were then sonicated in ice-cold Tris-HCl (0.1 M, pH 7.5) containing EDTA (0.1 mM) and dithiothreitol (2.5 mM). ODC activity of the sonicates was determined by measuring the release of $^{14}CO_2$ from carboxyl-labelled L-ornithine in the presence of saturating levels of pyridoxal 5-phosphate (0.1 mM) and L-ornithine (0.2 mM) [271]. The corresponding radioactivity was detected using a liquid scintillation counter. The ODC level is expressed as nmoles/10^6 cells.

2.12.2.2. SSAT activity

SSAT is the rate-limiting enzyme of the polyamine catabolic pathway, being involved in the conversion of spermine and spermidine back to putrescine. SSAT can be readily detected after induction of polyamine catabolism when cells are treated with polyamine analogues. Earlier studies have shown that overexpression of SSAT can been found in several human tumour cell types treated with specific antineoplastic polyamine analogues [272,273].

To determine the SSAT activity, L56Br-C1 cells were seeded as described for the proliferation assay. After 24 h of treatment with 10 µM BENSpm, Pd-BENSpm, Pd-Spm, CPENSpm or Pt-CPENSpm, cell were collected, counted in a hemocytometer, pelleted and stored at -80°C until analysis. Samples were then sonicated in Tris-HCl (50 mM, pH 7.5) containing sucrose (0.25 M). SSAT activity of the sonicates was determined by measuring the

synthesis of ^{14}[C]acetylspermidine after incubation of total cell extracts with ^{14}[C]acetyl-coenzyme A and spermidine. The ^{14}[C]acetylspermidine formed by active SSAT was captured on filter discs. The corresponding radioactivity was detected using a liquid scintillation counter [270]. The SSAT level is expressed as nmoles/10^6 cells.

2.12.3. Polyamine Analysis

Measurements of biogenic polyamines, polyamine analogues or their metabolites in tissues, cells or body fluids are of utmost importance in biochemistry, biology and oncology [274]. The intracellular polyamine levels are tightly regulated and can be affected by treatment with different substances.

In this study, high-performance liquid chromatography (HPLC) was used to measure the polyamine levels in cell extracts. HPLC is a chromatographic technique that uses a liquid mobile phase to separate components in a sample through the use of a higher pressure that pushes the solvent through the column, allowing the establishment of chemical or physical interactions between the sample and the chromatography column.

L56Br-C1 cells for polyamine analysis were seeded as described for the proliferation assay. After 24 h of treatment with 10 μM BENSpm, Pd-BENSpm, Pd-Spm, CPENSpm or Pt-CPENSpm, cells were collected, counted in a hemocytometer, pelleted and stored at -20°C until analysis. The cells were then sonicated in perchloric acid (0.2 M), kept at 4°C over night to precipitate proteins, and then the samples were centrifuged. After centrifugation, the polyamines were found in the supernatant. Finally, chromatographic separation and quantitative determination of these polyamine pools in breast cancer cell extracts were carried out by HPLC using θ-phthaldialdehyde as the reagent [275]. The polyamine levels are expressed as nmoles/10^6 cells.

2.13. Methods using Flow Cytometry

Flow cytometry (FCM) is a method used to measure properties of single cells, by suspending them in a stream of rapidly moving fluid that allows the cells to pass one by one through a laser beam. Depending on the granularity of the cells, the laser light will scatter differently. If any fluorescent molecules are present in the cells, they will be able to emit light after laser excitation. Detectors will pick up both scattered and emitted light. Then, by passing

them through an electronic detection apparatus, information on the physical and chemical structure of each individual cell can be provided and analysed in the form of histograms. In this study, the results obtained with FCM were used to analyse cell cycle phase distribution, cell death and cell cycle kinetics and to identify cell surface markers.

2.13.1. Cell Cycle Phase Distribution and Cell Death Analysis

The cell cycle involves a complex sequence of events that include cell growth, genome duplication and mitosis. The DNA distribution of a cell population provides important information about the cell cycle phase distribution and cell death. FCM was applied to investigate the effects of the tested compounds on the cell cycle phase distribution and on the induction of cell death. For the investigation of cell death, both attached and suspended (dead or dying cells floating in the medium) cells were harvested together.

Cells were seeded as described for the proliferation assay and then allowed to attach and grow for 24 h, prior to addition of the test compounds at the desired concentrations (25 or 100 µM for NSpd, Pd-NSpd or Pt-NSpd and 10 µM for BENSpm, Pd-BENSpm, Pd-Spm, CPENSpm or Pt-CPENSpm). After 24, 48 and 72 h of treatment, cells were collected, counted in a hemocytometer, pelleted, resuspended, then fixed in ice-cold 70% ethanol and stored at -20°C until analysis. Before FCM analysis of the DNA content, cells were pelleted, washed with PBS and then incubated with propidium iodide (PI)-nuclear isolation medium (PBS containing 100 µg/ml PI, 0.60% Nonidet P-40 and 100 µg/ml Ribonuclease A (RNase A)) overnight at 4°C to stain the DNA [276]. PI (Fig. 26) is a fluorochrome excitable at 488 nm, resulting in red fluorescence at 620 nm where the intensity of the emitted red fluorescence is a measurement of the DNA content within the cell nucleus. PI binds stoichiometrically to double-stranded regions of nucleic acids (DNA and RNA). Therefore, in order to determine only the DNA content of the cell nuclei, RNase A and nonidet P-40 were included in the PI staining solution to digest RNA and disrupt the cell membrane, respectively. Immediately prior to FCM analysis, the nuclear suspension was suctioned through a syringe and filtered through a nylon mesh. The samples were analysed with respect to DNA content using an Ortho Cytoron Absolute flow cytometer (for NSpd-, Pd-NSpd- or Pt-NSpd-treated cells) or an Accuri C6 flow cytometer (for BENSpm-, Pd-BENSpm-, Pd-Spm-, CPENSpm- or Pt-CPENSpm-treated cells) [132]. Computerised analysis of FCM-derived data (cell cycle phase distribution) was performed using the MultiCycle® software (Phoenix Flow Systems, San Diego, CA, USA). The appearance of signals with DNA content

lower than that of G_1 cells (sub-G_1 region) due to DNA degradation and nuclear fragmentation is considered to be a marker of cell death. Hence, apoptotic and necrotic cells were detected as a sub-G_1 peak.

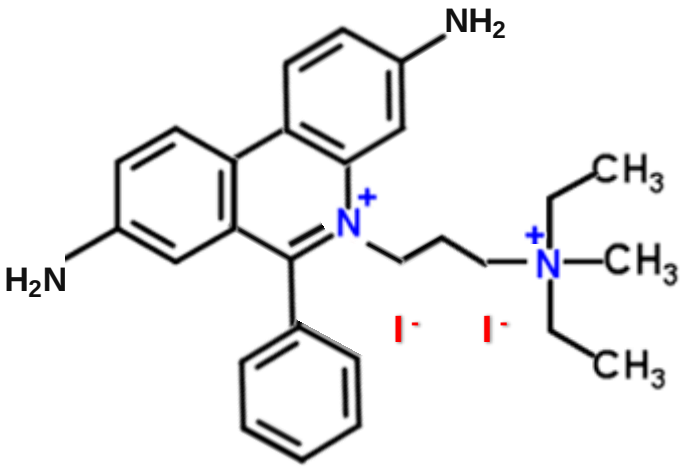

Figure 26: Molecular structure of propidium iodide (PI).

2.13.2. Cell Cycle Kinetic Analysis

Cell cycle kinetics refers to the rate of movement of a cell through the distinct cell cycle phases and can be analysed by using a bromodeoxyuridine (BrdUrd)-DNA flow cytometry method. BrdUrd (Fig. 27) is a thymidine analogue containing a bromine substitution of the methyl group. After addition to the cell culture medium, BrdUrd is taken up by the cells in the same way as thymidine, and is then incorporated into the newly synthesised DNA in cells in the S phase of the cell cycle, thereby replacing thymidine during DNA replication and serving as a suitable marker for cell proliferation [277].

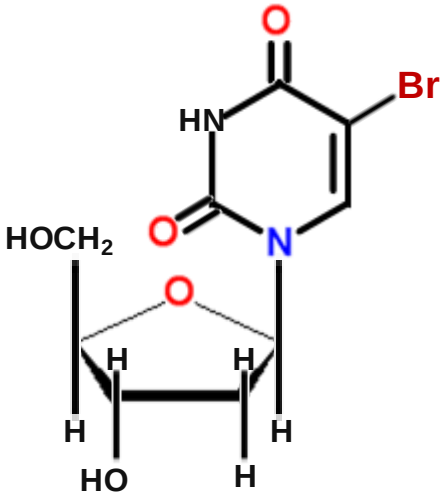

Figure 27: Molecular structure of bromodeoxyuridine (BrdUrd).

In this study, a BrdUrd-DNA flow cytometry technique was used to investigate the effects of the different potential therapeutic agents under study on cell cycle progression, after evaluation of the changes that took place in the cell cycle phase distribution. This technique, which allows the simultaneous measurement of the cellular DNA content along with the cellular amount of incorporated BrdUrd, can be divided into four main steps:

1) BrdUrd Labelling

Cells were seeded in a number of Petri dishes (9 cm diameter) in 12 ml of medium at a density of 0.4 x 10^6 cells/Petri dish (MCF-10A and JIMT-1) or 1.3 x 10^6 cells/Petri dish (L56Br-C1 and MCF-7) and then allowed to attach and grow for 24 h, prior to addition of 25 μM NSpd, Pd-NSpd or Pt-NSpd. In each experiment, the number of Petri dishes seeded with cells was at least so many to be able to harvest at least three for each treatment at each time point. After seeding, the cells in each Petri dish were treated independently. After 72 h of treatment, cells were labelled with BrdUrd (5 μM) for 30 minutes (cells in S phase incorporate the BrdUrd into their DNA), followed by a complete medium removal, washing the cell layer with medium containing 0.5% FCS at 37°C (to ensure that no more BrdUrd labelling occurs) and addition of fresh BrdUrd-free medium with and without the compounds (to allow progression of the cells through the cell cycle). Next, cells were harvested by trypsinisation at specific time points post-labelling (0, 3, 6, 9 and 12 h), pelleted, resuspended and fixed in ice-cold 70% ethanol and stored at -20°C until analysis.

2) Cell Labelling

The preparation of the cells for FCM-mediated assessment of DNA and BrdUrd contents was carried out as previously described in detail by [129,132]. Briefly, cells were incubated with a freshly made pepsin-HCl solution (0.1 M) for 30 minutes to digest cellular proteins. After washing with PBS, the cells nuclei were incubated in HCl (2 M) for exactly 20 minutes, in order to partially denature DNA, resulting in intermittent double-stranded DNA stretches with single-stranded DNA loops. The partial DNA denaturation is assumed to be stoichiometric *i.e.* proportional to the DNA content. Next, cells were incubated with a primary monoclonal antibody against BrdUrd that only binds to BrdUrd exposed in the single-stranded DNA loops, and the primary antibody was then detected by the use of a secondary FITC-conjugated antibody. The nuclei were then stained with PI, which binds to the double-stranded regions of DNA. Since BrdUrd is light sensitive, all the analysis was performed under restrained light conditions.

3) FCM Analysis of DNA and BrdUrd Contents

The FCM analysis of DNA content (red fluorescence) and BrdUrd content (green fluorescence) was monitored with an Ortho Cytoron Absolute flow cytometer with an argon ion laser as excitation light source. In the flow cytometer, both fluorochromes (PI and FITC) were excited at 488 nm. The DNA and BrdUrd contents were recorded as the fluorescence intensity at 620 and 520 nm, respectively.

4) Data Analysis

The computer analysis of the data was performed using Multi2D® and MultiCycle® software programs (Phoenix Flow Systems, San Diego, CA, USA). The data was analysed and calculations made as previously described [129,278].

The lengths of the S and G_2+M phases were calculated as previously described. The length of the S phase corresponds to the DNA replication time and was obtained by following the progression of the BrdUrd-labelled cells through the S phase, according to the principles of Begg e*t al.* [279], as previously described [280]. The length of G_2+M phase corresponds to the time required for cells to proceed through the G_2 and M phases of the cell cycle [278]. In order to calculate the movement of cells through the G_2+M phase, the percentage of BrdUrd-labelled divided cells (originally found in S phase) in relation to the total number of BrdUrd-

labelled cells was plotted against the post-labelling time, being the intercept of the line with the x-axis an approximate measure of the length of this phase.

2.13.3. Identification of Cell Surface Markers

Several types of solid tumours, including breast cancer, display a functional hierarchy of cancer cells but only a small subpopulation of self-renewing stem like cells (known as CSCs) can give rise to the differentiated cells that forms the bulk of the tumour. In human breast cancers, these breast CSC are enriched in a population of cells with a $CD44^+/CD24^{-/low/}$epithelial-specific antigen $(ESA)^+$ phenotype. The cellular heterogeneity of human breast tissues has been characterised based on the expression of the cell surface markers CD44 and CD24 and it has been shown that primary human breast cancer cells with a $CD44^+/CD24^-$ phenotype resulted in increased tumour formation *in vivo* [46].

In this thesis, the effect of treatment with the different compounds was investigated on the putative cancer stem cell population $CD44^+CD24^-$ in the JIMT-1 breast cancer cell line. JIMT-1 cells were seeded in a number of Petri dishes (5 cm diameter) in 5 ml of medium at a density of 0.6 x 10^6 cells/Petri dish and then allowed to attach and grow for 24 h, prior to addition of 10 µM BENSpm, Pd-BENSpm, Pd-Spm, CPENSpm or Pt-CPENSpm. In each experiment, the number of Petri dishes seeded with cells was at least so many to be able to harvest at least three for each treatment at each time point. After seeding, the cells in each Petri dish were treated independently. After 72 h of treatment, cells were detached and dissociated from the surface by the use of Accutase treatment, thereby preventing the disruption of the cell surface proteins CD44 and CD24. After washing the live cells with ice-cold PBS containing 1% FCS, they were then incubated with the monoclonal antibodies CD44-FITC and CD24-PE for 15 minutes, while shaking on ice. Finally, cells were washed again with ice-cold PBS containing 1% FCS and identified based on their expression of the cell surface markers CD44 and CD24 using an Accuri C6 flow cytometer. The data was analysed using the CFlow software (BD Biosciences, San Jose, CA, USA).

2.14. Colony Forming Efficiency Assay

The colony forming efficiency (CFE) assay is a clonogenic test that measures the ability of single cells to form colonies when inoculated at low density. Unlike other

conventional biochemical methods, CFE is a highly sensitive assay that does not measure a specific biological effect, but instead determines the ability of a cancer cell to form a viable colony after treatment with a certain compound [281]. In addition, it has been shown that the human tumour CFE assay can be efficiently used for the screening of new and promising drugs against selected tumour types (breast, colorectal, kidney, lung, melanomas and ovarian) [282].

$$\textbf{\textit{Colony Forming Efficiency}}\ (\%) = \frac{Number\ of\ formed\ colonies}{Number\ of\ seeded\ cells}\ x\ 100 \qquad (2.5)$$

For the CFE assay, cells were seeded as described for the proliferation assay and then allowed to attach and grow for 24 h, prior to addition of the test compounds at the desired concentrations (25 μM for NSpd, Pd-NSpd or Pt-NSpd and 10 μM for BENSpm, Pd-BENSpm, Pd-Spm, CPENSpm or Pt-CPENSpm). After 72 h of treatment, cells were resuspended in agarose-containing medium (0.3% agarose) at cloning density, *i.e.* 1 cell per microliter, and seeded in 48 well plates coated with poly(2-hydroxyethyl methacrylate) (polyHEMA). After an incubation period of 14 days, the number of colonies was counted using an inverted phase contrast microscope [283].

2.15. Determination of the Intracellular Pd(II) and Pt(II) Accumulation

Inductively Coupled Plasma Mass Spectrometry (ICP-MS) (Fig. 28) is a powerful technique used to obtain an accurate and precise elemental analysis through the ionisation of the elements present in the sample with inductively coupled plasma, followed by the separation and quantification of the resultant ions in a mass spectrometer.

In this study, ICP-MS was used to determine the intracellular accumulation of Pd(II) or Pt(II) in cells treated with Pd(II)- or Pt(II)-polyamine chelates. Cells were seeded in a number of Petri dishes (9 cm diameter) in 12 ml of medium at a density of 1 x 10^6 cells/Petri dish (MCF-10A) or 2 x 10^6 cells/Petri dish (JIMT-1 and L56Br-C1) and then allowed to attach and grow for 24 h, prior to addition of the test compounds at the desired concentrations (25 μM for NSpd, Pd-NSpd or Pt-NSpd and 10 μM for BENSpm, Pd-BENSpm, Pd-Spm, CPENSpm or Pt-CPENSpm). In each experiment, the number of Petri dishes seeded with cells was at least so many to be able to harvest at least three for each treatment at each time

point. After seeding, the cells in each Petri dish were treated independently. After 72 h of treatment, cells were washed with ice-cold PBS, harvested by trypsinisation, counted in a hemocytometer, pelleted by centrifugation and stored at -80°C until analysis. Prior to analysis, the pellets were digested in 65% HNO_3 for 2 h at 65°C, diluted to a 5% acid solution and finally centrifuged at 600 *g* for 14 minutes. The analysis of metal content was performed by ICP-MS (Thermo X7), as previously described [186]. The data of metal content was used to calculate the intracellular concentration of each complex (based on the corresponding stoichiometry).

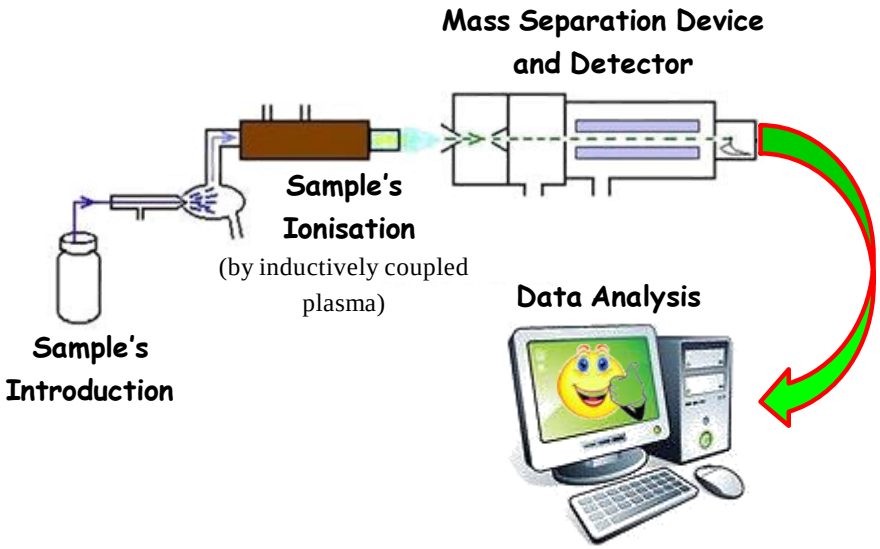

Figure 28: Schematic representation of an inductively-coupled plasma mass spectrometer for detection of Pd(II) and Pt(II).

2.16. Methods to Classify Drugs as Potential DNA Damage Induction Agents

In the present study, the two complementary methods described below were used to determine if the compounds under study caused DNA damage. This was investigated in two ways: indirectly by the evaluation of induction of genes involved in DNA damage detection and repair; and directly by investigating DNA strand breaks.

2.16.1. Anthem's Genotox Screen Assay

The Anthem's Genotox screen is a patented human cell-based technology that employs the genetically engineered HCT116 human colon carcinoma cell line. The assay was

developed as a mammalian genotoxicity screen that can be used for the detection of potential genotoxins during drug development, prior to their *in vivo* evaluation. In addition, the genetically engineered cell line allows the identification of pathways activated by treatment with compounds by the use of particular reporter genes. A single cell clone of the HCT116 cell line carries the Genotox early-sensor cassettes. The cassette includes the p21 and GADD153 promoters and p53 response elements and are respectively and operatively linked to Renilla luciferase, firefly luciferase and β-galactosidase reporter genes.

In this study, the Anthem's *in vitro* reporter-based Genotox assay was applied to elucidate if the compounds were genotoxic and to get an insight into which molecular pathways were activated. Shortly, 1.3 x 10^4 Genotox early-sensor HCT116 cells were seeded per well in 96-well plates 16 h before tested compound treatment. The cells were incubated in replicates with five concentrations (1, 10, 25, 50 and 100 µM) of NSpd, Pd-NSpd, Pt-NSpd, BENSpm or Pd-BENSpm. Aminoguanidine hemisulfate was added to the FCS containing cell culture medium to a final concentration of 1 mM for cells treated with NSpd, Pd-NSpd or Pt-NSpd. Cells treated with methyl methanesulfonate (400, 200 and 100 µM) were included as assay positive control and vehicle-treated (1% DMSO) cells as negative control. At 72 h post-incubation, the cells were gently washed twice with PBS and lysed using lysis buffer (750 mM HEPES, 1.25% Triton X-100, 5 mg/mL porcine gelatin, 50% glycerol and 0.25% antifoam). The cell lysates were processed for Renilla luciferase, firefly luciferase and β-galactosidase reporter assays. Briefly, 20 µl of the cell lysate was reacted with substrates (coelentrazine and D-luciferin for Renilla luciferase and firefly luciferase, respectively and ortho-nitrophenyl-β-galactoside for β-galactosidase) and assay buffers (Luciferase assay buffer: 1 M Tricine, 0.5 M $MgSO_4$, 0.5 M EDTA and 1 M DTT; β-galactosidase buffer: 60 mM Na_2HPO4, 60 mM NaH_2PO_4, 10 mM KCl and 1 mM $MgSO_4$) in white luminometer plates (for luciferase assays) or absorbance plate (for β-galactosidase activity assay). The assay plates were then read using a BioTek plate reader and the raw data were recorded. The results are expressed as average fold induction of reporter gene expression in comparison to the vehicle treated controls. The test compound is considered as genotoxic if the average fold reporter gene induction at any of the tested dose is over 1.5 fold (i.e. a 50% increase compared to vehicle treated controls).

2.16.2. Single Cell Gel Electrophoresis or Comet Assay

The Single Cell Gel Electrophoresis (SCGE) assay or Comet assay (Fig. 29) is a sensitive and fast technique used for the detection of DNA double strand breaks in individual cells [284]. This method can be employed for both *in vitro* and *in vivo* studies and allows the evaluation of DNA damage and repair, biomonitoring and genotoxicity [285].

In this study, the SCGE assay was used to investigate if compounds induced DNA strand breaks. The SCGE assay was performed as previously described [286-288].

Cells were seeded in a number of Petri dishes (5 cm diameter) in 5 ml of medium at a density of 0.3 x 10^6 cells/Petri dish (MCF-10A) or 0.7 x 10^6 cells/Petri dish (JIMT-1 and L56Br-C1) and then allowed to attach and grow for 24 h, prior to addition of the test compounds at the desired concentrations (25 μM for NSpd, Pd-NSpd or Pt-NSpd and 10 μM for BENSpm, Pd-BENSpm, Pd-Spm, CPENSpm or Pt-CPENSpm). In each experiment, the number of Petri dishes seeded with cells was at least so many to be able to harvest at least three for each treatment at each time point. After seeding, the cells in each Petri dish were treated independently. After 72 h of treatment, cells were harvested and, since trypsin itself induces DNA damage, special attention was given to using an exact trypsinisation time. The cells were then counted in a hemocytometer, pelleted and diluted in low melting agarose. The mixture was added to a Gel Bond® membrane and it was allowed to solidify completely, followed by the addition of an extra agarose layer. This cell-containing gel was first incubated in lysis buffer for 1 h in the dark (to expose the nucleoid) and then in a high pH electrophoresis buffer (to unwind the DNA helix), followed by electrophoresis that allowed the migration of DNA strand pieces towards the anode, while intact chromosomal DNA was kept intact inside the nucleoid. Finally, the samples were washed in neutralisation buffer (to renature the complementary DNA strands) and stained with ethidium bromide (EtBr), a fluorochrome that intercalates in the DNA. The comets were observed with an Olympus AX70 fluorescence microscope where damaged DNA appeared as comets, with the head constituting the nucleoid and the tail representing the migrated DNA, while an intact nucleoid without a tail corresponded to undamaged DNA. The cells were photographed with an Olympus DP50 digital camera and the images were obtained using Viewfinder Lite and Studio Lite 1.0 software (Olympus Optical Co Ltd., Japan).

The CometScore™ Freeware was used to analyse the comets in cells treated with NSpd, Pd-NSpd or Pt-NSpd. The evaluation of the DNA damage in these comets was performed by measuring the TMOM (tail moment) that corresponds to the product of the

DNA percentage in the tail by the tail length. An increase in the percentage of DNA found in the tail and the tail length reflects an increase in DNA damage.

Seven to 22 random images were captured for each sample treated with BENSpm, Pd-BENSpm, Pd-Spm, CPENSpm or Pt-CPENSpm. In each image, all nucleoids were counted by visual inspection. Then, nucleoids with comet tails were visually counted in each image. A nucleoid with comet tail was defined as a nucleoid with a visible tail independent of tail size. A mean was calculated for the images of each sample. At least 30 comets were scored for each sample. Afterwards, the mean of the samples for each treatment was calculated (in %).

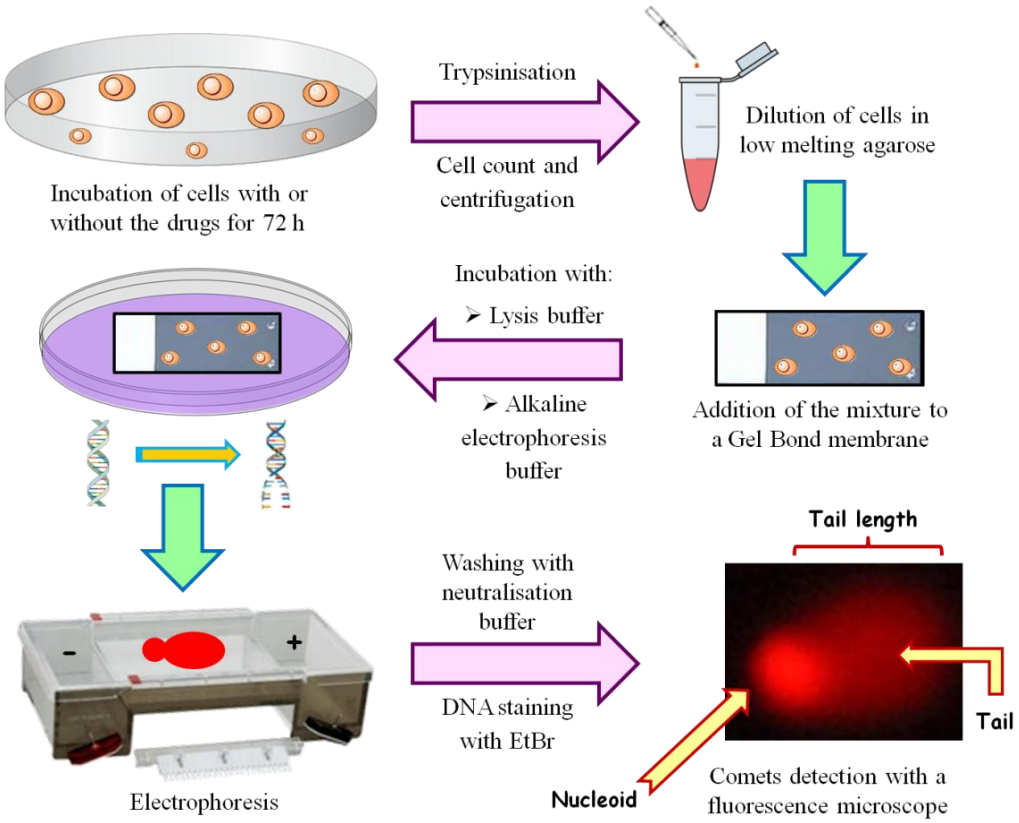

Figure 29: Schematic representation of the single cell gel electrophoresis (SCGE) assay.

2.17. GSH-Glo™ Gluthathione Assay

The GSH-Glo™ Glutathione assay is a luminescence-based method used for the detection and quantification of the total glutathione (GSH) levels in cells, tissue extracts or blood. GSH is an antioxidant largely found in eukaryotic cells that plays a critical role in

many metabolic processes. This is a simple, fast and highly sensitive assay that requires less sample than, for instance, HPLC or fluorimetric methods.

The glutathione assay was performed according to the instructions of the manufacturer (GSH-Glo™ Glutathione Assay Technical Bulletin TB369, Promega Biotech AB, Nacka, Sweden). Briefly, cells were trypsinised, counted in a hemocytometer, pelleted and resuspended in cell culture medium. Aliquots of 180 µl cell suspension containing 3000 (MCF-10A) or 8000 (JIMT-1 and L56Br-C1) cells were seeded in the wells of white, opaque flat-bottomed 96-well plates. At 48 h of drug treatment with 10 µM BENSpm, Pd-BENSpm, Pd-Spm, CPENSpm or Pt-CPENSpm, the medium was removed from the plates very carefully. Next, luciferin-NT and glutathione S-transferase were added to GSH-Glo™ reaction buffer to make GSH-Glo™ reagent, which was further added to the wells of the plates. Before a 30-minute incubation period at room temperature, the plates were swirled gently and briefly. Then, the luciferin detection reagent was added to the wells of the plates, which were again gently and briefly swirled, followed by incubation for 15 minutes at room temperature. Finally, luminescence was monitored in a Labsystems iEMS Reader MF using the DeltaSoft II v.4.14 software (Biometallics Inc., Princeton, NJ, USA).

2.18. Western Blot Analysis

Western blotting, also called immunoblotting or protein blotting, is one of the most widely used immunochemical techniques in molecular biology research. The method was introduced by Towbin and co-workers in 1979 [289] and antibodies are used to detect and identify specific proteins bound in a sample bound to a membrane. The proteins are detected mainly according to their size [289]. The method can be divided into several steps:

1) The sample is loaded on a gel and the proteins are separated according to their size by denaturing gel electrophoresis;

2) The proteins are blotted from the gel to a nitrocellulose membrane;

3) The blot is then blocked with a protein such as albumin or casein in dry milk, followed by incubation with primary antibodies, which are able to bind to the protein of interest and then secondary antibodies;

4) The proteins are detected on the membrane surface by addition of enhanced chemiluminiscence (ECL) solution, which is converted to light by the secondary antibodies labelled with horseradish peroxidase. The intensity of the signal obtained correlates to the abundance of antigen (protein of interest) on the membrane.

In this work, Western blot analysis was used to investigate to which extent polyamine depletion affected the expression of the AzI protein in different human breast cell lines. Cells were seeded in a number of replicate cultures and were allowed to attach and grow for 24 h, prior to addition of the test compounds to the desired concentrations. After 24, 48 and 72 h of treatment, cells were collected, counted in a hemocytometer, pelleted at 700x *g* for 10 minutes at 4°C and stored at -80°C until analysis. Then, a known number of pelleted cells were resuspended in sample loading buffer (200 µl per 10^6 cells; 62.5 mM Tris-HCL, pH 6.8, 20% glycerol, 2% sodium dodecyl sulfate, 5% β-mercaptoethanol and 0.5% bromophenol blue), sonicated, heat-denaturated at 95°C for 5 minutes and then put on ice immediately. Aliquots of the cell lysates were loaded into wells of precast polyacrylamide gels (according to the cell number) and the proteins were electrophoretically separated under reducing conditions (according to size) in a Xcell *Sure Lock*™ Mini-Cell system at a constant 150 V for 1.5 hours, in NuPAGE© MOPS running buffer. Separated proteins were transferred to ECL® nitrocellulose membranes by use of the iBlot™ Dry Blotting system. The membranes were incubated with 5% non-fat dry milk in PBS-T (PBS containing 0.05% Tween 20, a polyethylene glycol sorbitan monolaurate) for 2.5 h at room temperature, in order to block remaining hydrophobic binding sites on the membrane and, consequently, to prevent nonspecific binding of the antibodies to the membrane surface. After an overnight incubation with the AzI primary antibody (kindly donated by Dr. Senya Matsufuji) at 4ºC, the membranes were washed and incubated, for 1 h at room temperature, with horseradish peroxidase-conjugated goat anti-mouse IgG secondary antibody (1:20000) in PBS-T. The protein bound antibodies were detected as bands with the ECL™ Advance Blotting Detection Kit. The ChemiDoc XRS system and the Quantity One software (Bio-Rad Laboratories Inc., Hercules, CA, USA) were used for imaging.

2.19. Statistical analysis

A two-tailed Student's t-test was used to assess the differences between the control and the treated samples. A 1-way ANOVA followed by the Newman-Keuls Multiple Comparison test was used for the statistical significance evaluation. Differences were considered statistically significant for $p < 0.05$.

III - Results

“Somewhere, something incredible is waiting to be known.”

Carl Sagan

3. Results

The very first step of this study consisted in the synthesis of novel Pd(II) and Pt(II) complexes with polyamine analogues, following optimised procedures previously used within the QFM-UC research group (for the synthesis of Pd(II) and Pt(II) complexes with biogenic polyamines).

3.1. Characterisation of the Compounds by Vibrational Spectroscopy

Vibrational spectroscopy techniques – FTIR and Raman – were used to structurally characterise the polyamine analogues BESpm, NSpd, BENSpm and CPENSpm and their newly synthesised complexes with Pd(II) and Pt(II) – Pd-NSpd, Pt-NSpd, Pd-BENSpm and Pt-CPENSpm. In addition, the most stable structures for the polyamine analogues under study were obtained through quantum mechanical methods, as the lowest energy geometries among the several possible conformations calculated for each molecule.

A full spectral assignment was performed for BESpm (Fig. 30), BESpm and CPENSpm (in the solid state) (Fig. 31) and for NSpd (Fig. 32) in the light of the data obtained by quantum mechanical methods – optimised geometries and predicted vibrational pattern. A good agreement was found between experimental and calculated wavenumbers, after scaling according to Merrick and co-workers [252] in order to correct for anarmonicity effects. The Raman spectra previously gathered for spermine (Spm) and spermidine [203] were used for comparison, which allowed an accurate and clear assignment of the features corresponding to the common molecular core between the biogenic polyamines and its analogues BESpm, BENSpm, CPENSpm and NSpd (Fig. 5). A quite good agreement was obtained in all cases (Tabs. 8 to 11).

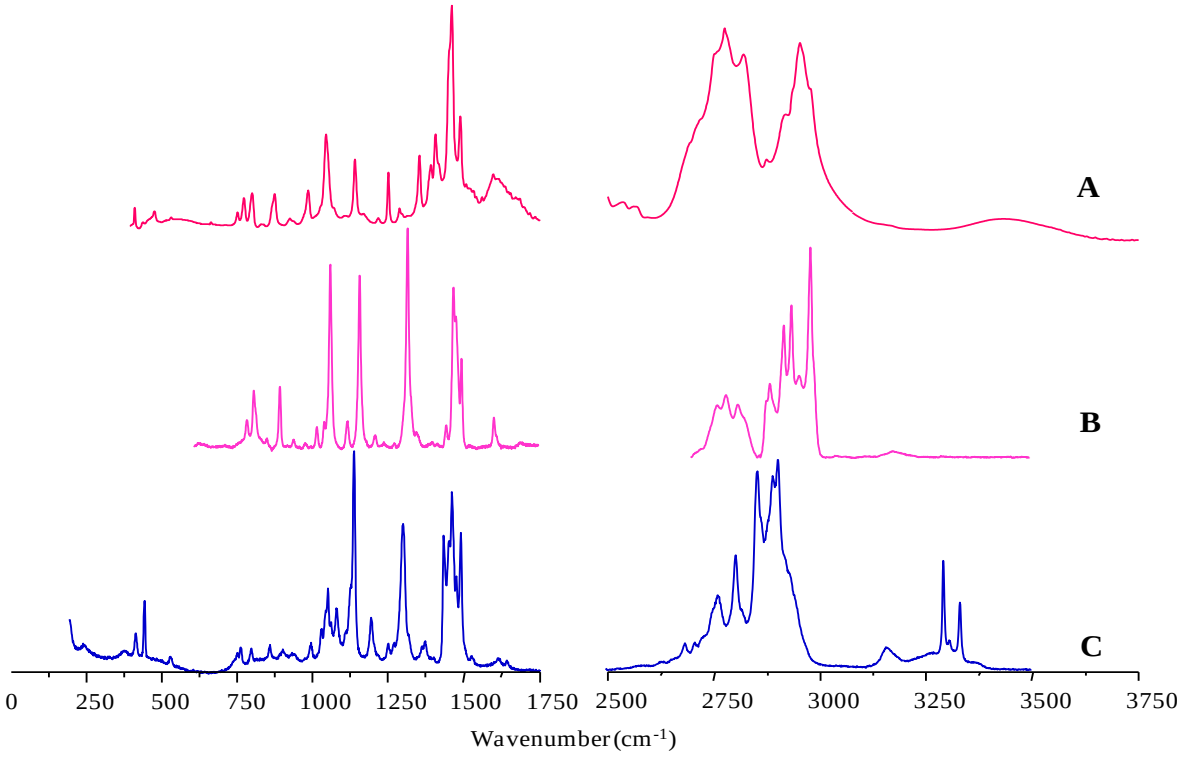

Figure 30: Experimental FTIR (A) and Raman (B) spectra for BESpm. The experimental Raman spectrum for Spm (**C**) is included for comparison [203].

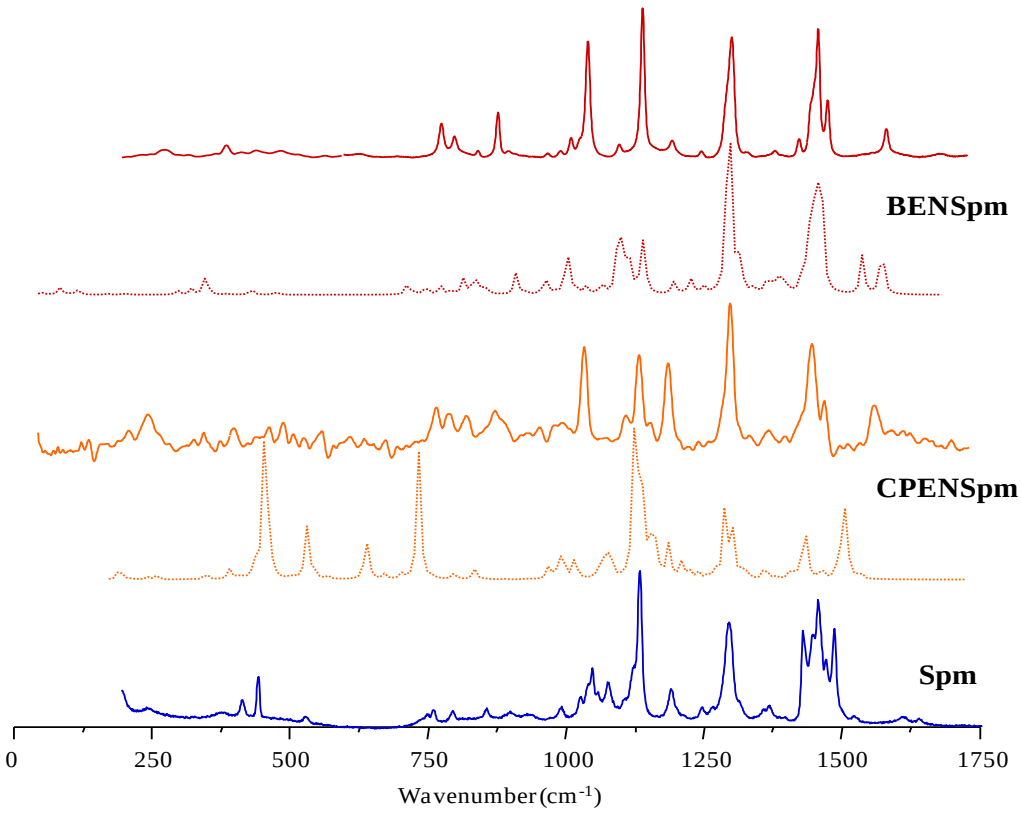

Figure 31: Experimental (solid line) and calculated (dotted line) Raman spectra for BENSpm and CPENSpm. The experimental Raman spectrum for Spm is included for comparison [203].

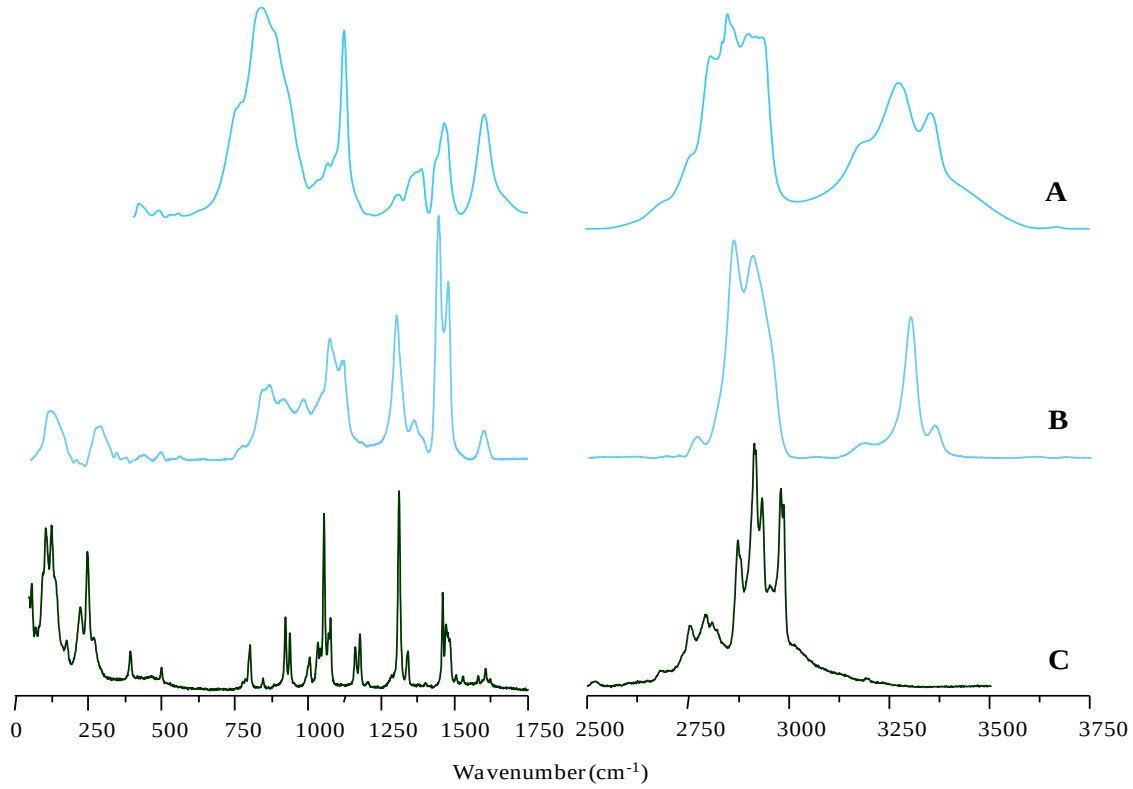

Figure 32: Experimental FTIR (A) and Raman (B) spectra for NSpd (pure liquid). The experimental Raman spectrum for spermidine (**C**) is included for comparison [203].

Tabs. 8 to 11 comprise the main vibrational features for the modified polyamines (Figs. 30 to 35): NH_2 symmetric and antisymmetric stretching vibrations, detected at *ca.* 3400 cm^{-1} (BESpm), at *ca.* 3100 (BENSpm and CPENSpm) and between 3180 and 3370 for NSpd; NH_2/NH_3 deformation modes at about 1600 cm^{-1} (as theoretically predicted); CH_2 deformations (twisting and wagging) as intense features from 1300-1400 (BESpm), 1450-1500 cm^{-1} (BENSpm and CPENSpm) and 1200-1400 cm^{-1}; strong signals predominantly due to NH_2/NH_3 deformations (also containing a contribution from CH_2 deformations), detected at *ca.* 1260 and 1200 cm^{-1} for BENSpm and CPENSpm, and between 1113 and 1126 cm^{-1} for NSpd; the NH_2 rocking vibration, in turn, was observed at 745-970 cm^{-1} for the terminally alkylated polyamines, while for NSpd a broad band, centred at 770 cm^{-1} was detected (particularly intense in infrared), encompassing both NH_2 and NH_3 rocking modes; CC and CN stretchings observed between 900 and 1100 cm^{-1} (for all the polyamine analogues). For the alkylated molecules BESpm, BENSpm and CPENSpm, a characteristic deformation mode of the terminal methyl group appeared around 1390-1500 cm^{-1} (Tabs. 8, 10 and 11). All the modified polyamines presently studied are solids, except for NSpd which is a liquid at room temperature leading to an expected broadening of the FTIR and Raman signals (Fig. 32).

Table 8: Main experimental (solid state) and calculated Raman and FTIR wavenumbers (cm^{-1}) for BESpm.

Experimental		[a]Calculated	[b]Approximate description
FTIR	Raman		
		3341	$\nu_{as}(NH_2) + \nu_{as}(NH_2)$
3433		3341	$\nu_{s}(NH_2) + \nu_{s}(NH_2)$
2978	2975	3028	$\nu_{as}(CH_3)$
2953	2948	3012	$\nu_{as}(CH_2) + \nu_{as}(CH_3)$
	2930	3012	$\nu_{as}(CH_2) + \nu_{as}(CH_3)$
2920	2913	2976	$\nu_{as}(CH_2)$
	2880	2947	$\nu_{s}(CH_2)$
2874	2871	2935	$\nu_{s}(CH_3) + \nu_{s}(CH_3)$
	2855	2919	$\nu_{s}(CH_2)$
2820	2804	2919	$\nu_{s}(CH_2)$
2775	2776	2911	$\nu_{s}(CH_2)$
2752	2755	2909	$\nu_{s}(CH_2)$
1596	1594	1571	$\delta_{sciss}(NH_2) + \delta_{sciss}(NH_2)$
		1519	$\delta_{sciss}(NH_2)$
1488	1488	1470	$\delta_{sciss}(NH_2) + \delta_{sciss}(CH_2)$
	1469	1466	$\delta_{sciss}(CH_2)$
1460	1461	1461	$\delta_{sciss}(CH_2) + \delta_{as}(CH_3)$
1451		1454	$\delta_{sciss}(CH_2) + \delta_{as}(CH_3)$
	1437	1438	$\omega(NH_2)$
1406	1407	1408	$t(NH_2) + \omega(CH_2)$
1391	1390	1392	$t(NH_2) + t(CH_2) + \omega(CH_2) + \delta_{as}(CH_3)$
1354	1336	1339	$\omega(CH_2) + t(CH_2)$
	1310	1313	$t(CH_2) + t(CH_2)$
1252	1264	1262	$\omega(NH_2) + \omega(CH_2)$
	1230	1231	$\omega(NH_2) + \omega(CH_2) + r(CH_2)$
	1201	1199	$r(CH_2)$
1142	1149	1154	$r(NH_2) + r(CH_2)$
	1110	1105	$t(NH_2) + t(CH_2)$
1047	1052	1083	$\nu(CC) + \nu(CN)$
	1031	1031	$\nu(CC) + \nu(CN)$
988	1008	984	$\nu(CC) + \nu(CN)$
	967	971	$\nu(CC) + \nu(CN)$
928	931	939	$\nu(CC) + \nu(CN)$
878	558	892	$r(NH_2) + r(CH_2) + t(CH_2) + \delta_{as}(CH_3)$
	842	851	$r(NH_2) + r(CH_2) + t(CH_2)$
804	798	811	$r(NH_2) + r(CH_2) + t(CH_2)$
777	776	777	$r(NH_2) + r(CH_2) + \delta_{as}(CH_3)$
756		748	$r(CH_2)$
483		488	$\delta(CCN)_{long}$
418		423	$\delta(CCN)_{long}$

[a]At the B3LYP/6-31G** level. Wavenumbers above 600 cm^{-1} are scaled by 0.9614 [252] (IR intensities in $km.mol^{-1}$. Raman scattering activities in $Å.amu^{-1}$). **ν** – stretching; **δ** – in-plane deformation; **t** – twisting; **r** – rocking; **ω** – wagging; **sciss** – scissoring; **s** – symmetric; **as** – antisymmetric; **long** – longitudinal.

Table 9: Main experimental and calculated Raman and FTIR wavenumbers (cm^{-1}) for NSpd, Pt-NSpd and Pd-NSpd.

NSpd			Pt-NSpd		Pd-NSpd		Approximate description
Exp.		[a]Cal	Exp.		Exp.		
FTIR	Raman		FTIR	Raman	FTIR	Raman	
3362	3362	3442	3262	3267	3269	3283	$\nu_s(NH_3)$
3278	3302	3346	3248	3250	3224	3227	$\nu_s(NH_3) + \nu_s(NH_2)$
3187	3188	3220	3215	3219	3172	3172	$\nu_{as}(NH_3) + \nu_{as}(NH_2)$
		3217	3148	3152	3154	3158	$\nu_s(NH_2)$
2939	2955	3137	2942	2942	2939	2940	$\nu_{as}(CH_2)$
2905	2909		2877	2915	2874	2903	$\nu_{as}(CH_2)$
2852	2861		2854	2878	2846	2876	$\nu_s(CH_2)$
1600	1600		1608		1605		$\delta_{sciss}(NH_2)$
1466	1478	1470	1462	1459	1460	1459	$\delta_{sciss}(CH_2)$
1439	1444	1410	1446		1449		$\delta_{sciss}(CH_2)$
1365	1360						$\delta_{sciss}(CH_2)$
1307	1300	1252	1258		1249		$\delta_{sciss}(CH_2) + t(CH_2)$
			1172	1170	1171		$\omega(CH_2) + t(CH_2) + \delta(NH_3) + \nu(CC)$
1126	1113	1186	1148		1146	1143	$\omega(CH_2) + t(CH_2) + \delta(NH_3) + \nu(CC)$
1070	1070	1112	1064	1036	1053	1062	$\omega(CH_2) + t(CH_2)$
			1035		1031		$\omega(CH_2) + t(CH_2)$
979	980	1018					$\nu(CC) + \nu(CN)$
915	915	970					$t(CH_2) + \delta_s(NH_3) + \delta_{sciss}(NH_2) + \nu(CC)$
884	865	906					$\delta_{sciss}(NH_2) + \omega(NH_2)$
843	841	880					$r(NH_3)$
766	772	766					$r(CH_2) + r(NH_3) + r(NH_2)$
557	554						$r(NH_3)$
			522	536 ([b]524)		522	$\nu_s(N^cMN)$
			483	482 ([b]508)	498	498	$\nu_{as}(N^cMN)$
				391		388	$\nu(Cl^cMCl)$
				333 ([b]323)		340	$\nu_s(Cl^cMCl)$
				316 ([b]317)		307	$\nu_{as}(Cl^cMCl)$
	281						[d]LAM
				229		225	δ(NMN)
				171		173	δ ClMCl)
	118						[d]TAM

[a]At the B3LYP/6-31G** level. Wavenumbers above 600 cm^{-1} are scaled by 0.9614 [252] (IR intensities in $km.mol^{-1}$. Raman scattering activities in $Å.amu^{-1}$). **ν** – stretching; **δ** – in-plane deformation; **t** – twisting; **r** – rocking; **ω** – wagging; **sciss** – scissoring; **s** – symmetric; **as** – antisymmetric. [b]From [290]. [c]M=Pt(II) or Pd(II). [d]LAM and TAM refer to longitudinal and transverse acoustic modes, respectively.

Table 10: Main experimental (solid state) and calculated Raman and FTIR wavenumbers (cm^{-1}) for BENSpm and Pd-BENSpm.

BENSpm			Pd-BENSpm		Approximate description
Exp.		[a]Calc.	Exp.		
FTIR	Raman		FTIR	Raman	
3147	3167	3342	3221	3229	$\nu_s(NH_2)$
3123					$\nu_s(NH_2)$
3083	3031	3028			$\nu_{as}(CH_3)$
		3011			$\nu_{as}(CH_2) + \nu_{as}(CH_3)$
2989	2976	2975	2981	2992	$\nu_{as}(CH_2)$
2951	2932	2947	2971	2968	$\nu_s(CH_2)$
		2934			$\nu_s(CH_3)$
2927	2909	2923	2923	2923	$\nu_s(CH_2)$
2889	2881		2865	2865	$\nu_s(CH_2)$
1635	1694		1625	1623	$\delta_{sciss}(NH_2)$
1596	1595	1623			$\delta_{sciss}(NH_2) + \delta_{sciss}(CH_2)$
1490	1488	1511			$\delta(CH_3)$
1461	1471	1500	1463	1455	$\omega(CH_2) + t(CH_2) + \omega(NH_2) + \delta(NH_2)$
1405	1437	1468	1439	1433	$\omega(CH_2) + t(CH_2) + \omega(NH_2) + \delta(NH_2)$
1394	1392	1456	1386	1388	$\delta_{sciss}(CH_2) + t(NH_2)$
1357		1405	1354	1355	$\delta_{sciss}(CH_2) + t(CH_2) + \omega(CH_2)$
	1312	1363	1306	1307	$\omega(CH_2) + t(CH_2) + t(NH_2)$
			1296	1293	$\omega(CH_2) + \omega(NH_2) + \delta(NH_2)$
1264	1257	1309	1281	1252	$\omega(CH_2) + t(CH_2) + t(NH_2)$
			1175	1178	$\omega(CH_2) + r(NH_2)$
1152	1149	1173	1146	1141	$\nu(CC) + \nu(CN)$
1050	1049	1084	1069	1074	$\nu(CC) + \nu(CN)$
1035	1035	1075	1038	1039	$\nu(CC) + \nu(CN)$
			1023	1014	$\nu(CC) + \nu(CN)$
999	999	1023	993	989	$\nu(CC) + \nu(CN)$
			966	936	$t(CH_2) + r(CH_2) + r(NH_2)$
906	884	931	892	887	$t(CH_2) + r(CH_2) + r(NH_2)$
			835	833	$r(NH_2)$
805	804	838	804	809	$r(CH_2) + r(NH_2)$
782	780	778	745	748	$r(CH_2) + r(NH_2)$
			697	700	$r(CH_2)$
				563	$\nu_s(NPdN)$
				505	$\nu_{as}(NPdN)$
				487	$\nu_{as}(NPdN)$
				424	$\nu_s(ClPdCl)$
				325	$\nu_{as}(ClPdCl)$
				295	$\delta(NPdN)$
				222	$\delta(ClMCl)$

[a]At the B3LYP/6-31G** level. Wavenumbers above 600 cm^{-1} are scaled by 0.9614 [252] (IR intensities in $km.mol^{-1}$. Raman scattering activities in $Å.amu^{-1}$). **ν** – stretching; **δ** – in-plane deformation; **t** – twisting; **r** – rocking; **ω** – wagging; **sciss** – scissoring; **s** – symmetric; **as** – antisymmetric.

Table 11: Main experimental (solid state) and calculated Raman and FTIR wavenumbers (cm^{-1}) for CPENSpm and Pt-CPENSpm.

BENSpm			Pd-BENSpm		Approximate description
Exp.		[a]Calc.	Exp.		
FTIR	Raman		FTIR	Raman	
3129		3330	3139	3165	$\nu_{as}(NH_2)$
3072	3070	3228		3061	$\nu_{s}(NH_2)$
		3215			$\nu_{as}(CH_3)$
2973	2973	3231	2960	2995	$\nu_{as}(CH_2)$
2935	2934	3135	2937	2939	$\nu_{s}(CH_2)$
	2907	3134			$\nu(CH)^{cyclop}$
		3121			$\nu_{s}(CH_3)$
2864	2878	2949	2879	2880	$\nu_{s}(CH_2)$
	2808	2885			$\nu(CH/CH_2)^{cyclop}$
1592			1608		$\delta_{sciss}(NH_2)$
1575	1577				$\delta_{sciss}(CH_2) + \delta_{sciss}(NH_2)$
1481	1485	1500			$\delta(CH_3)$
1452	1463		1465	1461	$\omega(CH_2) + t(CH_2) + \delta(NH_2) + \omega(NH_2)$
1408	1414	1477	1455	1451	$\delta_{sciss}(CH_2)$
1391	1385	1464	1386	1373	$\delta_{sciss}(CH_2)$
1355	1349	1391			$\delta_{sciss}(CH_2) + t(CH_2)$
	1314	1333	1320	1310	$\omega(CH_2) + t(CH_2) + t(NH_2)$
1263	1256	1289			$\omega(CH_2) + t(CH_2) + t(NH_2)$
1212	1201	1199	1191	1196	$\omega(CH_2) + t(CH_2)^{cyclop} + t(NH_2)$
1148	1147	1175	1159		$\omega(CH_2) + t(NH_2)$
1049	1048	1104	1048		$\nu(CC) + \nu(CN)$
1027		1033			$\nu(CC) + \nu(CN)$
1000		1013			$\nu(CC) + \nu(CN)$
	884	920	878		$t(CH_2) + r(CH_2) + t(NH_2) + \omega(NH_2)$
830	833	858	834	831	$t(CH_2) + r(CH_2) + t(NH_2)$
800	802	807	808	810	$t(CH_2)^{cyclop}$
777	778	786	773	779	$r(CH_3) + r(NH_2)$
				516	$\nu_{s}(NPtN)$
				483	$\nu_{as}(NPtN)$
				386	$\nu_{s}(ClPtCl)$
				368	$\nu_{s}(ClPtCl)$
				321	$\nu_{as}(ClPtCl)$
	252				$\nu(CC)^{cyclop}$
				220	$\delta(NPtN)$
	216				[b]LAM
				197	$\delta(ClPtCl)$
				168	$\delta(ClPtCl)$

[a]At the B3LYP/6-31G** level. Wavenumbers above 600 cm^{-1} are scaled by 0.9614 [252] (IR intensities in $km.mol^{-1}$. Raman scattering activities in $Å.amu^{-1}$). **ν** – stretching; **δ** – in-plane deformation; **t** – twisting; **r** – rocking; **ω** – wagging; **sciss** – scissoring; **s** – symmetric; **as** – antisymmetric. [b]LAM refers to a longitudinal acoustic mode.

Bands from the rocking deformations of the terminal NH_3 groups were clearly detected for NSpd at 841/843 cm^{-1} by both FTIR (very intense band) and Raman (Table 9, Fig. 32), and were absent in BESpm, BENSpm and CPENSpm (Figs. 30, 33 and 34), while the bands assigned to NH_2 symmetric and antisymmetric deformations were observed (as theoretically predicted) at *ca.* 1600 cm^{-1} for the four modified polyamines.

Furthermore, the cyclopropyl-containing polyamine, CPENSpm, displayed several bands characteristic from this group (Table 11): the CH_2 twisting modes, at 1201 cm^{-1}, quite intense in the Raman spectrum (Table 11, Fig. 34) while hardly observed by infrared; methylene deformations at 800 cm^{-1}, present in both the FTIR and the Raman pattern (Fig. 34); and the ring C–C stretching, detected by Raman at 252 cm^{-1} (Fig. 34). As opposed to NSpd, the Raman bands corresponding to the amine stretching modes were not detected.

In addition, some acoustic modes were detected in the Raman spectra presently obtained (Tabs. 9 and 11): the symmetric LAM (accordion mode) at 281 and 216 cm^{-1} for NSpd and CPENSpm, respectively (Figs. 32 and 34), and one TAM was observed for NSpd at 120 cm^{-1} (Fig. 32).

Regarding the newly synthesised chelates, upon metal binding, the vibrational pattern of the ligands underwent clear changes: no bands assigned to the NH_2/NH_3 groups were detected, namely $\delta(NH_2)$ around 1600 cm^{-1}, as well as $r(NH_3)$ (Figs. 33, 34 and 35) (*e.g.* for NSpd, $\delta(NH_3)$ at *ca.* 555/770 cm^{-1} and $\delta(NH_3)$ at *ca.* 1120 cm^{-1}). Additionally, a marked shift of NH stretching bands to higher frequencies were plainly detected by FTIR for the terminally alkylated ligands BENSpm and CPENSpm (Figs. 33 and 34, second region) – ascribed to the change from $\nu(NH_2)$/ $\nu(NH_3)$ symmetric and antisymmetric vibrations, in the free ligands, to the corresponding modes for the metal-coordinated amine groups. For the non-alkylated polyamine NSpd, in turn, these features ($\nu(NH_2)$/ $\nu(NH_3)$) were detected for both the complex and the uncoordinated molecule, undergoing a significant intensity decrease upon metal binding (Fig. 35). Concomitantly, distinct new signals appeared in the Raman pattern below *ca.* 600 cm^{-1}, characteristic of the metal coordination profile: deformations, between 165 and 225 cm^{-1} (δ(Cl–M–Cl)) and 220 to 295 cm^{-1} (δ(N–M–N)), as well as symmetric and antisymmetric (Cl–M–Cl) and (N–M–N) stretching modes, between 305 to 425 cm^{-1} and 480 to 565 cm^{-1}, respectively (Tabs. 9 to 11). A Pd for Pt substitution (in the NSpd complexes) was found to lead to a change in the band profile assigned to the symmetric and antisymmetric (metal–N) stretching modes – either a broad feature or a well resolved two-band pattern in the 460–540 cm^{-1} interval (Fig. 35).

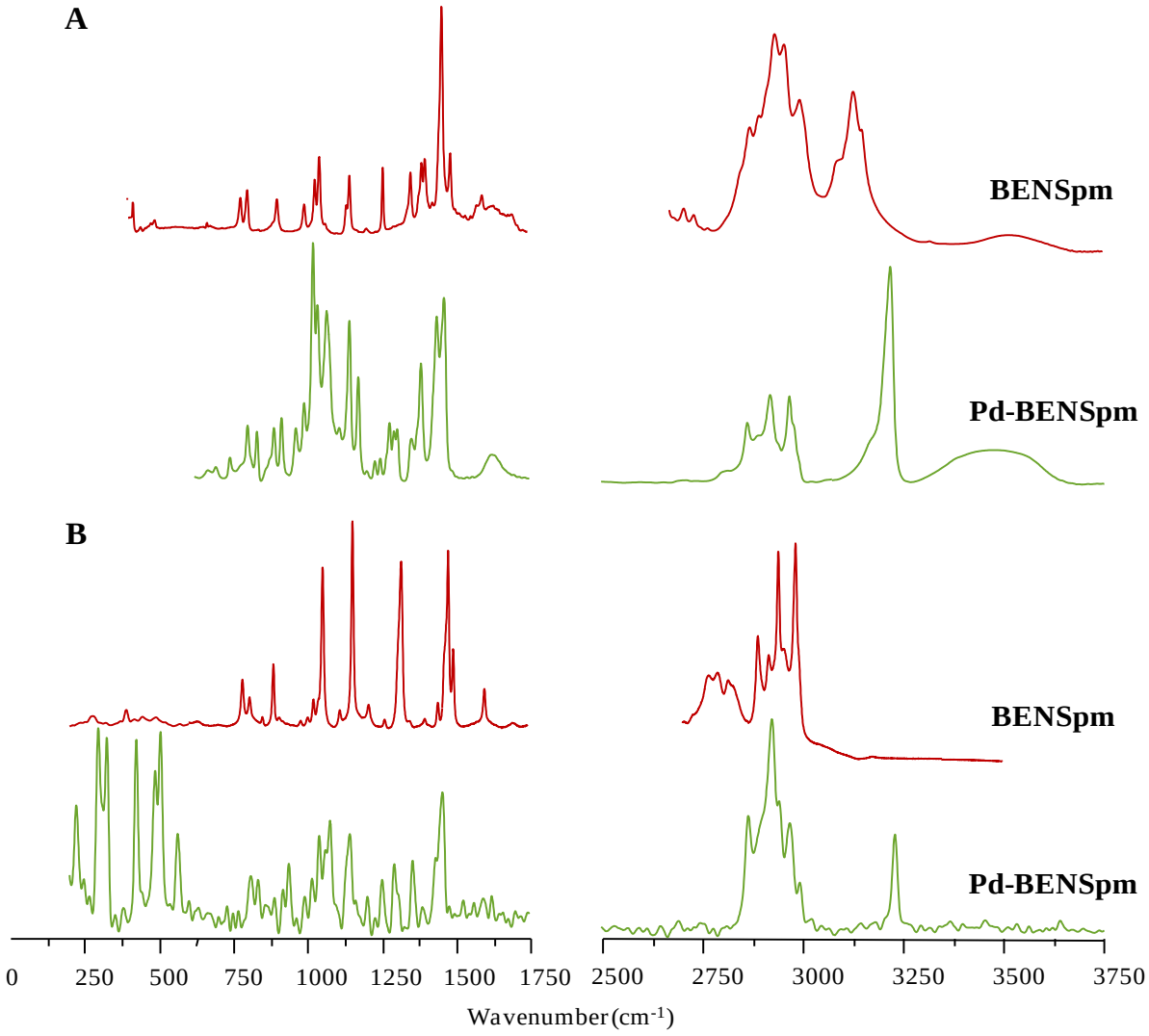

Figure 33: Experimental FTIR (A) and Raman (B) spectra for BENSpm and Pd-BENSpm.

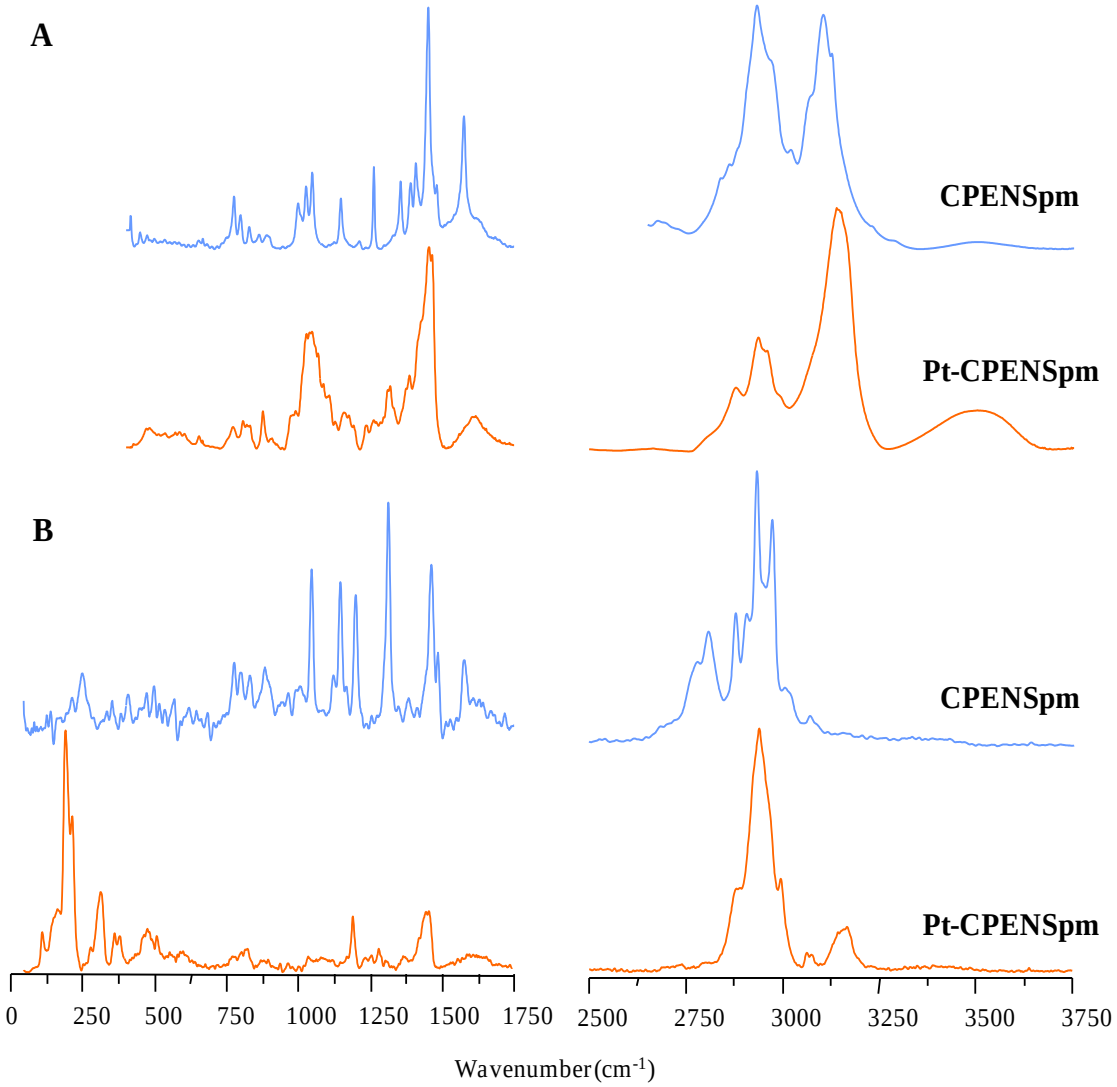

Figure 34: Experimental FTIR (A) and Raman (B) spectra for CPENSpm and Pt-CPENSpm.

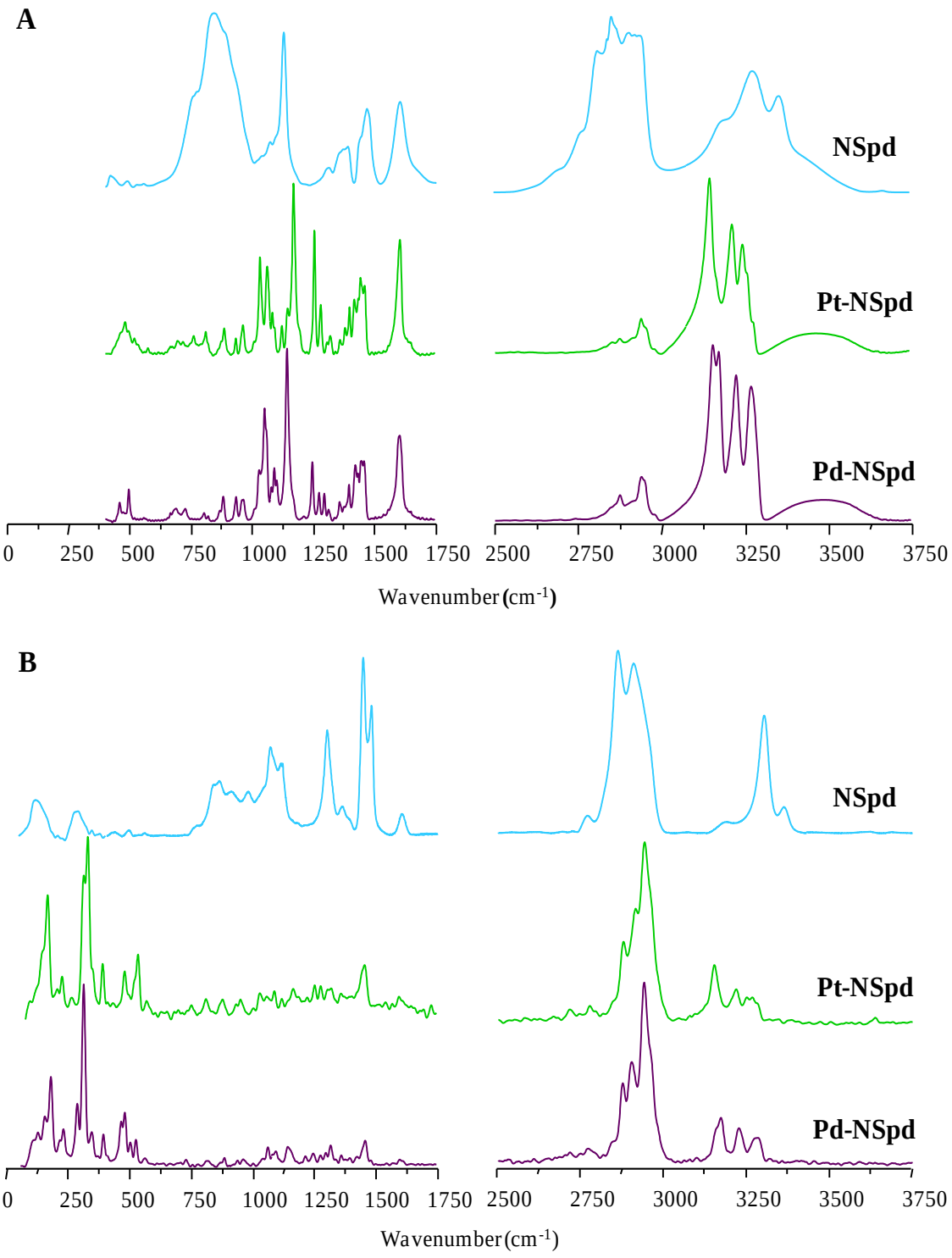

Figure 35: Experimental FTIR (A) and Raman (B) spectra for NSpd, Pt-NSpd and Pd-NSpd.

3.2. Evaluation of the Cellular Impact

After the structural characterisation of the polyamine analogues and their Pd(II) and Pt(II) complexes by vibrational spectroscopy, their effects on a range of human breast cancer cell lines were anaylsed using a variety of cell biological techniques.

This section is divided in two parts. First the antiproliferative effect of the polyamine analogue (NSpd) was tested on various breast cancer cell lines and one normal-like breast cell line, and compared with those of its Pd(II) and Pt(II) chelates. Second the antiproliferative effect of two other polyamine analogues (BENSpm and CPENSpm) and their Pd(II) or Pt(II) complexes were analysed using the same breast cell lines and the results interpreted in the light of their structural features.

3.2.1. NSpd, Pd-NSpd and Pt-NSpd

In the present work, the spermidine analogue NSpd and its newly synthesised trinuclear Pd(II) and Pt(II) complexes, Pd-NSpd and Pt-NSpd [190], were evaluated regarding their antiproliferative activity against four different human breast cancer cell lines (JIMT-1, L56Br-C1, MCF-7 and MDA-MB-231) and one immortalised normal-like breast epithelial line (MCF-10A).

MTT Reduction

In order to evaluate the toxicity of NSpd, Pd-NSpd or Pt-NSpd against the five cell lines investigated, a MTT dose response test that is assumed to reflect cell number was performed, using concentrations ranging from 0.1 to 100 μM [112,291]. This assay showed that MTT reduction decreased in all cases when increasing both concentration as well as time of treatment, although the reactions to each treatment varied between the five cell lines (Fig. 36). The dose response curves show that while Pt-NSpd was found to be the least cytotoxic compound, Pd-NSpd and NSpd were more toxic and gave in general similar dose responses. The results also show that L56Br-C1 was the most sensitive cell line (Fig. 36 **D**–**F**). The effects of drug treatment were more obvious between 10 and 100 μM concentrations, for both 48 and 72 h of treatment.

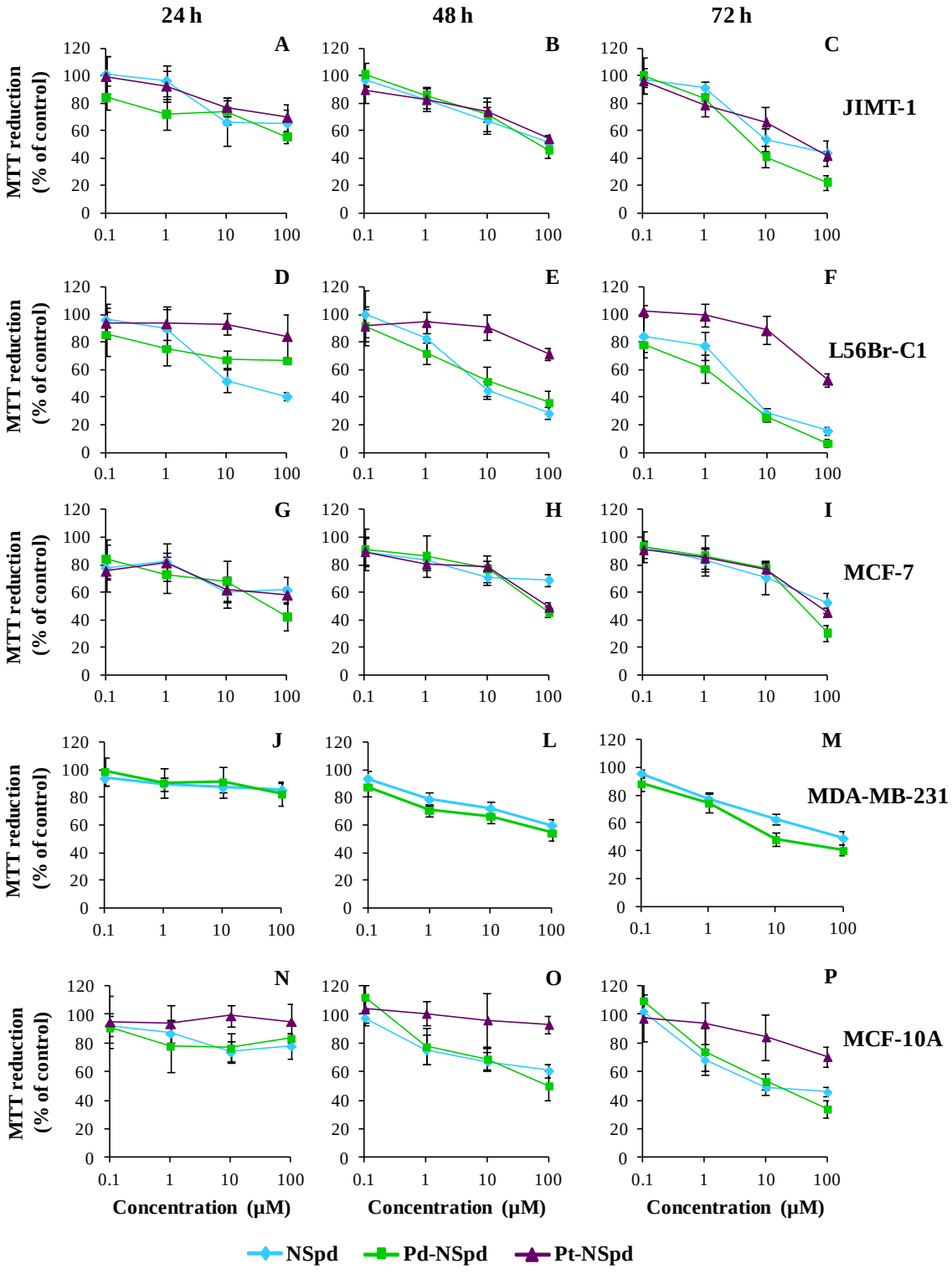

Figure 36: Dose response effect of NSpd, Pd-NSpd or Pt-NSpd treatment. The four breast cancer cell lines JIMT-1 (**A**–**C**), L56Br-C1 (**D**–**F**), MCF-7 (**G**–**I**), MDA-MB-231 (**J**–**M**) and the normal-like breast cell line MCF-10A (**N**–**P**) were used. Twenty-four h after seeding of cells in 96-well plates, the polyamine analogue and its complexes were added to the final concentrations shown in the figure and were treated for 24, 48 and 72 h, before evaluation using an MTT assay. The results are expressed as % of control (n=12 independent samples from two independent experiments) with bars representing ± SD.

Effect of Short and Long Time Treatment on Cell Proliferation

Based on the dose response curves, we decided to compare 25 and 100 µM concentrations for further investigations. We examined the effect of NSpd, Pd-NSpd or Pt-NSpd treatment on cell proliferation using both concentrations. The proliferation of MCF-10A cells (Fig. 37 **D**) was only slightly affected by treatment with a 25 µM concentration of NSpd, Pd-NSpd or Pt-NSpd, while in JIMT-1 and MCF-7 cells the proliferation was more affected than in MCF-10A cells and differential effects of the drugs were clearly discernible (Fig. 37 **A**, **C**). L56Br-C1 cells were the most sensitive cells to these compounds and there was even a decrease in cell number implicating cell death after 72 h of treatment with NSpd and Pd-NSpd (Fig. 37 **B**). Figure 38 shows the morphology of the cells after 72 h of treatment with the compounds. L56Br-C1 cells had to be rinsed with PBS to remove all dead floating cells before photography of attached cells that were found in small patches.

For the 100 µM concentration, the results obtained exhibited more distinct differences between the tested compounds and the cell lines than after treatment with a 25 µM concentration (Fig. 37 **E**–**I**). MCF-10A cells were still the least sensitive cells with smallest differences between the various treatments (Fig. 37 **H**). Pd-NSpd treatment appeared to totally inhibit cell proliferation in JIMT-1 and MCF-7 cells almost immediately, while Pt-NSpd and NSpd slowed cell proliferation in these cell lines, with the former being slightly more efficient than the later (Fig. 37 **E**, **G**). In L56Br-C1 cells, treatment with 100 µM NSpd, Pd-NSpd or Pt-NSpd immediately inhibited cell proliferation and a marked reduction in cell number was observed in Pd-NSpd-treated cultures (Fig. 37 **F**), implicating cell death. Proliferation of MDA-MB-231 cells was clearly reduced by treatment with NSpd and Pd-NSpd, the latter displaying a stronger antiproliferative effect (Fig. 37 **I**).

The effect of repeated cycles of 72 h treatment with 25 µM NSpd, Pd-NSpd or Pt-NSpd followed by 96 h of drug withdrawal, on cell proliferation (Fig. 37 **J**–**M**) was also investigated. MCF-10A normal-like breast cells were not affected by repeated treatment cycles with either NSpd or Pt-NSpd and were only slightly affected by Pd-NSpd (Fig. 37 **M**). In L56Br-C1 cells, repeated treatment cycles with NSpd or Pd-NSpd resulted in unchanged and decreasing cell numbers, respectively, compared to the number of cells seeded at time 0, while repeated treatment with Pt-NSpd only slightly affected the cell number compared to control (Fig. 37 **K**). In JIMT-1 and MCF-7 cells, the accumulated cell number was lower for cells treated with either NSpd or Pd-NSpd, but not with Pt-NSpd, when compared with untreated cells, especially after the second treatment cycle (Fig. 37 **J**, **L**).

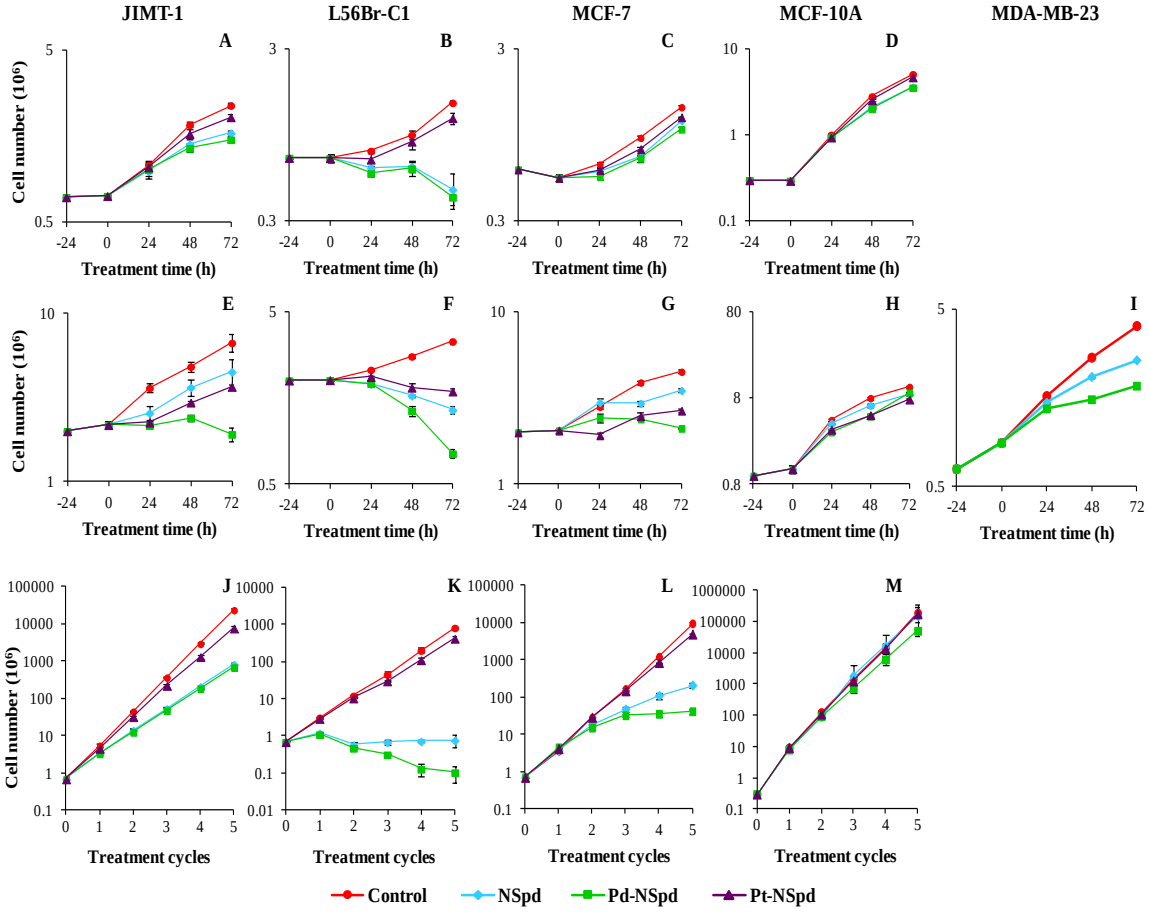

Figure 37: Effect of NSpd, Pd-NSpd or Pt-NSpd treatment on the proliferation of JIMT-1, L56Br-C1, MCF-7, MCF-10A and MDA-MB-231 cells. Twenty-four h after seeding of cells (0 h time of treatment in the figure), NSpd, Pd-NSpd or Pt-NSpd was added to give a final concentration of 25 µM (**A**–**D**) or 100 µM (**E**–**I**). Cells were harvested by trypsinisation and counted in a hemocytometer. The results are presented as mean values (n=3–6 independent samples from one or two independent experiments) and bars represent ± SD. When not visible, the bars are covered by the symbols. **J**–**M**: Cells were seeded and NSpd, Pd-NSpd or Pt-NSpd was added to the final concentration of 25 µM after 24 h of seeding. After 72 h of treatment, the drug-containing medium was aspirated and drug free culture medium was added. After an additional 72 h of incubation (recovery time), cells were harvested by trypsinisation and counted in a hemocytometer. These 7 days were defined as one treatment cycle. The total recovery time between each treatment was 96 h. The cells were reseeded at the same density as at the previous passage and treated with the same drug for the next treatment cycle. All together this was repeated for 5 treatment cycles. The data are presented as the total amount of cells (mean values (n=3–6 samples from one or two independent experiments) and bars represent ± SD) that theoretically would have accumulated if all cells had been reseeded with a known cell density after each treatment cycle. When not visible, the bars are covered by the symbols. Please note that the y-axis has different scales for the different cell lines because of different rates of cell proliferation.

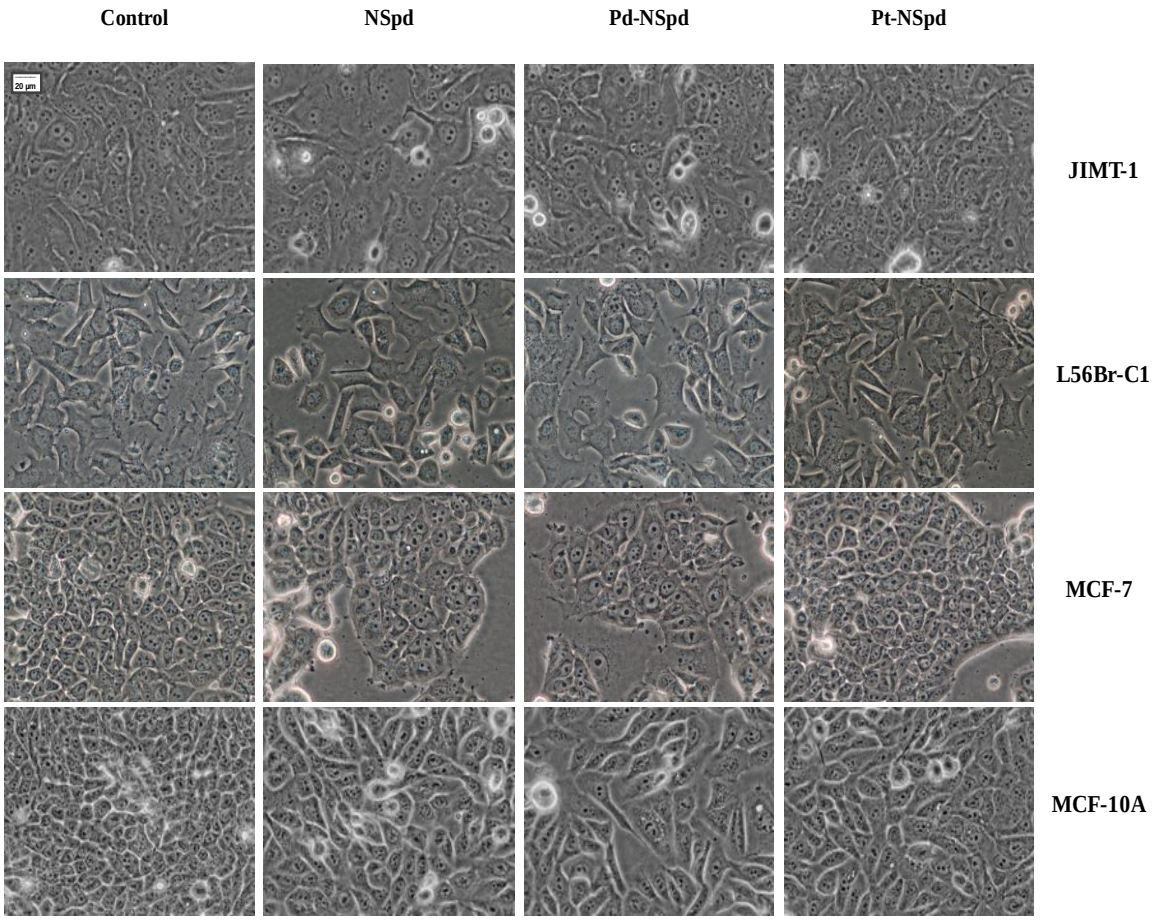

Figure 38: Phase contrast images of JIMT-1, L56Br-C1, MCF-7 and MCF-10A cells treated with NSpd, Pd-NSpd or Pt-NSpd. Twenty-four h after seeding the cells, NSpd, Pd-NSpd or Pt-NSpd was added to give a final concentration of 25 µM. After 72 h of treatment, the cells were photographed with a digital camera attached to a phase contrast microscope. The L56Br-C1 cultures were rinsed with PBS to remove all dead cells floating which were prominent in NSpd- and Pd-NSd-treated cultures, where attached cells were found in small groups seen in the image.

Drug Competition for ^{3}H-spermidine Uptake

This assay was used to evaluate the ability of NSpd, Pd-NSpd or Pt-NSpd to competitively inhibit the uptake of ^{3}H-spermidine in the four breast cell lines, using five different concentrations of the compounds. Fig. 39 shows that, in all cell lines, only NSpd was clearly found to compete with ^{3}H-spermidine, resulting in a 50% inhibition of ^{3}H-spermidine uptake at a 6 to 8 µM NSpd concentration. The dosage needed for a 50% inhibition of ^{3}H-spermidine uptake was about 100 times higher for Pt-NSpd than for its polyamine ligand, in all of the four cell lines investigated. As opposed to Pt-NSpd, Pd-NSpd caused a 50%

inhibition of ^{3}H-spermidine uptake, at concentrations that were only twice as high as NSpd in JIMT-1 cells (about 15 µM) and between five and six times higher in the other cell lines.

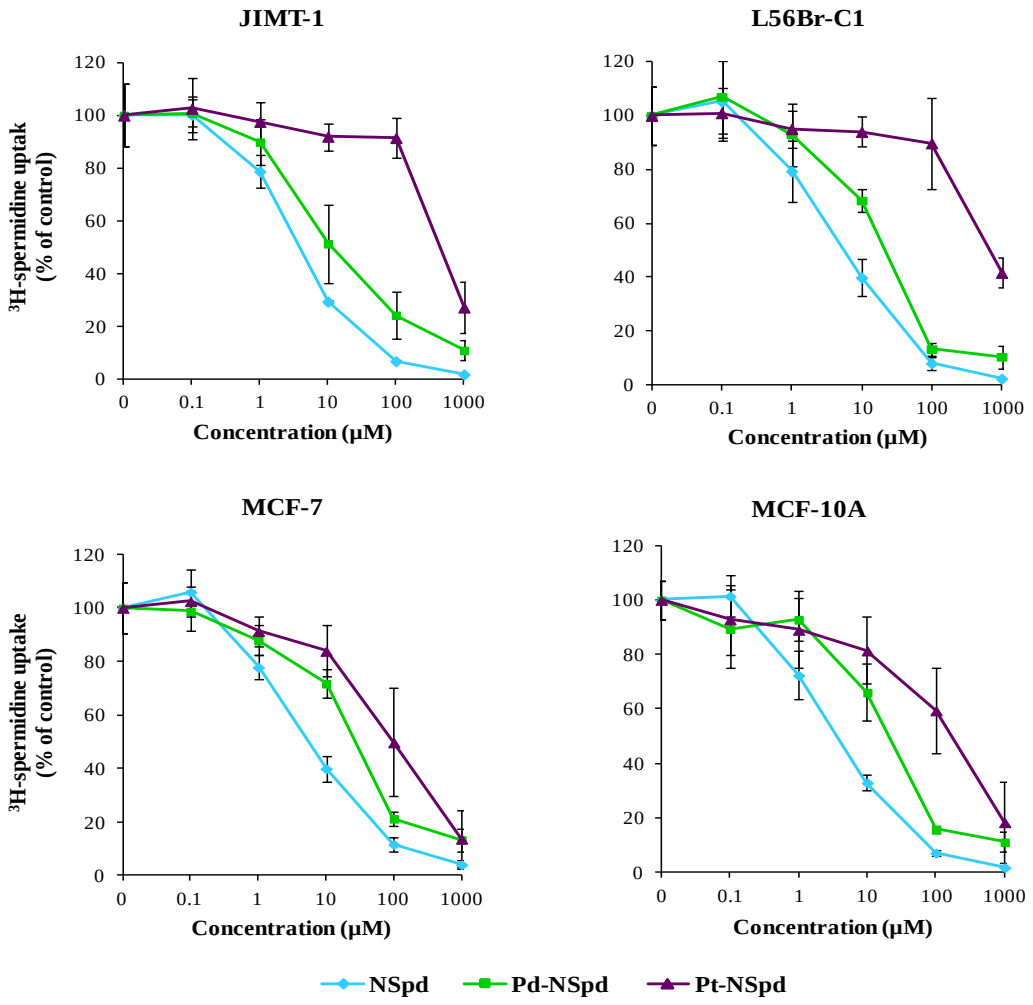

Figure 39: Effect of NSpd, Pd-NSpd or Pt-NSpd on the uptake of ^{3}H-spermidine in JIMT-1, L56Br-C1, MCF-7 and MCF-10A cells. The cells were seeded in 12-well plates and incubated for 48 h, whereupon the polyamine analogue and its complexes were added to give the final concentrations shown in the figure. The concentration of ^{3}H-spermidine used was 1 µM. The results are presented as mean values (n=4 samples from two independent experiments) and bars represent ± SD.

ODC Activity

In all cell lines, there was an evident rise in ODC activity during the first day after seeding (Fig. 40). Thereafter, ODC activity decreased rapidly in all cell lines except in L56Br-C1 cells, where it remained elevated for at least another day before slowly decreasing. Treatment with NSpd or Pd-NSpd clearly decreased the ODC activity in all the cell lines examined, except for the JIMT-1 cells where only minor differences were seen (Fig. 40). The

effect on ODC activity was most evident in L56Br-C1 cells, as the ODC activity remained relatively high in the control cells for the entire experimental period. Pt-NSpd only slightly inhibited the ODC activity in all cell lines analysed.

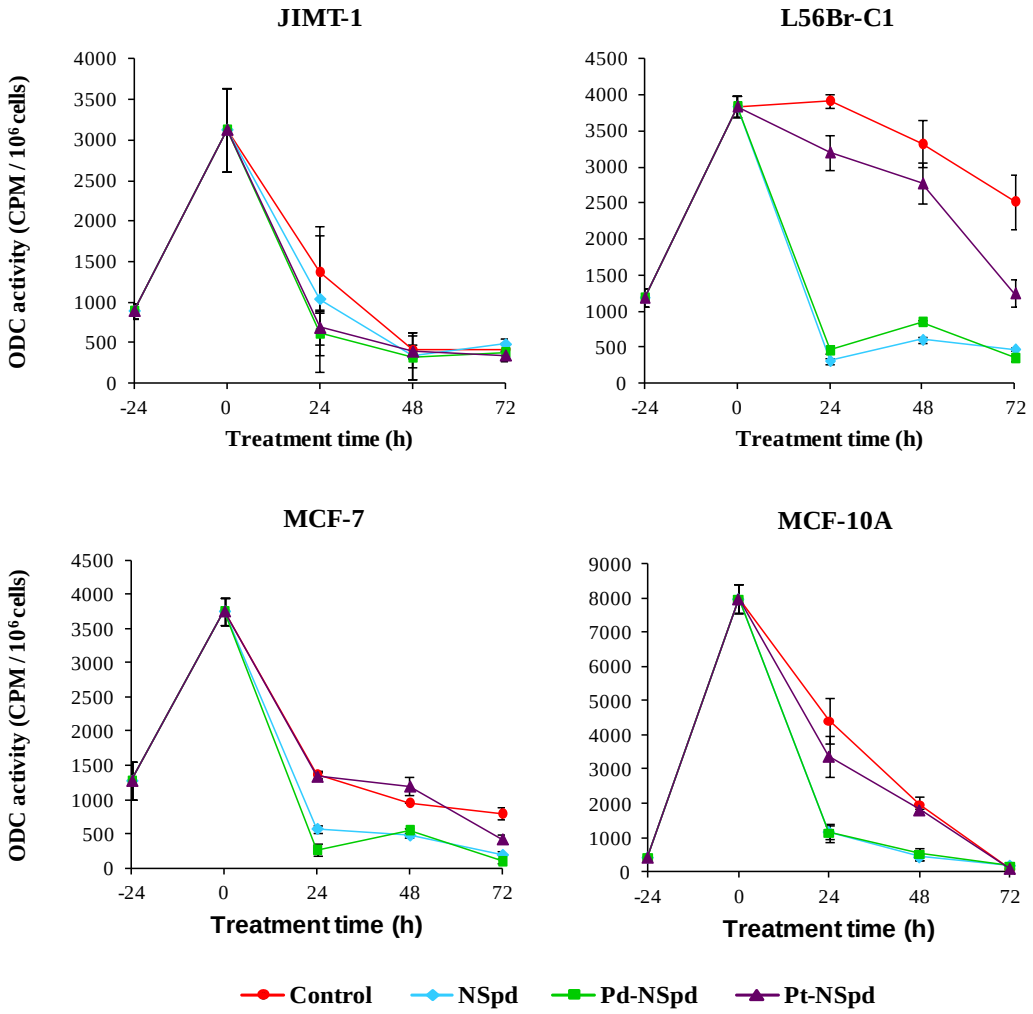

Figure 40: ODC activity in JIMT-1, L56Br-C1, MCF-7 and MCF-10A cells treated with NSpd, Pd-NSpd or Pt-NSpd. Twenty-four h after seeding of cells (0 h time of treatment in the figure), NSpd, Pd-NSpd or Pt-NSpd was added to give a final concentration of 25 µM. The ODC activity was determined using a radiometric assay. The results are presented as mean values (n=3 independent samples from one independent experiment) and bars represent ± SD.

Cell Cycle Phase Distribution and Cell Death

FCM represents a fast method to determine the cell cycle phase distribution based on the stoichiometric binding of a fluorescent probe to DNA. As the drugs used in the present study were shown to affect cell proliferation, FCM was used to further examine whether there were changes in the cell cycle phase distribution induced by the compounds and whether they induced cell death (studied by monitoring the appearance of a sub-G_1 peak). Only data from treatment with 100 μM are shown (Fig. 41), as the pattern of changes was similar, but less pronounced, after treatment with 25 μM.

The data show that the only cell line in which the percentage of cells in the sub-G_1 region increased substantially was the L56Br-C1 cell line (Fig. 41). When treating L56Br-C1 cells with NSpd or Pd-NSpd, cell death was induced after 48 h of treatment as indicated by the increased number of cells in the sub-G_1 region, which further increased after 72 h of treatment. No cell death was observed in the other cell lines analysed.

The most obvious changes in cell cycle phase distribution were found in JIMT-1 and L56Br-C1 cells, while there were no clear changes compared to control in MCF-7 and MCF-10A cells (Fig. 41). In JIMT-1 cells, the percentage of cells in the G_1 phase increased from 30 to almost 70% during the first 24 h of treatment with 100 μM Pd-NSpd and then remained at that level. During the same time period, the percentage of cells in the S phase decreased from 60 to 20%. Less evident differences in cell cycle phase distribution were observed in NSpd and Pt-NSpd-treated JIMT-1 cells. In L56Br-C1, the percentage of cells in the G_1 phase decreased, while it increased in both the S and G_2 phases after treatment with Pd-NSpd. Although not as striking, treatment with NSpd or Pt-NSpd resulted in similar changes in cell cycle phase distribution in the L56Br-C1 cells.

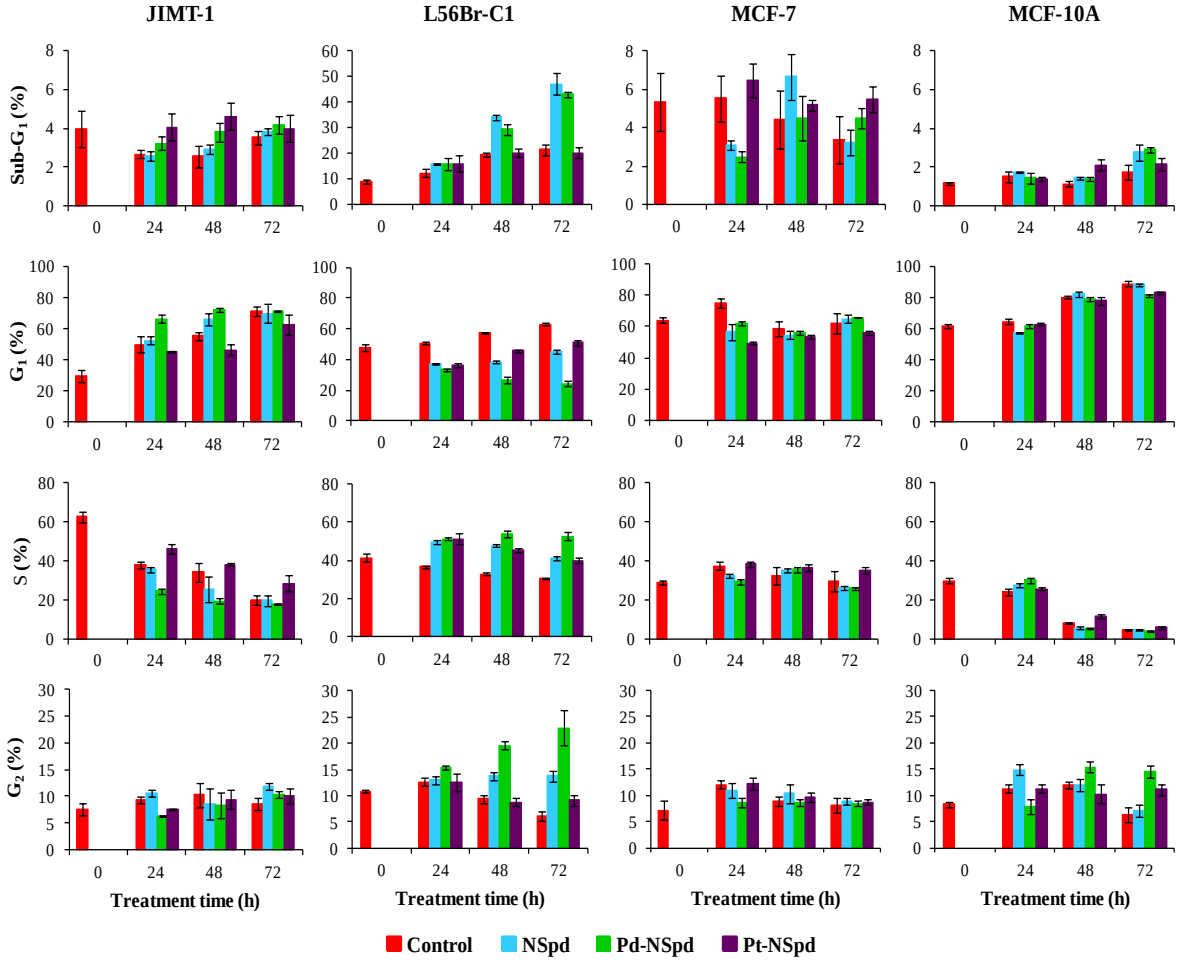

Figure 41: Sub-G_1 region and cell cycle phase distribution of JIMT-1, L56Br-C1, MCF-7 and MCF-10A cells treated with NSpd, Pd-NSpd or Pt-NSpd. Twenty-four h after seeding the cells, NSpd, Pd-NSpd or Pt-NSpd was added to give a final concentration of 100 µM. At 24, 48 and 72 h of treatment, both detached and attached cells were harvested, pooled and fixed in 70% ice-cold ethanol. The nuclei were stained with PI and the analysis was performed using FCM. The results are presented as mean values (n=3–6 independent samples from one or two independent experiments) and bars represent ± SD.

Cell Cycle Kinetics

Since we found effects on the cell cycle phase distribution and cell death in L56Br-C1 cells, it was of interest to further study cell cycle kinetics. For this purpose, the length of both S and G_2+M phases were evaluated by the use of a BrdUrd-FCM method [129,280].

The length of the S phase corresponds to the DNA replication time and was calculated by following the movement of BrdUrd-labelled cells during the cell cycle according to the

principles of Begg *et al* [279], as previously described [132,280]. The S phase was significantly prolonged in all cell lines after 72 h of NSpd or Pd-NSpd treatment, compared to control cells (Table 12). However, the prolongation was different in the four cell lines. Pt-NSpd treatment resulted in the smallest increase in S phase length and no increase in MCF-10A cells.

The length of G_2+M phase was also evaluated and corresponds to the time required for cells to proceed through the G_2 and M phases of the cell cycle [278]. The data indicated a prolongation of the G_2+M phase in all four cell lines after 72 h of treatment with NSpd, Pd-Npd or Pt-NSpd, compared to control cells.

Table 12: Effect of NSpd, Pd-NSpd or Pt-NSpd treatment on the length of the S and G_2+M phases[1].

S phase lenght (h)				
Cell Line	***Control***	***NSpd***	***Pd-NSpd***	***Pt-NSpd***
JIMT-1	13.1 ±1.0	21.4 ± 0.9 ***	20.2 ± 1.3 ***	14.1 ± 1.0
L56Br-C1	15.7 ± 1.0	18.5 ± 1.6 ***	22.5 ± 1.3 ***	16.7 ± 0.5 *
MCF-7	11.8 ± 1.1	15.2 ± 2.4 **	14.8 ± 1.7 **	13.3 ± 1.4 *
MCF-10A	7.6 ± 0.3	8.7 ± 1.1 *	15.7 ± 1.1 ***	7.1 ± 0.1
G_2/M phase lenght (h)				
Cell Line	***Control***	***NSpd***	***Pd-NSpd***	***Pt-NSpd***
JIMT-1	4.5	5.7	5.7	5.1
L56Br-C1	5.8	7.5	7.5	7.2
MCF-7	4.2	5.1	5.3	4.9
MCF-10A	3.7	6.2	5.8	4.3

[1]Cells were seeded and the drugs (25 µM) were added 24 h later. After 72 h of treatment, the cells were labelled with BrdUrd for 30 minutes, before the cells were allowed to progress through the cell cycle in BrdUrd free medium. Cells were sampled for analysis of DNA and BrdUrd contents by FCM at 3, 6, 9 and 12 h post-labelling. Data was collected from one experiment, n=5–12. * $p < 0.05$; ** $p < 0.01$; *** $p < 0.001$.

Effect of NSpd, Pd-NSpd or Pt-NSpd Treatment on Colony Forming Efficiency

This assay is designed to measure the ability of cells to proliferate and form colonies in an anchorage independent manner and it can be used to assess the sensitivity of human tumours to anticancer drugs. The normal-like cell line MCF-10A does not form colonies in soft agar and was not used in this assay. In the breast cancer cell lines, the colony forming efficiency decreased by all treatments compared to the control, with Pd-NSpd being the most effective compound and Pt-NSpd the least effective one (Table 13).

Table 13: Effect of NSpd, Pd-NSpd or Pt-NSpd treatment on colony forming efficiency in soft agar[1].

Cell line	*JIMT-1*	*L56Br-C1*	*MCF-7*
Control (%)	24.2 ± 2.1	30.7 ± 2.3	28.3 ± 2.7
NSpd (%)	14.2 ± 3.1 (58.5)	14.1 ± 2.6 (46)	18.5 ± 2.1 (65.5)
Pd-NSpd (%)	12.3 ± 2.4 (50.8)	12.1 ± 2.7 (39.4)	15.8 ± 2.4 (55.9)
Pt-NSpd (%)	19.3 ± 2.8 (79.8)	24.0 ± 1.3 (78.1)	24.2 ± 1.7 (85.5)

[1]Cells were seeded and the drugs (25 μM) were added 24 h later. After 72 h of treatment, the cells were harvested, counted and reseeded at low density in soft agar. Colonies were counted after 14 days of incubation. The results are presented as mean values (n=3 independent cultures) ± SD and as percentage of control (in brackets).

Intracellular Pd(II) and Pt(II) Accumulation

The cellular contents of Pd(II) and Pt(II) complexes after treatment with 25 μM Pd-NSpd and Pt-NSpd, respectively, for 72 h were estimated by measuring the amount of Pd(II) and Pt(II) in the cells using ICP-MS. As shown in Fig. 42, the intracellular concentrations of Pd-NSpd and Pt-NSpd were considerably higher in the most sensitive cell line, L56Br-C1 compared to the least sensitive one, MCF-10A. Moreover, the concentration of Pt-NSpd was 2–3 times as high as that of Pd-NSpd in MCF-10A cells (Fig. 42 **B**), whereas in L56Br-C1 cells the concentrations were similar (Fig. 42 **A**).

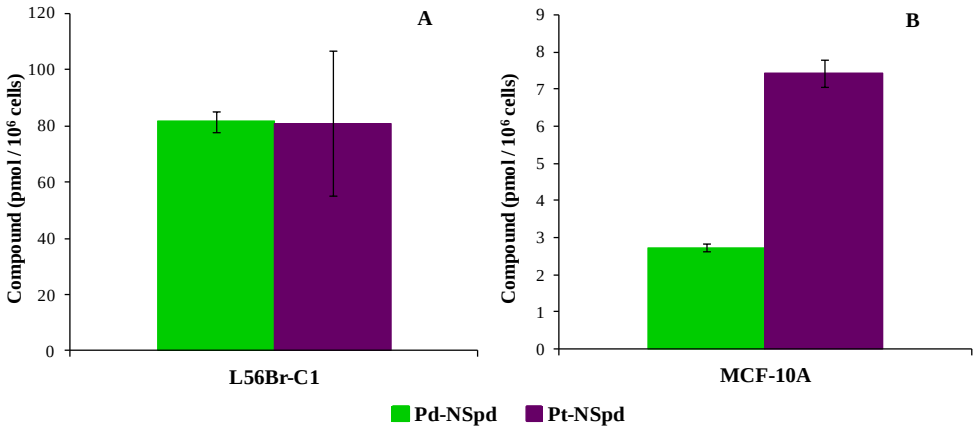

Figure 42: Intracellular accumulation of Pd-NSpd and Pt-NSpd in L56Br-C1 and MCF-10A cells. At 72 h of treatment with 25 µM of Pd-NSpd and Pt-NSpd, cells were harvested, pooled and digested in HNO_3 (see Materials and Methods). The supernatant was used for analysis of Pd(II) and Pt(II) by ICP-MS and the data used to calculate the intracellular Pd-NSpd and Pt-NSpd concentrations. The results are presented as mean values (n=3 independent samples from one independent experiment) and bars represent ± SD.

Assessment of the Genotoxic Potentials of NSpd, Pd-NSpd and Pt-NSpd

The Anthem's Genotox screen is a patented human cell-based technology that employs a genetically engineered stable p53 proficient HCT116 cell line. This mammalian genotoxicity screen can help in the identification of potential genotoxins in an early phase of drug development, before *in vivo* assessment, and also to identify pathways activated through the utilisation of reporter genes. In the present study, this assay was used as a complement to the SCGE assay, to analyse if the test compounds were potential genotoxins. A compound is considered to be genotoxic if the average reporter gene induction at any dose tested is over 1.5 fold. Taking this into account, Fig. 43 shows that 100 µM NSpd induced both p21 and p53, Pt-NSpd induced only p21 at the concentrations of 50 and 100 µM and Pd-NSpd did not induce either of the early DNA damage sensors (p21, GADD153 and p53) at any concentration in the Anthem's Genotox screen. Thus, NSpd and Pt-NSpd (Fig. 43 **A**, **C**) were found to be potential genotoxins, but not Pd-NSpd (Fig. 43 **B**).

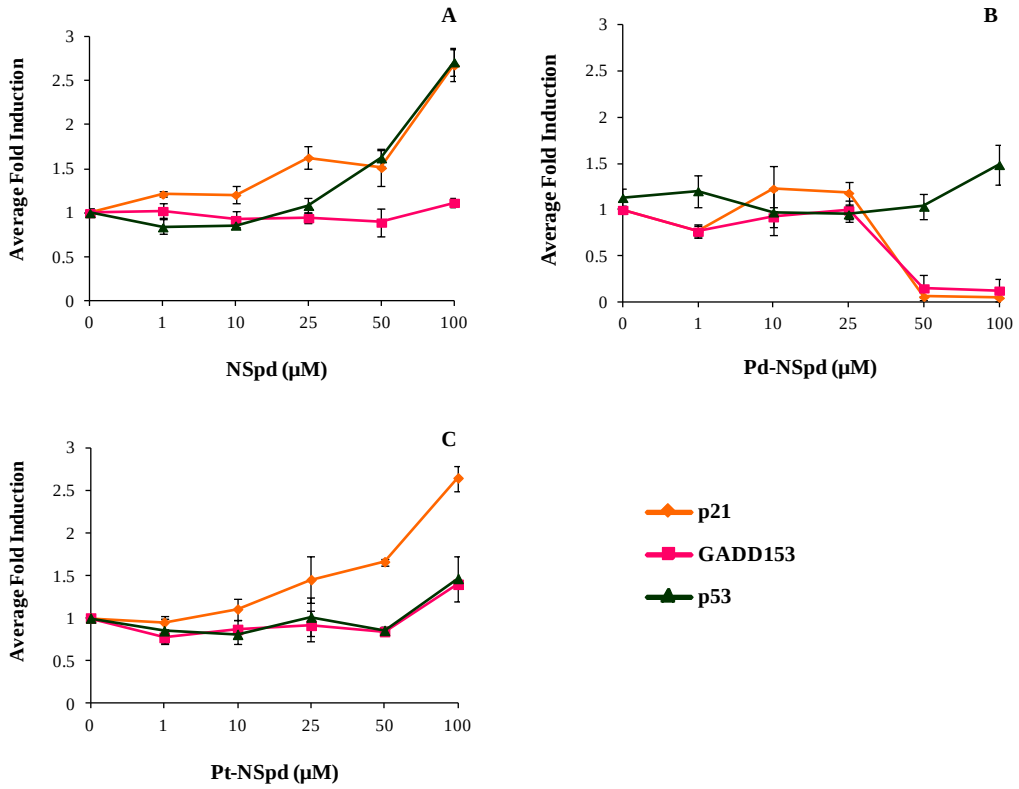

Figure 43: Genotoxic effect of NSpd, Pd-NSpd or Pt-NSpd in genetically engineered reporter-based HCT-p21-GADD-p53 cells. The genetically engineered reporter-based HCT-p21-GADD-p53 cells carrying the DNA damage early sensors p21, GADD153 and p53 were seeded in 96-well plates and allowed to attach for 16 h. The p21 promotor was operatively linked to Renilla luciferase reporter gene, the GADD 153 promotor operatively linked to firefly luciferase reporter gene and the p53 response elements operatively linked to β-galactosidase reporter gene. Sixteen h after seeding, the compounds to be tested were added to the final concentrations shown in the figure and incubated for 72 h. Samples were analysed for Renilla luciferase, firefly luciferase and β-galactosidase. The results are presented as mean values (n=3 independent samples from one independent experiment) and bars represent ± SD.

Single Cell Gel Electrophoresis

The SCGE assay was performed to investigate if the compounds induced DNA strand breaks. None of the compounds induced any significant amount of DNA strand breaks with a 25 µM concentration in any of the cell lines tested. Only data for the most sensitive cell line (L56Br-C1) are shown (Fig. 44). Figure 44 **A** shows representative comets from the different treatments. The tail length and the %DNA in the tail was evaluated for each comet and plotted in cytograms (Fig. 44 **B**). TMOM for each cell was calculated and plotted (Fig. 44 **C)**. Figure 44 **D** shows a table with the mean TMOM value of the 10% highest TMOM values.

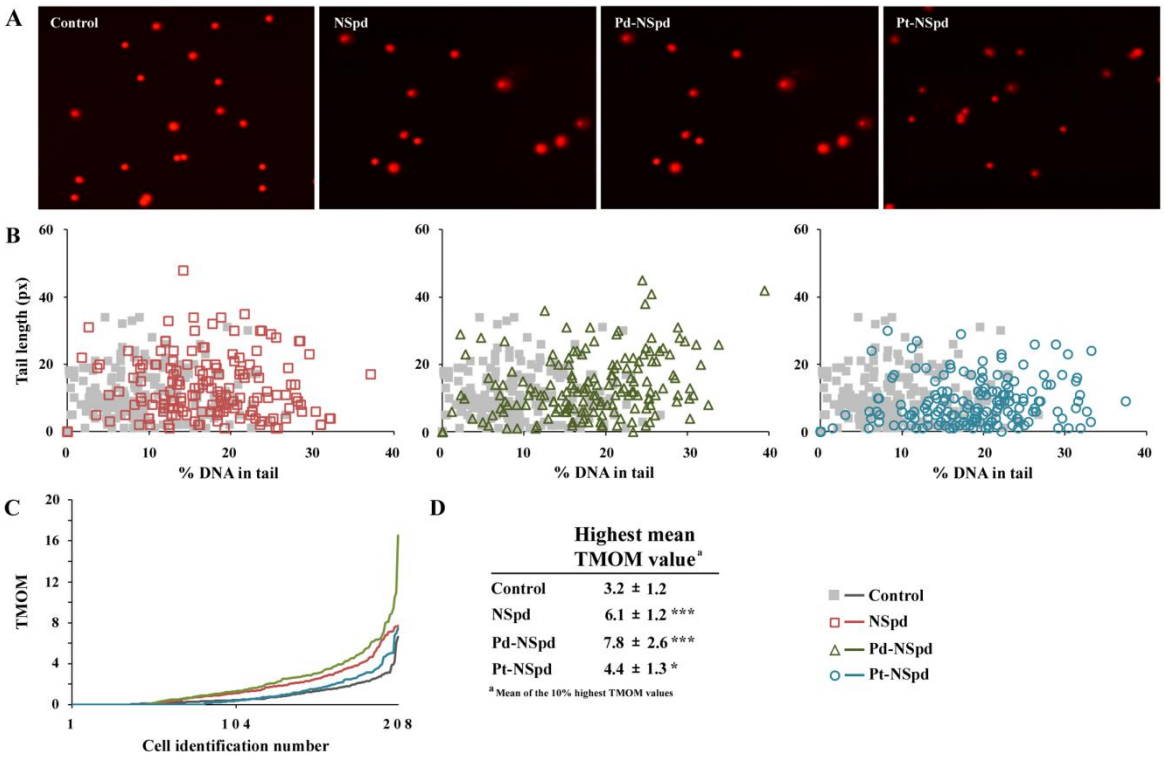

Figure 44: SCGE assay for the evaluation of DNA damage in L56Br-C1 cells. Twenty-four h after seeding of L56Br-C1 cells, NSpd, Pd-NSpd or Pt-NSpd was added to give a final concentration of 25 µM. After 72 h of treatment, cells were harvested for SCGE analysis. The EtBr-stained nucleoids were photographed and then examined using the Comet Score™ Freeware. **A**: Images of comets obtained by the SCGE assay. DNA damage results in comets with head and tail, whereas undamaged DNA results in a round head. **B**: Percentage DNA in tail on the x-axis *versus* tail length on the y-axis for individual cells. **C**: Tail moment TMOM (%DNA in tail multiplied by tail length) for individual cells. Data were collected from three independent experiments, n=207 cells. **D**: Table showing the mean TMOM value of the 10% highest TMOM values *i.e.* 20 highest values ± SD. *$p < 0.05$ compared to control; ***$p < 0.001$ compared to control.

Effect of NSpd, Pd-NSpd or Pt-NSpd Treatment on the Antizyme Inhibitor Levels

The expression levels of AzI were determined by Western blot analysis in the normal-like breast cell line MCF-10A and in the breast cancer cell lines JIMT-1, MCF-7 and L56Br-C1. A strong band corresponding to the molecular weight of AzI (49 kDa) was found in all the cell lines examined (Fig. 45). In JIMT-1 cells, the AzI signal appeared stronger for all time points in cells treated with Pd-NSpd, compared to control and NSpd-treated cells (Fig. 45). In MCF-10A cells, a strong AzI signal was observed 24 h after seeding (when treatment started), which remained elevated for at least another day, before slowly decreasing. There were no major differences between the treatments (Fig. 45). In MCF-7 cells, treatment with

NSpd or Pd-NSpd appeared to increase the cellular AzI levels at 24 and 72 h after treatment, compared to control cells (Fig. 45). However, no major difference was observed between the two treatments. In L56Br-C1 cells, treatment with Pd-NSpd decreased the AzI levels after 48 and 72 h, while NSpd treatment did not affect the cellular AzI levels, compared to control (Fig. 46). No major differences were observed between the various treatments after 24 h. A small increase in the AzI levels was observed after 48 h of treatment with Pt-NSpd.

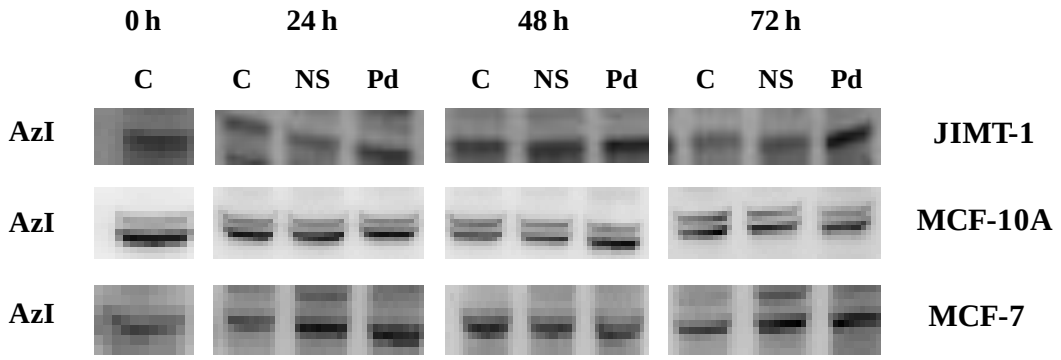

Figure 45: Effect of NSpd or Pd-NSpd treatment on the AzI protein levels in JIMT-1, MCF-10A and MCF-7 cells. Twenty-four h after seeding of cells (0 h time of treatment in the figure), NSpd or Pd-NSpd was added to a final concentration of 25 µM. Western blot analysis was used to detect the AzI protein. Loading was based on cell number: 75000 cells per lane. The data are representative of two independent cultures from one experiment. C: control, NS: NSpd, Pd: Pd-NSpd.

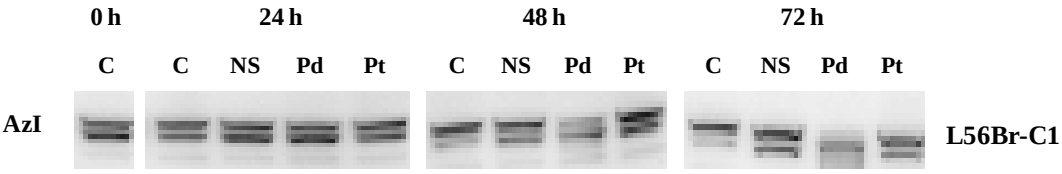

Figure 46: Effect of NSpd, Pd-NSpd or Pt-NSpd treatment on the AzI protein levels in L56Br-C1 cells. Twenty-four h after seeding of cells (0 h time of treatment in the figure), NSpd, Pd-NSpd or Pt-NSpd was added to a final concentration of 25 µM. Western blot analysis was used to detect the AzI protein. Loading was based on cell number: 75000 cells per lane. The data are representative of two independent cultures from one experiment. C: control, NS: NSpd, Pd: Pd-NSpd, Pt: Pt-NSpd.

3.2.2. BENSpm, CPENSpm, Pd-BENSpm, Pd-Spm and Pt-CPENSpm

It has been previously shown that several breast cancer cell lines were highly sensitive to treatment with Pd(II)-polyamine analogues and that these chelates were more toxic than their Pt(II) counterparts against the same breast cancer cell lines [169]. This led us to investigate the cytotoxic effects of two known and widely used polyamine analogues, BENSpm and CPENSpm, and three synthesised complexes, Pd-BENSpm, Pd-Spm and Pt-CPENSpm on three different human breast cancer cell lines (JIMT-1, L56Br-C1 and MCF-7) and one immortalised normal-like breast epithelial line (MCF-10A).

MTT Reduction

The MTT assay was used to analyse the toxicity of BENSpm, Pd-BENSpm, CPENSpm or Pt-CPENSpm against the four cell lines investigated, using concentrations that ranged from 0.1 to 100 µM. In general, MTT reduction decreased, when increasing concentration as well as time of treatment. However, the reactions to each treatment differed between the four cell lines (Fig. 47). The dose response curves show that Pt-CPENSpm was found to be the least cytotoxic compound and that BENSpm, Pd-BENSpm and CPENSpm all had similar effects on the individual cell lines. In fact, Pt-CPENSpm treatment resulted in similar toxicity in all cell lines. Since BENSpm, Pd-BENSpm or CPENSpm treatment was highly cytotoxic in L56Br-C1 cells, the difference between those three drugs and Pt-CPENSpm was most obvious in this particular cell line. Based on these data and on previously published data on BENSpm and CPENSpm [107,112,292-294], the concentration 10 µM was used for further studies.

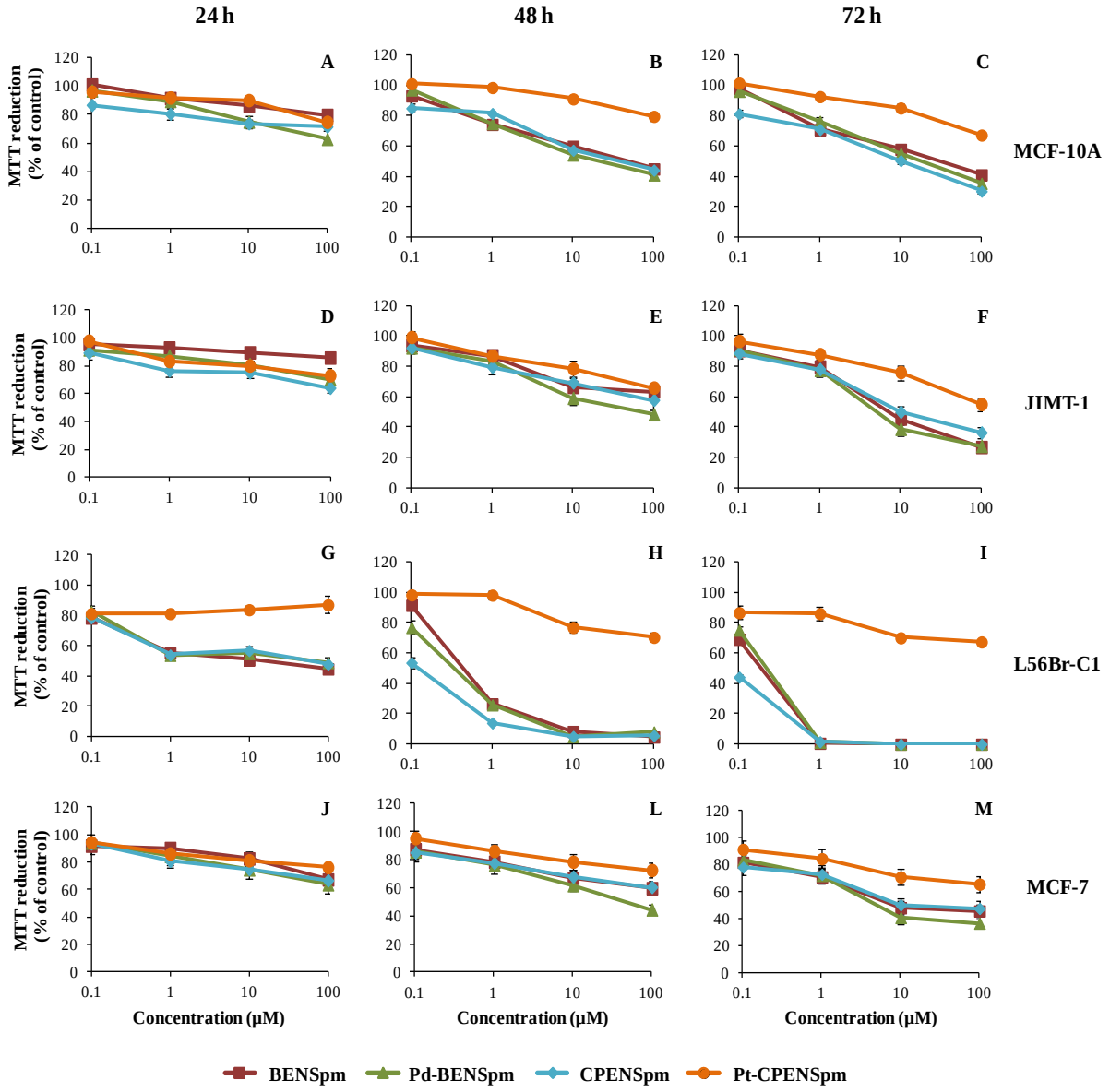

Figure 47: Dose response effect of BENSpm, Pd-BENSpm, CPENSpm or Pt-CPENSpm treatment. The normal-like breast cell line MCF-10A (**A**–**C**) and the three breast cancer cell lines JIMT-1 (**D**–**F**), L56Br-C1 (**G**–**I**) and MCF-7 (**J**–**M**) were used. Twenty-four h after seeding of cells in 96-well plates, the compounds to be tested were added to the final concentrations shown in the figure and the cells were treated for 24, 48 and 72 h, before evaluation using an MTT assay. The results are expressed as % of control (n=12 independent samples from two independent experiments) with bars representing ± SEM. When not visible, the bars are covered by the symbols.

Effect of Short Time Exposure on Cell Proliferation

We next investigated the effects of the compounds on cell proliferation (Fig. 48 **A**-**D**). As shown in the MTT assay, Pt-CPENSpm was the least cytotoxic compound (Fig. 47). Actually, Pt-CPENSpm did not affect proliferation of MCF-10A (Fig. 48 **A**) and L56Br-C1 (Fig. 48 **C**) cells, but slightly inhibited proliferation of JIMT-1 (Fig. 48 **B**) and MCF-7 (Fig. 48 **D**) cells. Pd-Spm treatment did not affect proliferation of MCF-10A cells, while BENSpm, Pd-BENSpm and CPENSpm slightly reduced the cell numbers at 48 h and 72 h of treatment (Fig. 48 **A**). In L56Br-C1 cells, treatment with BENSpm, Pd-BENSpm or CPENSpm resulted in a decrease in cell number after 48 h and 72 h compared to the cell number at 24 h, implicating cell death (Fig. 48 **C**). Pd-Spm also resulted in a slight decrease in cell number in L56Br-C1 cells. In JIMT-1 (Fig. 48 **B**) as well as in MCF-7 (Fig. 48 **D**) cells, the inhibition of cell proliferation was similar after treatment with BENSpm, Pd-BENSpm, CPENSpm or Pd-Spm. In conclusion, the cell proliferation assay shows that the least sensitive cell line was MCF-10A and the most sensitive one was L56Br-C1.

Effect of Long Time Exposure on Cell Proliferation

In addition to the 72 h proliferation study, we also evaluated the effect of repeated treatment cycles with 10 µM BENSpm, Pd-BENSpm, Pd-Spm, CPENSpm or Pt-CPENSpm on cell proliferation of MCF-10A, JIMT-1 and L56Br-C1 cells (Fig. 48 **E**–**G**). The cells were cultivated in cycles with drug treatment for 72 h along with drug free periods of 96 h in between, for a total period of 5 cycles. Proliferation of MCF-10A normal-like breast cells were not affected by repeated treatment cycles with either Pt-CPENSpm or Pd-Spm (Fig. 48 **E**), while repeated treatments with these compounds had a somewhat inhibitory effect on the growth of JIMT-1 cells (Fig. 48 **F**). In L56Br-C1 cells, repeated treatments with Pd-Spm resulted in a reduction of cell number after 4 treatment cycles. Repeated treatment with BENSpm, Pd-BENSpm or CPENSpm resulted in a decrease in cell number, compared to the number of cells seeded at time 0, in all cell lines (Fig. 48 **E–G**).

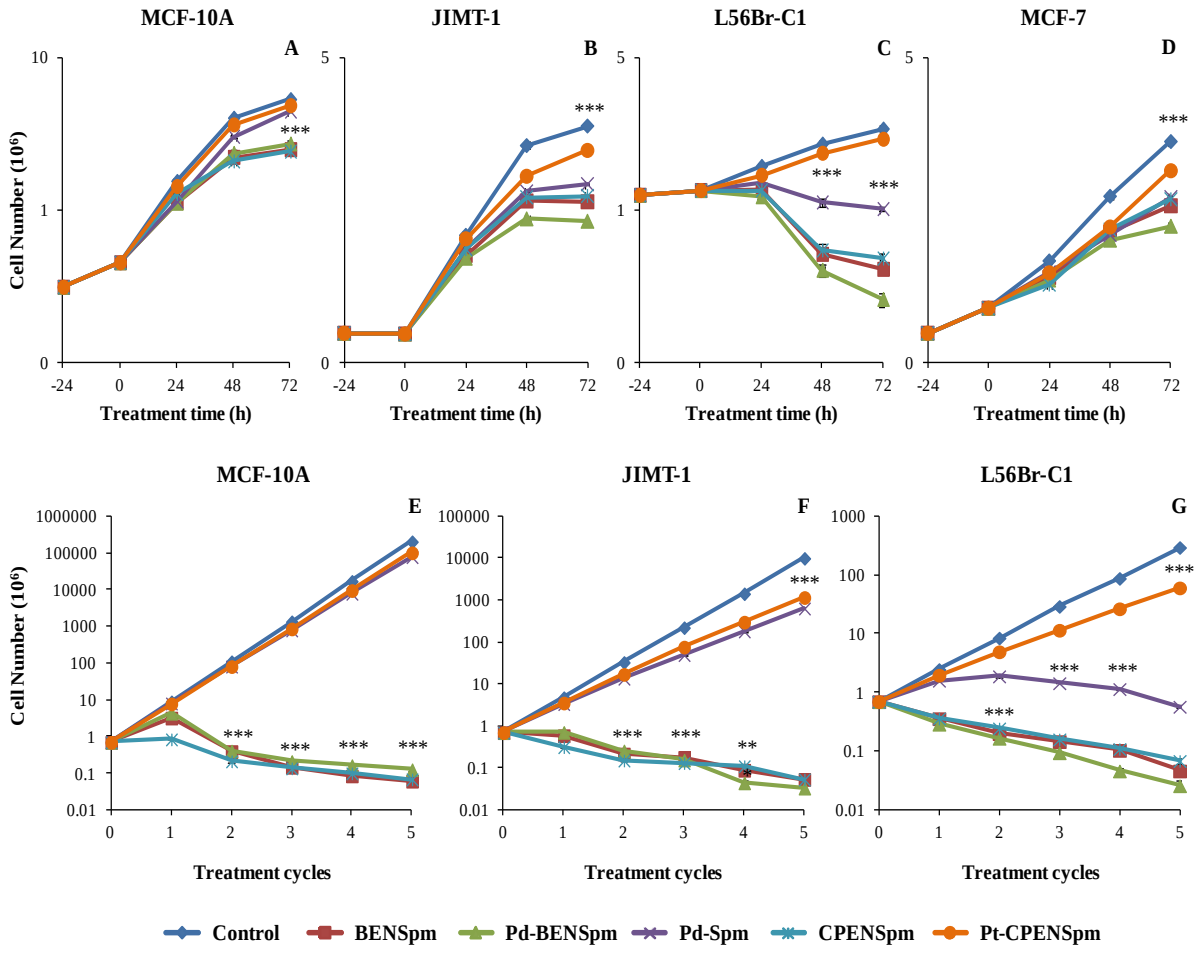

Figure 48: Effect of BENSpm, Pd-BENSpm, Pd-Spm, CPENSpm or Pt-CPENSpm treatment on the cell proliferation. Twenty-four h after seeding of MCF-10A, JIMT-1, L56Br-C1 and MCF-7 cells (0 h time of treatment in the figure), BENSpm, Pd-BENSpm, Pd-Spm, CPENSpm or Pt-CPENSpm was added to a final concentration of 10 µM (**A**–**D**). Cells were harvested by trypsinisation and counted in a hemocytometer. The results are presented as mean values (n=6 samples from two independent experiments) and bars represent ± SEM. The bars are covered by the symbols. **E**–**G**: Cells were seeded and BENSpm, Pd-BENSpm, Pd-Spm, CPENSpm or Pt-CPENSpm was added to the final concentration of 10 µM, after 24 h of seeding. After 72 h of treatment, the drug-containing medium was aspirated and drug free culture medium was added. After an additional 72 h of incubation, cells were harvested by trypsinisation and counted in a hemocytometer. These 7 days were defined as one treatment cycle. The cells were reseeded at the same density as at the previous passage and treated with the same drug for the next treatment cycle. All together this was repeated for 5 treatment cycles. The total recovery time between repeated treatments was 96 h. The results are presented as mean values (n=3 samples from one independent experiment) and bars represent ± SEM. The bars are covered by the symbols. Please note that the y-axis has different scales for the different cell lines because of different rates of cell proliferation. *** $p < 0.001$ compared to control for the curves below the symbol.

Intracellular Pd(II) and Pt(II) Accumulation

ICP-MS was used to quantify the Pd(II) or Pt(II) content in cells treated with 10 µM Pd-BENSpm, Pd-Spm or Pt-CPENSpm for 72 h and the data were used to calculate the intracellular concentrations of the drugs (Fig. 49). The data demonstrate that the intracellular concentration of Pd-BENSpm was approximately 20, 40 and 360 pmol/10^6 cells in MCF-10A (Fig. 49 **A**), JIMT-1 (Fig. 49 **B**) and L56Br-C1 (Fig. 49 **C**) cells, respectively. The Pd-Spm and Pt-CPENSpm concentrations were between 2 and 15 pmoles/10^6 cells in the three cell lines, with the highest concentrations in MCF-10A cells and the lowest concentrations in L56Br-C1 cells.

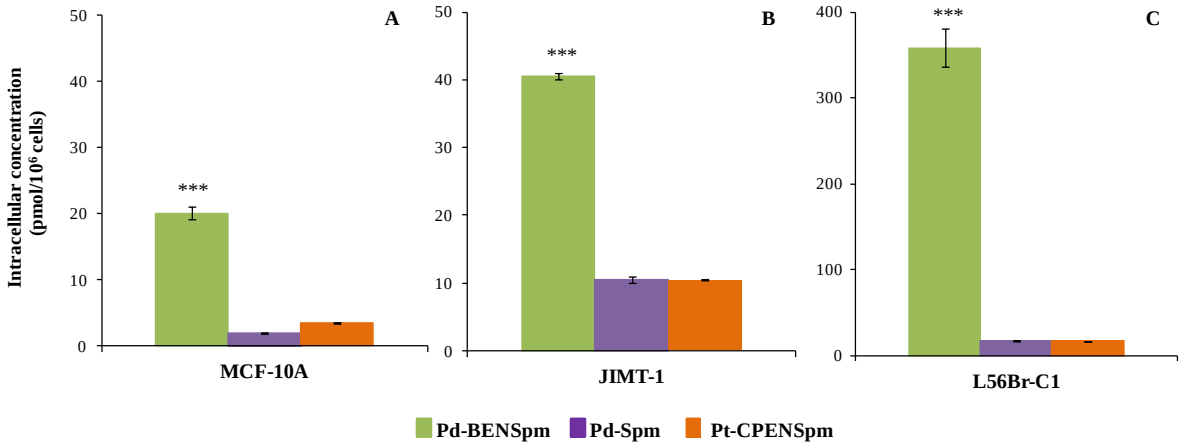

Figure 49: Intracellular concentration of Pd-BENSpm, Pd-Spm and Pt-CPENSpm in MCF-10A, JIMT-1 and L56Br-C1 cells. At 72 h of treatment with 10 µM of Pd-BENSpm, Pd-Spm or Pt-CPENSpm, cells were harvested, pooled and digested in HNO_3 (see Materials and Methods). The supernatant was used for analysis of Pd(II) and Pt(II) by ICP-MS and the data used to calculate the intracellular Pd-BENSpm, Pd-Spm and Pt-CPENSpm concentrations in MCF-10A (**A**), JIMT-1 (**B**) and L56Br-C1 (**C**) cells. The results are presented as mean values (n=3 independent samples from one independent experiment) and bars represent ± SEM. *** $p < 0.001$ compared to Pd-Spm or Pt-CPENSpm treatment.

Analysis of Polyamine Levels

Since L56Br-C1 was found to be the most sensitive cell line, it was of interest to measure the polyamine levels in these cells (by HPLC), after 24 h of incubation with 10 µM of BENSpm, Pd-BENSpm, Pd-Spm, CPENSpm or Pt-CPENSpm (Fig. 50). As expected, the putrescine (Fig. 50 **A**), spermidine (Fig. 50 **B**) and spermine (Fig. 50 **C**) contents decreased

significantly upon treatment with BENSpm, Pd-BENSpm or CPENSpm, compared to control. Pt-CPENSpm treatment resulted in a minor increase in polyamine levels compared to control, while Pd-Spm treatment only had a neglible effect (Fig. 50 **A**–**C**).

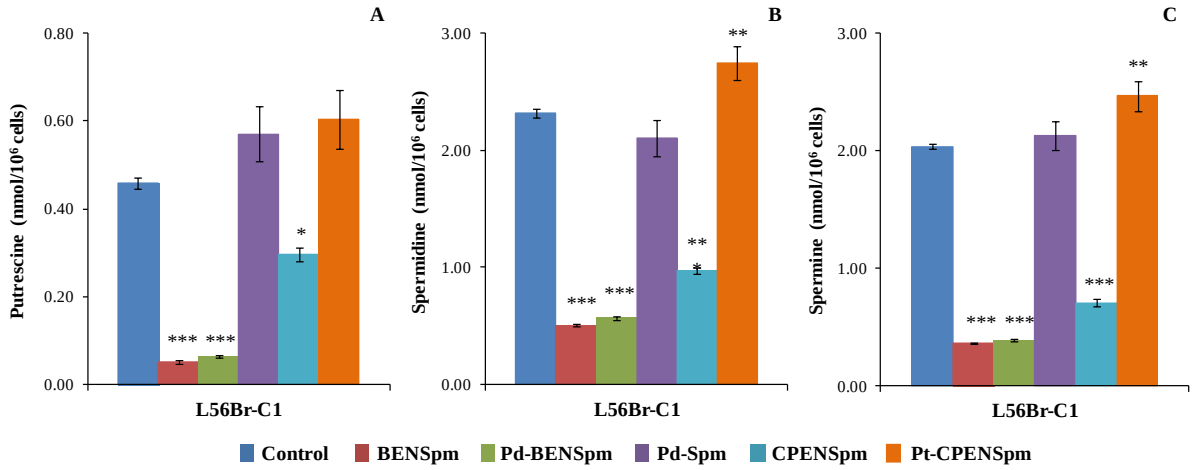

Figure 50: Effect of BENSpm, Pd-BENSpm, Pd-Spm, CPENSpm or Pt-CPENSpm treatment on the polyamine content in L56Br-C1 cells. After 24 h of treatment with 10 µM of BENSpm, Pd-BENSpm, Pd-Spm, CPENSpm or Pt-CPENSpm, cells were harvested, counted in a hemocytometer and then putrescine (**A**), spermidine (**B**) and spermine (**C**) contents were determined by HPLC. The results are presented as mean values (n=3 independent samples from one independent experiment) and bars represent ± SEM. When not visible, the bars are covered by the symbols. * $p < 0.05$ compared to control; ** $p < 0.01$ compared to control; *** $p < 0.001$ compared to control.

SSAT Activity

Since the polyamines were efficiently depleted by BENSpm and Pd-BENSpm, the next step was to measure the activity of the polyamine catabolic enzyme SSAT. The SSAT activity was very low in the untreated L56Br-C1 cells, but increased dramatically after treatment with BENSpm, Pd-BENSpm or CPENSpm (Fig. 51). The increase in SSAT activity was twice as high in cells treated with BENSpm or Pd-BENSpm than in CPENSpm-treated cells. In Pd-Spm- or Pt-CPENSpm-treated cells the SSAT activity was found to be zero.

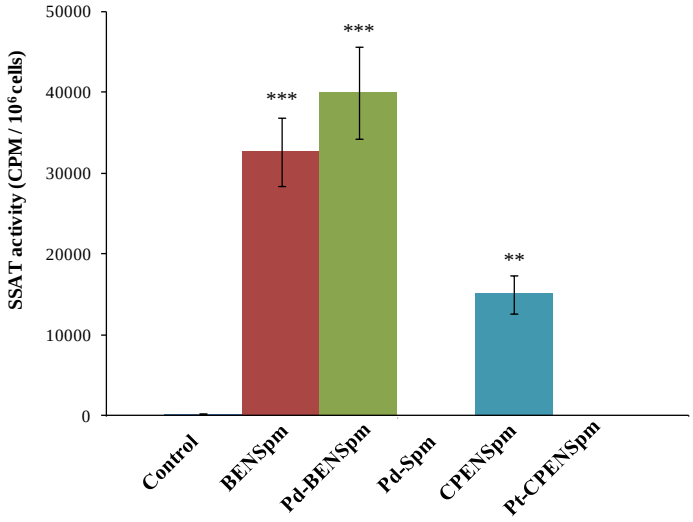

Figure 51: SSAT activity in L56Br-C1cells treated with BENSpm, Pd-BENSpm, Pd-Spm, CPENSpm or Pt-CPENSpm. After 24 h of treatment with 10 µM of BENSpm, Pd-BENSpm, Pd-Spm, CPENSpm or Pt-CPENSpm, cells were harvested, counted in a hemocytometer and then the SSAT activity was determined using a radiometric assay. The results are presented as mean values (n=6 independent samples from two independent experiments) and bars represent ± SEM. ** $p < 0.01$ compared to control; *** $p < 0.001$ compared to control.

Cell Cycle Phase Distribution and Cell Death

Since the various compounds used in the present study were shown to affect cell proliferation differently, the effects of BENSpm, Pd-BENSpm, Pd-Spm, CPENSpm or Pt-CPENSpm on cell cycle phase distribution as well as on cell death were analysed by FCM.

The data show that the only cell line in which the percentage of cells in the sub-G_1 region, which reflects cell death, increased substantially was the L56Br-C1 cell line (Fig. 52). When treating L56Br-C1 cells with BENSpm, Pd-BENSpm or CPENSpm, cell death was already induced after 48 h of treatment. No cell death was observed in MCF-10A and JIMT-1 cells. As also seen in Fig. 52, a large fraction of untreated L56Br-C1 cells was found in the sub-G_1 region indicating (or demonstrating) a high degree of spontaneous apoptotic cell death [295].

In MCF-10A cells, the number of cells in the G_1 phase increased from around 50% to 80% between 24 and 48 h of treatment with BENSpm, Pd-BENSpm or CPENSpm. During the same time period, the percentage of cells in the S phase decreased from 40 to 10%. Less evident changes were found in the cell cycle phase distribution of JIMT-1 cells after treatment (Fig. 52), with the exception of Pd-Spm treatment, which increased the number of cells in S

phase approximately 10% after 24 and 48 h of treatment, compared to the other treatments. In L56Br-C1 cells, cell death was so prominent that is was not possible to evaluate the DNA histograms at 48 and 72 h of treatment.

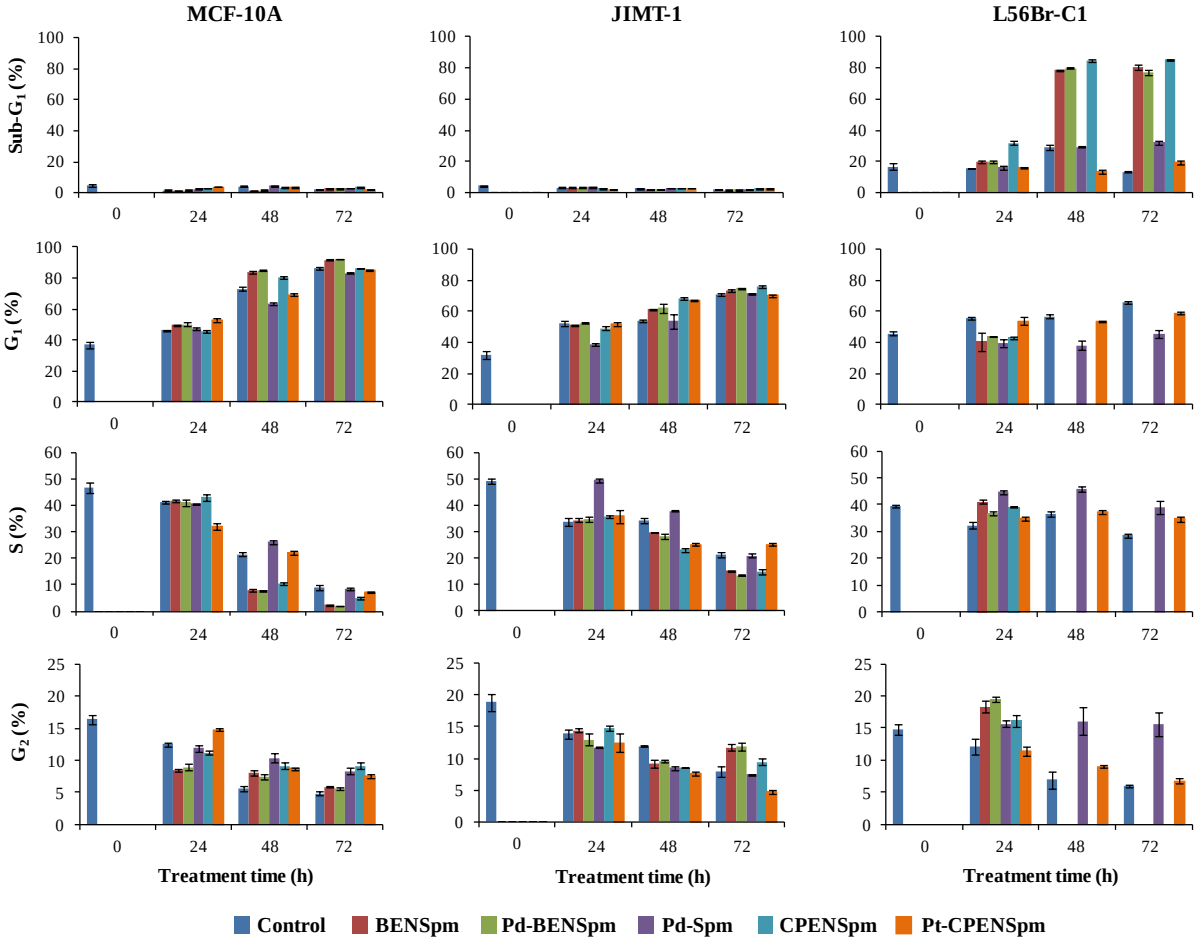

Figure 52: Sub-G_1 region and cell cycle phase distribution of MCF-10A, JIMT-1 and L56Br-C1 cells treated with BENSpm, Pd-BENSpm, Pd-Spm, CPENSpm or Pt-CPENSpm. Twenty-four h after seeding the cells, BENSpm, Pd-BENSpm, Pd-Spm, CPENSpm or Pt-CPENSpm was added to a final concentration of 10 µM. At 24, 48 and 72 h of treatment, both detached and attached cells were harvested, pooled and fixed in 70% ice-cold ethanol. The nuclei were stained with PI and the analysis was performed using FCM. The results are presented as mean values (n=3 independent samples from one independent experiment) and bars represent ± SEM.

Identification of the Cancer Stem Cell Population $CD44^+CD24^-$

To investigate the effects on the putative breast CSC population, here defined as $CD44^+CD24^-$ [283], JIMT-1 cells were treated for 72 h with 10 µM BENSpm, Pd-BENSpm, Pd-Spm, CPENSpm or Pt-CPENSpm and the data was analysed by FCM. As shown in Fig.

53 (**A**, **B)**, treatment with both BENSpm and Pd-BENSpm significantly reduced the levels of the $CD44^{+}CD24^{-}$ subpopulation from 50% (total population in the control cells) to 30% and 33%, respectively, whereas treatment with Pd-Spm, CPENSpm and Pt-CPENSpm gave a not statistically significant increase in the $CD44^{+}CD24^{-}$ subpopulation (Fig. 53).

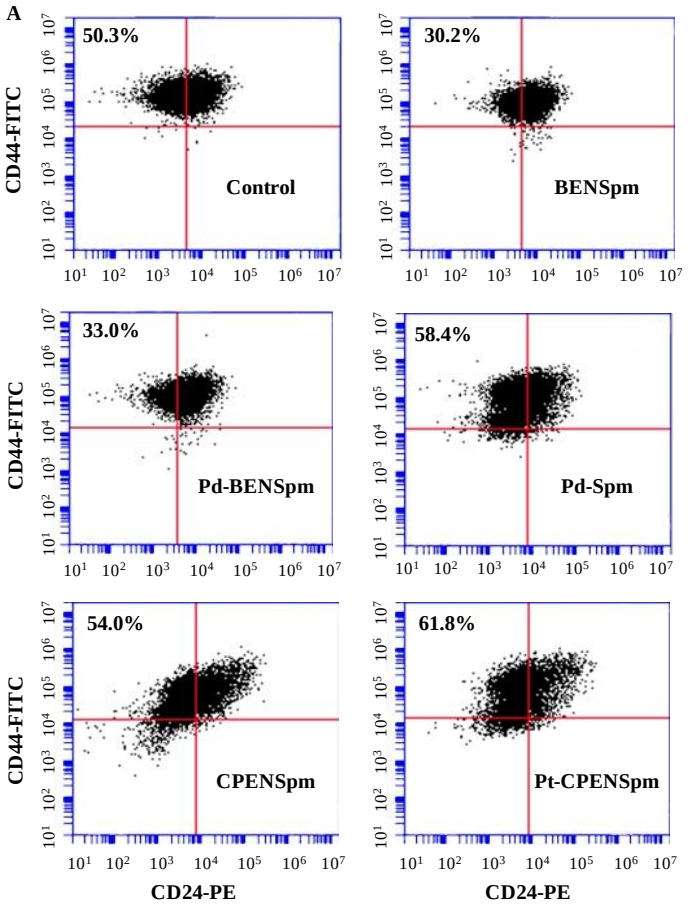

B

Treatment (72h)	$CD44^{+}CD24^{-}$ (% ± SEM)
Control	50.3 ± 0.9
BENSpm	30.2 ± 1.2 ***
Pd-BENSpm	33.0 ± 1.5 ***
Pd-Spm	58.4 ± 4.2
CPENSpm	54.0 ± 4.6
Pt-CPENSpm	61.8 ± 2.1

Figure 53: Effect of BENSpm, Pd-BENSpm, Pd-Spm, CPENSpm or Pt-CPENSpm treatment on the $CD44^{+}CD24^{-}$ putative cancer stem cell population in JIMT-1 cells. After 72 h of treatment with 10 µM of the drugs, cells were harvested with Accutase and identified based on their expression of the cell surface markers CD44 and CD24 by FCM. **A**: Representative cytograms of the flow cytometric analysis of cell surface-expressed CD44 and CD24 in the JIMT-1 breast cancer cell line. **B**: Table showing the data obtained with each treatment. The results are presented as percentage of total population (n=9 independent samples from three independent experiments) ± SEM. *** $p < 0.001$ compared to control.

Colony Forming Efficiency

The immortalised normal-like cell line MCF-10A does not form colonies in soft agar and was not used in this assay. In the JIMT-1 and L56Br-C1 breast cancer cell lines, all the treatments decreased the CFE, compared to the control (Table 14). The CFE was similar in JIMT-1 and L56Br-C1 control cells, around 30%. Pd-BENSpm treatment was most efficient in reducing the number of colonies and L56Br-C1 was the most sensitive cell line to all the treatments (Table 14).

Table 14: Effect of BENSpm, Pd-BENSpm, Pd-Spm, CPENSpm or Pt-CPENSpm treatment on colony forming efficiency in soft agar[1].

Cell line	*JIMT-1*	*L56Br-C1*
Control (%)	29.4 ± 1.0	32.7 ± 1.9
BENSpm (%)	15.1 ± 0.5 (51.2) ***	10.8 ± 0.5 (33.0) ***
Pd-BENSpm (%)	12.1 ± 0.3 (41.3) ***	7.8 ± 0.1 (23.7) ***
Pd-Spm (%)	20.5 ± 0.3 (69.7) ***	17.0 ± 1.0 (51.8) ***
CPENSpm (%)	16.4 ± 0.8 (55.7) ***	11.8 ± 1.0 (36.2) ***
Pt-CPENSpm (%)	24.1 ± 0.4 (82.1) ***	24.0 ± 0.5 (73.2) ***

[1]Cells were seeded and the drugs (10 μM) were added 24 h later. After 72 h of treatment, the cells were harvested, counted and reseeded at low density in soft agar. Colonies were counted 14 days after incubation. The results are presented as mean values (n=3 independent cultures) ± SEM or as percentage of control (in brackets). *** $p < 0.001$ compared to control.

Assessment of the Genotoxic Potentials of BENSpm and Pd-BENSpm

Regarding genotoxicity classification, a test compound is considered to be genotoxic if the average reporter gene induction at any dose tested is over 1.5 fold. The Anthem's Genotox screen was used for assessing the genotoxic potential of BENSpm and Pd-BENSpm, in a genetically engineered stable p53 proficient HCT116 cell line.

Fig. 54 shows that both p21 and p53, but not GADD153, where induced by BENSpm (Fig. 54 **A**) and Pd-BENSpm (Fig. 54 **B**) treatments, at 5 and 10 μM concentrations. Thus, both compounds can be considered as genotoxins in this screen, indicating that they may induce DNA strand breaks.

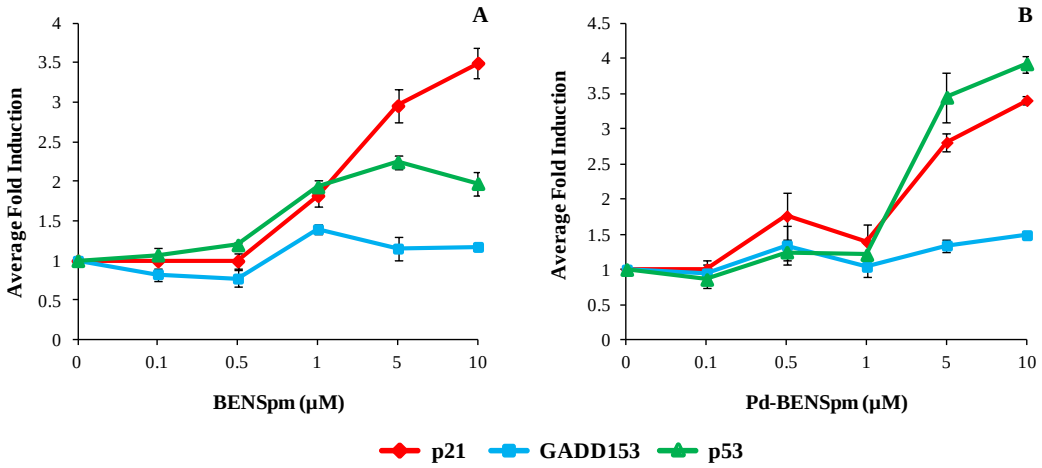

Figure 54: Genotoxic effect of BENSpm or Pd-BENSpm in genetically engineered reporter-based HCT-p21-GADD-p53 cells. The genetically engineered reporter-based HCT-p21-GADD-p53 cells carrying the DNA damage early sensors p21, GADD153 and p53 were seeded in 96-well plates and allowed to attach for 16 h. The p21 promotor was operatively linked to Renilla luciferase reporter gene, the GADD 153 promotor operatively linked to firefly luciferase reporter gene and the p53 response elements operatively linked to β-galactosidase reporter gene. Sixteen h after seeding, the polyamine analogue and its complex were added to the final concentrations shown in the figure and incubated for 72 h. The samples were analysed for Renilla luciferase, firefly luciferase and β-galactosidase. The results are presented as mean values (n=3 independent samples from one independent experiment) and bars represent ± SD.

Single Cell Gel Electrophoresis

The SCGE assay was performed to investigate if any of the compounds induced DNA strand breaks. Table 15 shows the percentage of comets in relation to the total number of nucleoids scored, after 72 h of treatment. There were fewer nucleoids with comets in control MCF-10A and JIMT-1 cells, compared to L56Br-C1 cells. All treatments resulted in an increase in the number of nucleoids with a comet in all cell lines, although the increase was most prominent in L56Br-C1 cells. Of the five tested compounds, Pd-BENSpm was the most efficient in increasing the number of nucleoids with comets. Figure 55 shows the comets of the most sensitive cell line (L56Br-C1).

Table 15: Effect of BENSpm, Pd-BENSpm, Pd-Spm, CPENSpm or Pt-CPENSpm treatment on the number of comets in MCF-10A, JIMT-1 and L56Br-C1 cell lines, evaluated by the SCGE assay[1].

Cell Line	*MCF-10A*	*JIMT-1*	*L56Br-C1*
Control	4.6 ±1.0	4.5 ± 1.5	8.1 ± 0.8
BENSpm	11.0 ± 1.6 **	18.3 ± 3.7 *	30.5 ± 2.4 ***
Pd-BENSpm	11.2 ± 1.0 **	23.8 ± 4.0 **	41.2 ± 3.8 ***
Pd-Spm	9.2 ± 0.9	14.3 ± 3.0 *	24.2 ± 2.4 **
CPENSpm	11.3 ± 1.5 **	16.1 ± 3.9 *	27.2 ± 2.2 ***
Pt-CPENSpm	9.0 ± 1.6	11.1 ± 2.0	18.4 ± 2.1 *

[1]Cells were seeded and the drugs (10 µM) were added 24 h later. After 72 h of treatment, the cells were harvested by trypsinisation and the SCGE assay was performed as previously described. The results show the percentage of comets in relation to the total number of nucleoids scored and are presented as mean values of three independent samples from one experiment (n=150 cells) ± SEM. * $p < 0.05$ compared to control; ** $p < 0.01$ compared to control; *** $p < 0.001$ compared to control.

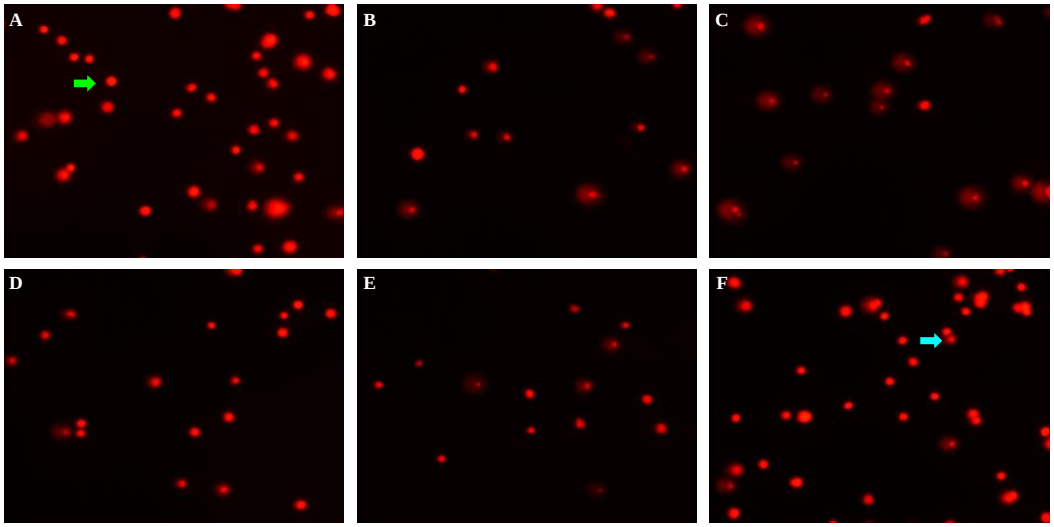

Figure 55: Evaluation of DNA damage in L56Br-C1 cells by the SCGE assay. Twenty-four h after seeding the cells, BENSpm, Pd-BENSpm, Pd-Spm, CPENSpm or Pt-CPENSpm was added to a final concentration of 10 µM. After 72 h of treatment, the cells were harvested for SCGE assay analysis. The EtBr-stained nucleoids were photographed with a digital camera attached to an epifluorescence microscope. The total number of nucleoids and the nucleoids with comet tails were visually counted in each image. A nucleoid with comet tail was defined as a nucleoid with a visible tail independent of tail size. For every sample, the % of nucleoids with a comet tail was calculated. Thus, for every treatment, three values (in %) were obtained, which were used for the calculation of mean ± SEM. The green arrows represent undamaged cells while the blue arrows represent the smallest nucleoids with comet tail counted. Images of comets obtained for the untreated (**A**), BENSpm- (**B**), Pd-BENSpm- (**C**), Pd-Spm- (**D**), CPENSpm- (**E**) or Pt-CPENSpm-treated (**F**) samples.

GSH-Glo™ Glutathione Assay

The GSH-Glo™ Glutathione assay is a luminescence-based method used for the detection and quantification of GSH levels in cells, tissue extracts or blood. Since the toxicity of cisplatin has been shown to be dependent on the cellular GSH level [296], we decided to investigate the effect of the compounds on the GSH level.

Table 16 shows that Pd-Spm treatment efficiently reduced the GSH levels in all cell lines. In Pd-Spm-treated cells, the level was below the detection limit of the assay and thus the value was set to 0. Treatment with BENSpm, Pd-BENSpm or CPENSpm resulted in a marked reduction of cellular GSH levels. The decrease in cellular GSH was most prominent in the L56Br-C1 cells. Pt-CPENSpm treatment, on the other hand, only slightly reduced or even increased the GSH level, depending on the cell line.

In addition to the effects of the various treatments on the GSH level, Table 16 also shows the effects on cell growth (given as % of cells relative to control at 48 h of treatment). The cell data are derived from the growth curves shown in Fig. 48 **A**–**C**. Comparing the GSH levels and cell growth, it is clear that there is no obvious correlation between decrease in GSH and reduction of cell number in any of the cell lines.

Table 16: Effect of BENSpm, Pd-BENSpm, Pd-Spm, CPENSpm or Pt-CPENSpm treatment on the levels of GSH in MCF-10A, JIMT-1 and L56Br-C1 cell lines, evaluated by the GSH-Glo™ Glutathione Assay[1].

Cell Line	***MCF-10A***					
	Control	**BENSpm**	**Pd-BENSpm**	**Pd-Spm**	**CPENSpm**	**Pt-CPENSpm**
GSH (nmol/10^6cells)	34.3 ± 1.7	25.8 ± 1.8	26.9 ± 2.6	0.0	22.7 ± 2.5	40.7 ± 2.5
GSH (% of control)		75.1***	78.4***	0.0***	66.2***	118.5**
Cells (% of control)		55.4	58.8	75.5	52.1	90.4
Cell Line	***JIMT-1***					
GSH (nmol/10^6cells)	30.9 ± 1.5	17.1 ± 1.9	7.9 ± 0.8	0.0	18.6 ± 2.4	20.0 ± 5.8
GSH (% of control)		55.1***	25.6***	0.0***	60.0***	64.8***
Cells (% of control)		65.9	57.6	70.8	67.7	79.4
Cell Line	***L56Br-C1***					
GSH (nmol/10^6cells)	15.1 ± 1.0	2.8 ± 0.4	0.5 ± 0.5	0.0	1.0 ± 0.2	21.3 ± 4.2
GSH (% of control)		18.6***	3.0***	0.0***	6.8***	140.3***
Cells (% of control)		19.0	14.9	41.5	20.1	87.0

[1]Cells were seeded in white opaque 96-well plates and the compounds were added 24 h later to a final concentration of 10 µM. After 48 h of treatment, the plates were removed from the incubator and the GSH-Glo™ Glutathione assay was performed according to the instructions of the manufacturer. The results of the GSH assay are presented as nmol/10^6 cells (mean ± SD) (n=3 independent samples from one experiment) and as percentage of control. In Pd-Spm-treated cells, the level was below the detection limit of the assay and thus the value was set to 0. The data in the row defined as Cells were derived from the growth curves (Fig. 48 **A**–**C**). The number of cells in each treatment as % of control was calculated at 48 h of treatment. ** $p < 0.01$ compared to control; *** $p < 0.001$ compared to control.

IV - Discussion

“The important thing in Science is not so much to obtain new facts as to discover new ways of thinking about them.”

Sir William Lawrence Bragg

4. Discussion

The leading aim of many research groups across the world is to find a proper and highly efficient anticancer drug that can be applied in the treatment of human tumours, overcoming the resistance often developed upon drug administration [133]. Among all types of cancer, the one that causes one of the highest death rates among women worldwide is still breast cancer [297]. For this reason, new treatment strategies are needed and the initial step is to synthesise new chemotherapeutic agents and further test them in breast cancer cell lines, in order to select promising candidates that can be used in the clinic.

In this thesis, three different modified (N-alkylated) biogenic polyamines (NSpd, BENSpm and CPENSpm) and their newly synthesised Pd(II) and Pt(II) chelates Pd-NSpd, Pt-NSpd, Pd-BENSpm, Pt-CPENSpm and Pd-Spm (Fig. 9) were structurally characterised by vibrational spectroscopy and analysed for their anticancer activity against various human breast cancer cell lines. This type of agents were chosen in view of the promising results already obtained for bi- and trinuclear Pd(II) and Pt(II) spermidine and spermine complexes, regarding their interaction with DNA and their antineoplastic properties [156,170,171,191-193].

Characterisation of the Compounds by Vibrational Spectroscopy

Linear alkylpolyamines, such as the biogenic polyamines spermidine and spermine or the presently investigated analogues, can adopt numerous conformations depending on the dihedral angles that determine their overall orientation, the most common ones being 60^o (*gauche*), 180^o (*trans*) and -60^o (*gauche´*). At physiological pH, all the nitrogen atoms of these polyamines are protonated, which hinders the formation of intramolecular (N)H ··· N or (C)H ··· N hydrogen bonds and favouring the *all-trans* conformation energetically. Under these conditions, electrostatic and steric effects determine the energetically favoured geometrie(s) for these molecules. Previous conformational analysis of α,ω-diamines ($H_2N(CH_2)_nNH_2$, n=2 to 10 and n=12), as well as of the larger spermidine (triamine) and spermine (tetramine) systems [201,203,298-302] have demonstrated that the *all-trans* conformation is the predominant or even the sole conformation at room temperature for this kind of totally extended polycationic molecules, in the solid state.

The conformational preferences of the compounds used in the present study were obtained through vibrational analysis – FTIR and Raman spectroscopies. Interpretation of the experimental data was assisted by the calculated geometries and corresponding vibrational pattern, and a quite good agreement was obtained.

The bands due to the rocking modes of the terminal NH_3 groups (particularly intense in infrared, Fig. 31) were only observed for NSpd, as expected, since BESpm, BENSpm and CPENSpm are alkylated at the terminal nitrogen atoms. However, the features occurring at about 1600 cm^{-1}, assigned to NH_2 symmetric and antisymmetric deformations (from the central amine groups), were detected in all the modified polyamines. As expected, the NH stretching vibrations have a larger IR intensity as compared to Raman. It is interesting to note that the Raman spectrum of NSpd displays quite strong $\nu(NH_3)$ modes from the terminal NH_3 groups (that are absent in the alkylated polyamines), while the corresponding vibrations for the central NH_2 moieties are hardly detectable.

Some of the typical acoustic modes of this kind of *all-trans* extended molecules, comprising repeated CH_2/NH_2 units [300,302] – either longitudinal (LAM's) or transverse (TAM's) – were detected in the low frequency region of the Raman spectra for NSpd and CPENSpm. Additionally, NSpd and BENSpm being centrossymmetric species, a complementary IR and Raman pattern was obtained, as opposed to their biogenic counterparts spermidine and spermine [201,203].

The polyamine chelates presently studied vary in their coordination pattern, according to the type of ligand – either tri- or tetramine: in $(MCl_2)_3(NSpd)_2$ (M-NSpd) (M = Pt(II) or Pd(II)), two of the metal ions are bound to each of the NSpd ligands, while the third is shared by both amines. In Pd-BENSpm and Pt-CPENSpm, in turn, the two metal centres coordinate to the four nitrogens of the spermine-like molecule (Fig. 10). The spectroscopic data presently gathered confirms this type of coordination, both Pt(II) and Pd(II) being known to have a significant affinity for nitrogen atoms. Hence, upon metal binding to the polyamines, some expected changes occurred in the vibrational features of the ligands. These include:

(i) intensity variation of the amine stretching bands – for BENSpm and CPENSpm they are hardly observable for the free ligands but become quite intense for the corresponding complexes (Figs. 32 and 33). In contrast, for NSpd and its complexes the intensity of these features lowers upon metal binding (Fig. 34);

(ii) marked shift of the NH stretching bands to higher frequencies;

(iii) loss of the main deformation bands assigned to the NH_2/NH_3 groups, namely $\delta(NH_2)$, $\delta(NH_3)$ and $r(NH_3)$ (Figs. 32 to 34);

(iv) detection of characteristic Raman bands below *ca.* 600 cm^{-1}, ascribed to (Cl-M-Cl) and (N-M-N) deformations, as well as to symmetric and antisymmetric (Cl–M–Cl) and (N–M–N) stretching modes (Figs. 32 to 34, Tabs. 9 to 11). These features allow to identify the presence of the complex after the synthetic procedure.

Overall, complexation of the polyamine ligands leads to a marked weakening of the Raman bands at higher wavenumbers (above 1000 cm^{-1}) relative to the very intense signals that appear below *ca.* 600 cm^{-1}, which are due to strong vibrational modes involving the metal and its first coordination sphere.

These results are in accordance with the previously gathered data for cisplatin and its Pd(II) homologue [200,205,211,290], as well as for the similar polynuclear spermidine (M_3Spd_2) and spermine (M_2Spm) chelates (M=Pt(II) or Pd(II)) [unpublished data]. Actually, comparison of the vibrational profile of the presently investigated cisplatin-like chelates, comprising two or three ($MCl_2(NH_3)_2$) moieties, with cisplatin's vibrational pattern [290] indicates that the deformation and stretching modes involving the metal centre, either Pt(II) or Pd(II), occur in defined spectral regions irrespective of the type of species – either the mononuclear cisplatin and its Pd(II) homologue, or the di- and trinuclear polyamine chelates – since they reflect a very similar metal coordination sphere (Table 9).

Evaluation of the Cellular Impact

Within the drug discovery field of cancer treatment, the study of the cellular impact of a potential anticancer agent by the use of methods that evaluate cell proliferation and cell cycle phase distribution, metabolic activity and cell death constitute important approaches. Since deregulation of cell proliferation is known to be a hallmark of cancer, the pathways involved are an essential source of new targets for cancer therapy [2].

Taking this into account, the next step was to test the cytotoxic activity of these compounds against a wide range of breast cancer cell lines, using different biological assays in an attempt to fully evaluate their cellular effects.

The four breast cancer cell lines (JIMT-1, L56Br-C1, MCF-7 and MDA-MB-231) and the immortalised normal-like breast epithelial cell line (MCF-10A) were first used to investigate the cytotoxic effects of the spermidine analogue NSpd and its newly synthesised

trinuclear Pd(II) and Pt(II) complexes (Pd-NSpd and Pt-NSpd, respectively). In general, the results showed that the different cell lines reacted differently to the treatment with NSpd, Pd-NSpd or Pt-NSpd, the normal-like MCF-10A line being the least sensitive.

As determined by the MTT assay, administration of NSpd, Pd-NSpd or Pt-NSpd resulted in decreased cell viability and an increased growth inhibition in a dose- and time-dependent manner. MCF-10A was shown to be the least affected cell line while L56Br-C1 was the most sensitive one. Interestingly, the polyamine analogue NSpd, which has not been tested before, presented a clear growth inhibitory effect. The effect obtained with the Pd(II) complex of NSpd was usually similar to that obtained with NSpd. However, a clear difference was seen between the two NSpd complexes. In fact, Pd-NSpd treatment resulted in much higher MTT reduction than Pt-NSpd treatment in all the cell lines tested, demonstrating it to be considerably more cytotoxic than the homologous Pt(II) complex.

Similar results were obtained in a cell proliferation assay in which the L56Br-C1 was the most sensitive cell line, whereas the MCF-10A cells were hardly affected by either of the drugs. In this assay, Pd-NSpd was shown to have a somewhat stronger antiproliferative effect on the breast cancer cell lines than NSpd. In addition, the Pd-NSpd effect was also stronger than that of the homologous Pt(II) complex. Results from repeated cycles of drug treatment and withdrawal demonstrated that the breast cancer cells did not easily recover from treatment with NSpd or Pd-NSpd. Again, the L56Br-C1 cells were the most sensitive ones, demonstrating an unchanged or decreased cell number after repeated cycles of treatment with NSpd or Pd-NSpd, respectively. Interestingly, the breast cancer cells appeared to recover quickly from the antiproliferative effect of Pt-NSpd. Only minor effects on cell proliferation were observed when treatment with Pt-NSpd was combined with withdrawal periods. The results are in accordance with those of published studies regarding other Pd or Pt-polyamine complexes, namely Pd(II)- and Pt(II)-spermine complexes [133,156,170,191,192], where the substitution of Pt(II) for Pd(II) increased the cytotoxicity of the drug [171]. Actually, this substitution was shown to significantly increase the anticancer effect against the human squamous carcinoma cell line (HSC-3) [156,170].

In most cell types, two classes of polyamine transport systems have been recognised: one that is sodium dependent with a preference for putrescine and one that is sodium independent with a preference for spermidine and spermine. The polyamine transport system is energy-, time-, temperature-, and concentration-dependent and saturable, suggesting it is a carrier-mediated transport. However, this system has a low specificity and, thus, can be

responsible for the transport of various molecules, like polyamine-based compounds, into the cell [53,85]. In general, and since the transporter is not specific for putrescine, spermidine or spermine, the affinity of the carrier increases to amines which have chain lengths resembling those of spermidine or spermine. It has also been shown that the primary nitrogen groups from the polyamines seem to be critical for uptake [87]. Primary amines are present in the linear NSpd, Pd-NSpd and Pt-NSpd (terminal amino groups), thus pointing to a possibility of these compounds being taken up by the polyamine transporter. In this study, it was shown that only NSpd competed efficiently with ^{3}H-spermidine uptake in all four cell lines, indicating that NSpd uses the same polyamine transport system as spermidine to enter the cell. Regarding the complexes, Pd-NSpd inhibited ^{3}H-spermidine uptake to a higher degree compared to Pt-NSpd, but still much less compared to NSpd. It is unclear how these chelates are transported into the cell but, since they share similarities with cisplatin, it is possible that they enter the cell in the same way. It was recently found that CTR1 and CTR2 modulate the uptake of Pt(II)-based anticancer drugs, such as cisplatin [137,143,149,151]. Currently, the CTR1 is known to act as a major Pt-drug transporter in several cell systems [143]. Therefore, the presently investigated complexes might also enter the cell using the CTR1 transporter or, since they are considerably more lipophilic than cisplatin (due to the presence of the alkylpolyamine ligands), by passive diffusion across the membrane to a larger extent. In addition they may partly use the polyamine transport system, as well. Again, minor structural differences can have important effects on activity, which was clearly shown through the substitution of a Pd by a Pt centre [170,171].

The differences in cytotoxicity observed between Pd-NSpd and Pt-NSpd complexes may be caused by differences in cellular uptake. Attempts to estimate the content of the complexes in L56Br-C1 and MCF-10A cells revealed a large difference between the two cell lines. The most sensitive cell line, L56Br-C1, contained more than 10-fold higher concentrations of Pd-NSpd or Pt-NSpd compared to the least sensitive cell line MCF-10A, after treatment with the complexes for 3 days. The reason for this difference is not known. No major differences were seen in the ability of the complexes to inhibit the ^{3}H-spermidine uptake in the cells, indicating that the uptake of the complexes may be unrelated to the polyamine transport system. Interestingly, the data showed that in MCF-10A cells the content of Pt-NSpd was higher than of Pd-NSpd after treatment with the complexes, suggesting a more efficient uptake of Pt-NSpd than of Pd-NSpd. The same was not shown in L56BR-C1 cells, which contained equal amounts of the complexes after treatment. Nevertheless, Pd-

NSpd exhibited stronger cytotoxicity than Pt-NSpd in all of the breast cancer cell lines tested, making it a more efficient agent from a cancer treatment approach.

High expression of ODC characterises some cancers, including breast cancer. Consequently, there has been a great effort to search for new compounds that can inhibit ODC activity in tumour cells [303]. In the present study, the increase in ODC activity in all cell lines registered 24 h after seeding is correlated to cell proliferation. The reason for ODC activity remaining elevated for somewhat longer time in L56Br-C1 cells, compared to the other cell lines, is not known. However, this cell line has the slowest growth rate of the ones used in the present study and it is conceivable that the duration of the ODC peak is somewhat connected to the growth rate of the cells. NSpd or Pd-NSpd treatment resulted in ODC inhibition in all the cell lines, except for the JIMT-1 cells. In comparison, no significant inhibition was observed with Pt-NSpd treatment. Although the ODC activity was significantly suppressed by NSpd or Pd-NSpd treatment in all cell lines, it is not clear if it contributes to the compounds cytotoxicity. Overall, there did not seem to be a clear correlation between the effects of the drugs on ODC activity and their antiproliferative effects (*i.e.* compare growth inhibitory effects and ODC suppression in JIMT-1 and MCF-10A cells). However, polyamine analogues are known to also activate the polyamine catabolic pathway leading to the depletion of the biogenic polyamines, which may be part of the growth inhibitory mechanism.

The DNA distribution of a cell population evaluated by FCM gives information about cell cycle phase distribution and cell death. The most consistent changes in cell cycle phase distribution were found in L56Br-C1 and JIMT-1 cells. Treatment of L56Br-C1 cells with Pd-NSpd or NSpd resulted in an increase in the percentage of cells in sub-G_1 region. This increase of the sub-G_1 fraction was substantially higher after 72 h of treatment, demonstrating that treatment with either Pd-NSpd or NSpd induced cell death in this cell line. Consequently, the whole cell cycle phase distribution was affected, resulting in a decrease in the percentage of cells in G_1 phase along with an increase in both S and G_2 phases. Since cell death was induced and no cell proliferation was observed, cell death presumably took place in G_1 cells. There was no marked cell death observed in JIMT-1, MCF-7 and MCF-10A cells by treatment with either of the drugs. However, in JIMT-1 cells, the percentage of cells in G_1 phase was increased already after 24 h of treatment with Pd-NSpd, indicating a block in this phase. This is also obvious from the growth curve analysis where we detected a block in cell proliferation at the same time point. In accordance with the results from the other growth experiments, no clear differences in cell cycle phase distribution were observed in MCF-10A

and MCF-7 cells treated with NSpd, Pd-NSpd or Pt-NSpd. Nevertheless, as small effects on the cell cycle progression may be highly significant from a pharmacological point of view, it was important to fully evaluate the cell cycle progression, namely the length of S and G_2+M phases, by the use of a DNA BrdUrd flow cytometric method. Compared to controls, NSpd and Pd-NSpd-treated cells showed a significant prolongation of the S phase as well as the G_2+M phase in all cell lines. The prolongation of both phases was less evident in Pt-NSpd-treated cells. Polyamines are known to stabilise DNA, so replacement of natural polyamines with analogues may result in DNA destabilisation that could have caused the S phase prolongation in NSpd-treated cells. On the other hand, the interaction of the chelates with DNA occurs by covalent linkage to the nitrogen atoms of the bases, mainly the N_7 of guanine and adenine, therefore disrupting the base-paring. These complexes form long-range, intra- and interstrand DNA adducts that are responsible for a more severe and less reparable damage than their counterparts (for instance, cisplatin) [133,135,178-180,304]. Effects on cell cycle kinetics are often related to cell cycle regulatory proteins and polyamine levels. However, in this study we did not analyse any cell cycle regulatory protein nor polyamine pools and thus no further conclusions can be drawn.

The results are further emphasised by the CFE in soft agar. The ability of forming colonies in soft agar is characteristic of malignant cells and reproduces the invasiveness of the cancer, so only the breast cancer cell lines were analysed. This assay showed a decrease in colony formation in all treated cells compared to the control, after 72 h of treatment. Again, this reduction was higher in NSpd or Pd-NSpd-treated cultures. The largest effect was obtained in the L56Br-C1 cell line with a decrease in colony forming efficiency of over 50%.

In the mammalian genotoxicity screen, NSpd and Pt-NSpd were found to be potential genotoxins at 50 µM and 100 µM concentrations. In contrast, Pd-NSpd did not show any genotoxicity at any of the concentrations tested in the mammalian genotoxicity screen, although we cannot rule out genotoxicity in other assays. SCGE assay did not shown any induction of DNA strand breaks with 25 µM NSpd, Pd-NSpd or Pt-NSpd treatment in any of the cell lines. However, taking these results together, we can expect that induction of DNA strand breaks could be detectable when using a higher concentration of the drug (50 µM for NSpd and 100 µM for Pt-NSpd).

It has been shown that high levels of AzI induce polyamine biosynthesis, thus leading to enhanced intracellular polyamine pools and, consequently, to promotion of cell proliferation and transformation [79,80,89,93]. In addition, AzI has been shown to be induced in growth-stimulated mouse fibroblasts, as well as in certain forms of human cancers,

suggesting a role for AzI in proliferation and cell cycle progression [90,305]. Therefore, it was of relevance to study how the treatments with the compounds affected the AzI levels in the various cell lines. However, although a strong AzI band was detected in all the cell lines analysed, no clear differences were observed between the different treatments. Therefore, the decrease in cell proliferation mainly observed in NSpd- and Pd-NSpd-treated cells cannot be explained by a decrease in AzI expression levels.

Taking into consideration the results obtained with NSpd and its Pd(II) and Pt(II) complexes, we next analysed the cytotoxic effects of the polyamine analogues BENSpm and CPENSpm, together with the metal-based polyamine complexes, Pd-BENSpm, Pd-Spm and Pt-CPENSpm on JIMT-1, L56Br-C1, MCF-7 and MCF-10A human breast cell lines.

Previous studies have shown that both BENSpm and CPENSpm effectively inhibit cell proliferation in breast cancer cell lines [107,112-114]. Interestingly, the platination of CPENSpm clearly induced a marked reduction in toxicity in all the cell lines analysed in the present study. In contrast, the palladination of BENSpm increased the cytotoxic effect of the compound. The reason for this difference in not known, but may be related to the cellular uptake, which was significantly higher for Pd-BENSpm than for Pt-CPENSpm. These results are in agreement with the data obtained for NSpd, Pd-NSpd and Pt-NSpd, where it was observed that platination of NSpd significantly reduced the cytotoxic effect of the compound, whereas palladination did not [306]. However, the difference in cytotoxicity between the Pd(II) and the Pt(II) complex of NSpd was not explained by a difference in uptake, thus indicating an alternative mechanism. Furthermore, the use of chelating ligands in this fashion may render a very stable Pt(II) compound with reduced lability compared to its parent compound cisplatin and its palladium counterparts and, therefore, less prone to react with the cellular targets.

The Pd(II) complex of spermine was used for comparison and was demonstrated to exert cytotoxic activity against the breast cancer cells tested. However, the natural polyamine spermine normally does not exhibit any major cytotoxic effects, as opposed to BENSpm and CPENSpm. Interestingly, only minor effects were observed with Pd-Spm in the normal-like breast epithelial cell line (MCF-10A). Pd-Spm has previously been demonstrated to also be cytotoxic against the breast cancer cell lines MCF-7 and MDA-MB-231 [192], as well as the human oral squamous carcinoma cell line HSC-3 [171]. In those studies, the effect of Pd-Spm seemed to be irreversible. No recovery was observed after withdrawal of the drug. Nevertheless, as shown in the present study, the cytotoxic effect of Pd-Spm was, at least,

partly reversible in the cell lines JIMT-1 and MCF-10A. The cytotoxic effects of Pd-BENSpm as well as of BENSpm and CPENSpm, on the other hand, appeared to be irreversible in all cell lines tested.

The cell line that presented an overall higher sensitivity to the compounds tested was the L56Br-C1 (in accordance with the previous results obtained with NSpd, Pd-NSpd and Pt-NSpd). Pd-BENSpm, BENSpm and CPENSpm were all strongly cytotoxic against L56Br-C1 cells, as revealed by growth inhibition, increased cell death, decreased colony forming efficiency, as well as induction of DNA strand breaks. The uptake of Pd-BENSpm was much more efficient in the L56Br-C1 cells than in the other cell lines tested, which may partly explain the sensitivity of this cell line for the Pd(II) complex. Another possible explanation for the difference in sensitivity may lie in different redox potentials in the cell lines. Determination of the GSH level showed that the GSH pool was about 50% lower in L56Br-C1 cells compared to MCF-10A and JIMT-1 cells.

Interestingly, we found that Pd-Spm lowered the GSH pool to an undetectable level in MCF-10A, JIMT-1 and L56Br-C1 cell lines, but this was not reflected in a similar decrease in cell number. The cell number was still high in MCF-10A and JIMT-1 cells and only reduced by 60% in L56Br-C1 cells. Pd-Spm was presumably inactivated by binding to GSH, thus resulting in a reduced cytotoxicity. The toxicity of cisplatin has been shown to be reduced by GSH [296]. GSH-binding to cisplatin is responsible for metabolic drug inactivation, thereby decreasing its bioavailability at the pharmacological target and hence its antitumour activity [307]. In addition, cisplatin resistance has sometimes been correlated with a rise in the levels of cellular GSH [307]. Moreover, Pd(II), which is more labile than Pt(II), is also more prone to bind to sulphur atoms than Pt(II), according to the soft and hard acid base theory [308]. The fact that the cell number did not decrease after 48 h of treatment with Pd-Spm may imply a very efficient synthesis of GSH, maintaining at least a low pool, although not detectable, of GSH sufficient for cell proliferation and survival. However, this notion has to be further investigated. BENSPM, Pd-BENSpm, and CPENSpm lowered the GSH pools but not to the same extent as Pd-Spm, implying that these compounds were not inactivated by GSH to the same extent as was Pd-Spm (even if these treatments all reduced the cell number to a larger extent than Pd-Spm treatment). The difference in effects on the GSH levels between Pd-BENSpm and Pd-Spm is very interesting since the compounds are structurally very similar. However, this may be due to the extra $–CH_2CH_3$ arm making the metal centre less available for nucleophilic attack and thus less susceptible to inactivation by GSH. Regarding the GSH lowering activity of Pd-Spm, it may be exploited in the search for anticancer redox

chemotherapeutics [307,309]. Treatment of MCF-10A and L56Br-C1 cells with Pt-CPENSpm, on the other hand, gave an increase in the GSH level at the same time as cell proliferation was reduced by about 10%. In JIMT-1 cells, Pt-CPENSpm treatment resulted in a reduced GSH level. Thus, we can conclude that there is no clear correlation between decrease in GSH levels and reduction of cell number in any of the cell lines.

Biogenic polyamines are essential for a variety of cellular processes, including cell growth [53,76]. Depletion of cellular polyamines may potentiate the effect of the cytotoxic agents and, eventually, result in growth arrest. Under physiological conditions, the polyamines are positively charged and bind strongly to negatively charged macromolecules, like DNA and RNA [53,76]. The binding of polyamines to DNA is believed to stabilise the DNA. Thus, interference with the cellular polyamine homeostasis may render the cells more sensitive to cytotoxic drugs that interact with DNA. Polyamine analogues have been shown to decrease cellular polyamine levels by inhibiting their biosynthesis as well as inducing their catabolism [101,295,310]. As shown in the present study, Pd-BENSpm, BENSpm and CPENSpm besides being highly cytotoxic, all induced SSAT, which catalyses the rate-limiting step in polyamine degradation, to very high levels in L56Br-C1 cells. High SSAT induction by BENSpm treatment was also previously found in L56Br-C1 cells [293]. The increase in SSAT was reflected in a concomitant decrease in cellular polyamine content. Moreover, platination of CPENSpm not only decreased the cytotoxic effect of the drug on L56Br-C1 cells, but also eliminated its effects on cellular SSAT activity and polyamine levels. Although there seems to be a strong correlation between the cytotoxic effects and polyamine depletion, the underlying mechanism is not known. However, it is also believed that the production of H_2O_2 and acetaldehyde formed in the polyamine oxidase-catalysed oxidation of the products of the SSAT reaction may also contribute to a cytotoxicity effect [293,311]. GSH is an essential metabolite in the molecular mechanisms involved in the detoxification of H_2O_2. The lower GSH pool in L56Br-C1 cells may thus also contribute to an increased sensitivity to the presence of H_2O_2 produced in polyamine catabolism.

It has recently been suggested that spermine oxidase, and not the acetylpolyamine oxidase as previously was thought, is the exclusive source of H_2O_2, at least in breast cancer cell lines treated with polyamine analogues [311]. It was shown that the H_2O_2 formed upon induction of polyamine catabolism in MDA-MB-231 cells treated with BENSpm was found to be solely derived from spermine oxidase [311].

Stem cell markers are often used to evaluate the aggressiveness and invasiveness of cancer. It has been found that individual tumours contain highly heterogeneous cell populations identified by cell surface markers and also by intracellular markers. The cell surface markers CD44 and CD24 are adhesion molecules and the $CD44^+CD24^-$ cells were suggested to be CSCs in a breast cancer model [44]. We have shown that treatment with the polyamine analogue PG-11047 reduced the putative $CD44^+CD24^-$ CSC population in JIMT-1 cells and decreased their CFE [283]. BENSpm, which is a polyamine analogue closely related to PG-11047, also reduced the CSC population evaluated by FCM and the CSC reducing effect was retained to a similar degree by Pd-BENSpm treatment (no significant difference was obtained between BENSpm and Pd-BENSpm). Although the antiproliferative effect of CPENSpm treatment was very much similar to that of BENSpm and Pd-BENSpm treatments, there was no effect on the putative $CD44^+CD24^-$ CSC population. Interestingly, all three compounds resulted in similar a decrease in CFE. Thus the CFE was markedly reduced, whereas the putative $CD44^+CD24^-$ CSC population was not, after treatment with CPENSpm. Moreover, Pt-CPENSpm treatment resulted in an increased putative $CD44^+CD24^-$ CSC population, in spite of a decrease in the CFE, compared to control. Thus, the data support the notion that other factors than only CD44 positivity and CD24 negativity define CSCs [312]. Also, we did the CFE in the presence of FCS which may support colony formation not only by CSCs but also by other progenitor cells, although this has not clearly been shown for breast cancer.

The Anthem's Genotox screen was used to determine if any of the compounds tested could be classified as potential genotoxins in the range of the concentrations analysed. This screen is highly sensitive and specific, when compared with currently available *in vitro* genotoxicity assays. By using this mammalian screen, BENSpm and Pd-BENSpm were found to induce p21 and p53 at 5 µM and 10 µM concentrations. Interestingly, Pd-BENSpm induced p21 to a higher degree than BENSpm which may contribute to the slight higher toxicity of Pd-BENSpm compared to BENSpm.

A close statistical comparison (not shown) between BENSpm and Pd-BENSpm showed that the latter was indeed somewhat more cytotoxic than the former. The cell number was significantly lower in Pd-BENSpm-treated cultures after 48 and 72 h of treatment than in BENSpm-treated cultures in all breast cancer cell lines. Pd-BENSpm treatment reduced the CFE significantly more than BENSpm treatment did. Pd-BENSpm treatment resulted in significantly more comets in SCGE than did BENSpm treatment in the two cancer cell lines JIMT-1 and L56Br-C1 but not in MCF-10A cells. Pd-BENSpm treatment also reduced the

GSH level significantly more than BENSpm treatment did in the two cancer cell lines. Thus, although the difference between BENSpm and Pd-BENSpm is small, Pd-BENSpm showed slightly higher toxicity against cancer cells and thus may be of some importance for further design of new metal-based polyamine analogues.

V - Conclusions

“Science knows no country, because knowledge belongs to humanity, and is the torch which illuminates the world.”

Louis Pasteur

5. Conclusions

Interference with polyamine homeostasis through administration of modified analogues, or the use of metal complexes with a view to affect cell growth *via* DNA covalent binding, are promising therapeutic approaches against cancer. In order to follow this type of strategies, a thorough knowledge of the conformational preferences of both modified polyamines and their chelates is crucial for understanding the mechanisms through which they are metabolised after being transported into the cell (pharmacokinetics) and the molecular basis of their interaction with the pharmacological target (pharmacodynamics).

The reported results show the successful syntheses and purification of Pd(II) and Pt(II) chelates with modified biogenic polyamines (tri- and tetramines), presently modified and improved relative to previously published methods. Additionally, the theoretical approach used to simulate these systems was suitable, as expected in the light of previous data published within this research group on cisplatin and cisplatin-like complexes [170,200,205,211].

As expected, and similarly to previously reported studies on biogenic polyamines, the *all-trans* geometry was found to be energetically favoured for the physiological, totally protonated, states of all the alkylated linear amines presently investigated. The polynuclear chelates display a stable geometry identical to that previously obtained for their analogues with spermine (M_2Spm) and spermidine (M_3Spd_2), comprising two or three cisplatin-like ($MCl_2(NH_3)_2$) moieties, respectively. Therefore, when interacting with DNA (their main biological target), they are able to bind to the purine/pirimidine bases through two or three different sites simultaneously, upon hydrolysis of the chloride leaving groups, *via* long-range intra- and interstrand interactions. This type of non-conventional interplay with the target, not available to mononuclear drugs such as cisplatin or carboplatin, greatly enhances their cytotoxicity while decreasing the success of repairing mechanisms.

This kind of conformational studies – both for the target and the potential chemotherapeutic agents – is the basis for a rational development of new anticancer drugs, coupling a higher (and hopefully selective) cytotoxic activity to an optimised therapeutic efficacy, as well as to the capacity of overcoming resistance to clinically used agents.

Concomitant biological studies – cytotoxicity and cell growth inhibition evaluation – were also performed for both the modified polyamines and their Pt(II) and Pd(II) chelates in human breast cancer cell lines, aiming at linking structural preferences to anticancer effect.

The studies performed on the cellular effects of the tested compounds are important for future attempts to improve cancer treatment and also to increase our understanding regarding the polyamines and their effects in the cell. The results obtained in these studies show that a variety of responses are induced after treatment with various polyamine analogues and their Pd(II) and Pt(II) complexes, in several human breast cancer cells. Different behaviours of the drugs were shown in the various cell lines, with L56Br-C1 being the most sensitive and MCF-10A the least sensitive one.

The overall data demonstrated that the Pd-NSpd complex displayed stronger antiproliferative effects on the human breast cancer cell lines tested, as compared to Pt-NSpd. Similar findings were observed when comparing the cytotoxic effects of trinuclear Pd(II) chelates of spermidine and spermine to those of their Pt(II) analogues [156,170,191,192]. The reason for this cytotoxicity enhancement is likely to be related to a more efficient interaction with DNA, yielding interstrand long-range adducts less prone to repair, and hence a more severe damage. Furthermore, this seems to be a selective effect, since the cytotoxicity activity of the Pd(II) and Pt(II) polyamine complexes varied depending on the cell line [156,170,191,192]. In general, cancer cells seemed more sensitive to the compounds than the non-neoplastic ones [156,169,192]. Overall, NSpd and Pd-NSpd were shown to have strong antiproliferative effects.

BENSpm, Pd-BENSpm and CPENSpm were found to have the strongest antineoplastic effect on the breast cancer cells tested. The growth inhibition induced by the compounds affected polyamine homeostasis considerably, which points to the importance of finding biomarkers for sensitivity and resistance in the treatment of breast cancer. It was also verified that some of the compounds were responsible for a damaging interaction with DNA, although the exact nature of this interplay remains to be identified. Nevertheless, the differences observed between the complexes may be related to differences in uptake, metabolism and/or reaching the target. In addition, it is known that a simple chemical modification in the structure of a compound may alter its binding profile to DNA and, consequently, its cytotoxic activity.

In conclusion, of the compounds studied, Pd-BENSpm may be regarded as a promising inorganic agent to be used for the development of new chemotherapy approaches against breast cancer, due to its slightly higher cancer cell toxicity coupled to lower side effect toxicity.

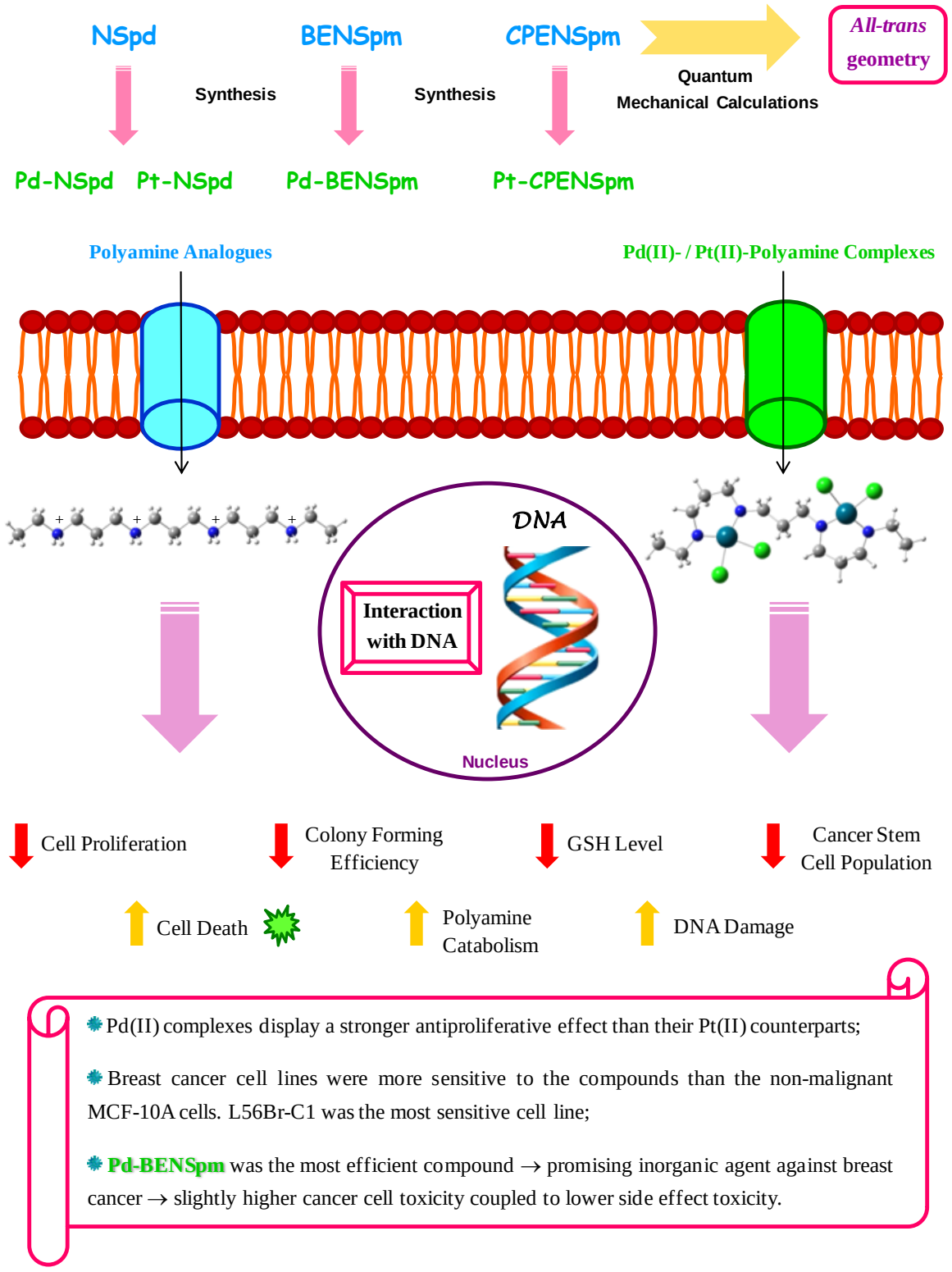

Figure 56: Schematic representation of the main conclusions resulting from this study.

Future Perspectives

Although many of the questions initially asked in this study were already answered, thus contributing to an improvement of knowledge within this research field, some others arose:

- How are these compounds transported into the cells?
- What cellular mechanisms are responsible for the cytotoxicity induced by the polyamine analogues and the Pd(II) complexes in the breast cells?

In order to address these questions, future work can be envisaged:

- Synthesis and conformational characterisation of new Pd(II) and Pt(II) complexes with other modified polyamines (such as BESpm), as well as of Pt(II)-BENSpm and Pd(II)-CPENSpm chelates (in order to do comparison with Pd-BENSpm and Pt-CPENSpm);
- Analysis of cell cycle regulatory protein levels;
- Study of SMO and PAO activity in breast cancer cells treated with these compounds;
- Cytotoxicity assessment of the compounds in cisplatin-resistant breast cancer cell lines;
- Biodistribution studies (namely by microRaman spectroscopy);
- Study of the actual binding to DNA using ICP-MS;
- Pretreatment (chemosensitisation) with DFMO, prior to drug administration;
- Analysis of the general toxicity in cell culture systems to evaluate side effects;
- Combination therapeutic schemes, aiming at a possible synergetic effect.

VI - References

“A man's friendships are one of the best measures of his worth.”

Charles Darwin

6. References

1. Morange M. (**2011**) History of cancer research. Chichester: *John Wiley & Sons Ltd*.
2. Hanahan D., Weinberg R. A. (**2011**) Hallmarks of cancer: the next generation. *Cell* **144**: 646-674.
3. Weinstein I. B., Case K. (**2008**) The history of Cancer Research: introducing an AACR Centennial series. *Cancer Res* **68**: 6861-6862.
4. WHO (**2012**) http://www.who.int/mediacentre/factsheets/fs317/en/index.html. *(accessed in March 2013).*
5. Malvezzi M., Bertuccio P., Levi F., La Vecchia C., Negri E. (**2012**) European cancer mortality predictions for the year 2012. *Ann Oncol* **23**: 1044-1052.
6. Society A. C. (**2012**) Cancer Facts & Figures 2012. Atlanta: *American Cancer Society*. pp. 1-68.
7. WHO: Mortality Profiles (**2013**) http://www.who.int/mediacentre/factsheets/fs297/en/. *(accessed in March 2013).*
8. Hong W. K., Bast R. C. J., Hait W. N., Kufe D. W., Pollock R. E., Weichselbaum R. R., Holland J. F., Frei III E. (**2010**) Holland-Frei Cancer Medicine. Shelton: *People's Medical Publishing House-USA.*
9. DeVita V. T., Lawrence T. S., Rosenberg S. A. (**2011**) Cancer: Principles and Practice of Oncology. Philadelphia: *Lippincott Williams & Wilkins*.
10. Cantor J. R., Sabatini D. M. (**2012**) Cancer cell metabolism: one hallmark, many faces. *Cancer Discov* **2**: 881-898.
11. NCI (**2013**) http://www.cancer.gov/cancertopics/cancerlibrary/what-is-cancer. *(accessed in March 2013).*
12. CRA (**2013**) http://www.cancer-research-awareness.com/types-of-cancer.html. *(accessed in March 2013).*
13. Umar A., Dunn B. K., Greenwald P. (**2012**) Future directions in cancer prevention. *Nature Reviews Cancer* **12**: 835-848.
14. Hanahan D., Weinberg R. A. (**2000**) The hallmarks of cancer. *Cell* **100**: 57-70.
15. Butcher L. D., Boland C. R. (**2012**) Tumour Formation: Number of Mutations Required. Chichester: *eLS. JohnWiley & Sons, Ltd.*
16. Cairns R. A., Harris I. S., Mak T. W. (**2011**) Regulation of Cancer Cell Metabolism. *Nature Reviews Cancer* **11**: 85-95.

17. Tlsty T. D., Briot A., Gualberto A., Hall I., Hess S., Hixon M., Kuppuswamy D., Romanov S., Sage M., White A. (**1995**) Genomic instability and cancer. *Mutat Res* **337**: 1-7.
18. Tryggvadottir L., Gislum M., Hakulinen T., Klint A., Engholm G., Storm H. H., Bray F. (**2010**) Trends in the survival of patients diagnosed with malignant melanoma of the skin in the Nordic countries 1964-2003 followed up to the end of 2006. *Acta Oncologica* **49**: 665-672.
19. WHO (**2013**) http://www.who.int/cancer/detection/breastcancer/en/. *(accessed in February 2013).*
20. Simstein R., Burow M., Parker A., Weldon C., Beckman B. (**2003**) Apoptosis, chemoresistance, and breast cancer: insights from the MCF-7 cell model system. *Exp Biol Med (Maywood)* **228**: 995-1003.
21. Richie R. C., Swanson J. O. (**2003**) Breast cancer: a review of the literature. *J Insur Med* **35**: 85-101.
22. Forouzanfar M. H., Foreman K. J., Delossantos A. M., Lozano R., Lopez A. D., Murray C. J., Naghavi M. (**2011**) Breast and cervical cancer in 187 countries between 1980 and 2010: a systematic analysis. *Lancet* **378**: 1461-1484.
23. Beiki O., Hall P., Ekbom A., Moradi T. (**2012**) Breast cancer incidence and case fatality among 4.7 million women in relation to social and ethnic background: a population-based cohort study. *Breast Cancer Res* **14**: R5.
24. WHO (**2013**) http://www.who.int/cancer/detection/breastcancer/en/index2.html. *(accessed in February 2013).*
25. DeSantis C., Siegel R., Jemal A. (**2011**) Breast Cancer: Facts & Figures 2011-2012. American Cancer Society Inc.: Atlanta.
26. NCI (**2012**) http://www.cancer.gov/cancertopics/pdq/treatment/breast/Patient/page2#Keypoint9. *(accessed in February 2013).*
27. Walters S., Maringe C., Butler J., Rachet B., Barrett-Lee P., Bergh J., Boyages J., Christiansen P., Lee M., Warnberg F., Allemani C., Engholm G., Fornander T., Gjerstorff M. L., Johannesen T. B., Lawrence G., McGahan C. E., Middleton R., Steward J., Tracey E., Turner D., Richards M. A., Coleman M. P. (**2013**) Breast cancer survival and stage at diagnosis in Australia, Canada, Denmark, Norway, Sweden and the UK, 2000-2007: a population-based study. *Br J Cancer*.

28. Yi M., Mittendorf E. A., Cormier J. N., Buchholz T. A., Bilimoria K., Sahin A. A., Hortobagyi G. N., Gonzalez-Angulo A. M., Luo S., Buzdar A. U., Crow J. R., Kuerer H. M., Hunt K. K. (**2011**) Novel staging system for predicting disease-specific survival in patients with breast cancer treated with surgery as the first intervention: time to modify the current American Joint Committee on Cancer staging system. *J Clin Oncol* **29**: 4654-4661.
29. Park Y. H., Lee S. J., Cho E. Y., Choi Y. L., Lee J. E., Nam S. J., Yang J. H., Shin J. H., Ko E. Y., Han B. K., Ahn J. S., Im Y. H. (**2011**) Clinical relevance of TNM staging system according to breast cancer subtypes. *Ann Oncol* **22**: 1554-1560.
30. Zhang J., Powell S. N. (**2005**) The role of the BRCA1 tumor suppressor in DNA double-strand break repair. *Mol Cancer Res* **3**: 531-539.
31. Althuis M. D., Fergenbaum J. H., Garcia-Closas M., Brinton L. A., Madigan M. P., Sherman M. E. (**2004**) Etiology of hormone receptor-defined breast cancer: a systematic review of the literature. *Cancer Epidemiol Biomarkers Prev* **13**: 1558-1568.
32. Pusztai L., Mazouni C., Anderson K., Wu Y., Symmans W. F. (**2006**) Molecular classification of breast cancer: limitations and potential. *Oncologist* **11**: 868-877.
33. Yanagawa M., Ikemot K., Kawauchi S., Furuya T., Yamamoto S., Oka M., Oga A., Nagashima Y., Sasaki K. (**2012**) Luminal A and luminal B (HER2 negative) subtypes of breast cancer consist of a mixture of tumors with different genotype. *BMC Res Notes* **5**: 376.
34. Bergamaschi A., Kim Y. H., Wang P., Sorlie T., Hernandez-Boussard T., Lonning P. E., Tibshirani R., Borresen-Dale A. L., Pollack J. R. (**2006**) Distinct patterns of DNA copy number alteration are associated with different clinicopathological features and gene-expression subtypes of breast cancer. *Genes Chromosomes Cancer* **45**: 1033-1040.
35. Neve R. M., Chin K., Fridlyand J., Yeh J., Baehner F. L., Fevr T., Clark L., Bayani N., Coppe J. P., Tong F., Speed T., Spellman P. T., DeVries S., Lapuk A., Wang N. J., Kuo W. L., Stilwell J. L., Pinkel D., Albertson D. G., Waldman F. M., McCormick F., Dickson R. B., Johnson M. D., Lippman M., Ethier S., Gazdar A., Gray J. W. (**2006**) A collection of breast cancer cell lines for the study of functionally distinct cancer subtypes. *Cancer Cell* **10**: 515-527.

36. Sorlie T., Perou C. M., Tibshirani R., Aas T., Geisler S., Johnsen H., Hastie T., Eisen M. B., van de Rijn M., Jeffrey S. S., Thorsen T., Quist H., Matese J. C., Brown P. O., Botstein D., Lonning P. E., Borresen-Dale A. L. (**2001**) Gene expression patterns of breast carcinomas distinguish tumor subclasses with clinical implications. *Proc Natl Acad Sci U S A* **98**: 10869-10874.
37. Ricardo S., Vieira A. F., Gerhard R., Leitao D., Pinto R., Cameselle-Teijeiro J. F., Milanezi F., Schmitt F., Paredes J. (**2011**) Breast cancer stem cell markers CD44, CD24 and ALDH1: expression distribution within intrinsic molecular subtype. *J Clin Pathol* **64**: 937-946.
38. Strebhardt K., Ullrich A. (**2008**) Paul Ehrlich's magic bullet concept: 100 years of progress. *Nat Rev Cancer* **8**: 473-480.
39. Li J., Chen F., Cona M. M., Feng Y., Himmelreich U., Oyen R., Verbruggen A., Ni Y. (**2012**) A review on various targeted anticancer therapies. *Target Oncol* **7**: 69-85.
40. Longo R., Torino F., Gasparini G. (**2007**) Targeted therapy of breast cancer. *Curr Pharm Des* **13**: 497-517.
41. Al-Hajj M., Wicha M. S., Benito-Hernandez A., Morrison S. J., Clarke M. F. (**2003**) Prospective identification of tumorigenic breast cancer cells. *Proc Natl Acad Sci U S A* **100**: 3983-3988.
42. Eaves C. J. (**2008**) Cancer stem cells: Here, there, everywhere? *Nature* **456**: 581-582.
43. O'Brien C. A., Kreso A., Jamieson C. H. (**2010**) Cancer stem cells and self-renewal. *Clin Cancer Res* **16**: 3113-3120.
44. Spillane J. B., Henderson M. A. (**2007**) Cancer stem cells: a review. *ANZ J Surg* **77**: 464-468.
45. Ailles L. E., Weissman I. L. (**2007**) Cancer stem cells in solid tumors. *Curr Opin Biotechnol* **18**: 460-466.
46. Fillmore C. M., Kuperwasser C. (**2008**) Human breast cancer cell lines contain stem-like cells that self-renew, give rise to phenotypically diverse progeny and survive chemotherapy. *Breast Cancer Res* **10**: R25.
47. Dean M., Fojo T., Bates S. (**2005**) Tumour stem cells and drug resistance. *Nature Reviews Cancer* **5**: 275-284.
48. Zhang M., Rosen J. F. (**2006**) Stem cells in the etiology and treatment of cancer. *Current Opinion in Genetics & Development* **16**: 60–64.

49. Clarke M. F., Dick J. E., Dirks P. B., Eaves C. J., Jamieson C. H., Jones D. L., Visvader J., Weissman I. L., Wahl G. M. (**2006**) Cancer stem cells--perspectives on current status and future directions: AACR Workshop on cancer stem cells. *Cancer Res* **66**: 9339-9344.
50. Rich J. N. (**2007**) Cancer stem cells in radiation resistance. *Cancer Res* **67**: 8980-8984.
51. Abraham B. K., Fritz P., McClellan M., Hauptvogel P., Athelogou M., Brauch H. (**2005**) Prevalence of CD44+/CD24-/low cells in breast cancer may not be associated with clinical outcome but may favor distant metastasis. *Clin Cancer Res* **11**: 1154-1159.
52. Heby O. (**1986**) Putrescine, Spermidine and Spermine. *NIPS* **1**: 12-15.
53. Wallace H. M., Fraser A. V., Hughes A. (**2003**) A perspective of polyamine metabolism. *Biochem J* **376**: 1-14.
54. Bachrach U. (**2010**) The early history of polyamine research. *Plant Physiol Biochem* **48**: 490-495.
55. Yatin M. (**2002**) Polyamines in living organisms. *Journal of Cell and Molecular Biology* **1**: 57-67.
56. Gugliucci A. (**2004**) Polyamines as clinical laboratory tools. *Clin Chim Acta* **344**: 23-35.
57. Gerner E. W., Meyskens F. L., Jr. (**2004**) Polyamines and cancer: old molecules, new understanding. *Nat Rev Cancer* **4**: 781-792.
58. Tabor C. W., Tabor H. (**1984**) Polyamines. *Annu Rev Biochem* **53**: 749-790.
59. Uemura T., Gerner E. W. (**2011**) Polyamine transport systems in mammalian cells and tissues. *Methods Mol Biol* **720**: 339-348.
60. Lovaas E. (**1997**) Antioxidative and metal-chelating effects of polyamines. *Adv Pharmacol* **38**: 119-149.
61. Heby O. (**1981**) Role of polyamines in the control of cell proliferation and differentiation. *Differentiation* **19**: 1-20.
62. Coffino P. (**2001**) Regulation of cellular polyamines by antizyme. *Nat Rev Mol Cell Biol* **2**: 188-194.
63. Igarashi K., Kashiwagi K. (**2010**) Modulation of cellular function by polyamines. *Int J Biochem Cell Biol* **42**: 39-51.
64. Pegg A. E., McCann P. P. (**1982**) Polyamine metabolism and function. *Am J Physiol* **243**: C212-221.
65. Cohen S. S. (**1998**) A Guide to the Polyamines. Oxford: *Oxford University Press*. 185-230 p.

66. Agostinelli E., Marques M. P. M., Calheiros R., Gil F. P., Tempera G., Viceconte N., Battaglia V., Grancara S., Toninello A. (**2010**) Polyamines: fundamental characters in chemistry and biology. *Amino Acids* **38**: 393-403.
67. Canizares F., Salinas J., de las Heras M., Diaz J., Tovar I., Martinez P., Penafiel R. (**1999**) Prognostic value of ornithine decarboxylase and polyamines in human breast cancer: correlation with clinicopathologic parameters. *Clin Cancer Res* **5**: 2035-2041.
68. Pegg A. E. (**2009**) Mammalian polyamine metabolism and function. *IUBMB Life* **61**: 880-894.
69. Yuan Q., Ray R. M., Viar M. J., Johnson L. R. (**2001**) Polyamine regulation of ornithine decarboxylase and its antizyme in intestinal epithelial cells. *Am J Physiol Gastrointest Liver Physiol* **280**: G130-138.
70. Moinard C., Cynober L., de Bandt J. P. (**2005**) Polyamines: metabolism and implications in human diseases. *Clin Nutr* **24**: 184-197.
71. Takao K., Rickhag M., Hegardt C., Oredsson S., Persson L. (**2006**) Induction of apoptotic cell death by putrescine. *Int J Biochem Cell Biol* **38**: 621-628.
72. Persson L. (**2009**) Polyamine homoeostasis. *Essays Biochem* **46**: 11-24.
73. Igarashi K., Kashiwagi K. (**2000**) Polyamines: mysterious modulators of cellular functions. *Biochem Biophys Res Commun* **271**: 559-564.
74. Wang J.-Y., Casero R. A. J. (**2006**) Polyamine Cell Signaling: Phisiology, Pharmacology and Cancer Research. Totowa, New Jersey: *Humana Press Inc.*
75. Nishioka K. (**1996**) Polyamines in Cancer: Basic mechanisms and clinical approaches. Georgetown: *R.G. Landes Company*.
76. Wallace H. M. (**2009**) The polyamines: past, present and future. *Essays Biochem* **46**: 1-
77. Cervelli M., Amendola R., Polticelli F., Mariottini P. (**2012**) Spermine oxidase: ten years after. *Amino Acids* **42**: 441-450.
78. Svensson F., Mett H., Persson L. (**1997**) CGP 48664, a potent and specific S-adenosylmethionine decarboxylase inhibitor: effects on regulation and stability of the enzyme. *Biochem J* **322 (Pt 1)**: 297-302.
79. Kahana C. (**2009**) Antizyme and antizyme inhibitor, a regulatory tango. *Cell Mol Life Sci* **66**: 2479-2488.
80. Pegg A. E., Feith D. J. (**2007**) Polyamines and neoplastic growth. *Biochem Soc Trans* **35**: 295-299.

81. Tolbert W. D., Zhang Y., Cottet S. E., Bennett E. M., Ekstrom J. L., Pegg A. E., Ealick S. E. (**2003**) Mechanism of human S-adenosylmethionine decarboxylase proenzyme processing as revealed by the structure of the S68A mutant. *Biochemistry* **42**: 2386-2395.
82. Pegg A. E. (**2008**) Spermidine/spermine-N(1)-acetyltransferase: a key metabolic regulator. *Am J Physiol Endocrinol Metab* **294**: E995-1010.
83. Casero R. A., Jr., Pegg A. E. (**1993**) Spermidine/spermine N1-acetyltransferase--the turning point in polyamine metabolism. *FASEB J* **7**: 653-661.
84. Pegg A. E., Feith D. J., Fong L. Y., Coleman C. S., O'Brien T. G., Shantz L. M. (**2003**) Transgenic mouse models for studies of the role of polyamines in normal, hypertrophic and neoplastic growth. *Biochem Soc Trans* **31**: 356-360.
85. Palmer A. J., Wallace H. M. (**2010**) The polyamine transport system as a target for anticancer drug development. *Amino Acids* **38**: 415-422.
86. Pegg A. E., Casero R. A., Jr. (**2011**) Current status of the polyamine research field. *Methods Mol Biol* **720**: 3-35.
87. Seiler N., Dezeure F. (**1990**) Polyamine transport in mammalian cells. *Int J Biochem* **22**: 211-218.
88. Heller J. S., Fong W. F., Canellakis E. S. (**1976**) Induction of a protein inhibitor to ornithine decarboxylase by the end products of its reaction. *Proc Natl Acad Sci U S A* **73**: 1858-1862.
89. Mangold U. (**2006**) Antizyme inhibitor: mysterious modulator of cell proliferation. *Cell Mol Life Sci* **63**: 2095-2101.
90. Mangold U. (**2005**) The antizyme family: polyamines and beyond. *IUBMB Life* **57**: 671-676.
91. Bercovich Z., Snapir Z., Keren-Paz A., Kahana C. (**2011**) Antizyme affects cell proliferation and viability solely through regulating cellular polyamines. *J Biol Chem* **286**: 33778-33783.
92. Lopez-Contreras A. J., Ramos-Molina B., Cremades A., Penafiel R. (**2010**) Antizyme inhibitor 2: molecular, cellular and physiological aspects. *Amino Acids* **38**: 603-611.
93. Olsen R. R., Zetter B. R. (**2011**) Evidence of a role for antizyme and antizyme inhibitor as regulators of human cancer. *Mol Cancer Res* **9**: 1285-1293.
94. Hayashi S., Murakami Y. (**1995**) Rapid and regulated degradation of ornithine decarboxylase. *Biochem J* **306 (Pt 1)**: 1-10.
95. Gerner E. W. (**2010**) Cancer chemoprevention locks onto a new polyamine metabolic target. *Cancer Prev Res (Phila)* **3**: 125-127.

96. Bachrach U. (**2004**) Polyamines and cancer: Minireview article. *Amino Acids* **26**: 307-309.
97. Criss W. E. (**2003**) A review of polyamines and cancer. *Turk J Med Sci* **33**: 195-205.
98. Thomas T., Thomas T. J. (**2001**) Polyamines in cell growth and cell death: molecular mechanisms and therapeutic applications. *Cell Mol Life Sci* **58**: 244-258.
99. Wallace H. M., Fraser A. V. (**2004**) Inhibitors of polyamine metabolism: review article. *Amino Acids* **26**: 353-365.
100. Seiler N. (**2003**) Thirty years of polyamine-related approaches to cancer therapy. Retrospect and prospect. Part 1. Selective enzyme inhibitors. *Curr Drug Targets* **4**: 537-564.
101. Wallace H. M., Niiranen K. (**2007**) Polyamine analogues - an update. *Amino Acids* **33**: 261-265.
102. Laukaitis C. M., Gerner E. W. (**2011**) DFMO: targeted risk reduction therapy for colorectal neoplasia. *Best Pract Res Clin Gastroenterol* **25**: 495-506.
103. Casero R. A., Jr., Woster P. M. (**2009**) Recent advances in the development of polyamine analogues as antitumor agents. *J Med Chem* **52**: 4551-4573.
104. Jeter J. M., Alberts D. S. (**2012**) Difluoromethylornithine: the proof is in the polyamines. *Cancer Prev Res (Phila)* **5**: 1341-1344.
105. Porter C. W., Bergeron R. J. (**1988**) Enzyme regulation as an approach to interference with polyamine biosynthesis--an alternative to enzyme inhibition. *Adv Enzyme Regul* **27**: 57-79.
106. Fraser A. V., Woster P. M., Wallace H. M. (**2002**) Induction of apoptosis in human leukaemic cells by IPENSpm, a novel polyamine analogue and anti-metabolite. *Biochem J* **367**: 307-312.
107. Oredsson S. M., Alm K., Dahlberg E., Holst C. M., Johansson V. M., Myhre L., Soderstjerna E. (**2007**) Inhibition of cell proliferation and induction of apoptosis by N(1),N(11)-diethylnorspermine-induced polyamine pool reduction. *Biochem Soc Trans* **35**: 405-409.
108. Thomas T., Thomas T. J. (**2003**) Polyamine metabolism and cancer. *J Cell Mol Med* **7**: 113-126.
109. Boncher T., Bi X., Varghese S., Casero R. A., Jr., Woster P. M. (**2007**) Polyamine-based analogues as biochemical probes and potential therapeutics. *Biochem Soc Trans* **35**: 356-363.

110. Davidson N. E., Hahm H. A., McCloskey D. E., Woster P. M., Casero R. A., Jr. (**1999**) Clinical aspects of cell death in breast cancer: the polyamine pathway as a new target for treatment. *Endocr Relat Cancer* **6**: 69-73.
111. Davidson N. E., Mank A. R., Prestigiacomo L. J., Bergeron R. J., Casero R. A., Jr. (**1993**) Growth inhibition of hormone-responsive and -resistant human breast cancer cells in culture by N1, N12-bis(ethyl)spermine. *Cancer Res* **53**: 2071-2075.
112. Holst C. M., Oredsson S. M. (**2005**) Comparison of three cytotoxicity tests in the evaluation of the cytotoxicity of a spermine analogue on human breast cancer cell lines. *Toxicol In Vitro* **19**: 379-387.
113. Hahm H. A., Dunn V. R., Butash K. A., Deveraux W. L., Woster P. M., Casero R. A., Jr., Davidson N. E. (**2001**) Combination of standard cytotoxic agents with polyamine analogues in the treatment of breast cancer cell lines. *Clin Cancer Res* **7**: 391-399.
114. Cervelli M., Bellavia G., Fratini E., Amendola R., Polticelli F., Barba M., Federico R., Signore F., Gucciardo G., Grillo R., Woster P. M., Casero R. A., Jr., Mariottini P. (**2010**) Spermine oxidase (SMO) activity in breast tumor tissues and biochemical analysis of the anticancer spermine analogues BENSpm and CPENSpm. *BMC Cancer* **10**: 555.
115. Bernacki R. J., Oberman E. J., Seweryniak K. E., Atwood A., Bergeron R. J., Porter C. W. (**1995**) Preclinical antitumor efficacy of the polyamine analogue N1, N11-diethylnorspermine administered by multiple injection or continuous infusion. *Clin Cancer Res* **1**: 847-857.
116. Wolff A. C., Armstrong D. K., Fetting J. H., Carducci M. K., Riley C. D., Bender J. F., Casero R. A., Jr., Davidson N. E. (**2003**) A Phase II study of the polyamine analog N1,N11-diethylnorspermine (DENSpm) daily for five days every 21 days in patients with previously treated metastatic breast cancer. *Clin Cancer Res* **9**: 5922-5928
117. Hakkinen M. R., Hyvonen M. T., Auriola S., Casero R. A., Jr., Vepsalainen J., Khomutov A. R., Alhonen L., Keinanen T. A. (**2010**) Metabolism of N-alkylated spermine analogues by polyamine and spermine oxidases. *Amino Acids* **38**: 369-381.
118. Hamana K., Matsuzaki S. (**1982**) Widespread occurrence of norspermidine and norspermine in eukaryotic algae. *J Biochem* **91**: 1321-1328.
119. Rodriguez-Garay B., Phillips G. C., Kuehn G. D. (**1989**) Detection of Norspermidine and Norspermine in Medicago sativa L. (Alfalfa). *Plant Physiol* **89**: 525-529.
120. Fuell C., Elliott K. A., Hanfrey C. C., Franceschetti M., Michael A. J. (**2010**) Polyamine biosynthetic diversity in plants and algae. *Plant Physiol Biochem* **48**: 513-520.

121. Prakash N. J., Bowlin T. L., Davis G. F., Sunkara P. S., Sjoerdsma A. (**1988**) Antitumor activity of norspermidine, a structural homologue of the natural polyamine spermidine. *Anticancer Res* **8**: 563-568.
122. Pledgie-Tracy A., Billam M., Hacker A., Sobolewski M. D., Woster P. M., Zhang Z., Casero R. A., Davidson N. E. (**2010**) The role of the polyamine catabolic enzymes SSAT and SMO in the synergistic effects of standard chemotherapeutic agents with a polyamine analogue in human breast cancer cell lines. *Cancer Chemother Pharmacol* **65**: 1067-1081.
123. Cooper G. M., Hausman R. E. (**2009**) The Cell: A Molecular Approach: *ASM Press* 1-766 p.
124. Israels E. D., Israels L. G. (**2000**) The cell cycle. *Oncologist* **5**: 510-513.
125. Harper J. V., Brooks G. (**2005**) The mammalian cell cycle: an overview. Totowa: *Humana Press*.
126. Johnson D. G., Walker C. L. (**1999**) Cyclins and cell cycle checkpoints. *Annu Rev Pharmacol Toxicol* **39**: 295-312.
127. Alm K., Oredsson S. (**2009**) Cells and polyamines do it cyclically. *Essays Biochem* **46**: 63-76.
128. Larsson S., Ryden T., Holst U., Oredsson S., Johansson M. (**2008**) Estimating the variation in S phase duration from flow cytometric histograms. *Math Biosci* **213**: 40-49.
129. Nasizadeh S., Myhre L., Thiman L., Alm K., Oredsson S., Persson L. (**2005**) Importance of polyamines in cell cycle kinetics as studied in a transgenic system. *Exp Cell Res* **308**: 254-264.
130. Oredsson S. M. (**2003**) Polyamine dependence of normal cell-cycle progression. *Biochem Soc Trans* **31**: 366-370.
131. Stein G. S., Pardee A. B. (**2004**) Cell Cycle and Growth Control: Biomolecular Regulation and Cancer. Hoboken: *John Wiley & Sons, Inc.*
132. Fredlund J. O., Johansson M., Baldetorp B., Oredsson S. M. (**1994**) Abnormal DNA synthesis in polyamine deficient cells revealed by bromodeoxyuridine-flow cytometry technique. *Cell Prolif* **27**: 243-256.
133. Ulukaya E., Ari F., Dimas K., Ikitimur E. I., Guney E., Yilmaz V. T. (**2011**) Anti-cancer activity of a novel palladium(II) complex on human breast cancer cells in vitro and in vivo. *Eur J Med Chem* **46**: 4957-4963.

134. Miklasova N., Fischer-Fodor E., Lonnecke P., Tomuleasa C. I., Virag P., Schrepler M. P., Miklas R., Dumitrescu L. S., Hey-Hawkins E. (**2012**) Antiproliferative effect of novel platinum(II) and palladium(II) complexes on hepatic tumor stem cells in vitro. *Eur J Med Chem* **49**: 41-47.
135. Marques M. P. M. (**2013**) Platinum and Palladium Polyamine Complexes as Anticancer Agents: The Structural Factor. *ISRN Spectroscopy*: 1-29.
136. Jakupec M. A., Galanski M., Arion V. B., Hartinger C. G., Keppler B. K. (**2008**) Antitumour metal compounds: more than theme and variations. *Dalton Trans*: 183-194.
137. Alderden R. A. (**2006**) The Discovery and Development of Cisplatin. *Journal of Chemical Education* **83**: 728-734.
138. Kauffman G. B. (**1997**) Alfred Werner's Research on the Platinum Metals: A Centennial Retrospect. *Platinum Metals Review* **41**: 34-40.
139. Rosenberg B., Vancamp L., Krigas T. (**1965**) Inhibition of Cell Division in Escherichia Coli by Electrolysis Products from a Platinum Electrode. *Nature* **205**: 698-699.
140. Rosenberg B., VanCamp L., Trosko J. E., Mansour V. H. (**1969**) Platinum compounds: a new class of potent antitumour agents. *Nature* **222**: 385-386.
141. FDA http://www.accessdata.fda.gov/scripts/cder/drugsatfda/index.cfm?fuseaction=Search.Overview&DrugName=CISPLATIN. *(accessed in March 2013)*.
142. Monneret C. (**2011**) Platinum anticancer drugs. From serendipity to rational design. *Ann Pharm Fr* **69**: 286-295.
143. Galluzzi L., Senovilla L., Vitale I., Michels J., Martins I., Kepp O., Castedo M., Kroemer G. (**2012**) Molecular mechanisms of cisplatin resistance. *Oncogene* **31**: 1869-1883.
144. Lebwohl D., Canetta R. (**1998**) Clinical development of platinum complexes in cancer therapy: an historical perspective and an update. *Eur J Cancer* **34**: 1522-1534.
145. Shamseddine A. I., Farhat F. S. (**2011**) Platinum-based compounds for the treatment of metastatic breast cancer. *Chemotherapy* **57**: 468-487.
146. Wang D., Lippard S. J. (**2005**) Cellular processing of platinum anticancer drugs. *Nat Rev Drug Discov* **4**: 307-320.
147. Brabec V., Kasparkova J. (**2005**) Modifications of DNA by platinum complexes. Relation to resistance of tumors to platinum antitumor drugs. *Drug Resist Updat* **8**: 131-146.
148. Esteban-Fernandez D., Moreno-Gordaliza E., Canas B., Palacios M. A., Gomez-Gomez M. M. (**2010**) Analytical methodologies for metallomics studies of antitumor Pt-containing drugs. *Metallomics* **2**: 19-38.

149. Basu A., Krishnamurthy S. (**2010**) Cellular responses to Cisplatin-induced DNA damage. *J Nucleic Acids* **2010**.
150. Siddik Z. H. (**2003**) Cisplatin: mode of cytotoxic action and molecular basis of resistance. *Oncogene* **22**: 7265-7279.
151. Wheate N. J., Walker S., Craig G. E., Oun R. (**2010**) The status of platinum anticancer drugs in the clinic and in clinical trials. *Dalton Trans* **39**: 8113-8127.
152. Eastman A. (**2006**) The Mechanism of Action of Cisplatin: From Adducts to Apoptosis. In: Lippert B., editor. Cisplatin: Chemistry and Biochemistry of a Leading Anticancer Drug. Zurich: *Verlag Helvetica Chimica Acta*.
153. Florea A.-M., D. B. (**2011**) Cisplatin as an Anti-Tumor Drug: Cellular Mechanisms of Activity, Drug Resistance and Induced Side Effects. *Cancers* **3**: 1351-1371.
154. Komeda S. (**2011**) Unique platinum-DNA interactions may lead to more effective platinum-based antitumor drugs. *Metallomics* **3**: 650-655.
155. Galanski M. (**2007**) Anticancer Platinum Complexes - State of the Art and Future Prospects. *Anticancer Agents Med Chem* **7**: 1-138.
156. Teixeira L. J., Seabra M., Reis E., da Cruz M. T., de Lima M. C., Pereira E., Miranda M. A., Marques M. P. M. (**2004**) Cytotoxic activity of metal complexes of biogenic polyamines: polynuclear platinum(II) chelates. *J Med Chem* **47**: 2917-2925.
157. Matos C. S., Batista de Carvalho A. L., Lopes R. P., Marques M. P. M. (**2012**) New strategies against prostate cancer--Pt(II)-based chemotherapy. *Curr Med Chem* **19**: 4678-4687.
158. Alcindor T., Beauger N. (**2011**) Oxaliplatin: a review in the era of molecularly targeted therapy. *Current Oncology* **18**: 18-25.
159. Brown S. D., Trotter K. D., Sutcliffe O. B., Plumb J. A., Waddell B., Briggs N. E., Wheate N. J. (**2012**) Combining aspects of the platinum anticancer drugs picoplatin and BBR3464 to synthesize a new family of sterically hindered dinuclear complexes; their synthesis, binding kinetics and cytotoxicity. *Dalton Trans* **41**: 11330-11339.
160. Beale P., Judson I., O'Donnell A., Trigo J., Rees C., Raynaud F., Turner A., Simmons L., Etterley L. (**2003**) A Phase I clinical and pharmacological study of cis-diamminedichloro(2-methylpyridine) platinum II (AMD473). *Br J Cancer* **88**: 1128-1134.
161. Battle A. R., Choi R., Hibbs D. E., Hambley T. W. (**2006**) Platinum(IV) analogues of AMD473 (cis-[PtCl2(NH3)(2-picoline)]): preparative, structural, and electrochemical studies. *Inorg Chem* **45**: 6317-6322.

162. Nowotnik D. P., Cvitkovic E. (**2009**) ProLindac (AP5346): a review of the development of an HPMA DACH platinum Polymer Therapeutic. *Adv Drug Deliv Rev* **61**: 1214-1219.
163. Fantini M., Gianni L., Santelmo C., Drudi F., Castellani C., Affatato A., Nicolini M., Ravaioli A. (**2011**) Lipoplatin treatment in lung and breast cancer. *Chemother Res Pract* **2011**: 125192.
164. Stathopoulos G. P., Boulikas T. (**2012**) Lipoplatin formulation review article. *J Drug Deliv* **2012**: 581363.
165. Fenske D. B., Cullis P. R. (**2008**) Liposomal nanomedicines. *Expert Opin Drug Deliv* **5**: 25-44.
166. Bryde S., de Kroon A. I. (**2009**) Nanocapsules of platinum anticancer drugs: development towards therapeutic use. *Future Med Chem* **1**: 1467-1480.
167. Koukourakis M. I., Giatromanolaki A., Pitiakoudis M., Kouklakis G., Tsoutsou P., Abatzoglou I., Panteliadou M., Sismanidou K., Sivridis E., Boulikas T. (**2010**) Concurrent liposomal cisplatin (Lipoplatin), 5-fluorouracil and radiotherapy for the treatment of locally advanced gastric cancer: a phase I/II study. *Int J Radiat Oncol Biol Phys* **78**: 150-155.
168. Seetharamu N., Kim E., Hochster H., Martin F., Muggia F. (**2010**) Phase II study of liposomal cisplatin (SPI-77) in platinum-sensitive recurrences of ovarian cancer. *Anticancer Res* **30**: 541-545.
169. Silva T. M., Andersson S., Sukumaran S. K., Marques M. P. M., Persson L., Oredsson S. (**2013**) Norspermidine and Novel Pd(II) and Pt(II) Polynuclear Complexes of Norspermidine as Potential Antineoplastic Agents Against Breast Cancer. *PLoS One* **8**: e55651.
170. Fiuza S. M., Amado A. M., Oliveira P. J., Sardão V. A., Batista de Carvalho L. A. E., Marques M. P. M. (**2006**) Pt(II) vs Pd(II) polyamine complexes as new anticancer drugs: A structure-activity study. *Lett Drug Des Discov* **3**: 149-151.
171. Soares A. S., Fiuza S. M., Gonçalves M. J., Batista de Carvalho L. A. E., Marques M. P. M., Urbano A. M. (**2007**) Effect of the Metal Center on the Antitumor Activity of the Analogous Dinuclear Spermine Chelates (PdCl2)2(Spermine) and (PtCl2)2(Spermine). *Lett Drug Des Discov* **4**: 460-463.
172. Benedetti B. T., Peterson E. J., Kabolizadeh P., Martinez A., Kipping R., Farrell N. P. (**2011**) Effects of noncovalent platinum drug-protein interactions on drug efficacy: use of fluorescent conjugates as probes for drug metabolism. *Mol Pharm* **8**: 940-948.

173. Liu Q., Qu Y., Van Antwerpen R., Farrell N. (**2006**) Mechanism of the membrane interaction of polynuclear platinum anticancer agents. Implications for cellular uptake. *Biochemistry* **45**: 4248-4256.
174. Navarro-Ranninger C., Zamora F., Perez J. M., Lopez-Solera I., Martinez-Carrera S., Masaguer J. R., Alonso C. (**1992**) Palladium(II) salt and complexes of spermidine with a six-member chelate ring. Synthesis, characterization, and initial DNA-binding and antitumor studies. *J Inorg Biochem* **46**: 267-279.
175. Navarro-Ranninger C., Perez J. M., Zamora F., Gonzalez V. M., Masaguer J. R., Alonso C. (**1993**) Palladium (II) compounds of putrescine and spermine. Synthesis, characterization, and DNA-binding and antitumor properties. *J Inorg Biochem* **52**: 37-49.
176. Navarro-Ranninger C., Ochoa P. A., Perez J. M., Gonzalez V. M., Masaguer J. R., Alonso C. (**1994**) Platinum (II) and (IV) spermidine complexes. Synthesis, characterization, and biological studies. *J Inorg Biochem* **53**: 177-190.
177. Amo-Ochoa P., Gonzalez V. M., Perez J. M., Masaguer J. R., Alonso C., Navarro-Ranninger C. (**1996**) Cytotoxicity, DNA binding, and reactivity against nucleosides of platinum (II) and (IV) spermine compounds. *J Inorg Biochem* **64**: 287-299.
178. Hegmans A., Kasparkova J., Vrana O., Kelland L. R., Brabec V., Farrell N. P. (**2008**) Amide-based prodrugs of spermidine-bridged dinuclear platinum. Synthesis, DNA binding, and biological activity. *J Med Chem* **51**: 2254-2260.
179. Malina J., Farrell N. P., Brabec V. (**2011**) DNA interstrand cross-links of an antitumor trinuclear platinum(II) complex: thermodynamic analysis and chemical probing. *Chem Asian J* **6**: 1566-1574.
180. Malina J., Kasparkova J., Farrell N. P., Brabec V. (**2011**) Walking of antitumor bifunctional trinuclear PtII complex on double-helical DNA. *Nucleic Acids Res* **39**: 720-728.
181. Farrell N. P., Dealmeida S. G., Skov K. A. (**1988**) Bis(Platinum) Complexes Containing 2 Platinum Cis-Diammine Units - Synthesis and Initial DNA-Binding Studies. *J Am Chem Soc* **110**: 5018-5019.
182. Farrell N. (**2004**) Polynuclear platinum drugs. *Met Ions Biol Syst* **42**: 251-296.
183. Roberts J. D., Peroutka J., Farrell N. (**1999**) Cellular pharmacology of polynuclear platinum anti-cancer agents. *J Inorg Biochem* **77**: 51-57.

184. Harris A. L., Ryan J. J., Farrell N. (**2006**) Biological consequences of trinuclear platinum complexes: comparison of [[trans-PtCl(NH3)2]2mu-(trans-Pt(NH3)2(H2N(CH2)6-NH2)2)]4+ (BBR 3464) with its noncovalent congeners. *Mol Pharmacol* **69**: 666-672.
185. Jodrell D. I., Evans T. R., Steward W., Cameron D., Prendiville J., Aschele C., Noberasco C., Lind M., Carmichael J., Dobbs N., Camboni G., Gatti B., De Braud F. (**2004**) Phase II studies of BBR3464, a novel tri-nuclear platinum complex, in patients with gastric or gastro-oesophageal adenocarcinoma. *Eur J Cancer* **40**: 1872-1877.
186. Wennerberg J., Kjellstrom J., Oredsson S. (**2012**) Increased toxicity of a trinuclear Pt-compound in a human squamous carcinoma cell line by polyamine depletion. *Cancer Cell Int* **12**: 20.
187. Komeda S., Moulaei T., Chikuma M., Odani A., Kipping R., Farrell N. P., Williams L. D. (**2011**) The phosphate clamp: a small and independent motif for nucleic acid backbone recognition. *Nucleic Acids Res* **39**: 325-336.
188. Roberts J. J., Pascoe J. M. (**1972**) Cross-linking of complementary strands of DNA in mammalian cells by antitumour platinum compounds. *Nature* **235**: 282-284.
189. Decatris M. P., Sundar S., O'Byrne K. J. (**2005**) Platinum-based chemotherapy in metastatic breast cancer: the Leicester (U.K.) experience. *Clin Oncol (R Coll Radiol)* **17**: 249-257.
190. Silva T. M., Oredsson S., Persson L., Woster P., Marques M. P. M. (**2012**) Novel Pt(II) and Pd(II) complexes with polyamine analogues: synthesis and vibrational analysis. *J Inorg Biochem* **108**: 1-7.
191. Marques M. P. M., Girao T., Pedroso De Lima M. C., Gameiro A., Pereira E., Garcia P. (**2002**) Cytotoxic effects of metal complexes of biogenic polyamines. I. Platinum(II) spermidine compounds: prediction of their antitumour activity. *Biochim Biophys Acta* **1589**: 63-70.
192. Fiuza S. M., Holy J., Batista de Carvalho L. A. E., Marques M. P. M. (**2011**) Biologic activity of a dinuclear Pd(II)-spermine complex toward human breast cancer. *Chem Biol Drug Des* **77**: 477-488.
193. Tummala R., Diegelman P., Fiuza S. M., Batista de Carvalho L. A. E., Marques M. P. M., Kramer D. L., Clark K., Vujcic S., Porter C. W., Pendyala L. (**2010**) Characterization of Pt-, Pd-spermine complexes for their effect on polyamine pathway and cisplatin resistance in A2780 ovarian carcinoma cells. *Oncol Rep* **24**: 15-24.

194. Powers D. C., Ritter T. (**2011**) Palladium(III) in Synthesis and Catalysis. *Top Organomet Chem* **503**: 129-156.
195. Abu-Surrah A. S., Al-Sa'doni H. H., Abdalla M. Y. (**2008**) Palladium-based chemotherapeutic agents: Routes toward complexes with good antitumor activity. *Cancer Therapy* **6**: 1-10.
196. Abu-Surrah A. S., Abu Safieh K. A., Ahmad I. M., Abdalla M. Y., Ayoub M. T., Qaroush A. K., Abu-Mahtheieh A. M. (**2010**) New palladium(II) complexes bearing pyrazole-based Schiff base ligands: synthesis, characterization and cytotoxicity. *Eur J Med Chem* **45**: 471-475.
197. Teixeira-Dias J. J. C. (**1986**) Espectroscopia Molecular: Fundamentos, Métodos e Aplicações. Lisboa: *Fundação Calouste Gulbenkian*.
198. Fiuza S. M., Gomes C., Teixeira L. J., Girao da Cruz M. T., Cordeiro M. N., Milhazes N., Borges F., Marques M. P. M. (**2004**) Phenolic acid derivatives with potential anticancer properties--a structure-activity relationship study. Part 1: methyl, propyl and octyl esters of caffeic and gallic acids. *Bioorg Med Chem* **12**: 3581-3589.
199. Herrmann C., Reiher M. (**2007**) First-Principles Approach to Vibrational Spectroscopy of Biomolecules. *Top Curr Chem* **268**: 85 - 132.
200. Amado A. M., Fiuza S. M., Marques M. P. M., Batista de Carvalho L. A. E. (**2007**) Conformational and vibrational study of platinum(II) anticancer drugs: cis-diamminedichloro-platinum(II) as a case study. *J Chem Phys* **127**: 185104.
201. Marques M. P. M., Batista de Carvalho L. A. E. (**2007**) Vibrational spectroscopy studies on linear polyamines. *Biochem Soc Trans* **35**: 374-380.
202. Amorim da Costa A. M., Marques M. P. M., Batista de Carvalho L. A. E. (**2002**) The carbon---hydrogen stretching region of the Raman spectra of 1,6-hexanediamine: N-deuteration, ionisation and temperature effects. *Vibrational Spectroscopy* **29**: 61-67.
203. Amorim da Costa A. M., Marques M. P. M., Batista de Carvalho L. A. E. (**2003**) Raman spectra of putrescine, spermidine and spermine polyamines and their N-deuterated and N-ionized derivatives. *Journal of Raman Spectroscopy* **34**: 357-366.
204. Amado A. M., Otero J. C., Marques M. P. M., Batista de Carvalho L. A. E. (**2004**) Spectroscopic and theoretical studies on solid 1,2-ethylenediamine dihydrochloride salt. *Chemphyschem* **5**: 1837-1847.
205. Fiuza S. M., Amado A. M., Dos Santos H. F., Marques M. P. M., Batista de Carvalho L. A. E. (**2010**) Conformational and vibrational study of cis-diamminedichloropalladium(II). *Phys Chem Chem Phys* **12**: 14309-14321.

206. Sathyanarayana D. N. (**2007**) Vibrational Spectroscopy: Theory And Applications: *New Age International (P) Ltd.* 716 p.
207. Colthup N. B., Daly L. H., Wiberley S. E. (**1975**) Introduction to Infrared and Raman Spectrosocpy. London: *Academic Press, Inc.* 523 p.
208. Šašić S., Ozaki Y. (**2010**) Raman, Infrared and Near-Infrared Chemical Imaging. Hoboken, N.J.: *John Wiley & Sons, Inc.*
209. Housecroft C. E., Sharpe A. (**2008**) Inorganic Chemistry. Harlow: *Pearson Education*.
210. Siebert F., Hildebrandt P. (**2008**) Vibrational Spectroscopy in Life Science. Weinheim: *Wiley-VCH*. 310 p.
211. Fiuza S. M., Amado A. M., Marques M. P. M., Batista de Carvalho L. A. E. (**2008**) Use of effective core potential calculations for the conformational and vibrational study of platinum(II) anticancer drugs. cis-Diamminedichloroplatinum(II) as a case study. *J Phys Chem A* **112**: 3253-3259.
212. Amado A. M., Fiuza S. M., Batista de Carvalho L. A. E., Marques M. P. M. (**2006**) Ab initio conformational study of platinum and palladium complexes towards the understanding of the potential anticancer activities. *Recent Progress in Computational Sciences and Engineering, Vols 7a and 7b* **7A-B**: 19-23.
213. Gunzler H., Gremlich H. U. (**2002**) IR Spectroscopy. An Introduction. Weinheim: *Wiley-VCH*.
214. Stuart B. (**2004**) Infrared Spectroscopy: Fundamentals and Applications: *John Wiley & Sons, Ltd*.
215. Stuart B. (**1997**) Biological Applications of Infrared Spectroscopy. England: *John Wiley & Sons, Ltd.*
216. Waynant R. W., Ilev I. K., Gannot I. (**2001**) Mid-infrared laser applications in medicine and biology. *Phil Trans R Soc Lond A* **359**.
217. Bassan P., Kohler A., Martens H., Lee J., Byrne H. J., Dumas P., Gazi E., Brown M., Clarke N., Gardner P. (**2010**) Resonant Mie scattering (RMieS) correction of infrared spectra from highly scattering biological samples. *Analyst* **135**: 268-277.
218. Bassan P., Byrne H. J., Lee J., Bonnier F., Clarke C., Dumas P., Gazi E., Brown M. D., Clarke N. W., Gardner P. (**2009**) Reflection contributions to the dispersion artefact in FTIR spectra of single biological cells. *Analyst* **134**: 1171-1175.
219. Aydin H. M., Hu B., Suso J. S., El Haj A., Yang Y. (**2011**) Study of tissue engineered bone nodules by Fourier transform infrared spectroscopy. *Analyst* **136**: 775-780.

220. Draux F., Jeannesson P., Gobinet C., Sule-Suso J., Pijanka J., Sandt C., Dumas P., Manfait M., Sockalingum G. D. (**2009**) IR spectroscopy reveals effect of non-cytotoxic doses of anti-tumour drug on cancer cells. *Anal Bioanal Chem* **395**: 2293-2301.
221. Pijanka J. K., Kohler A., Yang Y., Dumas P., Chio-Srichan S., Manfait M., Sockalingum G. D., Sule-Suso J. (**2009**) Spectroscopic signatures of single, isolated cancer cell nuclei using synchrotron infrared microscopy. *Analyst* **134**: 1176-1181.
222. Bird B., Miljkovic M. S., Remiszewski S., Akalin A., Kon M., Diem M. (**2012**) Infrared spectral histopathology (SHP): a novel diagnostic tool for the accurate classification of lung cancer. *Lab Invest* **92**: 1358-1373.
223. Diem M., Miljković M., Bird B., Chernenko T., Schubert J., Marcsisin E., Mazur A., Kingston E., Zuser E., Papamarkakis K., Laver N. (**2012**) Applications of Infrared and Raman Microspectroscopy of Cells and Tissue in Medical Diagnostics: Present Status and Future Promises. *Spectroscopy: An International Journal* **27**: 463-496.
224. Matthaus C., Bird B., Miljkovic M., Chernenko T., Romeo M., Diem M. (**2008**) Chapter 10: Infrared and Raman microscopy in cell biology. *Methods Cell Biol* **89**: 275-308.
225. Lasch P., Chiriboga L., Yee H., Diem M. (**2002**) Infrared spectroscopy of human cells and tissue: detection of disease. *Technol Cancer Res Treat* **1**: 1-7.
226. Kondepati V. R., Heise H. M., Backhaus J. (**2008**) Recent applications of near-infrared spectroscopy in cancer diagnosis and therapy. *Anal Bioanal Chem* **390**: 125-139.
227. Pijanka J., Sockalingum G. D., Kohler A., Yang Y., Draux F., Parkes G., Lam K. P., Collins D., Dumas P., Sandt C., van Pittius D. G., Douce G., Manfait M., Untereiner V., Sule-Suso J. (**2010**) Synchrotron-based FTIR spectra of stained single cells. Towards a clinical application in pathology. *Lab Invest* **90**: 797-807.
228. Raman C. V., Krishnan K. S. (**1928**) A new type of secondary radiation. *Nature* **121**: 501-502.
229. Kalantri P. P., Somani R. R., Makhija D. T. (**2010**) Raman spectroscopy: A potential technique in analysis of pharmaceuticals. *Der Chemica Sinica* **1**: 1-12.
230. http://www.raman.de/htmlEN/basics/intensityEng.html. *(accessed in March 2013).*
231. Martyshkin D. V., Ahuja R. C., Kudriavtsev A., Mirov S. B. (**2004**) Effective suppression of fluorescence light in Raman measurements using ultrafast time gated charge coupled device camera. *Review of Scientific Instruments* **75**: 630-635.
232. http://www.raman.de/htmlEN/technology/fluoreEng.html. *(acessed in February 2013).*
233. Movasaghi Z., Rehman S., Rehman I. U. (**2007**) Raman Spectroscopy of Biological Tissues. *Applied Spectroscopy Reviews* **42**: 493-541.

234. Tu A. T. (**2003**) Use of Raman Spectroscopy in Biological Compounds. *Journal of the Chinese Chemical Society* **50**: 1-10.
235. Marques M. P. M., Batista de Carvalho L. A. E. (**2009**) Raman microspectroscopy. Applications in life sciences. Image Analysis in Life Sciences. Kerala: *Research Signpost*.
236. Neuberger A., Deenen L. L. M. v. (**1988**) Modern Physical Methods in Biochemistry. Amsterdam: *Elsevier Science*.
237. Milhazes N., Borges F., Calheiros R., Marques M. P. M. (**2004**) Identification of synthetic precursors of amphetamine-like drugs using Raman spectroscopy and ab initio calculations: beta-Methyl-beta-nitrostyrene derivatives. *Analyst* **129**: 1106-1117.
238. Nawaz H., Bonnier F., Knief P., Howe O., Lyng F. M., Meade A. D., Byrne H. J. (**2010**) Evaluation of the potential of Raman microspectroscopy for prediction of chemotherapeutic response to cisplatin in lung adenocarcinoma. *Analyst* **135**: 3070-3076.
239. Kneipp K., Kneipp H., Kneipp J. (**2006**) Surface-enhanced Raman scattering in local optical fields of silver and gold nanoaggregates-from single-molecule Raman spectroscopy to ultrasensitive probing in live cells. *Acc Chem Res* **39**: 443-450.
240. Lasch P., Kneipp J. (**2008**) Biomedical Vibrational Spectrometry. Hoboken, NJ: *John Wiley & Sons*. 386 p.
241. Bitar R. A., Martinho Hda S., Tierra-Criollo C. J., Zambelli Ramalho L. N., Netto M. M., Martin A. A. (**2006**) Biochemical analysis of human breast tissues using Fourier-transform Raman spectroscopy. *J Biomed Opt* **11**: 054001.
242. http://www.horiba.com/fileadmin/uploads/Scientific/Documents/Raman/Polymers01.pdf. *(accessed in February 2013).*
243. Fiuza S. M. (**2009**) Complexos Polinucleares de Paládio (II) como Novos Agentes Anticancerígenos: Relações Estrutura-Actividade: Coimbra University. 258 p.
244. Codina G., Caubet A., Lopez C., Moreno V., Molins E. (**1999**) Palladium(II) and platinum(II) polyamine complexes: X-ray crystal structures of (SP-4-2)-chloro{N-[(3-amino-kappa N)-propyl]propane-1,3-diamine-kappa N,kappa N '}palladium(1+) tetrachloropalladate (2-) (2 : 1) and (R,S)-tetrachloro[mu-(spermine)]dipalladium(II) (={mu-{N,N '-bis[(3-amino-kappa N)propyl]butane-1,4-diamine-kappa N :kappa N '}}tetrachlorodipalladium). *Helvetica Chimica Acta* **82**: 1025-1037.

245. Frisch M. J., Trucks G. W., Schlegel H. B., Scuseria G. E., Robb M. A., Cheeseman J. R., Montgomery J. A., Vreven J., T. , Kudin K. N., Burant J. C., Millam J. M., Iyengar S. S., Tomasi J., Barone V., Mennucci B., Cossi M., Scalmani G., Rega N., Petersson G. A., Nakatsuji H., Hada M., Ehara M., Toyota K., Fukuda R., Hasegawa J., Ishida M., Nakajima T., Honda Y., Kitao O., Nakai H., Klene M., Li X., Knox J. E., Hratchian H. P., Cross J. B., Bakken V., Adamo C., Jaramillo J., Gomperts R., Stratmann R. E., Yazyev O., Austin A. J., Cammi R., Pomelli C., Ochterski J. W., Ayala P. Y., Morokuma K., Voth G. A., Salvador P., Dannenberg J. J., Zakrzewski V. G., Dapprich S., Daniels A. D., Strain M. C., Farkas O., Malick D. K., Rabuck A. D., Raghavachari K., Foresman J. B., Ortiz J. V., Cui Q., Baboul A. G., Clifford S., Cioslowski J., Stefanov B. B., Liu G., Liashenko A., Piskorz P., Komaromi I., Martin R. L., Fox D. J., Keith T. A., Al-Laham M. A., Peng C. Y., Nanayakkara A., Challacombe M., Gill P. M. W., Johnson B. G., Chen W. C., Wong M. W., Gonzalez C., Pople J. A. (**2004**) G. Gaussian 03, Revision D.01. *Gaussian, Inc, Wallingford, CT*.

246. Lee C., Yang W., Parr R. G. (**1988**) Development of the Colle-Salvetti correlation-energy formula into a functional of the electron density. *Phys Rev B Condens Matter* **37**: 785-789.

247. Miehlich B., Savin A., Stoll H., Preuss H. (**1989**) Results Obtained with the Correlation-Energy Density Functionals of Becke and Lee, Yang and Parr. *Chemical Physics Letters* **157**: 200-206.

248. Becke A. D. (**1988**) Density-functional exchange-energy approximation with correct asymptotic behavior. *Phys Rev A* **38**: 3098-3100.

249. Becke A. D. (**1993**) Density-Functional Thermochemistry .3. The Role of Exact Exchange. *Journal of Chemical Physics* **98**: 5648-5652.

250. Petersson G. A., Bennett A., Tensfeldt T. G., Allaham M. A., Shirley W. A., Mantzaris J. (**1988**) A Complete Basis Set Model Chemistry .1. The Total Energies of Closed-Shell Atoms and Hydrides of the 1st-Row Elements. *Journal of Chemical Physics* **89**: 2193-2218.

251. Peng C. Y., Ayala P. Y., Schlegel H. B., Frisch M. J. (**1996**) Using redundant internal coordinates to optimize equilibrium geometries and transition states. *Journal of Computational Chemistry* **17**: 49-56.

252. Merrick J. P., Moran D., Radom L. (**2007**) An evaluation of harmonic vibrational frequency scale factors. *J Phys Chem A* **111**: 11683-11700.

253. Tanner M., Kapanen A. I., Junttila T., Raheem O., Grenman S., Elo J., Elenius K., Isola J. (**2004**) Characterization of a novel cell line established from a patient with Herceptin-resistant breast cancer. *Mol Cancer Ther* **3**: 1585-1592.
254. Nagy P., Friedlander E., Tanner M., Kapanen A. I., Carraway K. L., Isola J., Jovin T. M. (**2005**) Decreased accessibility and lack of activation of ErbB2 in JIMT-1, a herceptin-resistant, MUC4-expressing breast cancer cell line. *Cancer Res* **65**: 473-482.
255. Koninki K., Barok M., Tanner M., Staff S., Pitkanen J., Hemmila P., Ilvesaro J., Isola J. (**2010**) Multiple molecular mechanisms underlying trastuzumab and lapatinib resistance in JIMT-1 breast cancer cells. *Cancer Lett* **294**: 211-219.
256. Johannsson O. T., Staff S., Vallon-Christersson J., Kytola S., Gudjonsson T., Rennstam K., Hedenfalk I. A., Adeyinka A., Kjellen E., Wennerberg J., Baldetorp B., Petersen O. W., Olsson H., Oredsson S., Isola J., Borg A. (**2003**) Characterization of a novel breast carcinoma xenograft and cell line derived from a BRCA1 germ-line mutation carrier. *Lab Invest* **83**: 387-396.
257. Jonsson G., Staaf J., Olsson E., Heidenblad M., Vallon-Christersson J., Osoegawa K., de Jong P., Oredsson S., Ringner M., Hoglund M., Borg A. (**2007**) High-resolution genomic profiles of breast cancer cell lines assessed by tiling BAC array comparative genomic hybridization. *Genes Chromosomes Cancer* **46**: 543-558.
258. Soule H. D., Vazguez J., Long A., Albert S., Brennan M. (**1973**) A human cell line from a pleural effusion derived from a breast carcinoma. *J Natl Cancer Inst* **51**: 1409-1416.
259. Levenson A. S., Jordan V. C. (**1997**) MCF-7: the first hormone-responsive breast cancer cell line. *Cancer Res* **57**: 3071-3078.
260. Ogretmen B., Safa A. R. (**1997**) Expression of the mutated p53 tumor suppressor protein and its molecular and biochemical characterization in multidrug resistant MCF-7/Adr human breast cancer cells. *Oncogene* **14**: 499-506.
261. Kurokawa H., Nishio K., Fukumoto H., Tomonari A., Suzuki T., Saijo N. (**1999**) Alteration of caspase-3 (CPP32/Yama/apopain) in wild-type MCF-7, breast cancer cells. *Oncol Rep* **6**: 33-37.
262. Cailleau R., Olive M., Cruciger Q. V. (**1978**) Long term human breast carcinoma cell lines of metastatic origin: preliminary characterization. *In Vitro* **14**: 911-915.
263. Brinkley B. R., Beall P. T., Wible L. J., Mace M. L., Turner D. S., Cailleau R. M. (**1980**) Variations in cell form and cytoskeleton in human breast carcinoma cells in vitro. *Cancer Res* **40**: 3118-3129.

264. Huguet E. L., McMahon J. A., McMahon A. P., Bicknell R., Harris A. L. (**1994**) Differential expression of human Wnt genes 2, 3, 4, and 7B in human breast cell lines and normal and disease states of human breast tissue. *Cancer Res* **54**: 2615-2621.
265. Soule H. D., Maloney T. M., Wolman S. R., Peterson W. D., Jr., Brenz R., McGrath C. M., Russo J., Pauley R. J., Jones R. F., Brooks S. C. (**1990**) Isolation and characterization of a spontaneously immortalized human breast epithelial cell line, MCF-10. *Cancer Res* **50**: 6075-6086.
266. Zientek-Targosz H., Kunnev D., Hawthorn L., Venkov M., Matsui S., Cheney R. T., Ionov Y. (**2008**) Transformation of MCF-10A cells by random mutagenesis with frameshift mutagen ICR191: a model for identifying candidate breast-tumor suppressors. *Mol Cancer* **7**: 51.
267. Mosmann T. (**1983**) Rapid colorimetric assay for cellular growth and survival: application to proliferation and cytotoxicity assays. *J Immunol Methods* **65**: 55-63.
268. Twentyman P. R., Luscombe M. (**1987**) A study of some variables in a tetrazolium dye (MTT) based assay for cell growth and chemosensitivity. *Br J Cancer* **56**: 279-285.
269. Sylvester P. W. (**2011**) Optimization of the tetrazolium dye (MTT) colorimetric assay for cellular growth and viability. *Methods Mol Biol* **716**: 157-168.
270. Matsui I., Wiegand L., Pegg A. E. (**1981**) Properties of spermidine N-acetyltransferase from livers of rats treated with carbon tetrachloride and its role in the conversion of spermidine into putrescine. *J Biol Chem* **256**: 2454-2459.
271. Janne J., Williams-Ashman H. G. (**1971**) On the purification of L-ornithine decarboxylase from rat prostate and effects of thiol compounds on the enzyme. *J Biol Chem* **246**: 1725-1732.
272. Casero R. A., Jr., Wang Y., Stewart T. M., Devereux W., Hacker A., Smith R., Woster P. M. (**2003**) The role of polyamine catabolism in anti-tumour drug response. *Biochem Soc Trans* **31**: 361-365.
273. Gabrielson E., Tully E., Hacker A., Pegg A. E., Davidson N. E., Casero R. A., Jr. (**2004**) Induction of spermidine/spermine N1-acetyltransferase in breast cancer tissues treated with the polyamine analogue N1, N11-diethylnorspermine. *Cancer Chemother Pharmacol* **54**: 122-126.
274. Muskiet F. A., Dorhout B., van den Berg G. A., Hessels J. (**1995**) Investigation of polyamine metabolism by high-performance liquid chromatographic and gas chromatographic profiling methods. *J Chromatogr B Biomed Appl* **667**: 189-198.

275. Seiler N., Knodgen B. (**1985**) Determination of Polyamines and Related-Compounds by Reversed-Phase High-Performance Liquid-Chromatography - Improved Separation Systems. *J Chromatogr* **339**: 45-57.
276. Thornthwaite J. T., Sugarbaker E. V., Temple W. J. (**1980**) Preparation of tissues for DNA flow cytometric analysis. *Cytometry* **1**: 229-237.
277. Dolbeare F., Gratzner H., Pallavicini M. G., Gray J. W. (**1983**) Flow cytometric measurement of total DNA content and incorporated bromodeoxyuridine. *Proc Natl Acad Sci U S A* **80**: 5573-5577.
278. Fredlund J. O., Oredsson S. M. (**1997**) Ordered cell cycle phase perturbations in Chinese hamster ovary cells treated with an S-adenosylmethionine decarboxylase inhibitor. *Eur J Biochem* **249**: 232-238.
279. Begg A. C., McNally N. J., Shrieve D. C., Karcher H. (**1985**) A method to measure the duration of DNA synthesis and the potential doubling time from a single sample. *Cytometry* **6**: 620-626.
280. Fredlund J. O., Oredsson S. M. (**1996**) Normal G1/S transition and prolonged S phase within one cell cycle after seeding cells in the presence of an ornithine decarboxylase inhibitor. *Cell Prolif* **29**: 457-466.
281. Katz D., Ito E., Lau K. S., Mocanu J. D., Bastianutto C., Schimmer A. D., Liu F. F. (**2008**) Increased efficiency for performing colony formation assays in 96-well plates: novel applications to combination therapies and high-throughput screening. *Biotechniques* **44**: ix-xiv.
282. Shoemaker R. H., Wolpert-DeFilippes M. K., Kern D. H., Lieber M. M., Makuch R. W., Melnick N. R., Miller W. T., Salmon S. E., Simon R. M., Venditti J. M., et al. (**1985**) Application of a human tumor colony-forming assay to new drug screening. *Cancer Res* **45**: 2145-2153.
283. Cirenajwis H., Smiljanic S., Honeth G., Hegardt C., Marton L. J., Oredsson S. M. (**2010**) Reduction of the putative CD44+CD24- breast cancer stem cell population by targeting the polyamine metabolic pathway with PG11047. *Anticancer Drugs* **21**: 897-906.
284. Fairbairn D. W., Olive P. L., O'Neill K. L. (**1995**) The comet assay: a comprehensive review. *Mutat Res* **339**: 37-59.

285. Collins A., Dusinska M., Franklin M., Somorovska M., Petrovska H., Duthie S., Fillion L., Panayiotidis M., Raslova K., Vaughan N. (**1997**) Comet assay in human biomonitoring studies: reliability, validation, and applications. *Environ Mol Mutagen* **30**: 139-146.
286. Alm K., Berntsson P., Oredsson S. M. (**1999**) Topoisomerase II is nonfunctional in polyamine-depleted cells. *J Cell Biochem* **75**: 46-55.
287. Johansson V. M., Oredsson S. M., Alm K. (**2008**) Polyamine depletion with two different polyamine analogues causes DNA damage in human breast cancer cell lines. *DNA Cell Biol* **27**: 511-516.
288. Freiburghaus C., Lindmark-Mansson H., Paulsson M., Oredsson S. (**2012**) Reduction of ultraviolet light-induced DNA damage in human colon cancer cells treated with a lactoferrin-derived peptide. *J Dairy Sci* **95**: 5552-5560.
289. Towbin H., Staehelin T., Gordon J. (**1979**) Electrophoretic transfer of proteins from polyacrylamide gels to nitrocellulose sheets: procedure and some applications. *Proc Natl Acad Sci U S A* **76**: 4350-4354.
290. Batista de Carvalho L. A. E., Marques M. P. M., Martin C., Parker S. F., Tomkinson J. (**2011**) Inelastic neutron scattering study of Pt(II) complexes displaying anticancer properties. *Chemphyschem* **12**: 1334-1341.
291. Berridge M. V., Tan A. S. (**1993**) Characterization of the cellular reduction of 3-(4,5-dimethylthiazol-2-yl)-2,5-diphenyltetrazolium bromide (MTT): subcellular localization, substrate dependence, and involvement of mitochondrial electron transport in MTT reduction. *Arch Biochem Biophys* **303**: 474-482.
292. McCloskey D. E., Woster P. M., Casero R. A., Jr., Davidson N. E. (**2000**) Effects of the polyamine analogues N1-ethyl-N11-((cyclopropyl)methyl)-4,8-diazaundecane and N1-ethylN-11-((cycloheptyl)methyl)-4,8-diazaundecane in human prostate cancer cells. *Clin Cancer Res* **6**: 17-23.
293. Holst C. M., Staaf J., Jonsson G., Hegardt C., Oredsson S. M. (**2008**) Molecular mechanisms underlying N1, N11-diethylnorspermine-induced apoptosis in a human breast cancer cell line. *Anticancer Drugs* **19**: 871-883.
294. Uimari A., Keinanen T. A., Karppinen A., Woster P., Uimari P., Janne J., Alhonen L. (**2009**) Spermine analogue-regulated expression of spermidine/spermine N1-acetyltransferase and its effects on depletion of intracellular polyamine pools in mouse fetal fibroblasts. *Biochem J* **422**: 101-109.

295. Hegardt C., Johannsson O. T., Oredsson S. M. (**2002**) Rapid caspase-dependent cell death in cultured human breast cancer cells induced by the polyamine analogue N(1),N(11)-diethylnorspermine. *Eur J Biochem* **269**: 1033-1039.
296. Chen H. H., Kuo M. T. (**2010**) Role of glutathione in the regulation of Cisplatin resistance in cancer chemotherapy. *Met Based Drugs* **2010**.
297. Pandey A., Kurup A., Shrivastava A., Radhi S., Nguyen D. D., Arentz C., D'Chuna N., Hardwick F., D'Souza M. J., Jenkins M., Grizzi F., Kast W. M., Cobos E., Rahman R., Chiriva-Internati M., Chiaramonte R., Platonova N. (**2012**) Cancer testes antigens in breast cancer: biological role, regulation, and therapeutic applicability. *Int Rev Immunol* **31**: 302-320.
298. Batista de Carvalho L. A. E., Lourenço L. E., Marques M. P. M. (**1999**) Conformational Study of 1,2-Diaminoethane by Combined Ab Initio MO Calculations and Raman Spectroscopy. *J Mol Struct* **482**: 639-646.
299. Amorim da Costa A.M., Marques M. P. M., Batista de Carvalho L. A. E. (**2002**) The Carbon-hydrogen Stretching Region of the Raman Spectra of 1,6-Hexane- diamine: N-Deuteration, Ionization and Temperature Effects. *Vibrational Spectroscopy* **29**: 61-67.
300. Marques M. P. M., Batista de Carvalho L. A. E., Tomkinson J. (**2002**) Study of Biogenic and α,ω-Polyamines by Combined Inelastic Neutron Scattering and Raman Spectroscopies, and Ab Initio MO Calculations. *Journal Physical Chemistry A* **106**: 2473-2482.
301. Amorim da Costa A. M., Batista de Carvalho L. A. E., Marques M. P. M. (**2004**) Intra- versus Interchain interactions in α,ω-Polyamines: A Raman Spectroscopy Study *Vibrational Spectroscopy* **35**: 165-171.
302. Batista de Carvalho L. A. E., Marques M. P. M., Tomkinson J. (**2006**) Transverse Acoustic Modes of Biogenic and α,ω-polyamines: A Study by Inelastic Neutron Scattering and Raman Spectroscopies Coupled to DFT Calculations *Journal Physical Chemistry A* **110**: 12947-12954.
303. Huang Y., Hager E. R., Phillips D. L., Dunn V. R., Hacker A., Frydman B., Kink J. A., Valasinas A. L., Reddy V. K., Marton L. J., Casero R. A., Jr., Davidson N. E. (**2003**) A novel polyamine analog inhibits growth and induces apoptosis in human breast cancer cells. *Clin Cancer Res* **9**: 2769-2777.

304. Rezler E. M., Fenton R. R., Esdale W. J., McKeage M. J., Russell P. J., Hambley T. W. (**1997**) Preparation, characterization, DNA binding, and in vitro cytotoxicity of the enantiomers of the platinum(II) complexes N-methyl-, N-ethyl- and N,N-dimethyl-(R)- and -(S)-3-aminohexahydroazepinedichloroplatinum(II). *J Med Chem* **40**: 3508-3515.
305. Keren-Paz A., Bercovich Z., Porat Z., Erez O., Brener O., Kahana C. (**2006**) Overexpression of antizyme-inhibitor in NIH3T3 fibroblasts provides growth advantage through neutralization of antizyme functions. *Oncogene* **25**: 5163-5172.
306. Silva T., Andersson S., Sukumaran S., Marques M. P. M., Persson L., Oredsson S. (**2013**) Norspermidine and Novel Pd(II) and Pt(II) Polynuclear Complexes of Norspermidine as Potential Antineoplastic Agents Against Breast Cancer. *PLoS One* **8**: e55651.
307. Wu W. J., Zhang Y., Zeng Z. L., Li X. B., Hu K. S., Luo H. Y., Yang J., Huang P., Xu R. H. (**2013**) beta-phenylethyl isothiocyanate reverses platinum resistance by a GSH-dependent mechanism in cancer cells with epithelial-mesenchymal transition phenotype. *Biochem Pharmacol* **85**: 486-496.
308. Lim M. C. (**1977**) Mixed-Ligand Complexes of Palladium(Ii) .1. Diaqua(Ethylenediamine)Palladium(Ii) Complexes of Glycylglycine and Glycinamide. *Journal of the Chemical Society-Dalton Transactions*: 15-17.
309. Wondrak G. T. (**2009**) Redox-directed cancer therapeutics: molecular mechanisms and opportunities. *Antioxid Redox Signal* **11**: 3013-3069.
310. Porter C. W., Ganis B., Libby P. R., Bergeron R. J. (**1991**) Correlations between polyamine analogue-induced increases in spermidine/spermine N1-acetyltransferase activity, polyamine pool depletion, and growth inhibition in human melanoma cell lines. *Cancer Res* **51**: 3715-3720.
311. Pledgie A., Huang Y., Hacker A., Zhang Z., Woster P. M., Davidson N. E., Casero R. A., Jr. (**2005**) Spermine oxidase SMO(PAOh1), Not N1-acetylpolyamine oxidase PAO, is the primary source of cytotoxic H2O2 in polyamine analogue-treated human breast cancer cell lines. *J Biol Chem* **280**: 39843-39851.
312. Ricardo S., Vieira A. F., Gerhard R., Leitao D., Pinto R., Cameselle-Teijeiro J. F., Milanezi F., Schmitt F., Paredes J. (**2011**) Breast cancer stem cell markers CD44, CD24 and ALDH1: expression distribution within intrinsic molecular subtype. *J Clin Pathol* **64**: 937-946.

Annexes

Annexe I – Symbols

Au	gold
Bi	bismuth
Cu	cooper
Fe	iron
Ga	gallium
Pt	platinum
Pd	palladium
Re	rhenium
Ru	ruthenium

h	Planck constant
k	Force constant
m	Atomic mass
v	Frequency
μ	Reduced mass

δ	In-plane Angular Deformation (symmetric – δ_s – or antisymmetric – δ_{as} or longitudinal – δ_{long}
r	rocking
sciss	scissoring
t	twisting
ν	Stretching (symmetric – ν_s – or antisymmetric – ν_{as})
ω	wagging

Annexe II – Abbreviations

3-AAP	3-Acetamidopropanal
A	Adenine base
AdoMet	*S*-Adenosylmethionine
AdoMetDC	*S*-Adenosylmethionine decarboxylase
APAO	Acetylpolyamine oxidase
Az	Antizyme
AzI	Antizyme inhibitor
BESpm	N^1,N^{12}-bis(ethyl)spermine
BENSpm	N^1,N^{11}-bis(ethyl)norspermine
BrdUrd	Bromodeoxyuridine
CCD	Charge coupled device
CDKs	Cyclin dependent kinases
CDKIs	Cyclin dependent kinase inhibitors
$CD44^+/CD24^-$	Cell surface feature present essentially in stem-like cells
CFE	Colony Forming Efficiency
Cisplatin	*Cis*-Diamminedichloroplatinum (II)
CPENSpm	N^1-cyclo-propylmethyl-N^{11}-ethylnorspermine
CSC	Cancer stem cell
CTR	Cooper transporter
dcAdoMet	decarboxylated *S*-Adenosylmethionine
DFMO	α-Difluoromethylornithine
DFT	Density Functional Theory
DMEM	Dulbecco's modified Eagle's medium
DMSO	Dimethyl sulphoxide
DNA	Deoxyribonucleic acid
ECL	Enhanced chemiluminiscence
EDTA	Ethylenediaminetetraacetic acid
ER	Estrogen receptor

EtBr	Ethidium bromide
FCM	Flow Cytometry
FCS	Fetal calf serum
FDA	Food and Drug Administration
FITC	Fluorescein isothiocyanate
FT	Fourier Transform
FTIR	Fourier Transform Infrared spectroscopy
FT-Raman	Fourier Transform Raman spectroscopy
G	Guanine base
G_0	Gap zero phase
G_1	Gap 1 phase
G_2	Gap 2 phase
GSH	Glutathione
^{3}H-spermidine	Radioactive-labelled spermidine
H_2O_2	Hydrogen peroxide
HER2	Human epidermal growth factor receptor 2
HMG	High mobility group
HPLC	High-Performance Liquid Chromatography
ICP-MS	Inductively Coupled Plasma Mass Spectrometry
IgG	Immunoglobulin
IR	Infrared
LAM	Longitudinal acoustic mode
laser	Light amplification by stimulated emission of radiation
M	Mitosis phase
MGBG	Methylglyoxal bis(guanylhydrazone)
MTT	3-(4,5-Dimethyl-thiazolyl-2)-2,5 diphenyltetrazolium bromide
NSpd	Norspermidine
ODC	Ornithine decarboxylase
PBS	Phosphate-buffered saline
PBS-T	Phosphate-buffered saline with 0.05% Tween 20

Pd-BENSpm	$(PdCl_2)_2$-N^1,N^{11}-bis(ethyl)norspermine
Pd-NSpd	$(PdCl_2)_3$-(norspermidine)$_2$
Pd-Spm	$(PdCl_2)_2$-spermine
PE	Phycoerythrin
PI	Propidium iodide
polyHEMA	Poly(2-hydroxyethyl methacrylate
PR	Progesterone receptor
Pt-CPENSpm	$(PtCl_2)_2$-N^1-cyclopropyl-methyl-N^{11}-ethylnorspermine
Pt-NSPd	$(PtCl_2)_3$-(norspermidine)$_2$
PTS	Polyamine transport system
QFM–UC	Molecular Physical-Chemistry research group, University of Coimbra
RNA	Ribonucleic acid
RNase A	Ribonuclease A
RPMI	Roswell ParK Memorial Institute medium
S	Synthesis phase
SAR	Structure-activity relationship
SCGE	Single Cell Gel Electrophoresis
SD	Standard deviation
SEM	Standard error of the mean
SMO	Spermine oxidase
Spm	Spermine
SSAT	Spermidine/spermine N^1-acetyltransferase
TAM	Transverse acoustic mode
TMOM	Tail moment
(s)	solid
(aq)	aqueous

Annexe III – Figures Index

Figure 56: Schematic representation of the main conclusions resulting from this study.

Annexe IV – Tables Index